

5-16-2003

An Overview of Tourmaline Mineralogy from Gem Tourmaline Producing Pegmatite Districts in Africa

Brian Giller
University of New Orleans

Follow this and additional works at: <https://scholarworks.uno.edu/td>

Recommended Citation

Giller, Brian, "An Overview of Tourmaline Mineralogy from Gem Tourmaline Producing Pegmatite Districts in Africa" (2003). *University of New Orleans Theses and Dissertations*. 18.
<https://scholarworks.uno.edu/td/18>

This Thesis is protected by copyright and/or related rights. It has been brought to you by ScholarWorks@UNO with permission from the rights-holder(s). You are free to use this Thesis in any way that is permitted by the copyright and related rights legislation that applies to your use. For other uses you need to obtain permission from the rights-holder(s) directly, unless additional rights are indicated by a Creative Commons license in the record and/or on the work itself.

This Thesis has been accepted for inclusion in University of New Orleans Theses and Dissertations by an authorized administrator of ScholarWorks@UNO. For more information, please contact scholarworks@uno.edu.

AN OVERVIEW OF TOURMALINE MINERALOGY FROM GEM TOURMALINE
PRODUCING PEGMATITE DISTRICTS IN AFRICA

A Thesis

Submitted to the Graduate Faculty of the
University of New Orleans
in partial fulfillment of the
requirements for the degree of

Master of Science
in
Geology

by

Brian S. Giller

B.S., James Madison University, 2000

May, 2003

ACKNOWLEDGEMENT

I would like to acknowledge my major professor, Dr. William B. “Skip” Simmons Jr. His helpful guidance, wealth of scientific knowledge, expectations of impeccability for me and desire to see me succeed brought out the absolute best of me as a person and my productivity as a graduate student. His critical reviews of this thesis were extremely helpful and are greatly appreciated.

Next, I would like to thank the members of my committee, Alexander U. Falster, Dr. Karen L. Webber, Dr. Michael A. Wise and Dr. Matthew W. Totten for their critical reviews of this manuscript and the valuable input, guidance and advice that they offered me throughout the duration of my graduate school career. Without you all, this project would not have been possible. To my major professor and all committee members, thank you very much for everything you have done for me. You all are like family to me.

To the individuals and organizations who supplied the specimens for analysis for this project, G.I.A., Wm. B. Simmons, A.U. Falster, Bill Larson, Bill Barker, Phillip Zahm, M.A. Wise, Paul Pohwat, Brendan Laurs, Lila Taylor, King Bambozoho III of Mali and John Patrick, I thank you all very much. This thesis would not have been possible without the samples you all provided.

Lastly, I would like to thank my family in Alexandria, Virginia and the many wonderful friends I have made while in New Orleans for their support during my graduate school career. To my Mom, Susan Giller and Dad, Martin Giller, sister Anne, brother Carl, Uncle Neal, Aunt Bev and cousins Kevin and Lisa, thank you. To my

friends at UNO, Jim Nizamoff, Pam Rein, Morgan Masau, Sirel White, John & Andrea Calvin, James Ronquillo, Sammy & Ali Bruiglio, Josh Sullivan, Leah Johanningmeier, Rebecca Murphy, Jeff & Jennifer Lewis, Lisa Dwyer, Chris Cannata, Louise Totten, Will Snyder, friends in Virginia and everybody else I have had the pleasure of knowing including geology department faculty members and former students, I extend many thanks for your friendship and support.

FOREWORD

It has always been assumed that tourmaline on the gem market was elbaite. This will soon change.

TABLE OF CONTENTS

Abstract	xii
Introduction.....	1
Previous Work	5
The Crystal Structure of the Tourmaline Group.....	7
Tourmaline Formulas.....	12
Causes of Color in the Tourmaline Group.....	13
Materials & Methods	16
General Results	21
Results.....	24
Nigerian Faceted Tourmaline	24
Namibian & Malian Tourmaline Slices and Fragments	88
Sanga Sanga, Tanzania Tourmaline Slices	117
Democratic Republic of Congo Tourmaline Slices	134
Mozambique Tourmaline Fragments	152
Namibian, Malian and Mozambique Tourmaline Cell-Edge Refinements	168
Discussion.....	171
Conclusions.....	180
References.....	184
Appendix 1.....	191
Appendix 2.....	202

Vita.....	204
-----------	-----

LIST OF TABLES

Table 1: Microprobe Detection Limits	20
Table 2: Microprobe Analyses, Nigerian Tourmaline	36
Table 3: Microprobe Analyses, Blue Nigerian Tourmaline.....	66
Table 4: Microprobe Analyses, Namibian Tourmaline	96
Table 5: Microprobe Analyses, Malian Tourmaline.....	105
Table 6: Microprobe Analyses, Tanzanian Tourmaline	122
Table 7: Microprobe Analyses, Congolese Tourmaline	140
Table 8: Microprobe Analyses, Mozambique Tourmaline	157
Table 9: Cell-Edge Data: Namibian, Malian and Mozambique Tourmaline.....	169

LIST OF FIGURES

Fig. 1: Political Map of Africa.....	3
Fig. 2: Pegmatite Schematic	4
Fig. 3: Tourmaline Structure Viewed Perpendicular to the a-axis.....	10
Fig. 4: Tourmaline Structure Viewed Perpendicular to the c-axis.....	11
Fig. 5: Mg- Y-site Al- Fe Ternary, African Tourmaline.....	22
Fig. 6: Ca- Y-site Al- Na Ternary, African Tourmaline.....	23
Fig. 7: Faceted Nigerian Tourmaline	26
Fig. 8: Nigerian Tourmaline Crystal.....	27
Fig. 9: Nigerian Tourmaline Crystal.....	27
Fig. 10: Ca- Xvac- Na Ternary, Nigerian Tourmaline.....	76
Fig. 11: Mn- Ti- Fe Ternary, Nigerian Tourmaline	77
Fig. 12: Li (calc.) vs. Fe Binary, Nigerian Tourmaline	77
Fig. 13: Fe vs. Mn Binary, Nigerian Tourmaline	79
Fig. 14: Li (calc.) vs. Mn Binary, Nigerian Tourmaline.....	79
Fig. 15: Li (calc.) vs. F Binary, Nigerian Tourmaline	80
Fig. 16: Li (calc.) vs. Al Binary, Nigerian Tourmaline	82
Fig. 17: Al vs. Fe Binary, Nigerian Tourmaline	82
Fig. 18: Fe vs. Ti Binary, Nigerian Tourmaline	83
Fig. 19: Mn vs. Ti Binary, Nigerian Tourmaline.....	85
Fig. 20: Na vs. F Binary, Nigerian Tourmaline	85

Fig. 21: Na vs. Ti+Fe+Mn Binary, Nigerian Tourmaline	86
Fig. 22: Color Intensity of Pink Stones vs. Mn Binary, Nigerian Tourmaline	86
Fig. 23: Color Intensity of Pink Stones vs. Avg. Mn Binary	87
Fig. 24: Photograph, Namibian Tourmaline Probemount.....	89
Fig. 25: Photograph, Namibian Tourmaline Probemount.....	89
Fig. 26: Ca- Xvac- Na Ternary, Namibian/Malian Tourmaline	107
Fig. 27: Mn- Ti- Fe Ternary, Namibian/Malian Tourmaline.....	108
Fig. 28: Li (calc.) vs. Fe Binary, Namibian/Malian Tourmaline	108
Fig. 29: Fe vs. Mn Binary, Namibian/Malian Tourmaline	109
Fig. 30: Li (calc.) vs. Mn Binary, Namibian/Malian Tourmaline.....	111
Fig. 31: Li (calc.) vs. F Binary, Namibian/Malian Tourmaline.....	111
Fig. 32: Li (calc.) vs. Al Binary, Namibian/Malian Tourmaline	112
Fig. 33: Al vs. Fe Binary, Namibian/Malian Tourmaline	112
Fig. 34: Fe vs. Ti Binary, Namibian/Malian Tourmaline	113
Fig. 35: Mn vs. Ti Binary, Namibian/Malian Tourmaline.....	115
Fig. 36: Na vs. F Binary, Namibian/Malian Tourmaline	115
Fig. 37: Na vs. Ti+Fe+Mn Binary, Namibian/Malian Tourmaline	116
Fig. 38: Photograph, Tanzanian Tourmaline	118
Fig. 39: Photograph, Tanzanian Tourmaline	118
Fig. 40: Ca- Xvac- Na Ternary, Tanzanian Tourmaline	125
Fig. 41: Mn- Ti- Fe Ternary, Tanzanian Tourmaline	126
Fig. 42: Li (calc.) vs. Fe Binary, Tanzanian Tourmaline.....	126
Fig. 43: Fe vs. Mn Binary, Tanzanian Tourmaline	127

Fig. 44: Li (calc.) vs. Mn Binary, Tanzanian Tourmaline	127
Fig. 45: Li (calc.) vs. F Binary, Tanzanian Tourmaline	129
Fig. 46: Li (calc.) vs. Al Binary, Tanzanian Tourmaline.....	129
Fig. 47: Al vs. Fe Binary, Tanzanian Tourmaline	130
Fig. 48: Fe vs. Ti Binary, Tanzanian Tourmaline.....	130
Fig. 49: Mn vs. Ti Binary, Tanzanian Tourmaline	131
Fig. 50: Na vs. F Binary, Tanzanian Tourmaline	131
Fig. 51: Na vs. Ti+Fe+Mn Binary, Tanzanian Tourmaline	133
Fig. 52: Photograph, Congolese Tourmaline	135
Fig. 53: Ca- Xvac- Na Ternary, Congolese Tourmaline.....	143
Fig. 54: Mn- Ti- Fe Ternary, Congolese Tourmaline	144
Fig. 55: Li (calc.) vs. Fe Binary, Congolese Tourmaline	144
Fig. 56: Fe vs. Mn Binary, Congolese Tourmaline.....	145
Fig. 57: Li (calc.) vs. Mn Binary, Congolese Tourmaline.....	145
Fig. 58: Li (calc.) vs. F Binary, Congolese Tourmaline	147
Fig. 59: Li (calc.) vs. Al Binary, Congolese Tourmaline	147
Fig. 60: Al vs. Fe Binary, Congolese Tourmaline	148
Fig. 61: Fe vs. Ti Binary, Congolese Tourmaline.....	148
Fig. 62: Mn vs. Ti Binary, Congolese Tourmaline	149
Fig. 63: Na vs. F Binary, Congolese Tourmaline	151
Fig. 64: Na vs. Ti+Fe+Mn Binary, Congolese Tourmaline.....	151
Fig. 65: Photograph, Mozambique tourmaline	153
Fig. 66: Ca- Xvac- Na Ternary, Mozambique Tourmaline	160

Fig. 67: Mn- Ti- Fe Ternary, Mozambique Tourmaline	161
Fig. 68: Li (calc.) vs. Fe Binary, Mozambique Tourmaline	161
Fig. 69: Fe vs. Mn Binary, Mozambique Tourmaline	162
Fig. 70: Li (calc.) vs. Mn Binary, Mozambique Tourmaline.....	162
Fig. 71: Li (calc.) vs. F Binary, Mozambique Tourmaline	163
Fig. 72: Li (calc.) vs. Al Binary, Mozambique Tourmaline	165
Fig. 73: Al vs. Fe Binary, Mozambique Tourmaline	165
Fig. 74: Fe vs. Ti Binary, Mozambique Tourmaline	166
Fig. 75: Mn vs. Ti Binary, Mozambique Tourmaline.....	166
Fig. 76: Na vs. F Binary, Mozambique Tourmaline	167
Fig. 77: Na vs. Ti+Fe+Mn Binary, Mozambique Tourmaline.....	167
Fig. 78: a vs. c Cell-Edge Diagram, Namibian, Malian and Mozambique Tourmaline ..	170

ABSTRACT

Suites of gem-quality faceted tourmaline, slices and fragments from Nigeria Namibia, Mali, Tanzania, Congo and Mozambique were quantitatively analyzed to determine mineralogy and minor element chemistry. The specimens range in color from colorless to pink, red, yellowish-brown, green, bluish-gray, blue, brown and black. The results show that these tourmalines are elbaite, liddicoatite, rossmanite and schorl.

Fe, Mn and Ti are the principal chromophores of the studied tourmaline. Fe is the most dominant and causes green, blue, dark-brown and black colors. Mn imparts pink and red hues. Correlations between Mn content and pink color intensity were not found. The $Mn^{2+} \leftrightarrow Ti^{4+}$ charge transfer causes yellowish-brown colors. A positive correlation of Na^+ with transition element content was found. Limited relationships between chemistry and locality were deciphered for Nigeria, Namibia and Tanzania on the basis of end-member content and Congo based on Mn, Mg and Ti content.

INTRODUCTON

The tourmaline group of minerals consists of fourteen known species. This group occurs in a wide variety of igneous, metamorphic and sedimentary environments (Simmons, 2003). Euhedral gem quality tourmaline is highly prized by mineral collectors and is of particular economic interest for being faceted into brilliant stones. Gem quality tourmaline crystallizes almost exclusively in rare-element and miarolitic class, LCT- (granitic pegmatites with a *L*=Lithium, *C*=Cesium & *T*=Tantalum signature) family pegmatites. Recent work has shown that a number of tourmaline species such as schorl, elbaite, liddicoatite, rossmanite and olenite occur in these types of pegmatites.

In the miarolitic cavities of geochemically evolved pegmatites, tourmaline crystals are associated with pocket wall minerals such as K-feldspar, quartz, Na-plagioclase and muscovite and or lepidolite, but gem-quality euhedral tourmaline crystals typically nucleate over early pocket minerals (Černý, 2000). Although tourmaline can form in any pegmatite zone from the border zone to the core, gem quality crystals that crystallize in miarolitic cavities (Fig. 2) are the most useful for the gem trade. Tourmaline is vital to petrologists for studying the chemical evolution of pegmatites. Additionally, gem quality tourmaline can also be associated with hydrothermal vein deposits and skarns.

There have been many recent studies on tourmaline from pegmatites in Russia, Madagascar, the Czech Republic, Canada, Namibia, Brazil, Tajikistan and the U.S.A. (Simmons, 2003; Simmons *et al.*, 2001; Simmons *et al.* 1997; Falster *et al.*, 1997, Selway

et al., 1999; Selway, 1999; Selway *et al.*, 1998a; Keller *et al.*, 1999; Henry & Dutrow, 2000; Gordienko *et al.*, 1997; Jolliff *et al.*, 1986; Hawthorne *et al.*, 1999 and others).

This and other work has resulted in the discovery of several new species of tourmaline including magnesiofoitite (Hawthorne *et al.*, 1999), rossmanite (Selway *et al.*, 1998a), foitite (MacDonald *et al.*, 1993), feruvite (Grice & Robinson, 1989) and their solid solution series in the last ten years. New species vanadiumdravite, “cralpoite”, “fluor-elbaite”, “fluor-dravite”, “fluor-schorl”, “oxy-elbaite” and “oxy-magnesiofoitite” are currently being classified. However, there has yet to be a broad based survey concerned with examining the mineralogy and compositional variation of gem quality tourmaline.

The primary objective of this thesis is to classify the mineralogy and chemical variability of African tourmaline reaching the gem market. This includes classifying these stones or crystals on the basis of the various tourmaline end-member(s) and their major and minor element chemistry. Other objectives are to link chemistry to color and finally to determine how variations in chemistry affect the unit cell dimensions of the crystal structure. This work is significant in the respect that such a large scale and inclusive mineralogical and chemical study of economically vital and aesthetically beautiful gem tourmaline has never been previously attempted. A map Africa showing the locations of the suites of tourmaline analyzed for this study is shown in Fig. 1.



Fig. 1: Political map of Africa outlining the locations of various pegmatite districts.

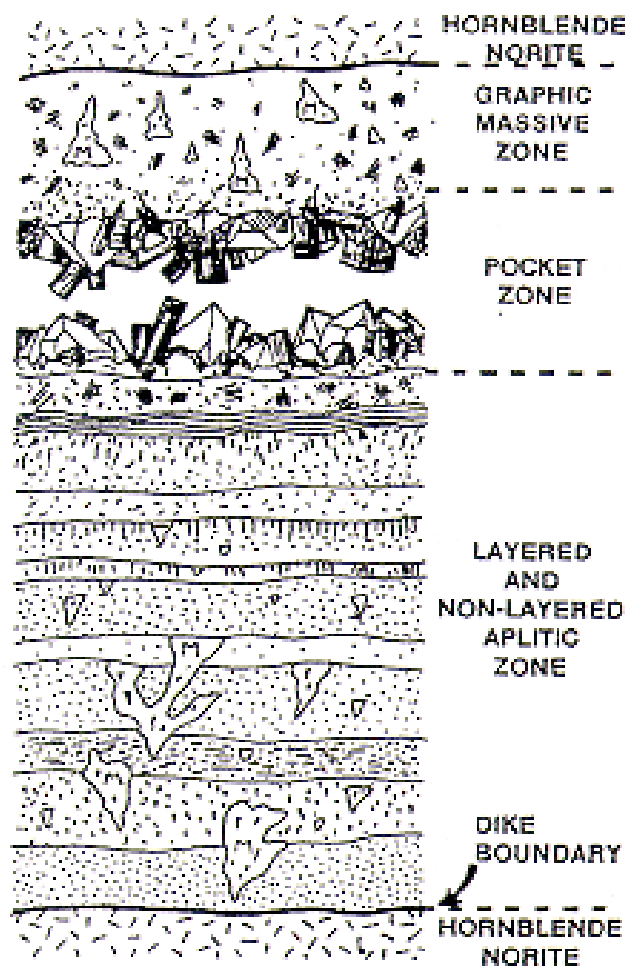


Fig. 2: A typical pegmatite dike in southern California with gem tourmaline in the pocket.
(modified from Foord, 1976)

PREVIOUS WORK

Tourmaline has previously been analyzed as a means of recording pegmatite consolidation by evaluating its chemical variations within sequentially crystallized internal pegmatite zones from different world localities.

The following studies of Russian tourmaline have been completed: Simmons *et al.*, (2001) analyzed tourmaline from six worldwide locations including Russia to determine its chemistry and relationship to pegmatite paragenesis. Simmons *et al.*, (1997) studied tourmaline from the elbaite sub-type pegmatites of the Malkhanski pegmatite district of Transbaikalia, Siberia, Russia.

In the United States several studies of tourmaline have been done. Falster *et al.*, (1997) collected tourmaline from the Animikie Red Ace pegmatite in Wisconsin, U.S.A. to study its chemistry and role in pegmatite evolution. Taylor *et al.*, (1997) observed tourmaline compositions from the Belo Horizonte no.1 pegmatite, Peninsular Ranges batholith, Southern California, U.S.A. Jolliff *et al.*, (1986) employed tourmaline as a means of deciphering pegmatite evolution and consolidation in the southern Black Hills, South Dakota, U.S.A.

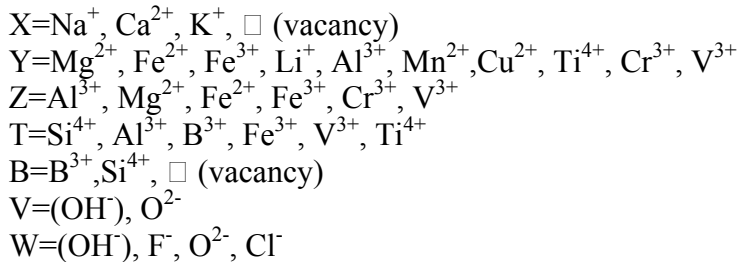
Tourmaline investigations in the Czech Republic include the following studies: Selway *et al.*, (1999) analyzed tourmaline from rare-element class, lepidolite subtype pegmatites from the Czech Republic and Canada to determine its compositional evolution. Novák & Selway (1997) analyzed tourmaline compositions from an elbaite sub-type pegmatite in Bližná, Czech Republic. Selway (1999) conducted a survey of the

compositional evolution of tourmaline in lepidolite, petalite and elbaite sub-type pegmatites.

Other investigations of pegmatitic tourmaline throughout the world include the following works: Henry and Dutrow (2000) examined fibrous tourmaline to determine its role as a recorder of pegmatite evolution. Keller *et al.*, (1999) conducted a study examining the chemical variability of tourmaline from pegmatites in the Southern Tin Belt (STB) in west-central Namibia to understand its petrologic significance. Bilal *et al.*, (1997) collected tourmaline samples from the São José da Safira area of the Eastern Brazilian Pegmatite Province (EBPP) to determine its chemical variability within individual pegmatites. Aurisicchio & Pezzotta (1997) performed analyses of over 80 tourmaline crystals from the pegmatites of Elba, Italy to study variations in chemistry and to use this information to make paragenetic inferences. Zolotarev (1997) studied the crystal chemistry of tourmalines from miarolitic pegmatites of the east Pamirs, Tajikistan.

THE CRYSTAL STRUCTURE OF THE TOURMALINE GROUP

The tourmaline group consists of minerals classified as complex hydrous cyclo-borosilicates. Tourmaline is trigonal, crystallizing in the acentric $3m$ point group (ditrigonal pyramidal) and the $R\bar{3}m$ space group with $Z=3$. At present, there are 14 valid I.M.A. approved species and more are currently being classified (Hawthorne & Henry, 1999). Because the 14 species are isostructural, extensive ionic substitution and solid solution occurs between these end-members. The structural formula of the tourmaline group can be expressed as $XY_3Z_6(BO_3)_3T_6O_{18}V_3W$. According to Hawthorne & Henry (1999), Keller *et al.*, (1999), Hawthorne (1997) and many others, the following metallic and non-metallic cations and anions fit into the following structural sites. Figs. 3 and 4 show drawings of the tourmaline structure and the locations of each site therein.



The X-site: The X-site is occupied by Na^+ , Ca^{2+} , K^+ cations or by vacancies (\square). The X-site is located in the center of the structural channels generated by the Si_6O_{18} rings. This site possesses nine or possibly ten-fold coordination and is bonded by six O^{2-} anions of the Si_6O_{18} ring and three O^{2-} anions of the B-triangles (Selway, 1999; Dietrich, 1985).

The Y-sites: The three Y-sites may contain a broad diversity of cations including but not exclusive to Mg^{2+} , Fe^{2+} , Fe^{3+} , Li^+ , Al^{3+} , Mn^{2+} , Cu^{2+} , Ti^{4+} , Cr^{3+} and V^{3+} . These

sites are distorted octahedra (Dietrich, 1985). The Y-sites possess a three-fold axis of rotation and are octahedrally coordinated by two O²⁻ anions of the BO₃ triangles, two O²⁻ anions from the anion-sites and two O²⁻ anions from the apices of the SiO₄ tetrahedra (Selway, 1999; Deer *et al.*, 1962). The Y-sites can also bond to the X-site cation (Selway, 1999).

The Z-sites: The six Z-sites contain Al³⁺, Mg²⁺, Fe²⁺, Fe³⁺, Cr³⁺ and V³⁺ cations. The Z-sites are octahedrally coordinated by eight O²⁻ anions. Each of the Z-site cations bond to one O²⁻ anion from the Y-site, two BO₃ group O²⁻ anions and three Si₆O₁₈ O²⁻ anions (Selway, 1999). These sites are distorted octahedra and are responsible for linking the V- and W-site structural islands together (Dietrich, 1985).

The T-sites: Each Si⁴⁺ cation is tetrahedrally coordinated by four O²⁻ anions comprising the SiO₄ tetrahedra. The SiO₄ tetrahedra are arranged in a six-fold ring, denoted T₆O₁₈. This Si₆O₁₈ ring is oriented perpendicular to the *c*-crystallographic axis and points toward the analogous (*c*⁻) termination of the crystal (Dietrich, 1985). Small amounts of Al³⁺, B³⁺, Fe³⁺, V³⁺ and Ti⁴⁺ can substitute for Si⁴⁺ (Keller *et al.*, 1999; Hawthorne, 1997).

The B-sites: The B-sites (BO₃ groups) house B³⁺ cations trigonally coordinated by three O²⁻ anions. The B-sites are oriented in a plane perpendicular to the *c*-axis of the crystal. The BO₃ triangles are linked via corner sharing to two Y-site octahedra and two Z-site octahedra. The BO₃ groups can also be connected to the X-site (Selway, 1999). It has been postulated that the B-triangles could be distorted due to the size and charge of the O²⁻ anions of the neighboring SiO₄ tetrahedra. Lowenstein (1956) and Keller *et al.*, (1999) have suggested the possibility of tetrahedrally coordinated B because of the

proximity of B to the O²⁻ anions of the SiO₄ tetrahedra. Keller *et al.*, (1999) have theorized the existence of ^[4]B in muscovite saturated pegmatite melts by stating that high ^[4]B/^[3]B ratios and low Fe-Mg activities limit tourmaline stability in such environments. Hughes *et al.*, (2001), Hughes *et al.*, (2000) and Tagg *et al.*, (1999) also propose the existence of ^[4]B in tourmaline. However, ^[4]B is not very probable in tourmaline or other minerals since this structural configuration is very unstable. Other than B³⁺ cations, there can be small amounts of Si⁴⁺ (Hughes *et al.*, 2001) or vacancies in this site.

The V and W-sites: These four sites contain the anions of the tourmaline structure. The three V-sites can hold (OH⁻) and O²⁻ anions. The W-site can house (OH⁻), F⁻ and O²⁻ anions (Hawthorne, 1997). The W-site can also house Cl⁻ (Keller *et al.*, 1999). This is the only crystallographic site in the tourmaline structure that F⁻ anions can occupy (Dutrow and Henry, 2000). The three V-sites are located immediately outside the Si₆O₁₈ ring and the fourth W-site is located in the center of the structure directly beneath the X-site in the center of the structural channel produced by the Si₆O₁₈ ring. Each anion-site is linked by O²⁻ anions of the Si₆O₁₈ ring (Dietrich, 1985).

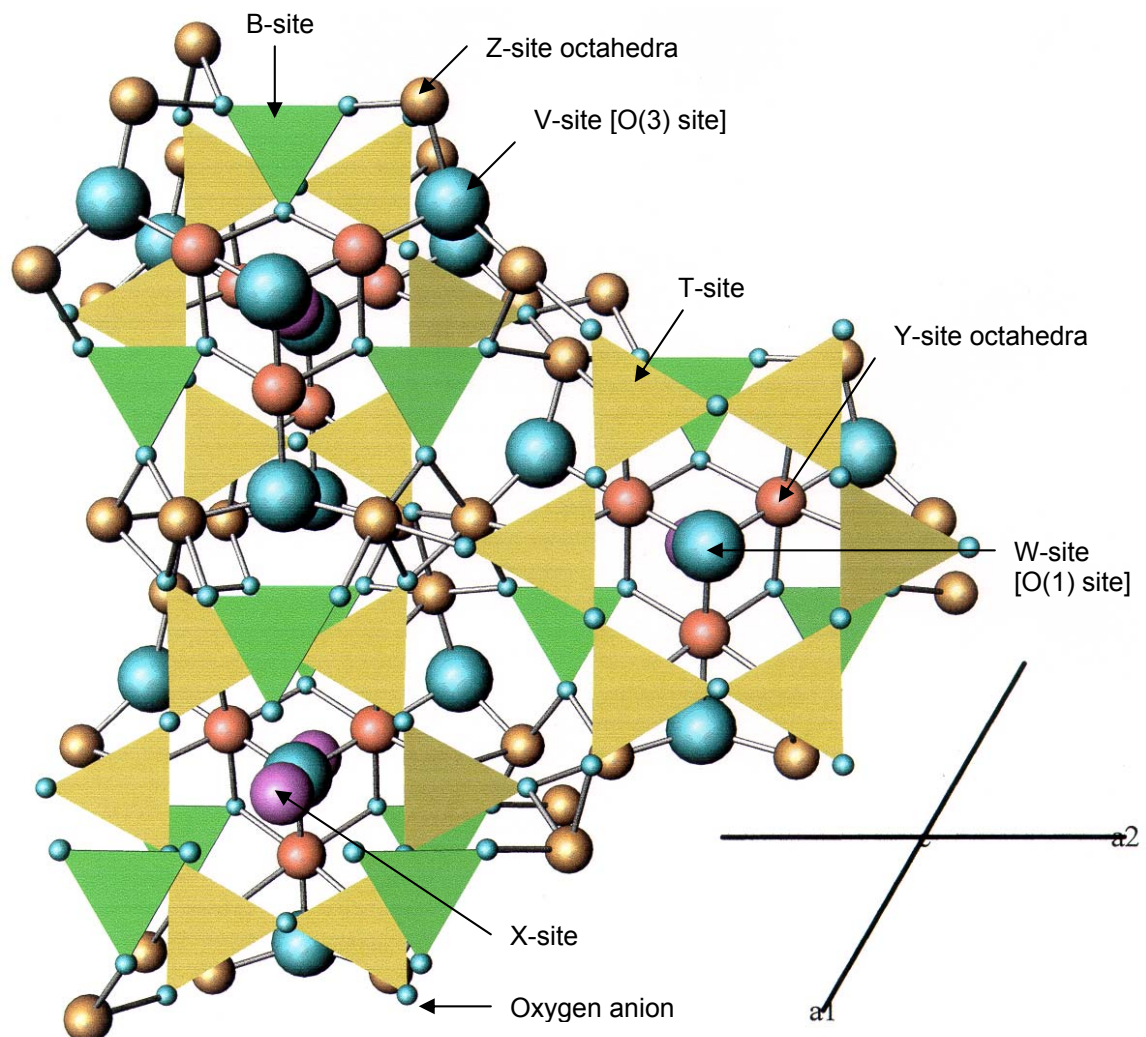


Fig. 3: Tourmaline structure viewed perpendicular to the a -axis.
(drawing produced by Atoms by Eric Dowty)

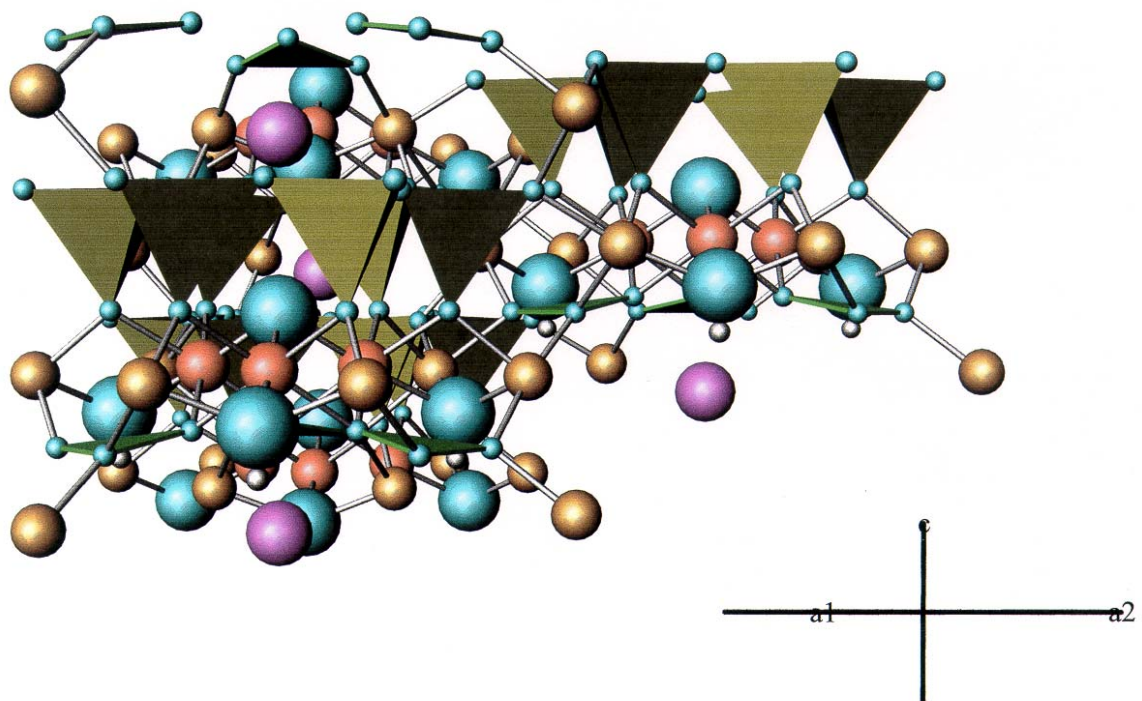


Fig. 4: Tourmaline structure viewed perpendicular to the c-axis.
(drawing produced by Atoms by Eric Dowty)

TOURMALINE FORMULAS

Valid IMA approved species

buergerite	$\text{Na}(\text{Fe}^{3+})_3\text{Al}_6(\text{BO}_3)_3\text{Si}_6\text{O}_{18}(\text{O})_3\text{F}$
chromdravite	$\text{NaMg}_3\text{Cr}_6(\text{BO}_3)_3\text{Si}_6\text{O}_{18}(\text{OH})_3(\text{OH})$
dravite	$\text{NaMg}_3\text{Al}_6(\text{BO}_3)_3\text{Si}_6\text{O}_{18}(\text{OH})_3(\text{OH})$
elbaite	$\text{Na}(\text{Li}_{1.5}\text{Al}_{1.5})\text{Al}_6(\text{BO}_3)_3\text{Si}_6\text{O}_{18}(\text{OH})_3(\text{OH})$
feruvite	$\text{Ca}(\text{Fe}^{2+})_3(\text{MgAl}_5)(\text{BO}_3)_3\text{Si}_6\text{O}_{18}(\text{OH})_3(\text{OH})$
foitite	$\square(\text{Fe}^{2+})_2(\text{Al},\text{Fe}^{3+})\text{Al}_6(\text{BO}_3)_3\text{Si}_6\text{O}_{18}(\text{OH})_3(\text{OH})$
liddicoatite	$\text{Ca}(\text{Li}_2\text{Al})\text{Al}_6(\text{BO}_3)_3\text{Si}_6\text{O}_{18}(\text{OH})_3\text{F}$
magnesiofoitite	$\square(\text{Mg}_2\text{Al})\text{Al}_6(\text{BO}_3)_3\text{Si}_6\text{O}_{18}(\text{OH})_3(\text{OH})$
olenite	$\text{NaAl}_3\text{Al}_6(\text{BO}_3)_3\text{Si}_6\text{O}_{18}(\text{O})_3(\text{OH})$
povondraite	$\text{Na}(\text{Fe}^{3+})_3(\text{Fe}^{3+})_6(\text{BO}_3)_3\text{Si}_6\text{O}_{18}(\text{O})_3(\text{OH})$
rossmanite	$\square(\text{Li},\text{Al}_2)\text{Al}_6(\text{BO}_3)_3\text{Si}_6\text{O}_{18}(\text{OH})_3(\text{OH})$
schorl	$\text{Na}(\text{Fe}^{2+})_3\text{Al}_6(\text{BO}_3)_3\text{Si}_6\text{O}_{18}(\text{OH})_3(\text{OH})$
uvite	$\text{CaMg}_3(\text{MgAl}_5)(\text{BO}_3)_3\text{Si}_6\text{O}_{18}(\text{OH})_3\text{F}$
vanadiumdravite	$\text{NaMg}_3\text{V}_6(\text{BO}_3)_3\text{Si}_6\text{O}_{18}(\text{OH})_3(\text{OH})$

Synthetic-hypothetical species

“tsilaisite”	$\text{NaMn}_3\text{Al}_6(\text{BO}_3)_3\text{Si}_6\text{O}_{18}(\text{OH})_3(\text{OH})$
--------------	---

(Formulas from Mandarino, 1999 and Anthony *et al.*, 1995)

CAUSES OF COLOR IN THE TOURMALINE GROUP

Chromophoric metallic cations, intervalence charge transfers (I.V.C.T.) and the effects of natural irradiation are responsible for the nearly limitless plethora of colors displayed by elbaite and other gem quality tourmaline species (Rossman, 1997).

Structural defects may also play a role in tourmaline coloration. Tourmaline color is directly related to its transition element content, especially Mn^{2+} , Mn^{3+} , Fe^{2+} , Fe^{3+} and Ti^{4+} (Simmons *et al.*, 2001).

Fe^{2+} is the principle coloring agent of elbaite and is a very powerful absorber of photons in the visible spectrum (Brown & Wise, 2001; Rossman, 1997). Fe^{2+} , Fe^{2+} and the $Fe^{2+} \rightarrow Ti^{4+}$ I.V.C.T. causes blue colors in gem tourmaline (Rossman, 1997). Blue-violet and violet hues are the result of high quantities of Fe with minor Ti causing the $Fe^{2+} \rightarrow Ti^{4+}$ I.V.C.T. This I.V.C.T. causes orange to orange-brown colors alone. Green hues are the result of Fe^{2+} or combinations of Fe^{2+} and the $Fe^{2+} \rightarrow Ti^{4+}$ I.V.C.T. described above (Rossman, 1997; Simmons *et al.*, 2001). Fe^{3+} can enhance this effect in addition to the pleochroic properties of gem-quality, Li-Al tourmaline (Rossman, 1997). According to Brown & Wise (2001), Fe^{2+} or Fe^{3+} are the principle causes of green hues in elbaite.

Mn is the cause of pink hues in tourmaline and the intensity of the pink color is currently thought to be directly related to the quantity of Mn in the structure (Rossman, 1991; Brown & Wise, 2001). Very high concentrations of Mn impart bright yellow hues in Li-Al tourmaline (Simmons *et al.*, 2001). Mn^{2+} is a much weaker absorber than Fe^{2+} and concentrations of 1.0-3.0 wt. % MnO is usually not enough to impart a color to Li-Al

tourmaline (Rossman, 1997). Thus, elbaite var. achroite may not contain the necessary quantities of chromophoric elements to result in coloration. Irradiation causes Mn²⁺ to oxidize to Mn³⁺ causing hues to change from colorless to various shades of pink and red (elbaite var. rubellite). Pairs of Fe³⁺ cations and their electronic interactions can also cause pink colors. The Mn²⁺→Ti⁴⁺ I.V.C.T. alone imparts the yellow to yellow-brown colors of tourmaline crystals containing substantial amounts of the “tsilaisite” molecule (Rossman, 1997). Dietrich (1985) states that the Mn²⁺→Ti⁴⁺ I.V.C.T. can also cause green hues in elbaite.

Cr³⁺ and V³⁺ cations impart an emerald green color to tourmaline specimens. Fe²⁺ can enhance this green color. According to Rossman (1997), cations other than those discussed above can sometimes impart a color to tourmaline. An example of this is Cu²⁺ which creates brilliant neon-blue hues in elbaites. Neon-blue cuprian elbaite crystals from Paraíba, Brazil contain up to 2.6 wt. % CuO at the Y-site (Rossman, 1991). Elevated Mn quantities alone can cause a yellow or golden color to elbaite crystals. Yellow, gem quality elbaite crystals from Zambia contain 6.0-7.0 wt. % MnO (Schmetzer & Bank, 1984b).

Irradiation is a significant factor in tourmaline coloration. These changes are caused by high energy photons that are capable of oxidizing or reducing cations and anions and trapping electrons at sites of radiation damage within the crystal structure (Reinitz & Rossman, 1988). The effects of irradiation can subsequently be removed by heating the sample or restored by re-exposing the crystal to further radiation.

Reinitz and Rossman (1988) performed a study of simulating the natural irradiation that elbaite crystals receive over geologic time to determine how this affects

color. Nearly colorless elbaite (var. achroite) from the San Diego mine, U.S.A. has an absorption spectra which displays features indicative of Mn²⁺. Upon exposure to radiation, the absorption spectrum loses its Mn²⁺ characteristics exponentially with increasing doses. Irradiation of Mn bearing elbaites cause Mn²⁺→Mn³⁺ oxidation and pink hues (Reinitz & Rossman, 1988). Heat repairs structural radiation damage and allows the crystals to become colorless. The authors found that both naturally irradiated and synthetically irradiated elbaite samples display identical spectroscopic features. Therefore, they conclude that the color of naturally pink elbaites is the result of radiation.

MATERIALS & METHODS

The acquired suite of faceted Nigerian tourmaline stones from the Bill Larson, Bill Barker and Phillip Zahm collections were placed table down in groups of 2-3 on glass slides for quantitative analysis. Clear fingernail polish was then applied to a 1 inch glass disc until it was sufficiently thick so that the apices of the crown made physical contact with the polish for a preliminary mount. Standard Bondo brand epoxy with hardener was then applied to the interstices of the gemstones, securing the mount. Each sample mount was made electrically conductive with 250Å of C using a carbon coater, applied under a vacuum of 1×10^{-5} Torr.

Non-faceted gem quality tourmaline fragments from Namibia, Congo, Mozambique and Mali were fashioned to a reasonable size with cutting pliers and were mounted both parallel and perpendicular to the c-crystallographic axis on 1 inch glass discs with epoxy. Tourmaline slices perpendicular to the c-axis from Namibia, Tanzania and Mozambique were simply glued to glass slides. All samples were then given sufficient time to set. For the Namibian and Mali fragments, an additional coating of epoxy plus hardener was applied to the disc mount until the crystals were submerged. After curing, the tourmaline fragments were initially ground flat with a diamond grinding wheel and polished using 1µm, 0.3µm and 0.05µm corundum polishing wheels. Samples were made electrically conductive with a carbon coater as described above.

The sample groups from the various countries include the following suites. The Nigerian samples are faceted stones labeled "a" through "x1" and "Lila-1-1" to "Lila-9-

8". Namibian tourmaline samples include rough and slices labeled ".3-1-1" to ".3-20-3" for the rough and "Nam-sl-a1" to "Nam-sl-d5". Tourmaline from Sanga Sanga, Tanzania are slices designated "Sanga-w1" to "Sanga-w7", "SS wm-1" to "SS wm-5" and "SS blue-2" to "SS blue-4". Congolese tourmaline specimens are also slices labeled "Congo k2" to "Congo k7", "Congo l1" to "Congo l7" and "Congo i2" to "Congo i5". The sample from Mozambique is a slice designated "Moz 1" to "Moz-10". Lastly is the specimen from Gao, Mali which is a fragment labeled ".3-13-1" to ".3-13-3".

Faceted, non-faceted samples and tourmaline slices were quantitatively analyzed for Si, Ti, Al, Bi, V, Cr, Fe, Mn, Mg, Ba, Cu, Pb, Ca, Zn, Na, K, F and Cl using an ARL-SEMQ electron microprobe operating in wavelength dispersive mode (WDS). Elements analyzed for but not detected for suites of the various countries were Bi, Cr, V, Ba, Cu, Pb, Zn, Mg, K and Cl. Three to ten spots per traverse were analyzed dependant upon the size of the specimen and the complexity of chemical zonation. Operating conditions were 15kV acceleration potential, 15nA beam current and a 2 μ m beam diameter. A variety of natural and synthetic compounds were employed as standards. These were calibrated using the operating conditions described above. Standards used were sillimanite (Al $K\alpha$), albite (Na $K\alpha$), adularia (K $K\alpha$ and Si $K\alpha$), fayalite (Fe $K\alpha$), titanite (Ti $K\alpha$), clinopyroxene (Mg $K\alpha$, Ca $K\alpha$, Si $K\alpha$ and Fe $K\alpha$), bismuth germanate (Bi $K\alpha$), vanadium (V) oxide (V $K\alpha$), rhodonite (Mn $K\alpha$) and fluortopaz (F $K\alpha$, Al $K\alpha$). Count times of 60 seconds were used for both the standards and samples. The M.A.N. (mean atomic number) standards that were used when applicable included the standards listed above plus hematite, periclase, fluorapatite and fluorite. Table 1 lists the detection limits of the elements described above.

The Fe content of the sample determined whether fayalite or clinopyroxene Fe $K\alpha$'s were used. The average Z of the material determined whether the adularia or the clinopyroxene Si $K\alpha$ was used.

Raw microprobe data was ZAF corrected and oxide weight percentages were calculated. Tourmaline formulae were processed using Microsoft Excel spreadsheets designed by the author over a period of one year. Non-detectable, low-Z constituents B, Li and OH were calculated via the stoichiometry as B_2O_3 , Li_2O and H_2O respectively to self consistency with B=3.000 apfu (atom per formula unit), Li=3- ΣY and OH=4-F. The weight percentages of B_2O_3 , Li_2O and H_2O were back-calculated using the “solver” macro in Microsoft Excel. These calculations were iterated to self consistency. Tourmaline formulas were first calculated to 24.5 oxygen anions. These 24.5 oxygen anions represent the oxygen atoms within the tourmaline structure that are bonded to heavier cations which are detectable with a microprobe. This spreadsheet was later modified to calculate the tourmaline formulas (in apfu) based upon 31 anions (O, OH, F and Cl) to yield the most accurate stoichiometry possible. O^{2-} content could not be determined with the methods or analytical instruments used.

Qualitative analyses were performed using an AMRAY 1820 scanning electron microscope operating in energy dispersive mode (EDS). Operating conditions were 15kV acceleration potential, 18mm working distance, 35° sample tilt and a 400 μ final aperture. Elements analyzed included Si, Ti, Al, Bi, V, Fe, Mn, Mg, Ca, Na, K and F. These elements were each analyzed using the $K\alpha$ X-ray line with the exception of Fe where the $K\beta$ was used to avoid interference with the Mn $K\beta$ line. X-ray maps were collected at 256x256 pixels with a dwell time of 200 milliseconds per pixel. X-ray line

scans were carried out using the multiple scan option with 16 steps at 2 seconds per step and 20-40 repeat scans.

Precision cell edge determinations of selected samples of rough were performed using a Scintag XDS-2000 X-ray diffractometer. A sufficient amount of a gem-quality tourmaline sample was separated using cutting pliers and pulverized using a steel impact mortar and pestle. This rough powder was then further crushed to a very fine powder with an agate mortar and pestle. Acetone was used to prevent loss of grains. This powder was allowed to dry and was run through a 200 mesh sieve to insure size uniformity. Smear mounts were prepared on 1 inch glass discs. Operating conditions were 35 kV, 15mA with a scan range of 10-80° 2θ, a step size of 0.01° and a dwell time of 4 seconds per step. Cu K_{α1} X-rays with a wavelength of 1.54060 Å were used. Pure milled quartz was used as an external X-ray standard. Unit cell dimensions were refined using the program “CELL” (designed by Wm. B. Simmons), a modified version of the least-squares indexing program originally designed by Appleman & Evans (1973) to process the observed d-spacing for the respective h k l and X-ray intensity. This calculation was iterated up to nine times.

Table 1: Detection limits of elements for the ARL-SEMQ electron microprobe.
(wt. % values have an accuracy of 99% confidence for a single line)

Al	--
Mg	0.16
Si	--
Ca	--
Ti	0.011
Fe	0.016
K	0.007
Mn	0.022
F	--
Cr	0.023
Na	0.064
Bi	0.022
V	0.017
Pb	0.012
Zn	0.097

GENERAL RESULTS

African Tourmaline

The Mg- Y-site Al- Fe ternary shown in Fig. 5 shows that the overwhelming majority of tourmaline from Nigeria, Namibia, Mali, Tanzania, Congo and Mozambique is Al [Li]-rich at the Y-site with the data falling towards the liddicoatite, rossmanite and elbaite end-members. Only a few stones or parts of stones from the Namibian suite and one analysis from the Congolese set plot towards the schorl end-member along the Y-site Al- Fe join. The Congolese samples display a slightly Mg-rich signature.

The more specific Ca- Y-site Al- Na ternary displayed in Fig. 6 shows that the examined tourmaline from Africa belongs to the liddicoatite-rossmanite-elbaite solid solution series. The Nigerian faceted stones and the slices from Sanga Sanga, Tanzania contain the most liddicoatite component of any of the localities surveyed. The rossmanite component is most prevalent in the Nigerian, Namibian and Tanzanian suites whereas only a few analyses from the Congolese and Namibian sets plot towards the schorl end-member of the Y-site Al- Na join.

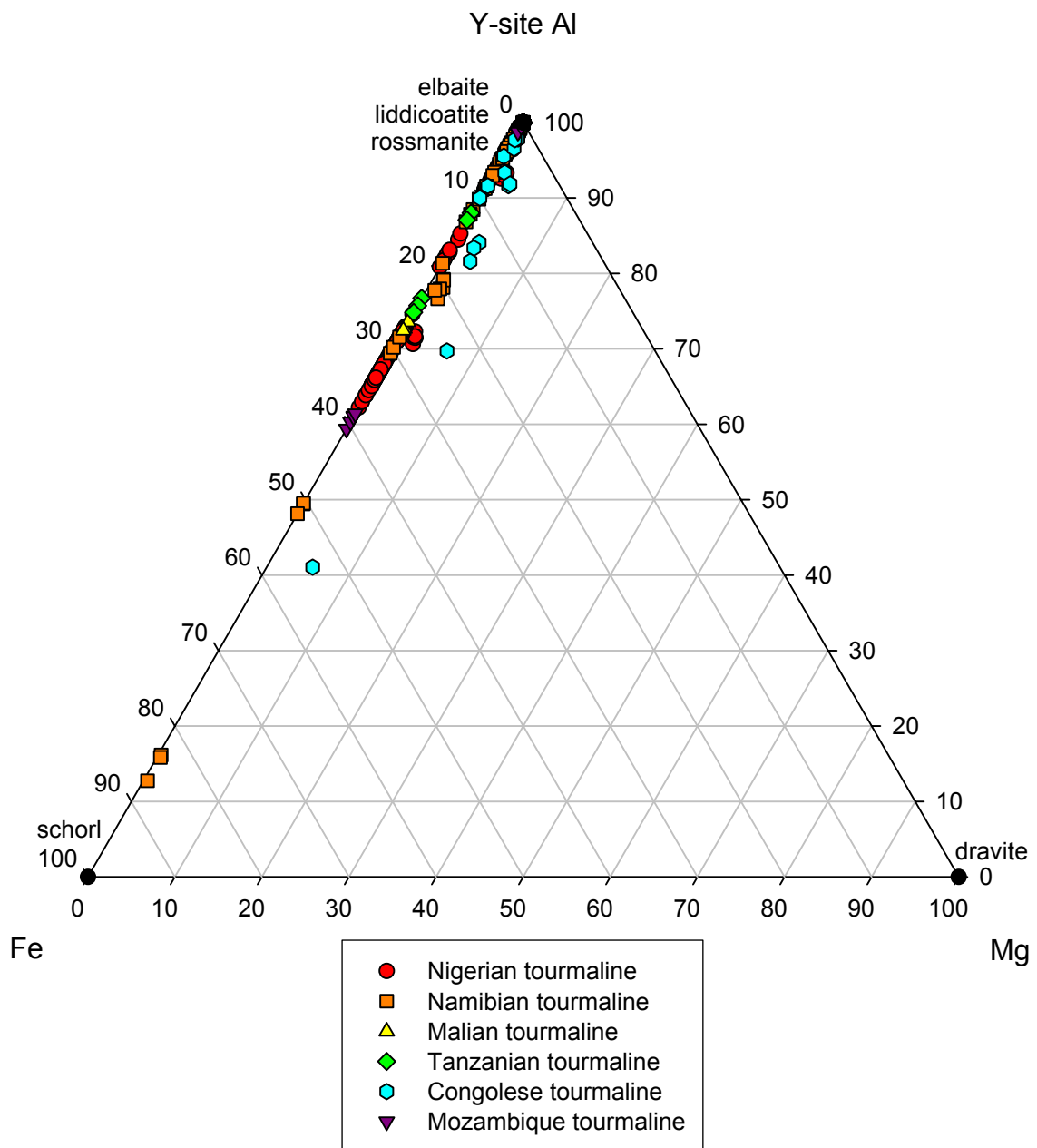


Fig. 5: Mg- Y-site Al- Fe ternary, African tourmaline.

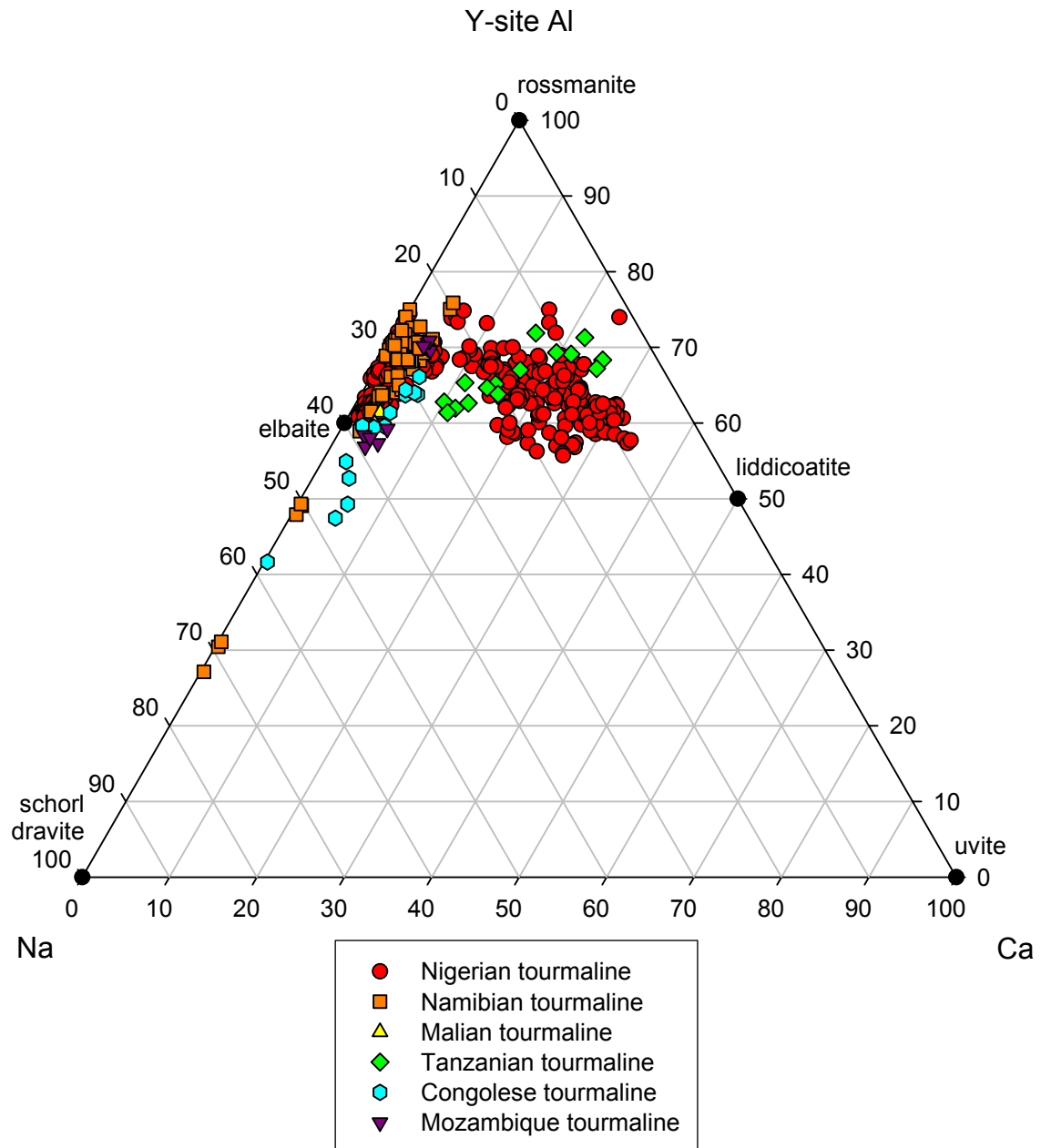


Fig. 6: Ca- Y-site Al- Na ternary, African tourmaline.

RESULTS

Nigerian Tourmaline

The Nigerian stones, shown in Fig. 7, range in color from colorless to near colorless, various hues of pink, reddish-purple, pinkish-red, red, greenish-yellow, yellowish-green, green, bluish-green and blue. There are eight bi-colored faceted stones in this suite. These include samples “h” (near colorless pink to near colorless green), “t” (near colorless green to pink), “u” (pale green to pink), “v” (red to near colorless red), “d1” (grayish-green to pink), “s1” (pink to pale bluish-gray), “t1” (yellowish green to pink) and “u1” (pale yellowish green to pink). The weight of the stones ranges from 2.014 to 10.57 carats. Examples of Nigerian tourmaline crystals from Nigeria are shown in Figs. 8 and 9.

Microprobe analyses of the suite of Nigerian cut stones can be found in Tables 2 and 3. The Nigerian suites of faceted tourmaline gemstones from the individual collections of Bill Larson, Bill Barker and Phillip Zahm belong to the liddicoatite-elbaite-rossmanite solid solution series based on X-site occupancy using the Ca-Xvac-Na ternary diagram (Fig. 10). The Zahm blue stones are elbaites. These stones plot predominantly in the liddicoatite and elbaite fields with four stones that are at least in part rossmanite within the Larson collection. One of the top facets of stone “g” is entirely composed of rossmanite with X-site vacancies more abundant than either Ca or Na at each analyzed spot. Stone “h” is bi-colored near colorless pink to near colorless green. Spots 1-2 are near colorless pink liddicoatite and the three remaining spots (3-5) are near colorless

green rossmanite. Spot 4 of pinkish-red stone “11” is rossmanite and the remaining spots are elbaite. Lastly, slightly pinkish-red stone “o” is composed of both elbaite and rossmanite with spots 1-3 being elbaite and spots 4-5 comprising rossmanite.

Other samples that are composed of zones of two species within the same stone from the Larson suite are stones “l”, “r1” and “s1”. Sample “l”, which is entirely pink is composed of elbaite and liddicoatite portions. Spots 1-4 are elbaite and spot 5 is liddicoatite. Stone “s1”, spot 1 is a pink elbaite after which the chemistry changes to liddicoatite on spots maintaining a pink hue 2-3. Spots 4-5 remain liddicoatite but the color changes to a pale bluish-gray. Finally sample “r1” is green throughout. The first spot is liddicoatite and the remaining spots are elbaite.

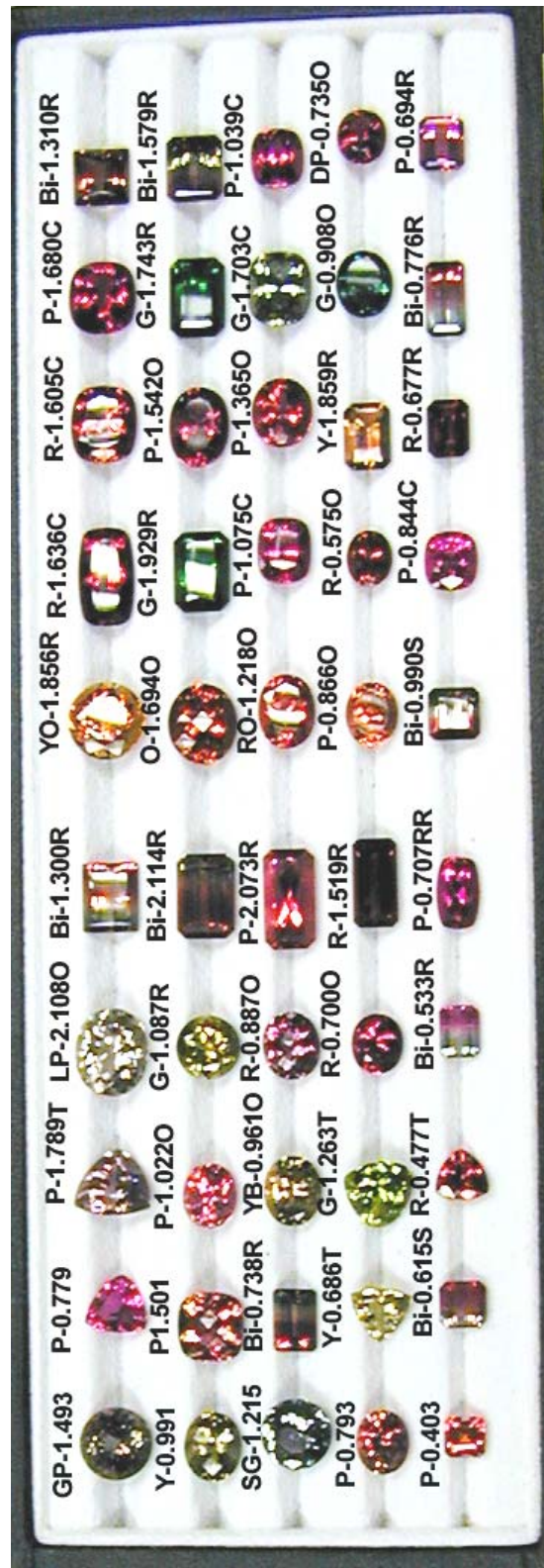


Fig. 7: Faceted Nigerian tourmaline of the Bill Larson & Bill Barker collections.



Fig. 8: Tourmaline crystal from Nigeria.



Fig. 9: Tourmaline crystal from Nigeria.

The T, B & Z-sites: SiO_2 ranges from 36.79 to 38.69 wt. %. This corresponds to 5.828 to 6.094 apfu Si at the T-site. The Si excess problem ($\text{Si} > 6.0$) will be discussed later in this paper. If there is less than 6.0 apfu Si in the formula, excess Y-site Al is partitioned into the T-site. B was assumed to fully occupy the B-site with 3.0 apfu. Calculated B_2O_3 varies from 10.72 to 11.26 wt. % with the lower quantities in the blue elbaites. There is sufficient Al to completely fill the octahedral Z-sites of all the Nigerian samples. Al totals are between 38.24 to 40.76 wt. % Al_2O_3 .

Y-site Al: Overall, octahedral Al varies from 1.176 to 1.572 apfu. These quantities are generally lower for the Zahm blue elbaites with 1.176 to 1.34 apfu Al. These quantities are generally highest for the pink stones, especially the rossmanites and are lowest for the green liddicoatites. Sample “g”, a pink rossmanite has the most Y-site Al with 1.529 to 1.572 apfu and stone “t1” (yellowish-green liddicoatite) has the least Al at this site with 1.201 to 1.24 apfu in the Larson/Barker collection. There is abundant compositional overlap displayed by the colorless to near colorless, pink, red, reddish-purple, yellowish-green, green and bluish-gray elbaites, liddicoatites and rossmanites. Liddicoatites and rossmanites span the entire range of Y-site Al quantities, with the rossmanites generally containing more Al apfu than the elbaites or liddicoatites.

Titanium: Ti quantities were generally very low to non-detectable except in a few liddicoatite and elbaite samples from the Larson/Barker set. The highest Ti quantities were observed in the liddicoatites. Overall, Ti ranges between 0 to 0.38 wt. % and 0 to 0.044 apfu. The most Ti observed was 0.38 wt. % and 0.044 apfu on spot 5 of sample “u1”, a pink liddicoatite. Pink (0 to 0.38 wt % & 0 to 0.044 apfu) and red samples (0 to 0.11 wt. % & 0 to 0.013 apfu) have the highest Ti. The colorless to near colorless stones

do not contain Ti except for spot 5 of stone v, a near colorless red spot with 0.01 wt. % and 0.001 apfu. Pale greenish-yellow sample “i” does not contain detectable Ti. Reddish-purple stone “k1” has up to 0.02 wt. % and 0.002 apfu Ti. Green samples range from 0 to 0.07 wt. % and 0 to 0.009 apfu. The Zahm blue elbaites and bluish-gray liddicoatites are devoid of Ti.

Bismuth: Bi varies from trace amounts below detection limits up to 0.09 wt. % Bi_2O_3 and 0 to 0.004 apfu Bi for stones of the Larson suite. The pink stones of this suite have the highest Bi varying between the ranges above. The most Bi was found in spot 2 of sample “j”, a near colorless to satin pink elbaite. Bi is usually present in only trace amounts in the blue elbaites but was observed randomly in detectable quantities. For the Zahm blue elbaites, Bi varies from 0 to 0.11 wt. % and 0 to 0.005 apfu. The most Bi was found in spot 7 of sample “Lila-9”.

Vanadium: V is almost completely absent or below detection limits for the Larson/Barker Nigerian suite of stones. The highest V concentration is 0.03 wt. % V_2O_3 and 0.004 apfu V for stone “n”, a yellowish-green elbaite. This value is insignificant due to large statistical errors at such low quantities. The blue elbaites of the Phillip Zahm collection are V-free with 0 to 0.08 wt. % and 0 to 0.01 apfu V. Spot 6 of “Lila-1” contains the most V.

Iron: For the pink stones of the Larson/Barker collections, Fe concentrations vary from 0 to 0.33 wt. % FeO and 0 to 0.043 apfu Fe. The colorless to near colorless pink stones contain from 0 to 0.25 wt. % and 0 to 0.032 apfu Fe. Fe is found in low quantities among the pink liddicoatites and elbaites but not in sample “g”, a rossmanite. The greatest Fe contents in the pink portion of sample “t1” a bi-colored yellowish-green

liddicoatite with 0.043 apfu Fe. The red elbaites and liddicoatites contain 0 to 0.11 wt. % and 0 to 0.014 apfu Fe. Reddish-purple sample “k1” has 0 to 0.05 wt. % and 0.001 to 0.006 apfu Fe. The rossmanite portion of sample “o” (spots 4-5) and sample “w1” (the only red liddicoatite) have detectable Fe. Generally there is a paucity of Fe among the colorless, pink and red samples.

Sample “i”, a greenish-yellow elbaite contains 0.16 to 0.26 wt. % and 0.021 to 0.035 apfu Fe. Fe is quite abundant in the various shades of green stones and ranges between 0 to 3.76 wt. % and 0 to 0.499 apfu. Generally, as the green stones become more intense in color, Fe content increases. The lowest Fe quantities are in sample “d1” (the light green liddicoatite domain) on spots 2 and 3 with only trace Fe. The very light green rossmanite zone of sample “h” (spots 3-5) has 0.38 to 0.56 wt. % and 0.050 to 0.073 apfu Fe. The largest amounts of Fe (3.60 to 3.76 wt. % and 0.476 to 0.499 apfu) are found in the green elbaites, especially sample “p1”. The bluish-gray gems are liddicoatites and include samples “c” and “s1” (spots 3-4). Fe varies from 0.14 to 0.59 wt. % and 0.018 to 0.076 apfu. The Zahm blue elbaites have the largest Fe concentrations with Fe ranging from 1.99-5.35 wt % and 0.266-0.714 apfu.

Manganese: For the colorless to near colorless pink stones of the Larsen/Barker set, Mn varies from 0.21 to 1.53 wt. % MnO and 0.028 to 0.206 apfu Mn. Mn quantities range from below detection limits to 1.84 wt. % MnO and 0 to 0.246 apfu for the pink stones. Overall, Mn quantities are generally lowest in the liddicoatites and rossmanites and greatest in the elbaites. Sample “y”, a pink elbaite has 1.72 to 1.84 wt. % and 0.232 to 0.246 apfu Mn. Sample “g” the pink rossmanite contains only trace Mn except for spot 4 which has 0.04 wt. % and 0.005 apfu. The red stones generally contain the same

range of Mn as the colorless to near colorless and pink stones except for sample “e1” which is the most Mn-rich with 0 to 4.65 wt. % and 0 to 0.630 apfu. The red rossmanites (spot 4 of sample “l1” and spots 4-5 of sample “o”) contain between 0.13 to 0.64 wt. % and 0.018 to 0.085 apfu. An abundance of Mn is observed in elbaite sample “e1” with 4.58 to 4.65 wt. % and 0.618 to 0.63 apfu.

Greenish-yellow stone “i” contains Mn ranging from 1.15 to 1.44 wt. % MnO and 0.028 to 0.194 apfu Mn. Green stones have compositions ranging from 0.10 to 1.86 wt. % MnO and 0.013 to 0.249 apfu Mn. Of the green stones, Mn is generally lowest in the green liddicoatites and rossmanites. The liddicoatite spot of sample “r1” (the rest is elbaite) has 0.28 wt % and 0.036 apfu Mn. The rossmanite zone of sample “h” contains 0.20 to 0.32 wt. % and 0.027 to 0.043 apfu Mn. The elbaites in general have the highest Mn quantities of the green stones with sample “f1” containing 1.78 to 1.86 wt. % and 0.238 to 0.249 apfu. Bluish-gray liddicoatites contain 0.32 to 0.42 wt. % and 0.043 to 0.055 apfu. Lastly, the Zahm blue elbaites contain 0.46 to 1.53 wt. % and 0.063 to 0.207 apfu Mn.

Magnesium: Mg is all but absent in the tourmalines from the Larson/Barker collection. Mg values range from 0 to 0.16 wt. % MgO and 0 to 0.037 apfu Mg in the green liddicoatites and elbaites. Mg is more abundant in the elbaitic stones. Sample “b”, a brownish-green liddicoatite, contains 0 to 0.03 wt. % and 0 to 0.007 apfu whereas pale pink sample “m” contains between 0 to 0.03 wt % and 0 to 0.008 apfu. The most Mg-rich tourmaline is sample “p1”, a slightly yellow-green elbaite which contains 0.11 to 0.16 wt. % and 0.026 to 0.037 apfu Mg. The Zahm blue elbaites contain trace Mg.

Calcium: Ca is most prevalent in the X-sites of the liddicoatites (2.13 to 4.38 wt. % CaO and 0.361 to 0.728 apfu Ca), especially the pink liddicoatites from the Larson/Barker suite. Conversely, the elbaites are the least Ca-rich with Ca ranging from 0.01 to 2.57 wt. % and 0.002 to 0.431 apfu, albeit some of the samples ("u", "l", "r" & "q") contain significant quantities of the liddicoatite molecule. Sample "g", a pink rossmanite has 0.66 to 0.78 wt. % and 0.111 to 0.131 apfu Ca. Other rossmanite zones such as spots 4-5 of stone "o" have between 1.62 to 1.78 wt. % and 0.275 to 0.299 apfu Ca. Spot 4 on gem "l1" contains 1.20 wt. % and 0.202 apfu Ca. Nigerian rossmanites can be Ca-rich. The very pale green rossmanitic zone of sample "h" varies between 1.93 to 2.24 wt. % and 0.325 to 0.374 apfu Ca. This domain is a vacancy dominant rossmanite with Ca predominating over Na at the X-site. The Zahm blue elbaites contain 0.12 to 0.52 wt. % and 0.021 to 0.088 apfu Ca.

Zinc: This element was not detected in any of the faceted stones from the Larson/Barker collections. In the Zahm blue elbaites, Zn is present in detectable amounts in random spots of samples "Lila-2, 3, 5 & 7". Zn fluctuates from 0 to 0.17 wt. % and 0 to 0.02 apfu Zn.

Calculated Lithium: Calculated Li quantities are higher in liddicoatites than in elbaites from the Larson/Barker set. Li varies from 1.69 to 2.54 wt. % Li₂O and 1.085 to 1.613 apfu Li in the elbaites. Some elbaite samples such as "j1", a pinkish-red stone are exceedingly rich in Li (2.36 to 2.54 wt. % and 1.487 to 1.613 apfu). The most Li-poor elbaites are generally the green stones such as sample "p1" which have Li quantities between 1.78 to 1.85 wt. % and 1.132 to 1.178 apfu. For the liddicoatites, Li ranges from 2.35 to 2.82 wt. % and 1.49 to 1.746 apfu. The most Li-rich liddicoatites are the pink

stones, especially sample “s” which has Li ranging from 2.75 to 2.82 wt. % and 1.717 to 1.746 apfu. The most Li-poor liddicoatite is the pink zone of stone “h”, containing 2.35 to 2.40 wt. % and 1.490 to 1.503 apfu. The rossmanite samples have Li quantities intermediate to the elbaites and liddicoatites (2.20 to 2.31 wt. % and 1.393 to 1.465 apfu). The Zahm blue elbaites contain 1.36 to 1.95 wt. % and 0.879 to 1.252 apfu Li.

Sodium: Among the Larson/Barker samples, Na is generally most prevalent in elbaites as opposed to the liddicoatites. The elbaites vary in Na content from 1.12 to 2.59 wt. % Na_2O and 0.338 to 0.788 apfu Na. The most Na-rich elbaite composition is 2.41 to 2.59 wt. % and 0.733 to 0.788 apfu for stone “f1”, a slightly yellowish-green elbaite. The most Na-poor elbaite composition ranges from 1.12 to 1.31 wt. % and 0.338 to 0.399 apfu for pink stone “l”. The liddicoatites vary from 0.52 to 1.49 wt. % and 0.159 to 0.451 apfu Na. The most Na-dominant liddicoatite composition is spot 2 on the pink zone of stone “s1” with 1.49 wt. % and 0.451 apfu. The most Na-depleted liddicoatite is pale pink stone “k” containing 0.52 to 0.64 wt. % and 0.159 to 0.195 apfu. The rossmanites generally have more Na than the liddicoatites but less than the elbaites and range from 0.61 to 1.43 wt. % and 0.186 to 0.435 apfu. The Zahm blue elbaites contain Na ranging from 1.71 to 2.62 wt. % and 0.532 to 0.811 apfu.

Potassium: The Larson/Barker tourmalines contain little to no K. Overall, K quantities range from 0 to 0.30 wt. % K_2O and 0 to 0.06 apfu K. The most K-rich tourmaline is sample “w1”, a pink-red liddicoatite with 0.13-0.30 wt. % and 0.027 to 0.06 apfu. The red and pink liddicoatites contain the most K of this suite. The rossmanites have no detectable K save for spot 4 on pinkish-red stone “l1” with 0.050 wt. % and 0.01 apfu. The Zahm blue elbaites have between 0 to 0.06 wt. % and 0 to 0.012 apfu K.

X-site totals: Occupancy at the X-site of tourmalines in the Larson/Barker suite varies from 0.511 to 0.998 apfu. The rossmanites have the lowest X-site totals with 0.511 to 0.63 apfu. The lowest X-site totals for a rossmanite are 0.511 to 0.577 apfu for the very pale green zone of stone “h”. The highest rossmanite totals are observed in spots 4-5 of slightly pinkish-red stone “o” and range between 0.568 to 0.630 apfu. Elbaites are intermediate with respect to X-site occupancy. The most occupied elbaite at the X-site is green stone “q” with 0.862 to 0.91 apfu. The least filled elbaite is pink sample “f” with 0.527 to 0.587 apfu. Liddicoatites are the most filled at the X-site. The most occupied liddicoatite is pink gem “x1” and contains 0.98 to 0.998 apfu. The least filled liddicoatite is bluish-gray sample “c” with X-site totals ranging from 0.651 to 0.693 apfu. Blue elbaites of the Zahm collection vary from 0.595 to 0.863 apfu X-site totals.

Hydroxyl anion and calculated water: Calculated H₂O ranges from 2.83 to 3.63 wt. % in the Larson/Barker collection. Quantities of OH vary from 2.944 to 3.827 apfu over the V and W-sites. There is a population of hydroxyl-liddicoatites where OH is greater than F at the W-site. Sample “x1” is a pink hydroxyl-liddicoatite with 3.508 to 3.567 apfu OH. Many of the elbaites in the Larson collection contain less than 3.5 apfu OH and therefore are occupied by other anions. In the Zahm suite, H₂O is in the range of 3.16 to 3.45 wt. %, whereas OH is from 3.405 to 3.676 apfu.

Fluorine: F contents are quite variable throughout samples from the Larson/Barker collection. F ranges from 0.35-1.77 wt % F and 0.174-0.877 apfu F. Overall, the highest F quantities are observed in liddicoatites but approximately half of the elbaite analyses are occupied predominantly by F at the W-site. These samples are classified as fluor-elbaites (Hawthorne & Henry, 1999). The most F-rich elbaite, sample

“q”, a yellowish-green fluor-elbaite contains 1.25 to 1.67 wt. % and 0.623 to 0.827 apfu F. The most F-depleted elbaite is bright pink stone “i1” with 0.35 to 0.76 wt. % and 0.174 to 0.38 apfu F. Stone “r”, a pink liddicoatite is the most F-rich tourmaline with 1.14 to 1.77 wt. % and 0.566 to 0.877 apfu. The pink domain of sample “t1” is the most F-poor liddicoatite and has 0.69 to 0.93 wt % and 0.339 to 0.459 apfu.

Rossmannites tend to be F-dominant as opposed to OH-rich at the W-site. Such compositions are classified as fluor-rossmanites (Hawthorne & Henry, 1999). Pink stone “g” a pink fluor-rossmanite contains the most F-poor spot of the Nigerian suite with 0.92 wt. % and 0.461 apfu and the gem has an overall composition of 0.92 to 1.17 wt. % and 0.461 to 0.585 apfu. The most F-rich fluor-rossmanite is spots 4-5 of sample “o” with 1.28 to 1.30 wt % and 0.635 to 0.642 apfu. The Zahm blue elbaites are generally F-poor but do contain fluor-elbaite in random spots. F fluctuates from 0.64 to 1.17 wt. % and 0.324 to 0.595 apfu F at the W-site.

Table 2: Microprobe analyses, Nigerian tourmaline.

Oxides		2d3	2d4	2d5	2-e1	2-e2	2-e3	2-e4	2-e5
sample		2d3	2d4	2d5	2-e1	2-e2	2-e3	2-e4	2-e5
color		pink	pink	pink	sl or pink	sl or pink	sl or pink	sl or pink	sl or pink
SiO ₂		38.22	38.12	38.20	38.27	38.21	38.03	38.29	38.08
TiO ₂		0.00	0.00	0.01	0.00	0.00	0.00	0.00	0.00
B ₂ O ₃ calc.		11.12	11.07	11.11	11.00	11.00	10.98	11.02	11.00
Al ₂ O ₃		40.38	40.17	40.12	39.83	39.83	39.90	39.80	40.08
Bi ₂ O ₃		0.02	0.01	0.02	0.00	0.00	0.01	0.00	0.01
V ₂ O ₃		0.00	0.00	0.00	0.00	0.00	0.00	0.00	0.00
FeO		0.00	0.01	0.00	0.13	0.17	0.13	0.16	0.15
MnO		0.07	0.06	0.11	0.83	0.81	0.82	0.86	0.86
MgO		0.00	0.00	0.00	0.00	0.00	0.00	0.00	0.00
CaO		2.96	2.93	3.11	1.24	1.34	1.35	1.33	1.30
Li ₂ O calc.		2.52	2.49	2.57	2.29	2.29	2.24	2.31	2.21
Na ₂ O		0.65	0.60	0.75	1.47	1.41	1.45	1.47	1.42
K ₂ O		0.06	0.00	0.04	0.00	0.03	0.00	0.00	0.00
H ₂ O calc.		3.31	3.30	3.30	3.29	3.28	3.26	3.30	3.30
F		1.12	1.09	1.13	1.07	1.10	1.11	1.07	1.04
Sub-total		100.42	99.83	100.47	99.43	99.47	99.29	99.59	99.44
O=F		-0.47	-0.46	-0.48	-0.45	-0.46	-0.47	-0.45	-0.44
Total		99.94	99.38	99.99	98.98	99.00	98.82	99.14	99.00
Ions (apfu)									
T: Si		5.972	5.985	5.973	6.043	6.036	6.021	6.041	6.016
Al		0.028	0.015	0.027	0.000	0.000	0.000	0.000	0.000
B: B		3.000	3.000	3.000	3.000	3.000	3.000	3.000	3.000
Z: Al		6.000	6.000	6.000	6.000	6.000	6.000	6.000	6.000
Y: Al		1.409	1.419	1.366	1.415	1.416	1.444	1.400	1.463
Ti		0.000	0.000	0.001	0.000	0.000	0.000	0.000	0.000
Bi		0.001	0.000	0.001	0.000	0.000	0.000	0.000	0.001
V		0.000	0.000	0.000	0.000	0.000	0.000	0.000	0.000
Fe ²⁺		0.000	0.001	0.000	0.017	0.022	0.018	0.021	0.019
Mn ²⁺		0.009	0.007	0.014	0.111	0.109	0.110	0.115	0.115
Mg		0.000	0.000	0.000	0.000	0.000	0.000	0.000	0.000
Li		1.581	1.572	1.617	1.457	1.453	1.428	1.464	1.403
X: Ca		0.495	0.493	0.521	0.210	0.227	0.228	0.224	0.220
Na		0.197	0.183	0.226	0.449	0.432	0.444	0.450	0.435
K		0.011	0.000	0.007	0.000	0.006	0.000	0.000	0.000
□ (vac.)		0.296	0.324	0.246	0.341	0.335	0.328	0.326	0.345
OH		3.445	3.459	3.440	3.468	3.453	3.442	3.469	3.478
F		0.555	0.541	0.560	0.532	0.547	0.558	0.531	0.522
species		Iiddicoatite	Iiddicoatite	Iiddicoatite	F-elbaite	F-elbaite	F-elbaite	F-elbaite	F-elbaite

Oxides		2f1	2f2	2f4	2f5	3g1	3g2	3g3	3g4
sample		bright pink	bright pink	bright pink	bright pink	pink	pink	pink	pink
SiO ₂		38.11	38.28	37.95	38.10	38.53	38.48	38.53	38.40
TiO ₂		0.00	0.00	0.00	0.00	0.00	0.00	0.00	0.00
B ₂ O ₃ calc.		10.91	10.92	10.91	10.94	11.04	11.04	11.04	11.01
Al ₂ O ₃		39.96	39.92	40.31	40.45	40.65	40.76	40.64	40.47
Bi ₂ O ₃		0.04	0.00	0.02	0.02	0.01	0.02	0.02	0.01
V ₂ O ₃		0.00	0.00	0.00	0.00	0.00	0.00	0.00	0.00
FeO		0.00	0.00	0.00	0.00	0.00	0.00	0.01	0.00
MnO		0.87	0.81	0.91	0.86	0.00	0.00	0.00	0.04
MgO		0.00	0.00	0.00	0.00	0.00	0.00	0.00	0.00
CaO		0.01	0.03	0.02	0.03	0.66	0.66	0.71	0.78
Li ₂ O calc.		2.15	2.19	2.05	2.06	2.30	2.27	2.30	2.31
Na ₂ O		1.88	1.69	1.84	1.74	1.43	1.35	1.37	1.39
K ₂ O		0.02	0.00	0.00	0.00	0.00	0.00	0.00	0.00
H ₂ O calc.		3.20	3.35	3.36	3.41	3.30	3.31	3.27	3.24
F		1.18	0.88	0.85	0.77	1.08	1.05	1.13	1.17
Sub-total		98.34	98.06	98.22	98.37	99.00	98.93	99.02	98.81
O=F		-0.50	-0.37	-0.36	-0.33	-0.45	-0.44	-0.48	-0.49
Total		97.85	97.68	97.86	98.04	98.55	98.48	98.55	98.32
Ions (apfu)									
T: Si		6.072	6.094	6.042	6.050	6.065	6.059	6.065	6.062
Al		0.000	0.000	0.000	0.000	0.000	0.000	0.000	0.000
B: B		3.000	3.000	3.000	3.000	3.000	3.000	3.000	3.000
Z: Al		6.000	6.000	6.000	6.000	6.000	6.000	6.000	6.000
Y: Al		1.502	1.491	1.565	1.569	1.541	1.564	1.540	1.529
Ti		0.000	0.000	0.000	0.000	0.000	0.000	0.000	0.000
Bi		0.002	0.000	0.001	0.001	0.000	0.001	0.001	0.000
V		0.000	0.000	0.000	0.000	0.000	0.000	0.000	0.000
Fe ²⁺		0.000	0.000	0.000	0.000	0.000	0.000	0.001	0.000
Mn ²⁺		0.118	0.110	0.123	0.116	0.000	0.000	0.000	0.005
Mg		0.000	0.000	0.000	0.000	0.000	0.000	0.000	0.000
Li		1.379	1.400	1.312	1.315	1.458	1.435	1.459	1.465
X: Ca		0.002	0.005	0.003	0.004	0.111	0.111	0.119	0.131
Na		0.582	0.522	0.569	0.534	0.435	0.412	0.419	0.425
K		0.004	0.000	0.000	0.000	0.000	0.000	0.000	0.000
□ (vac.)		0.413	0.473	0.428	0.461	0.454	0.477	0.462	0.444
OH		3.404	3.557	3.572	3.612	3.465	3.476	3.436	3.415
F		0.596	0.443	0.428	0.388	0.535	0.524	0.564	0.585
species		F-elbaite		elbaite	elbaite	F-rossman	F-rossman	F-rossman	F-rossman

Oxides		3g5	3h1	3h2	3h3	3h4	3h5	3i1	3i2
sample		pink	pi & nr cls	pi & nr cls	grn & ~cls	grn & ~cls	grn & ~cls	pale g yel	pale g yel
color		38.32	37.96	38.30	38.22	38.37	38.25	38.47	38.30
SiO ₂		0.00	0.00	0.00	0.00	0.00	0.00	0.00	0.00
TiO ₂		11.01	11.01	11.15	11.06	11.09	11.12	11.07	10.98
Al ₂ O ₃		40.71	40.15	40.67	40.66	40.55	40.71	40.31	39.82
Bi ₂ O ₃		0.00	0.08	0.01	0.01	0.02	0.03	0.01	0.03
V ₂ O ₃		0.00	0.00	0.00	0.00	0.01	0.00	0.00	0.00
FeO		0.00	0.18	0.25	0.38	0.47	0.56	0.21	0.26
MnO		0.00	0.21	0.23	0.20	0.27	0.33	1.32	1.27
MgO		0.00	0.00	0.00	0.00	0.00	0.00	0.00	0.00
CaO		0.77	2.13	2.34	1.93	2.03	2.24	0.61	0.57
Li ₂ O calc.		2.25	2.35	2.40	2.20	2.24	2.24	2.12	2.15
Na ₂ O		1.30	1.06	1.06	0.61	0.67	0.67	1.66	1.61
K ₂ O		0.00	0.00	0.00	0.00	0.00	0.00	0.04	0.00
H ₂ O calc.		3.36	3.22	3.31	3.37	3.34	3.30	3.29	3.22
F		0.92	1.22	1.14	0.95	1.02	1.13	1.13	1.19
Sub-total		98.66	99.58	100.86	99.59	100.08	100.58	100.20	99.41
O=F		-0.39	-0.51	-0.48	-0.40	-0.43	-0.47	-0.47	-0.50
Total		98.27	99.06	100.38	99.19	99.65	100.10	99.73	98.90
Ions (apfu)									
T: Si		6.048	5.988	5.967	6.007	6.010	5.978	6.040	6.062
Al		0.000	0.012	0.033	0.000	0.000	0.022	0.000	0.000
B: B		3.000	3.000	3.000	3.000	3.000	3.000	3.000	3.000
Z: Al		6.000	6.000	6.000	6.000	6.000	6.000	6.000	6.000
Y: Al		1.572	1.455	1.434	1.530	1.487	1.476	1.461	1.428
Ti		0.000	0.000	0.000	0.000	0.000	0.000	0.000	0.000
Bi		0.000	0.003	0.000	0.000	0.001	0.001	0.000	0.001
V		0.000	0.000	0.000	0.000	0.001	0.000	0.000	0.000
Fe ²⁺		0.000	0.024	0.032	0.050	0.061	0.073	0.028	0.035
Mn ²⁺		0.000	0.028	0.031	0.027	0.036	0.043	0.175	0.170
Mg		0.000	0.000	0.000	0.000	0.000	0.000	0.000	0.000
Li		1.427	1.490	1.503	1.393	1.414	1.406	1.336	1.365
X: Ca		0.131	0.361	0.390	0.325	0.341	0.374	0.102	0.096
Na		0.399	0.324	0.321	0.186	0.202	0.203	0.504	0.494
K		0.000	0.000	0.000	0.000	0.000	0.000	0.007	0.000
□ (vac.)		0.470	0.316	0.288	0.489	0.457	0.423	0.387	0.410
OH		3.539	3.391	3.441	3.529	3.492	3.442	3.441	3.402
F		0.461	0.609	0.559	0.471	0.507	0.557	0.559	0.598
species		rossmanite	liddicoatite	liddicoatite	rossmanite	F-rossman	F-rossman	F-elbaite	F-elbaite

Oxides		3i3	3i5	4j1	4j2	4j3	4j4	4k1	4k2
sample		pale g yel	pale g yel	~cl&sat pi	~cl&sat pi	~cl&sat pi	~cl&sat pi	pale pink	pale pink
color		38.31	38.11	38.01	38.26	38.23	38.31	37.86	37.84
SiO ₂		0.00	0.00	0.00	0.00	0.00	0.00	0.00	0.00
TiO ₂		10.97	10.96	10.91	10.94	10.94	10.95	11.13	11.08
Al ₂ O ₃		39.79	39.73	39.75	39.78	39.88	39.79	39.88	39.75
Bi ₂ O ₃		0.01	0.01	0.00	0.09	0.00	0.01	0.02	0.01
V ₂ O ₃		0.00	0.00	0.00	0.00	0.00	0.00	0.00	0.00
FeO		0.16	0.19	0.04	0.03	0.02	0.03	0.00	0.01
MnO		1.15	1.44	1.53	1.43	1.34	1.32	0.85	0.78
MgO		0.00	0.00	0.00	0.00	0.00	0.00	0.00	0.00
CaO		0.55	0.67	0.07	0.07	0.07	0.05	3.90	3.66
Li ₂ O calc.		2.19	2.12	2.07	2.12	2.12	2.15	2.60	2.55
Na ₂ O		1.65	1.67	2.02	1.79	1.87	1.91	0.54	0.52
K ₂ O		0.01	0.00	0.00	0.08	0.00	0.01	0.00	0.00
H ₂ O calc.		3.32	3.21	3.32	3.46	3.45	3.31	3.31	3.32
F		0.99	1.19	0.95	0.66	0.69	0.98	1.12	1.05
Sub-total		99.09	99.31	98.67	98.68	98.61	98.80	101.20	100.58
O=F		-0.42	-0.50	-0.40	-0.28	-0.29	-0.41	-0.47	-0.44
Total		98.67	98.81	98.27	98.40	98.32	98.39	100.73	100.13
Ions (apfu)									
T: Si		6.068	6.046	6.054	6.078	6.072	6.081	5.913	5.936
Al		0.000	0.000	0.000	0.000	0.000	0.000	0.087	0.064
B: B		3.000	3.000	3.000	3.000	3.000	3.000	3.000	3.000
Z: Al		6.000	6.000	6.000	6.000	6.000	6.000	6.000	6.000
Y: Al		1.428	1.428	1.462	1.448	1.465	1.444	1.254	1.286
Ti		0.000	0.000	0.000	0.000	0.000	0.000	0.000	0.000
Bi		0.000	0.000	0.000	0.004	0.000	0.000	0.001	0.000
V		0.000	0.000	0.000	0.000	0.000	0.000	0.000	0.000
Fe ²⁺		0.021	0.025	0.005	0.003	0.003	0.004	0.000	0.001
Mn ²⁺		0.154	0.194	0.206	0.192	0.180	0.177	0.112	0.103
Mg		0.000	0.000	0.000	0.000	0.000	0.000	0.000	0.000
Li		1.396	1.353	1.326	1.353	1.352	1.375	1.634	1.609
X: Ca		0.094	0.115	0.011	0.011	0.011	0.008	0.652	0.614
Na		0.506	0.512	0.624	0.550	0.575	0.587	0.162	0.159
K		0.002	0.000	0.000	0.016	0.000	0.002	0.000	0.000
□ (vac.)		0.399	0.373	0.365	0.422	0.414	0.402	0.186	0.227
OH		3.504	3.401	3.523	3.668	3.652	3.508	3.448	3.478
F		0.496	0.599	0.477	0.332	0.348	0.492	0.552	0.522
species		elbaite	F-elbaite	elbaite	elbaite	elbaite	elbaite	liddicoatite	liddicoatite

Oxides								
sample	4k3	4k4	4k5	4I1	4I2	4I3	4I4	4I5
color	pale pink	pale pink	pale pink	pink	pink	pink	pink	pink
SiO ₂	37.80	38.11	37.76	38.33	38.41	38.22	38.41	38.23
TiO ₂	0.00	0.00	0.00	0.00	0.00	0.00	0.00	0.00
B ₂ O ₃ calc.	11.06	11.09	11.08	11.11	11.12	11.09	11.13	11.13
Al ₂ O ₃	39.63	39.34	39.71	40.40	40.55	40.50	40.66	40.52
Bi ₂ O ₃	0.02	0.01	0.01	0.01	0.07	0.01	0.00	0.01
V ₂ O ₃	0.00	0.00	0.00	0.01	0.00	0.00	0.00	0.00
FeO	0.00	0.01	0.03	0.00	0.00	0.00	0.00	0.00
MnO	0.78	0.85	0.80	0.24	0.21	0.21	0.24	0.25
MgO	0.00	0.00	0.00	0.00	0.00	0.00	0.00	0.00
CaO	3.61	3.75	3.73	2.07	2.02	1.93	2.01	2.28
Li ₂ O calc.	2.56	2.61	2.58	2.42	2.39	2.38	2.37	2.44
Na ₂ O	0.60	0.58	0.64	1.29	1.18	1.31	1.12	1.22
K ₂ O	0.00	0.00	0.00	0.00	0.01	0.00	0.00	0.00
H ₂ O calc.	3.26	3.25	3.27	3.24	3.30	3.28	3.27	3.27
F	1.17	1.22	1.17	1.25	1.13	1.15	1.21	1.20
Sub-total	100.50	100.82	100.77	100.37	100.40	100.08	100.41	100.55
O=F	-0.49	-0.51	-0.49	-0.53	-0.47	-0.48	-0.51	-0.51
Total	100.01	100.31	100.28	99.84	99.92	99.60	99.91	100.04
Ions (apfu)								
T: Si	5.939	5.973	5.922	5.996	6.000	5.989	5.998	5.972
Al	0.061	0.027	0.078	0.004	0.000	0.011	0.002	0.028
B: B	3.000	3.000	3.000	3.000	3.000	3.000	3.000	3.000
Z: Al	6.000	6.000	6.000	6.000	6.000	6.000	6.000	6.000
Y: Al	1.278	1.238	1.261	1.443	1.466	1.469	1.480	1.431
Ti	0.000	0.000	0.000	0.000	0.000	0.000	0.000	0.000
Bi	0.001	0.000	0.000	0.000	0.003	0.000	0.000	0.000
V	0.000	0.000	0.000	0.002	0.000	0.000	0.000	0.000
Fe ²⁺	0.000	0.001	0.003	0.000	0.000	0.000	0.000	0.000
Mn ²⁺	0.104	0.113	0.106	0.032	0.028	0.028	0.032	0.033
Mg	0.000	0.000	0.000	0.000	0.000	0.000	0.000	0.000
Li	1.617	1.646	1.630	1.523	1.503	1.503	1.487	1.535
X: Ca	0.608	0.629	0.627	0.347	0.338	0.323	0.336	0.382
Na	0.184	0.177	0.195	0.390	0.358	0.399	0.338	0.368
K	0.000	0.000	0.000	0.000	0.002	0.000	0.001	0.000
□ (vac.)	0.208	0.194	0.178	0.263	0.302	0.278	0.326	0.250
OH	3.420	3.398	3.421	3.383	3.443	3.433	3.405	3.407
F	0.580	0.602	0.579	0.617	0.557	0.567	0.595	0.593
species	liddicoatite	liddicoatite	liddicoatite	F-elbaite	F-elbaite	F-elbaite	F-elbaite	liddicoatite

Oxides		5m1	5m2	5m3	5m4	5m5	5n1	5n2	5n3
sample		pl pi & y g	pl pi & y g	pl pi & y g	pl pi & y g	pl pi & y g	yel green	yel green	yel green
color		37.66	37.90	37.79	38.23	38.17	37.97	38.46	38.37
SiO ₂		0.03	0.02	0.00	0.04	0.02	0.00	0.00	0.01
TiO ₂		11.07	11.11	11.05	11.17	11.18	10.94	11.04	11.04
Al ₂ O ₃		39.84	39.94	39.80	40.10	40.24	39.79	40.03	39.95
Bi ₂ O ₃		0.01	0.01	0.00	0.01	0.01	0.00	0.00	0.00
V ₂ O ₃		0.00	0.00	0.00	0.00	0.00	0.00	0.00	0.00
FeO		0.30	0.31	0.27	0.31	0.31	0.62	0.64	0.73
MnO		0.29	0.25	0.21	0.29	0.25	0.54	0.56	0.62
MgO		0.00	0.02	0.00	0.03	0.01	0.09	0.05	0.08
CaO		3.55	3.57	3.42	3.47	3.55	0.68	0.68	0.72
Li ₂ O calc.		2.60	2.59	2.56	2.58	2.59	2.15	2.22	2.20
Na ₂ O		0.84	0.70	0.68	0.69	0.64	1.85	1.74	1.89
K ₂ O		0.00	0.00	0.00	0.00	0.00	0.00	0.00	0.01
H ₂ O calc.		3.28	3.25	3.20	3.26	3.30	3.20	3.22	3.22
F		1.15	1.22	1.29	1.25	1.17	1.20	1.25	1.24
Sub-total		100.60	100.90	100.28	101.43	101.42	99.04	99.88	100.05
O=F		-0.48	-0.51	-0.54	-0.53	-0.49	-0.51	-0.53	-0.52
Total		100.12	100.39	99.74	100.90	100.93	98.53	99.35	99.53
Ions (apfu)									
T: Si		5.909	5.927	5.942	5.945	5.933	6.031	6.054	6.040
Al		0.091	0.073	0.058	0.055	0.067	0.000	0.000	0.000
B: B		3.000	3.000	3.000	3.000	3.000	3.000	3.000	3.000
Z: Al		6.000	6.000	6.000	6.000	6.000	6.000	6.000	6.000
Y: Al		1.278	1.290	1.318	1.296	1.306	1.448	1.427	1.411
Ti		0.003	0.002	0.000	0.004	0.002	0.000	0.000	0.001
Bi		0.000	0.001	0.000	0.000	0.000	0.000	0.000	0.000
V		0.000	0.000	0.000	0.000	0.000	0.001	0.000	0.000
Fe ²⁺		0.039	0.041	0.035	0.041	0.040	0.082	0.084	0.096
Mn ²⁺		0.038	0.033	0.028	0.038	0.033	0.073	0.075	0.082
Mg		0.000	0.004	0.000	0.008	0.001	0.022	0.011	0.018
Li		1.641	1.630	1.618	1.613	1.616	1.374	1.403	1.391
X: Ca		0.597	0.598	0.575	0.579	0.591	0.116	0.115	0.121
Na		0.254	0.213	0.208	0.207	0.192	0.570	0.532	0.576
K		0.000	0.000	0.000	0.000	0.000	0.000	0.000	0.002
□ (vac.)		0.149	0.189	0.217	0.214	0.217	0.314	0.353	0.301
OH		3.431	3.395	3.361	3.385	3.426	3.395	3.379	3.382
F		0.569	0.605	0.639	0.615	0.574	0.605	0.621	0.617
species		Iiddicoatite	Iiddicoatite	Iiddicoatite	Iiddicoatite	Iiddicoatite	F-elbaite	F-elbaite	F-elbaite

Oxides		5n4	5n5	5o1	5o2	5o3	5o4	5o5	6p1
sample		yel green	yel green	sl pink red	colorless				
color		38.25	38.00	38.33	38.37	38.42	38.17	38.42	38.15
SiO ₂		0.00	0.00	0.00	0.00	0.01	0.00	0.00	0.00
TiO ₂		10.98	10.94	11.03	11.04	11.05	11.00	11.11	11.24
Al ₂ O ₃		39.80	39.72	39.97	39.96	39.78	40.00	40.53	40.68
Bi ₂ O ₃		0.00	0.00	0.01	0.05	0.02	0.02	0.01	0.00
V ₂ O ₃		0.03	0.00	0.00	0.00	0.02	0.00	0.00	0.00
FeO		0.68	0.67	0.09	0.06	0.05	0.08	0.07	0.00
MnO		0.56	0.54	0.53	0.53	0.64	0.62	0.64	0.33
MgO		0.05	0.08	0.00	0.01	0.00	0.00	0.00	0.00
CaO		0.67	0.65	1.54	1.58	1.67	1.62	1.78	3.67
Li ₂ O calc.		2.19	2.17	2.36	2.38	2.42	2.30	2.28	2.65
Na ₂ O		1.72	1.88	1.26	1.30	1.36	1.14	1.09	0.73
K ₂ O		0.00	0.00	0.00	0.00	0.00	0.00	0.00	0.02
H ₂ O calc.		3.30	3.30	3.24	3.26	3.28	3.43	3.22	3.30
F		1.03	1.01	1.20	1.17	1.13	0.77	1.30	1.22
Sub-total		99.27	98.96	99.54	99.68	99.84	99.14	100.46	101.99
O=F		-0.43	-0.42	-0.51	-0.49	-0.48	-0.32	-0.55	-0.51
Total		98.84	98.53	99.04	99.19	99.37	98.81	99.91	101.48
Ions (apfu)									
T: Si		6.054	6.037	6.041	6.040	6.043	6.029	6.008	5.898
Al		0.000	0.000	0.000	0.000	0.000	0.000	0.000	0.102
B: B		3.000	3.000	3.000	3.000	3.000	3.000	3.000	3.000
Z: Al		6.000	6.000	6.000	6.000	6.000	6.000	6.000	6.000
Y: Al		1.423	1.435	1.423	1.414	1.375	1.447	1.471	1.310
Ti		0.000	0.000	0.000	0.000	0.001	0.000	0.000	0.000
Bi		0.000	0.000	0.000	0.002	0.001	0.001	0.000	0.000
V		0.004	0.000	0.000	0.000	0.003	0.000	0.000	0.000
Fe ²⁺		0.090	0.089	0.011	0.008	0.006	0.010	0.009	0.000
Mn ²⁺		0.075	0.073	0.070	0.070	0.086	0.082	0.085	0.044
Mg		0.013	0.018	0.000	0.002	0.000	0.000	0.000	0.000
Li		1.394	1.384	1.495	1.504	1.529	1.460	1.434	1.646
X: Ca		0.113	0.110	0.260	0.267	0.282	0.275	0.299	0.608
Na		0.527	0.580	0.386	0.395	0.414	0.349	0.331	0.219
K		0.000	0.000	0.000	0.000	0.000	0.000	0.000	0.003
□ (vac.)		0.360	0.310	0.354	0.338	0.304	0.376	0.370	0.170
OH		3.486	3.493	3.402	3.418	3.436	3.615	3.358	3.402
F		0.514	0.507	0.598	0.582	0.564	0.385	0.642	0.598
species		F-elbaite	F-elbaite	F-elbaite	F-elbaite	F-elbaite	rossmanite	F-rossman	liddicoatite

Oxides		6p2	6p3	6p4	6p5	6q1	6q2	6q3	6q4
sample		colorless	colorless	colorless	colorless	yel green	yel green	yel green	yel green
SiO ₂		38.03	37.61	37.90	37.65	37.89	37.68	37.69	37.87
TiO ₂		0.00	0.00	0.00	0.00	0.05	0.07	0.04	0.03
B ₂ O ₃ calc.		11.16	11.01	11.08	11.07	11.06	11.02	11.10	11.10
Al ₂ O ₃		40.09	39.42	39.72	39.71	39.41	39.38	39.95	39.77
Bi ₂ O ₃		0.00	0.00	0.00	0.00	0.00	0.00	0.00	0.00
V ₂ O ₃		0.00	0.00	0.00	0.00	0.00	0.00	0.00	0.00
FeO		0.00	0.01	0.00	0.00	0.78	0.74	0.88	0.95
MnO		0.28	0.35	0.30	0.35	0.78	0.69	0.69	0.69
MgO		0.00	0.00	0.00	0.00	0.00	0.00	0.00	0.00
CaO		3.75	3.63	3.59	3.77	2.56	2.50	2.57	2.46
Li ₂ O calc.		2.68	2.64	2.66	2.68	2.43	2.44	2.40	2.39
Na ₂ O		0.75	0.78	0.79	0.85	1.49	1.58	1.52	1.55
K ₂ O		0.01	0.00	0.02	0.00	0.03	0.03	0.03	0.01
H ₂ O calc.		3.33	3.23	3.31	3.33	3.22	3.21	3.18	3.17
F		1.10	1.21	1.09	1.03	1.26	1.25	1.36	1.40
Sub-total		101.18	99.87	100.45	100.43	100.95	100.59	101.40	101.37
O=F		-0.46	-0.51	-0.46	-0.44	-0.53	-0.53	-0.57	-0.59
Total		100.71	99.37	99.99	99.99	100.42	100.07	100.83	100.78
Ions (apfu)									
T: Si		5.922	5.939	5.943	5.911	5.954	5.940	5.902	5.932
Al		0.078	0.061	0.057	0.089	0.046	0.060	0.098	0.068
B: B		3.000	3.000	3.000	3.000	3.000	3.000	3.000	3.000
Z: Al		6.000	6.000	6.000	6.000	6.000	6.000	6.000	6.000
Y: Al		1.281	1.274	1.284	1.259	1.251	1.256	1.275	1.274
Ti		0.000	0.000	0.000	0.000	0.005	0.009	0.005	0.003
Bi		0.000	0.000	0.000	0.000	0.000	0.000	0.000	0.000
V		0.000	0.000	0.000	0.000	0.000	0.000	0.000	0.000
Fe ²⁺		0.000	0.002	0.000	0.000	0.102	0.098	0.115	0.125
Mn ²⁺		0.037	0.046	0.040	0.046	0.104	0.092	0.091	0.091
Mg		0.000	0.000	0.000	0.000	0.000	0.000	0.000	0.000
Li		1.682	1.678	1.675	1.694	1.537	1.545	1.513	1.507
X: Ca		0.625	0.614	0.602	0.634	0.431	0.423	0.430	0.413
Na		0.228	0.238	0.241	0.258	0.454	0.481	0.462	0.469
K		0.002	0.000	0.004	0.000	0.007	0.006	0.005	0.002
□ (vac.)		0.145	0.148	0.153	0.108	0.108	0.090	0.102	0.116
OH		3.459	3.398	3.461	3.487	3.376	3.377	3.326	3.308
F		0.541	0.602	0.539	0.513	0.624	0.623	0.674	0.692
species		Iiddicoatite	Iiddicoatite	Iiddicoatite	Iiddicoatite	F-elbaite	F-elbaite	F-elbaite	F-elbaite

Oxides								
sample	7s4	7s5	6t2	6t3	6t4	6t5	7u1	7u2
color	sat pink	sat pink	nr cls grn	nr cls grn	pink	pink	pale green	pale green
SiO ₂	38.38	37.66	38.45	38.21	38.22	38.05	38.19	38.07
TiO ₂	0.00	0.00	0.00	0.00	0.00	0.00	0.00	0.00
B ₂ O ₃ calc.	11.26	11.19	10.97	10.96	10.93	10.91	11.09	11.10
Al ₂ O ₃	40.10	40.41	39.38	39.60	39.56	39.67	40.32	40.44
Bi ₂ O ₃	0.01	0.01	0.03	0.02	0.02	0.00	0.00	0.00
V ₂ O ₃	0.00	0.00	0.00	0.00	0.00	0.00	0.00	0.01
FeO	0.01	0.00	0.23	0.24	0.08	0.06	0.21	0.28
MnO	0.31	0.29	1.66	1.72	1.59	1.36	0.13	0.10
MgO	0.00	0.00	0.00	0.00	0.00	0.00	0.00	0.00
CaO	4.31	4.38	0.06	0.07	0.08	0.06	2.09	2.09
Li ₂ O calc.	2.81	2.76	2.19	2.10	2.13	2.12	2.41	2.42
Na ₂ O	0.63	0.60	2.16	2.21	2.00	2.05	1.28	1.41
K ₂ O	0.00	0.00	0.01	0.02	0.01	0.01	0.01	0.01
H ₂ O calc.	3.46	3.26	3.36	3.48	3.55	3.31	3.23	3.24
F	0.90	1.27	0.90	0.64	0.48	0.95	1.26	1.24
Sub-total	102.17	101.83	99.39	99.25	98.64	98.56	100.21	100.39
O=F	-0.38	-0.54	-0.38	-0.27	-0.20	-0.40	-0.53	-0.52
Total	101.80	101.29	99.01	98.98	98.44	98.16	99.68	99.87
Ions (apfu)								
T: Si	5.921	5.846	6.089	6.058	6.076	6.063	5.987	5.962
Al	0.079	0.154	0.000	0.000	0.000	0.000	0.013	0.038
B: B	3.000	3.000	3.000	3.000	3.000	3.000	3.000	3.000
Z: Al	6.000	6.000	6.000	6.000	6.000	6.000	6.000	6.000
Y: Al	1.212	1.239	1.351	1.400	1.412	1.449	1.437	1.428
Ti	0.000	0.000	0.000	0.000	0.000	0.000	0.000	0.000
Bi	0.000	0.000	0.001	0.001	0.001	0.000	0.000	0.000
V	0.000	0.000	0.000	0.000	0.000	0.000	0.000	0.001
Fe ²⁺	0.001	0.000	0.031	0.031	0.010	0.008	0.027	0.037
Mn ²⁺	0.040	0.038	0.223	0.231	0.215	0.183	0.017	0.013
Mg	0.000	0.000	0.000	0.000	0.000	0.000	0.000	0.000
Li	1.746	1.722	1.395	1.338	1.363	1.360	1.518	1.521
X: Ca	0.713	0.728	0.010	0.012	0.014	0.011	0.351	0.351
Na	0.189	0.181	0.663	0.678	0.616	0.634	0.390	0.429
K	0.000	0.000	0.002	0.003	0.002	0.003	0.002	0.001
□ (vac.)	0.098	0.091	0.325	0.307	0.368	0.353	0.257	0.219
OH	3.562	3.374	3.548	3.679	3.760	3.522	3.373	3.386
F	0.438	0.625	0.452	0.320	0.240	0.478	0.627	0.614
species	OH-liddi	liddicoatite	elbaite	elbaite	elbaite	elbaite	F-elbaite	F-elbaite

Oxides	8w2	8w3	8w4	8w5	8x1	8x2	8x3	8x4
sample	8w2	8w3	8w4	8w5	8x1	8x2	8x3	8x4
color	pink	pink	pink	pink	pink red	pink red	pink red	pink red
SiO ₂	38.40	38.69	38.22	38.22	38.27	37.97	38.19	38.28
TiO ₂	0.00	0.01	0.00	0.00	0.00	0.00	0.00	0.00
B ₂ O ₃ calc.	11.21	11.24	11.16	11.16	11.09	11.02	11.04	11.06
Al ₂ O ₃	40.12	40.17	40.35	40.45	40.49	40.59	40.27	40.41
Bi ₂ O ₃	0.00	0.01	0.00	0.00	0.00	0.00	0.00	0.00
V ₂ O ₃	0.01	0.00	0.00	0.00	0.00	0.00	0.00	0.00
FeO	0.03	0.03	0.02	0.01	0.04	0.02	0.03	0.00
MnO	0.12	0.15	0.18	0.12	0.30	0.26	0.27	0.27
MgO	0.00	0.00	0.00	0.00	0.00	0.00	0.00	0.00
CaO	3.53	3.44	3.18	3.14	1.65	1.53	1.63	1.59
Li ₂ O calc.	2.71	2.70	2.57	2.57	2.35	2.26	2.35	2.34
Na ₂ O	0.93	0.86	0.77	0.79	1.51	1.31	1.40	1.35
K ₂ O	0.00	0.01	0.00	0.01	0.00	0.00	0.00	0.00
H ₂ O calc.	3.36	3.36	3.33	3.28	3.29	3.24	3.39	3.26
F	1.07	1.09	1.10	1.20	1.12	1.19	0.89	1.17
Sub-total	101.49	101.76	100.88	100.95	100.11	99.39	99.46	99.74
O=F	-0.45	-0.46	-0.46	-0.51	-0.47	-0.50	-0.38	-0.49
Total	101.04	101.30	100.42	100.45	99.64	98.89	99.09	99.25
Ions (apfu)								
T: Si	5.954	5.980	5.954	5.950	5.996	5.987	6.011	6.014
Al	0.046	0.020	0.046	0.050	0.004	0.013	0.000	0.000
B: B	3.000	3.000	3.000	3.000	3.000	3.000	3.000	3.000
Z: Al	6.000	6.000	6.000	6.000	6.000	6.000	6.000	6.000
Y: Al	1.286	1.297	1.363	1.373	1.473	1.529	1.470	1.482
Ti	0.000	0.001	0.000	0.000	0.000	0.000	0.000	0.000
Bi	0.000	0.000	0.000	0.000	0.000	0.000	0.000	0.000
V	0.001	0.000	0.000	0.000	0.000	0.000	0.000	0.000
Fe ²⁺	0.004	0.004	0.002	0.002	0.005	0.002	0.004	0.000
Mn ²⁺	0.016	0.020	0.023	0.016	0.040	0.034	0.036	0.036
Mg	0.000	0.000	0.000	0.000	0.000	0.000	0.000	0.000
Li	1.692	1.678	1.611	1.609	1.481	1.435	1.490	1.481
X: Ca	0.586	0.570	0.531	0.524	0.277	0.259	0.274	0.268
Na	0.280	0.258	0.232	0.237	0.457	0.400	0.428	0.410
K	0.000	0.003	0.001	0.002	0.000	0.000	0.000	0.000
□ (vac.)	0.134	0.170	0.236	0.237	0.265	0.341	0.297	0.322
OH	3.477	3.467	3.459	3.409	3.443	3.406	3.556	3.420
F	0.522	0.533	0.541	0.591	0.557	0.594	0.444	0.580
species	liddicoatite	liddicoatite	liddicoatite	liddicoatite	F-elbaite	F-elbaite	elbaite	F-elbaite

Oxides		8x5	9y1	9y2	9y3	9y5	9z1	9z2	9z3
sample		pink red	bright pink	bright pink	bright pink	bright pink	pink	pink	pink
color		38.27	38.23	38.10	38.12	38.47	38.30	38.36	38.50
SiO ₂		0.00	0.00	0.00	0.00	0.00	0.00	0.00	0.00
TiO ₂		11.09	10.99	10.94	10.93	11.01	11.05	11.07	11.07
Al ₂ O ₃		40.51	39.93	39.84	39.76	39.77	40.48	40.67	40.47
Bi ₂ O ₃		0.00	0.00	0.02	0.02	0.03	0.01	0.01	0.01
V ₂ O ₃		0.00	0.00	0.00	0.00	0.01	0.00	0.00	0.00
FeO		0.01	0.02	0.00	0.02	0.00	0.00	0.00	0.00
MnO		0.28	1.83	1.72	1.73	1.84	0.06	0.05	0.07
MgO		0.00	0.00	0.00	0.00	0.00	0.00	0.00	0.00
CaO		1.73	0.07	0.06	0.05	0.08	0.88	0.89	0.86
Li ₂ O calc.		2.35	2.06	2.05	2.05	2.13	2.35	2.33	2.37
Na ₂ O		1.38	2.15	2.04	1.97	2.09	1.96	1.81	1.74
K ₂ O		0.00	0.01	0.01	0.02	0.01	0.00	0.02	0.01
H ₂ O calc.		3.28	3.37	3.50	3.28	3.44	3.26	3.22	3.28
F		1.15	0.90	0.58	1.05	0.76	1.16	1.27	1.13
Sub-total		100.03	99.56	98.88	99.00	99.65	99.52	99.68	99.52
O=F		-0.48	-0.38	-0.24	-0.44	-0.32	-0.49	-0.54	-0.48
Total		99.55	99.18	98.63	98.56	99.33	99.03	99.14	99.05
Ions (apfu)									
T: Si		5.999	6.045	6.050	6.059	6.071	6.023	6.023	6.047
Al		0.001	0.000	0.000	0.000	0.000	0.000	0.000	0.000
B: B		3.000	3.000	3.000	3.000	3.000	3.000	3.000	3.000
Z: Al		6.000	6.000	6.000	6.000	6.000	6.000	6.000	6.000
Y: Al		1.482	1.443	1.457	1.449	1.398	1.502	1.525	1.491
Ti		0.000	0.000	0.000	0.000	0.000	0.000	0.000	0.000
Bi		0.000	0.000	0.001	0.001	0.001	0.000	0.000	0.000
V		0.000	0.000	0.000	0.000	0.001	0.000	0.000	0.000
Fe ²⁺		0.002	0.003	0.000	0.003	0.000	0.000	0.000	0.000
Mn ²⁺		0.037	0.245	0.232	0.233	0.246	0.008	0.006	0.009
Mg		0.000	0.000	0.000	0.000	0.000	0.000	0.000	0.000
Li		1.480	1.310	1.311	1.313	1.354	1.489	1.469	1.500
X: Ca		0.291	0.013	0.010	0.009	0.013	0.149	0.149	0.145
Na		0.418	0.660	0.629	0.606	0.640	0.598	0.551	0.531
K		0.000	0.001	0.002	0.003	0.002	0.000	0.003	0.002
□ (vac.)		0.291	0.326	0.359	0.381	0.344	0.253	0.297	0.322
OH		3.430	3.552	3.710	3.475	3.620	3.424	3.369	3.439
F		0.570	0.448	0.290	0.525	0.380	0.575	0.631	0.561
species		F-elbaite	elbaite	elbaite	F-elbaite	elbaite	F-elbaite	F-elbaite	F-elbaite

Oxides	10c1-5	10d1-1	10d1-2	10d1-3	10d1-4	10d1-5	11e1-1	11e1-2
sample	pi & y or	gray green	gray green	gray green	pink	pink	pink red	pink red
color	37.56	38.30	38.05	38.06	37.79	38.09	37.67	38.07
SiO ₂	0.03	0.00	0.00	0.00	0.00	0.00	0.04	0.02
TiO ₂	11.08	11.10	11.12	11.06	11.07	11.11	10.85	10.91
Al ₂ O ₃	40.27	40.61	40.35	40.46	40.33	40.32	38.56	38.38
Bi ₂ O ₃	0.02	0.01	0.02	0.03	0.01	0.00	0.00	0.02
V ₂ O ₃	0.00	0.01	0.00	0.00	0.00	0.00	0.00	0.00
FeO	0.10	0.02	0.00	0.00	0.00	0.00	0.03	0.01
MnO	0.13	0.13	0.13	0.13	0.18	0.21	4.63	4.58
MgO	0.00	0.00	0.00	0.00	0.00	0.00	0.00	0.00
CaO	3.36	2.93	2.92	2.25	2.81	2.73	0.07	0.07
Li ₂ O calc.	2.59	2.37	2.56	2.38	2.51	2.51	1.69	1.83
Na ₂ O	0.90	0.10	1.03	0.94	1.02	1.02	2.09	2.21
K ₂ O	0.00	0.00	0.00	0.01	0.01	0.00	0.01	0.02
H ₂ O calc.	3.27	3.28	3.29	3.24	3.24	3.33	3.47	3.40
F	1.17	1.17	1.15	1.21	1.22	1.07	0.59	0.77
Sub-total	100.48	100.03	100.62	99.78	100.18	100.38	99.68	100.28
O=F	-0.49	-0.49	-0.48	-0.51	-0.51	-0.45	-0.25	-0.32
Total	99.99	99.54	100.13	99.27	99.66	99.93	99.44	99.96
Ions (apfu)								
T: Si	5.890	5.995	5.945	5.981	5.932	5.959	6.032	6.063
Al	0.110	0.005	0.055	0.019	0.068	0.041	0.000	0.000
B: B	3.000	3.000	3.000	3.000	3.000	3.000	3.000	3.000
Z: Al	6.000	6.000	6.000	6.000	6.000	6.000	6.000	6.000
Y: Al	1.332	1.484	1.375	1.475	1.394	1.394	1.277	1.204
Ti	0.003	0.000	0.000	0.000	0.000	0.000	0.005	0.003
Bi	0.001	0.000	0.001	0.001	0.000	0.000	0.000	0.001
V	0.000	0.001	0.000	0.000	0.000	0.000	0.000	0.000
Fe ²⁺	0.013	0.002	0.000	0.000	0.000	0.000	0.004	0.001
Mn ²⁺	0.018	0.018	0.018	0.018	0.023	0.028	0.628	0.618
Mg	0.000	0.000	0.000	0.000	0.000	0.000	0.001	0.000
Li	1.633	1.494	1.607	1.505	1.583	1.577	1.085	1.173
X: Ca	0.565	0.491	0.488	0.380	0.473	0.457	0.011	0.012
Na	0.274	0.031	0.311	0.288	0.309	0.311	0.647	0.683
K	0.000	0.000	0.000	0.002	0.002	0.000	0.002	0.003
□ (vac.)	0.161	0.477	0.201	0.331	0.216	0.232	0.340	0.302
OH	3.421	3.422	3.432	3.398	3.394	3.472	3.702	3.615
F	0.579	0.578	0.568	0.601	0.606	0.528	0.297	0.385
species	liddicoatite	liddicoatite	liddicoatite	liddicoatite	liddicoatite	liddicoatite	elbaite	elbaite

Oxides	11e1-3	11e1-4	11e1-5	11f1-1	11f1-2	11f1-3	11f1-5	11g1-1
sample	11e1-3	11e1-4	11e1-5	11f1-1	11f1-2	11f1-3	11f1-5	11g1-1
color	pink red	pink red	pink red	sl yel grn	sl yel grn	sl yel grn	sl yel grn	bright pink
SiO ₂	38.11	37.79	38.19	38.20	38.21	38.24	38.22	38.18
TiO ₂	0.07	0.09	0.03	0.00	0.03	0.04	0.02	0.00
B ₂ O ₃ calc.	10.90	10.86	10.94	11.08	11.03	11.11	11.05	10.96
Al ₂ O ₃	38.31	38.42	38.58	39.56	39.18	39.97	39.58	40.10
Bi ₂ O ₃	0.00	0.00	0.00	0.04	0.01	0.03	0.02	0.01
V ₂ O ₃	0.00	0.00	0.00	0.00	0.00	0.00	0.00	0.00
FeO	0.02	0.00	0.00	2.07	2.01	1.86	1.74	0.00
MnO	4.59	4.64	4.65	1.85	1.86	1.80	1.78	0.87
MgO	0.00	0.00	0.00	0.01	0.00	0.02	0.01	0.00
CaO	0.08	0.06	0.06	0.28	0.27	0.26	0.25	0.05
Li ₂ O calc.	1.82	1.73	1.79	1.85	1.90	1.85	1.89	2.18
Na ₂ O	2.01	1.99	2.03	2.59	2.42	2.43	2.41	2.17
K ₂ O	0.01	0.01	0.01	0.03	0.01	0.01	0.02	0.01
H ₂ O calc.	3.28	3.38	3.43	3.30	3.24	3.29	3.24	3.52
F	1.02	0.77	0.72	1.11	1.20	1.14	1.21	0.56
Sub-total	100.22	99.74	100.43	101.96	101.35	102.06	101.43	98.60
O=F	-0.43	-0.32	-0.30	-0.47	-0.51	-0.48	-0.51	-0.24
Total	99.79	99.42	100.12	101.49	100.85	101.58	100.92	98.36
Ions (apfu)								
T: Si	6.077	6.050	6.067	5.991	6.022	5.980	6.009	6.053
Al	0.000	0.000	0.000	0.000	0.000	0.020	0.000	0.000
B: B	3.000	3.000	3.000	3.000	3.000	3.000	3.000	3.000
Z: Al	6.000	6.000	6.000	6.000	6.000	6.000	6.000	6.000
Y: Al	1.199	1.248	1.224	1.313	1.278	1.347	1.334	1.492
Ti	0.008	0.011	0.004	0.000	0.004	0.005	0.002	0.000
Bi	0.000	0.000	0.000	0.002	0.000	0.001	0.001	0.000
V	0.000	0.000	0.000	0.000	0.000	0.000	0.000	0.000
Fe ²⁺	0.003	0.000	0.000	0.271	0.264	0.244	0.229	0.000
Mn ²⁺	0.620	0.630	0.625	0.246	0.249	0.238	0.238	0.116
Mg	0.000	0.000	0.000	0.002	0.000	0.004	0.002	0.000
Li	1.170	1.111	1.147	1.167	1.205	1.161	1.195	1.391
X: Ca	0.014	0.011	0.010	0.047	0.045	0.043	0.043	0.008
Na	0.620	0.617	0.625	0.788	0.738	0.736	0.733	0.668
K	0.002	0.002	0.001	0.005	0.002	0.003	0.003	0.002
□ (vac.)	0.365	0.370	0.364	0.160	0.215	0.218	0.221	0.322
OH	3.483	3.611	3.637	3.448	3.401	3.436	3.398	3.718
F	0.516	0.389	0.363	0.552	0.599	0.564	0.602	0.282
species	F-elbaite	elbaite	elbaite	F-elbaite	F-elbaite	F-elbaite	F-elbaite	elbaite

Oxides	11g1-2	11g1-3	11g1-4	11g1-5	12h1-1	12h1-2	12h1-3	12h1-4
sample	bright pink	bright pink	bright pink	bright pink	pink	pink	pink	pink
color	38.18	38.22	38.46	38.44	38.27	38.22	38.38	38.32
SiO ₂	0.00	0.00	0.00	0.00	0.00	0.01	0.02	0.00
TiO ₂	10.96	11.00	11.05	11.01	11.15	11.06	11.07	11.14
Al ₂ O ₃	40.27	40.34	40.39	40.12	40.63	39.99	39.72	40.68
Bi ₂ O ₃	0.00	0.01	0.00	0.00	0.01	0.01	0.01	0.01
V ₂ O ₃	0.00	0.00	0.00	0.00	0.00	0.00	0.00	0.02
FeO	0.00	0.00	0.00	0.00	0.14	0.11	0.08	0.10
MnO	0.85	0.87	0.90	0.92	0.35	0.33	0.37	0.29
MgO	0.00	0.00	0.00	0.00	0.00	0.00	0.00	0.00
CaO	0.05	0.06	0.05	0.06	2.40	2.39	2.36	2.30
Li ₂ O calc.	2.13	2.15	2.20	2.23	2.39	2.43	2.51	2.38
Na ₂ O	1.96	2.18	2.25	2.14	0.99	1.00	1.09	0.94
K ₂ O	0.02	0.01	0.01	0.01	0.00	0.03	0.00	0.03
H ₂ O calc.	3.51	3.49	3.60	3.49	3.26	3.20	3.19	3.24
F	0.58	0.64	0.44	0.66	1.24	1.31	1.32	1.28
Sub-total	98.50	98.97	99.34	99.07	100.81	100.10	100.14	100.72
O=F	-0.24	-0.27	-0.19	-0.28	-0.52	-0.55	-0.56	-0.54
Total	98.26	98.70	99.16	98.79	100.29	99.54	99.58	100.19
Ions (apfu)								
T: Si	6.053	6.041	6.050	6.068	5.968	6.004	6.026	5.976
Al	0.000	0.000	0.000	0.000	0.032	0.000	0.000	0.024
B: B	3.000	3.000	3.000	3.000	3.000	3.000	3.000	3.000
Z: Al	6.000	6.000	6.000	6.000	6.000	6.000	6.000	6.000
Y: Al	1.525	1.515	1.488	1.464	1.435	1.403	1.351	1.454
Ti	0.000	0.000	0.000	0.000	0.000	0.001	0.002	0.000
Bi	0.000	0.000	0.000	0.000	0.000	0.001	0.000	0.000
V	0.000	0.000	0.000	0.000	0.000	0.000	0.000	0.002
Fe ²⁺	0.000	0.000	0.000	0.000	0.018	0.015	0.011	0.013
Mn ²⁺	0.114	0.117	0.119	0.123	0.046	0.044	0.049	0.039
Mg	0.000	0.000	0.000	0.000	0.000	0.000	0.000	0.000
Li	1.361	1.368	1.393	1.413	1.501	1.536	1.586	1.492
X: Ca	0.008	0.010	0.009	0.010	0.400	0.402	0.397	0.384
Na	0.603	0.667	0.685	0.653	0.298	0.306	0.333	0.285
K	0.003	0.002	0.001	0.001	0.000	0.005	0.001	0.005
□ (vac.)	0.386	0.321	0.305	0.335	0.301	0.287	0.269	0.326
OH	3.712	3.681	3.779	3.672	3.391	3.348	3.344	3.370
F	0.289	0.319	0.221	0.328	0.609	0.651	0.655	0.629
species	elbaite	elbaite	elbaite	elbaite	liddicoatite	liddicoatite	liddicoatite	liddicoatite

Oxides		12h1-5	12i1-1	12i1-2	12i1-3	12j1-1	12j1-2	12j1-3	12j1-4
sample		pink	bright pink	bright pink	bright pink	pink red	pink red	pink red	pink red
color		38.17	38.28	38.27	38.38	38.19	38.17	37.60	38.18
SiO ₂		0.02	0.00	0.00	0.00	0.03	0.02	0.01	0.00
TiO ₂		11.08	11.01	10.98	11.01	10.99	11.08	10.95	11.09
B ₂ O ₃ calc.		40.12	40.66	40.42	40.52	38.82	39.89	39.45	39.88
Al ₂ O ₃		0.01	0.01	0.00	0.00	0.01	0.01	0.01	0.00
Bi ₂ O ₃		0.00	0.00	0.00	0.00	0.01	0.00	0.00	0.00
V ₂ O ₃		0.16	0.00	0.01	0.02	0.11	0.07	0.08	0.08
FeO		0.39	0.29	0.33	0.37	0.97	1.04	1.00	1.06
MnO		0.00	0.00	0.00	0.00	0.00	0.00	0.00	0.00
MgO		2.46	0.01	0.02	0.02	2.16	2.19	2.23	2.21
CaO		2.40	2.20	2.23	2.22	2.54	2.36	2.36	2.39
Li ₂ O calc.		0.95	2.13	2.12	2.05	1.53	1.31	1.40	1.43
Na ₂ O		0.02	0.00	0.00	0.00	0.02	0.01	0.02	0.00
K ₂ O		3.21	3.63	3.44	3.44	3.18	3.20	3.26	3.39
H ₂ O calc.		1.29	0.35	0.73	0.76	1.28	1.32	1.09	0.93
F		100.24	98.56	98.54	98.79	99.82	100.65	99.47	100.64
Sub-total		-0.54	-0.15	-0.31	-0.32	-0.54	-0.56	-0.46	-0.39
O=F		99.70	98.41	98.23	98.47	99.28	100.10	99.01	100.25
Total									
Ions (apfu)									
T: Si		5.989	6.043	6.055	6.058	6.041	5.987	5.966	5.981
Al		0.011	0.000	0.000	0.000	0.000	0.013	0.034	0.019
B: B		3.000	3.000	3.000	3.000	3.000	3.000	3.000	3.000
Z: Al		6.000	6.000	6.000	6.000	6.000	6.000	6.000	6.000
Y: Al		1.409	1.566	1.538	1.539	1.238	1.362	1.345	1.345
Ti		0.002	0.000	0.000	0.000	0.004	0.002	0.001	0.000
Bi		0.000	0.000	0.000	0.000	0.000	0.000	0.000	0.000
V		0.000	0.000	0.000	0.000	0.001	0.000	0.000	0.000
Fe ²⁺		0.020	0.000	0.001	0.003	0.014	0.010	0.010	0.011
Mn ²⁺		0.052	0.039	0.045	0.049	0.130	0.139	0.135	0.141
Mg		0.000	0.000	0.000	0.000	0.000	0.000	0.000	0.000
Li		1.517	1.395	1.417	1.410	1.613	1.487	1.509	1.503
X: Ca		0.413	0.002	0.003	0.004	0.366	0.368	0.380	0.371
Na		0.288	0.651	0.650	0.629	0.469	0.398	0.432	0.435
K		0.003	0.000	0.000	0.001	0.003	0.002	0.004	0.000
□ (vac.)		0.297	0.347	0.347	0.367	0.162	0.233	0.185	0.194
OH		3.361	3.827	3.634	3.620	3.360	3.345	3.454	3.541
F		0.639	0.174	0.367	0.380	0.640	0.655	0.546	0.459
species		liddicoatite	elbaite	elbaite	elbaite	F-elbaite	F-elbaite	F-elbaite	elbaite

Oxides	12j1-5	13k1-1	13k1-2	13k1-3	13k1-4	13k1-5	13l1-1	13l1-2
sample	pink red	red purple	red purple	red purple	red purple	red purple	pink red	pink red
color	38.28	37.61	38.18	37.87	38.31	38.41	38.38	38.51
SiO ₂	0.00	0.00	0.02	0.00	0.00	0.00	0.00	0.00
TiO ₂	11.08	11.03	11.17	11.07	11.15	11.17	11.07	11.10
Al ₂ O ₃	39.81	40.27	40.40	40.13	40.21	40.43	40.57	40.63
Bi ₂ O ₃	0.01	0.00	0.01	0.01	0.00	0.00	0.01	0.01
V ₂ O ₃	0.00	0.00	0.00	0.00	0.00	0.00	0.00	0.00
FeO	0.08	0.02	0.05	0.03	0.02	0.00	0.04	0.04
MnO	0.94	0.38	0.37	0.34	0.37	0.33	0.10	0.08
MgO	0.00	0.00	0.00	0.00	0.00	0.00	0.00	0.00
CaO	2.10	2.81	2.94	2.82	2.88	2.76	1.23	1.21
Li ₂ O calc.	2.39	2.44	2.54	2.50	2.54	2.51	2.34	2.37
Na ₂ O	1.44	0.91	1.05	1.04	1.00	0.97	1.48	1.59
K ₂ O	0.01	0.00	0.00	0.00	0.03	0.00	0.05	0.00
H ₂ O calc.	3.45	3.25	3.27	3.21	3.26	3.32	3.23	3.23
F	0.80	1.18	1.23	1.28	1.25	1.12	1.24	1.27
Sub-total	100.37	99.89	101.23	100.31	101.02	101.03	99.73	100.04
O=F	-0.34	-0.50	-0.52	-0.54	-0.53	-0.47	-0.52	-0.53
Total	100.03	99.40	100.71	99.77	100.50	100.56	99.21	99.50
Ions (apfu)								
T: Si	6.002	5.924	5.941	5.945	5.969	5.974	6.024	6.027
Al	0.000	0.076	0.059	0.055	0.031	0.026	0.000	0.000
B: B	3.000	3.000	3.000	3.000	3.000	3.000	3.000	3.000
Z: Al	6.000	6.000	6.000	6.000	6.000	6.000	6.000	6.000
Y: Al	1.357	1.399	1.350	1.370	1.354	1.385	1.506	1.495
Ti	0.000	0.000	0.002	0.000	0.000	0.000	0.000	0.000
Bi	0.000	0.000	0.000	0.000	0.000	0.000	0.000	0.000
V	0.000	0.000	0.000	0.000	0.000	0.000	0.000	0.000
Fe ²⁺	0.010	0.003	0.006	0.003	0.002	0.001	0.005	0.005
Mn ²⁺	0.125	0.050	0.049	0.045	0.048	0.043	0.013	0.011
Mg	0.000	0.000	0.000	0.000	0.000	0.000	0.000	0.000
Li	1.507	1.547	1.592	1.581	1.595	1.571	1.476	1.489
X: Ca	0.352	0.474	0.490	0.474	0.481	0.460	0.207	0.202
Na	0.437	0.278	0.317	0.317	0.302	0.291	0.450	0.484
K	0.002	0.000	0.000	0.000	0.007	0.000	0.010	0.000
□ (vac.)	0.210	0.248	0.194	0.208	0.210	0.248	0.334	0.314
OH	3.604	3.412	3.394	3.365	3.384	3.448	3.385	3.371
F	0.396	0.588	0.605	0.634	0.616	0.552	0.615	0.629
species	elbaite	liddicoatite	liddicoatite	liddicoatite	liddicoatite	liddicoatite	F-elbaite	F-elbaite

Oxides	13I1-3	13I1-4	13I1-5	13m1-1	13m1-2	13m1-3	13m1-5	14n1-1
sample	pink red	pink red	pink red	pink	pink	pink	pink	dk red pi
color	38.43	38.46	38.46	38.29	38.30	38.55	38.38	38.37
SiO ₂	0.00	0.00	0.00	0.00	0.00	0.00	0.00	0.00
TiO ₂	11.11	11.06	11.05	11.22	11.24	11.18	11.16	10.97
Al ₂ O ₃	40.73	40.62	40.37	40.66	40.74	40.23	40.46	39.42
Bi ₂ O ₃	0.00	0.01	0.00	0.01	0.01	0.01	0.01	0.02
V ₂ O ₃	0.00	0.00	0.00	0.01	0.00	0.00	0.02	0.01
FeO	0.03	0.00	0.03	0.05	0.09	0.04	0.08	0.04
MnO	0.09	0.13	0.09	0.16	0.17	0.17	0.16	2.07
MgO	0.00	0.00	0.00	0.00	0.00	0.00	0.00	0.00
CaO	1.19	1.20	1.16	3.17	3.23	2.96	2.83	0.02
Li ₂ O calc.	2.34	2.31	2.37	2.60	2.60	2.58	2.50	2.13
Na ₂ O	1.65	1.17	1.43	0.96	0.92	0.92	0.80	2.22
K ₂ O	0.01	0.05	0.00	0.01	0.02	0.01	0.00	0.01
H ₂ O calc.	3.20	3.21	3.25	3.30	3.29	3.25	3.27	3.21
F	1.33	1.28	1.18	1.20	1.23	1.28	1.23	1.21
Sub-total	100.11	99.50	99.41	101.63	101.85	101.18	100.90	99.70
O=F	-0.56	-0.54	-0.50	-0.51	-0.52	-0.54	-0.52	-0.51
Total	99.55	98.97	98.91	101.13	101.33	100.64	100.38	99.19
Ions (apfu)								
T: Si	6.015	6.042	6.048	5.930	5.922	5.991	5.976	6.076
Al	0.000	0.000	0.000	0.070	0.078	0.009	0.024	0.000
B: B	3.000	3.000	3.000	3.000	3.000	3.000	3.000	3.000
Z: Al	6.000	6.000	6.000	6.000	6.000	6.000	6.000	6.000
Y: Al	1.513	1.522	1.482	1.351	1.347	1.359	1.400	1.359
Ti	0.000	0.000	0.000	0.000	0.000	0.000	0.000	0.000
Bi	0.000	0.000	0.000	0.001	0.000	0.000	0.000	0.001
V	0.000	0.000	0.000	0.001	0.000	0.000	0.002	0.001
Fe ²⁺	0.003	0.000	0.004	0.006	0.011	0.005	0.011	0.005
Mn ²⁺	0.012	0.018	0.012	0.022	0.022	0.022	0.021	0.277
Mg	0.000	0.000	0.000	0.000	0.000	0.000	0.000	0.000
Li	1.472	1.461	1.501	1.621	1.620	1.614	1.565	1.357
X: Ca	0.199	0.202	0.195	0.526	0.535	0.493	0.473	0.003
Na	0.501	0.356	0.437	0.287	0.275	0.277	0.243	0.683
K	0.001	0.010	0.000	0.001	0.005	0.002	0.000	0.003
□ (vac.)	0.299	0.432	0.368	0.186	0.185	0.228	0.285	0.312
OH	3.341	3.365	3.414	3.412	3.397	3.372	3.394	3.394
F	0.658	0.635	0.586	0.588	0.603	0.628	0.606	0.606
species	F-elbaite	F-rossman	F-elbaite	Iiddicoatite	Iiddicoatite	Iiddicoatite	Iiddicoatite	F-elbaite

Oxides	14n1-2	14n1-3	14n1-4	14n1-5	14o1-1	14o1-2	14o1-3	14o1-4
sample	dk red pi	dk red pi	dk red pi	dk red pi	pink	pink	pink	pink
color	38.51	38.27	38.40	38.21	38.21	38.04	38.15	38.04
SiO ₂	0.00	0.00	0.00	0.00	0.00	0.00	0.00	0.00
TiO ₂	11.00	10.93	10.98	10.93	11.21	11.14	11.17	11.13
Al ₂ O ₃	39.43	39.29	39.42	39.40	40.36	39.96	40.10	40.03
Bi ₂ O ₃	0.00	0.00	0.00	0.00	0.01	0.01	0.00	0.01
V ₂ O ₃	0.01	0.00	0.00	0.00	0.00	0.00	0.00	0.00
FeO	0.00	0.00	0.04	0.00	0.00	0.01	0.03	0.00
MnO	2.05	1.95	1.93	1.82	0.43	0.39	0.42	0.34
MgO	0.00	0.00	0.00	0.00	0.00	0.00	0.00	0.00
CaO	0.01	0.02	0.01	0.02	3.78	3.84	3.77	3.66
Li ₂ O calc.	2.17	2.15	2.17	2.15	2.63	2.66	2.64	2.63
Na ₂ O	2.25	2.14	2.29	2.25	0.53	0.57	0.58	0.59
K ₂ O	0.00	0.00	0.00	0.00	0.00	0.00	0.00	0.04
H ₂ O calc.	3.30	3.29	3.42	3.38	3.30	3.25	3.27	3.29
F	1.04	1.02	0.77	0.83	1.19	1.25	1.23	1.17
Sub-total	99.77	99.05	99.41	98.99	101.65	101.13	101.37	100.93
O=F	-0.44	-0.43	-0.32	-0.35	-0.50	-0.53	-0.52	-0.49
Total	99.34	98.62	99.09	98.64	101.15	100.60	100.85	100.44
Ions (apfu)								
T: Si	6.086	6.085	6.080	6.074	5.925	5.933	5.935	5.938
Al	0.000	0.000	0.000	0.000	0.075	0.067	0.065	0.062
B: B	3.000	3.000	3.000	3.000	3.000	3.000	3.000	3.000
Z: Al	6.000	6.000	6.000	6.000	6.000	6.000	6.000	6.000
Y: Al	1.344	1.364	1.357	1.381	1.301	1.279	1.288	1.303
Ti	0.000	0.000	0.000	0.000	0.000	0.000	0.000	0.000
Bi	0.000	0.000	0.000	0.000	0.000	0.000	0.000	0.000
V	0.001	0.000	0.000	0.000	0.000	0.000	0.000	0.000
Fe ²⁺	0.000	0.001	0.005	0.001	0.000	0.001	0.004	0.000
Mn ²⁺	0.274	0.263	0.258	0.245	0.057	0.052	0.055	0.045
Mg	0.000	0.000	0.000	0.000	0.000	0.000	0.000	0.000
Li	1.381	1.373	1.381	1.374	1.642	1.668	1.654	1.652
X: Ca	0.002	0.004	0.002	0.003	0.628	0.642	0.628	0.613
Na	0.688	0.659	0.701	0.692	0.161	0.174	0.176	0.179
K	0.001	0.000	0.000	0.001	0.000	0.000	0.000	0.007
□ (vac.)	0.309	0.337	0.297	0.304	0.212	0.185	0.196	0.201
OH	3.482	3.488	3.614	3.582	3.417	3.381	3.393	3.424
F	0.518	0.512	0.386	0.418	0.583	0.619	0.607	0.576
species	F-elbaite	F-elbaite	elbaite	elbaite	liddicoatite	liddicoatite	liddicoatite	liddicoatite

Oxides								
sample	15q1-3	15q1-4	15q1-5	15r1-1	15r1-2	15r1-3	15r1-4	15r1-5
color	pale y grn	pale y grn	pale y grn	blue green	blue green	blue green	blue green	blue green
SiO ₂	37.85	37.85	37.61	38.17	38.04	38.10	38.18	38.11
TiO ₂	0.00	0.00	0.00	0.00	0.00	0.01	0.00	0.00
B ₂ O ₃ calc.	10.87	10.91	10.86	11.11	11.07	11.07	11.11	11.08
Al ₂ O ₃	39.00	39.12	39.12	40.07	39.94	39.97	40.05	39.93
Bi ₂ O ₃	0.01	0.00	0.02	0.00	0.01	0.01	0.01	0.01
V ₂ O ₃	0.00	0.00	0.00	0.00	0.00	0.00	0.00	0.00
FeO	0.48	0.53	0.50	0.58	0.54	0.52	0.60	0.48
MnO	1.64	1.72	1.68	0.28	0.28	0.27	0.28	0.28
MgO	0.00	0.00	0.00	0.00	0.00	0.00	0.00	0.00
CaO	0.55	0.52	0.54	2.39	2.26	2.30	2.34	2.27
Li ₂ O calc.	2.12	2.12	2.06	2.43	2.43	2.41	2.42	2.45
Na ₂ O	2.04	2.33	2.22	1.32	1.46	1.30	1.33	1.48
K ₂ O	0.00	0.01	0.01	0.02	0.01	0.01	0.01	0.01
H ₂ O calc.	3.15	3.19	3.20	3.23	3.24	3.26	3.24	3.23
F	1.28	1.21	1.16	1.28	1.22	1.18	1.24	1.25
Sub-total	98.97	99.52	98.98	100.87	100.51	100.41	100.81	100.58
O=F	-0.54	-0.51	-0.49	-0.54	-0.51	-0.50	-0.52	-0.53
Total	98.44	99.01	98.49	100.33	100.00	99.92	100.29	100.06
Ions (apfu)								
T: Si	6.050	6.029	6.018	5.970	5.970	5.979	5.974	5.976
Al	0.000	0.000	0.000	0.030	0.030	0.021	0.026	0.024
B: B	3.000	3.000	3.000	3.000	3.000	3.000	3.000	3.000
Z: Al	6.000	6.000	6.000	6.000	6.000	6.000	6.000	6.000
Y: Al	1.348	1.342	1.378	1.356	1.358	1.371	1.360	1.355
Ti	0.000	0.000	0.000	0.000	0.000	0.001	0.000	0.000
Bi	0.000	0.000	0.001	0.000	0.000	0.000	0.000	0.000
V	0.000	0.000	0.000	0.000	0.000	0.000	0.000	0.000
Fe ²⁺	0.064	0.070	0.067	0.076	0.071	0.068	0.079	0.063
Mn ²⁺	0.222	0.232	0.228	0.036	0.037	0.036	0.037	0.037
Mg	0.000	0.000	0.000	0.000	0.000	0.000	0.000	0.000
Li	1.366	1.355	1.327	1.531	1.534	1.523	1.523	1.544
X: Ca	0.093	0.088	0.093	0.401	0.380	0.387	0.392	0.381
Na	0.631	0.720	0.688	0.399	0.445	0.395	0.403	0.449
K	0.000	0.003	0.001	0.004	0.002	0.002	0.002	0.002
□ (vac.)	0.276	0.189	0.218	0.196	0.173	0.216	0.202	0.167
OH	3.355	3.391	3.415	3.368	3.394	3.413	3.386	3.382
F	0.646	0.609	0.585	0.632	0.605	0.587	0.614	0.618
species	F-elbaite	F-elbaite	F-elbaite	Iiddicoatite	F-elbaite	F-elbaite	F-elbaite	F-elbaite

Oxides	15s1-1	15s1-1	15s1-2	15s1-3	15s1-4	16t1-1	16t1-2	16t1-3
sample	15s1-1	15s1-1	15s1-2	15s1-3	15s1-4	16t1-1	16t1-2	16t1-3
color	pink	pink	pink	pl gray b	pl gray b	yel green	yel green	yel green
SiO ₂	38.51	38.28	37.90	37.61	38.04	37.87	38.05	37.97
TiO ₂	0.00	0.00	0.00	0.00	0.00	0.00	0.00	0.00
B ₂ O ₃ calc.	11.10	11.06	11.10	11.06	11.17	11.20	11.12	11.16
Al ₂ O ₃	39.85	39.89	39.73	39.94	39.86	40.11	39.61	39.89
Bi ₂ O ₃	0.01	0.01	0.01	0.01	0.01	0.00	0.00	0.00
V ₂ O ₃	0.00	0.00	0.00	0.00	0.00	0.00	0.00	0.01
FeO	0.08	0.10	0.10	0.22	0.59	0.63	0.58	0.69
MnO	0.47	0.41	0.54	0.39	0.42	0.51	0.43	0.52
MgO	0.00	0.00	0.01	0.00	0.00	0.00	0.00	0.00
CaO	1.88	2.08	2.94	2.83	3.14	3.52	3.28	3.29
Li ₂ O calc.	2.50	2.44	2.61	2.54	2.61	2.62	2.59	2.56
Na ₂ O	1.51	1.27	1.49	1.42	1.44	1.23	1.14	1.14
K ₂ O	0.05	0.01	0.01	0.00	0.00	0.01	0.00	0.00
H ₂ O calc.	3.22	3.26	3.21	3.19	3.22	3.36	3.43	3.33
F	1.28	1.17	1.31	1.31	1.34	1.06	0.85	1.09
Sub-total	100.47	99.96	100.95	100.54	101.82	102.11	101.08	101.65
O=F	-0.54	-0.49	-0.55	-0.55	-0.56	-0.44	-0.36	-0.46
Total	99.93	99.47	100.40	99.98	101.26	101.67	100.72	101.19
Ions (apfu)								
T: Si	6.030	6.017	5.936	5.911	5.921	5.878	5.945	5.915
Al	0.000	0.000	0.064	0.089	0.079	0.122	0.055	0.085
B: B	3.000	3.000	3.000	3.000	3.000	3.000	3.000	3.000
Z: Al	6.000	6.000	6.000	6.000	6.000	6.000	6.000	6.000
Y: Al	1.353	1.389	1.269	1.311	1.233	1.215	1.240	1.239
Ti	0.000	0.000	0.000	0.000	0.000	0.000	0.000	0.000
Bi	0.000	0.000	0.000	0.000	0.001	0.000	0.000	0.000
V	0.000	0.000	0.000	0.000	0.000	0.000	0.000	0.001
Fe ²⁺	0.010	0.014	0.013	0.029	0.076	0.082	0.076	0.090
Mn ²⁺	0.063	0.055	0.071	0.052	0.055	0.067	0.056	0.068
Mg	0.000	0.000	0.001	0.000	0.000	0.000	0.000	0.000
Li	1.573	1.542	1.645	1.607	1.636	1.636	1.628	1.602
X: Ca	0.316	0.349	0.494	0.477	0.523	0.585	0.549	0.549
Na	0.460	0.387	0.451	0.432	0.436	0.370	0.345	0.345
K	0.010	0.001	0.002	0.001	0.000	0.002	0.000	0.000
□ (vac.)	0.215	0.263	0.053	0.090	0.041	0.043	0.106	0.105
OH	3.366	3.417	3.351	3.349	3.340	3.482	3.579	3.462
F	0.634	0.583	0.649	0.651	0.660	0.518	0.421	0.538
species	F-elbaite	F-elbaite	Iiddicoatite	Iiddicoatite	Iiddicoatite	Iiddicoatite	OH-Iiddi	Iiddicoatite

Oxides	17w1-4	17w1-5	17x1-1	17x1-3	17x1-4
sample	17w1-4	17w1-5	17x1-1	17x1-3	17x1-4
color	pink red	pink red	pink	pink	pink
SiO ₂	38.37	38.07	38.00	38.10	38.04
TiO ₂	0.10	0.00	0.00	0.00	0.00
B ₂ O ₃ calc.	11.18	11.24	11.19	11.20	11.23
Al ₂ O ₃	39.97	40.40	40.13	40.05	40.35
Bi ₂ O ₃	0.00	0.00	0.00	0.00	0.00
V ₂ O ₃	0.00	0.00	0.00	0.01	0.00
FeO	0.01	0.00	0.00	0.00	0.00
MnO	0.16	0.14	0.07	0.11	0.13
MgO	0.00	0.00	0.00	0.00	0.00
CaO	3.23	3.63	3.63	3.59	3.56
Li ₂ O calc.	2.68	2.79	2.79	2.79	2.78
Na ₂ O	0.94	1.12	1.08	1.11	1.24
K ₂ O	0.17	0.30	0.26	0.25	0.19
H ₂ O calc.	3.44	3.44	3.44	3.39	3.44
F	0.89	0.93	0.88	1.00	0.92
Sub-total	101.12	102.06	101.47	101.61	101.87
O=F	-0.37	-0.39	-0.37	-0.42	-0.39
Total	100.74	101.67	101.10	101.19	101.48
Ions (apfu)					
T: Si	5.967	5.886	5.903	5.915	5.890
Al	0.033	0.114	0.097	0.085	0.110
B: B	3.000	3.000	3.000	3.000	3.000
Z: Al	6.000	6.000	6.000	6.000	6.000
Y: Al	1.292	1.248	1.251	1.244	1.251
Ti	0.012	0.000	0.000	0.000	0.000
Bi	0.000	0.000	0.000	0.000	0.000
V	0.000	0.000	0.000	0.002	0.000
Fe ²⁺	0.001	0.000	0.000	0.000	0.000
Mn ²⁺	0.021	0.018	0.009	0.015	0.018
Mg	0.000	0.000	0.000	0.000	0.000
Li	1.675	1.734	1.740	1.740	1.731
X: Ca	0.538	0.601	0.605	0.597	0.591
Na	0.283	0.336	0.324	0.335	0.371
K	0.034	0.060	0.051	0.050	0.037
□ (vac.)	0.145	0.002	0.020	0.018	0.002
OH	3.564	3.544	3.567	3.509	3.551
F	0.437	0.456	0.434	0.491	0.449
species	OH-liddi	OH-liddi	OH-liddi	OH-liddi	OH-liddi

Table 3: Microprobe analyses, blue Nigerian tourmaline.

Oxides	Lila-1-1	Lila-1-2	Lila-1-3	Lila-1-4	Lila-1-5	Lila-1-6	Lila-1-7	Lila-1-8
sample color	blue							
SiO ₂	37.60	37.42	37.22	37.57	37.44	37.59	37.51	37.90
TiO ₂	0.00	0.00	0.00	0.00	0.00	0.00	0.00	0.00
B ₂ O ₃ calc.	10.89	10.84	10.83	10.91	10.88	10.87	10.87	10.89
Al ₂ O ₃	38.89	38.88	38.77	39.03	38.89	38.81	38.89	38.86
Bi ₂ O ₃	0.00	0.00	0.00	0.00	0.00	0.00	0.00	0.00
V ₂ O ₃	0.00	0.06	0.00	0.00	0.00	0.08	0.00	0.00
FeO	2.22	2.11	2.31	2.09	2.14	2.09	2.21	1.99
MnO	1.44	1.27	1.40	1.38	1.53	1.26	1.29	1.27
MgO	0.00	0.00	0.00	0.00	0.00	0.00	0.00	0.00
CaO	0.52	0.32	0.41	0.47	0.49	0.35	0.34	0.36
CuO	0.00	0.00	0.00	0.00	0.00	0.00	0.00	0.00
PbO	0.00	0.00	0.00	0.00	0.00	0.00	0.00	0.00
ZnO	0.02	0.05	0.05	0.02	0.04	0.02	0.00	0.03
Li ₂ O calc.	1.86	1.85	1.84	1.90	1.87	1.90	1.88	1.95
Na ₂ O	2.28	2.36	2.47	2.44	2.45	2.40	2.47	2.04
K ₂ O	0.00	0.02	0.02	0.00	0.00	0.01	0.02	0.03
H ₂ O calc.	3.24	3.33	3.25	3.38	3.26	3.36	3.26	3.34
F	1.09	0.88	1.02	0.82	1.04	0.82	1.03	0.88
Sub-total	100.04	99.37	99.59	100.00	100.03	99.55	99.78	99.55
O=F	-0.46	-0.37	-0.43	-0.34	-0.44	-0.34	-0.44	-0.37
Total	99.59	99.01	99.16	99.66	99.59	99.21	99.34	99.18
Ions (apfu)								
T: Si	6.000	5.997	5.973	5.987	5.979	6.010	5.996	6.047
Al	0.000	0.003	0.027	0.013	0.021	0.000	0.004	0.000
B: B	3.000	3.000	3.000	3.000	3.000	3.000	3.000	3.000
Z: Al	6.000	6.000	6.000	6.000	6.000	6.000	6.000	6.000
Y: Al	1.313	1.340	1.305	1.317	1.299	1.312	1.323	1.306
Ti	0.000	0.000	0.000	0.000	0.000	0.000	0.000	0.000
Bi	0.000	0.000	0.000	0.000	0.000	0.000	0.000	0.000
V	0.000	0.007	0.000	0.000	0.000	0.010	0.000	0.000
Fe ²⁺	0.296	0.283	0.310	0.278	0.286	0.280	0.296	0.266
Mn ²⁺	0.195	0.173	0.191	0.186	0.207	0.171	0.175	0.172
Mg	0.000	0.000	0.000	0.000	0.000	0.000	0.000	0.000
Cu	0.000	0.000	0.000	0.000	0.000	0.000	0.000	0.000
Pb	0.000	0.000	0.000	0.000	0.000	0.000	0.000	0.000
Zn	0.003	0.006	0.006	0.002	0.005	0.002	0.000	0.004
Li	1.193	1.192	1.188	1.216	1.203	1.224	1.207	1.252
X: Ca	0.088	0.055	0.071	0.079	0.083	0.059	0.058	0.061
Na	0.706	0.734	0.767	0.755	0.759	0.744	0.766	0.632
K	0.000	0.004	0.003	0.000	0.000	0.001	0.003	0.006
□ (vac.)	0.206	0.207	0.159	0.166	0.158	0.196	0.172	0.301
OH	3.452	3.555	3.480	3.588	3.476	3.588	3.477	3.557
F	0.548	0.445	0.520	0.411	0.524	0.412	0.523	0.442
species	F-elbaite	elbaite	F-elbaite	elbaite	F-elbaite	elbaite	F-elbaite	elbaite

Oxides	Lila-3-1	Lila-3-2	Lila-3-3	Lila-3-4	Lila-3-5	Lila-3-6	Lila-3-7	Lila-3-8
sample								
color	blue	blue	blue	blue	blue	blue	blue	blue
SiO ₂	37.18	36.92	36.88	36.99	37.01	37.10	37.08	37.21
TiO ₂	0.00	0.00	0.00	0.00	0.00	0.00	0.00	0.00
B ₂ O ₃ calc.	10.93	10.82	10.82	10.82	10.85	10.83	10.83	10.88
Al ₂ O ₃	39.13	38.86	38.62	38.54	38.68	38.54	38.45	38.88
Bi ₂ O ₃	0.01	0.00	0.04	0.00	0.00	0.03	0.01	0.00
V ₂ O ₃	0.00	0.00	0.00	0.03	0.00	0.03	0.00	0.00
FeO	4.51	3.91	4.65	4.61	4.42	4.36	4.68	4.37
MnO	1.32	1.26	1.18	1.21	1.34	1.27	1.24	1.20
MgO	0.00	0.00	0.00	0.00	0.00	0.00	0.00	0.00
CaO	0.17	0.15	0.13	0.13	0.13	0.15	0.14	0.12
CuO	0.00	0.00	0.00	0.00	0.00	0.00	0.00	0.00
PbO	0.00	0.00	0.00	0.00	0.00	0.00	0.00	0.00
ZnO	0.11	0.08	0.12	0.10	0.07	0.05	0.06	0.06
Li ₂ O calc.	1.52	1.56	1.49	1.50	1.52	1.54	1.52	1.53
Na ₂ O	2.46	2.37	2.41	2.42	2.47	2.39	2.45	2.37
K ₂ O	0.02	0.00	0.00	0.00	0.03	0.03	0.02	0.00
H ₂ O calc.	3.24	3.32	3.29	3.28	3.38	3.32	3.26	3.26
F	1.13	0.88	0.93	0.97	0.77	0.89	1.00	1.04
Sub-total	101.71	100.13	100.56	100.58	100.66	100.53	100.73	100.93
O=F	-0.47	-0.37	-0.39	-0.41	-0.33	-0.38	-0.42	-0.44
Total	101.24	99.77	100.17	100.18	100.34	100.15	100.31	100.49
Ions (apfu)								
T: Si	5.910	5.930	5.926	5.939	5.931	5.951	5.948	5.944
Al	0.090	0.070	0.074	0.061	0.069	0.049	0.052	0.056
B: B	3.000	3.000	3.000	3.000	3.000	3.000	3.000	3.000
Z: Al	6.000	6.000	6.000	6.000	6.000	6.000	6.000	6.000
Y: Al	1.240	1.287	1.238	1.231	1.235	1.238	1.218	1.264
Ti	0.000	0.000	0.000	0.000	0.000	0.000	0.000	0.000
Bi	0.001	0.000	0.002	0.000	0.000	0.001	0.000	0.000
V	0.000	0.000	0.000	0.004	0.000	0.003	0.000	0.000
Fe ²⁺	0.600	0.525	0.624	0.619	0.593	0.585	0.628	0.584
Mn ²⁺	0.177	0.172	0.161	0.164	0.182	0.172	0.168	0.163
Mg	0.000	0.000	0.000	0.000	0.000	0.000	0.000	0.000
Cu	0.000	0.000	0.000	0.000	0.000	0.000	0.000	0.000
Pb	0.000	0.000	0.000	0.000	0.000	0.000	0.000	0.000
Zn	0.013	0.009	0.014	0.011	0.008	0.006	0.007	0.007
Li	0.969	1.007	0.961	0.970	0.982	0.994	0.978	0.982
X: Ca	0.029	0.026	0.023	0.022	0.023	0.026	0.024	0.021
Na	0.757	0.739	0.750	0.752	0.766	0.744	0.762	0.732
K	0.004	0.000	0.000	0.001	0.005	0.005	0.003	0.001
□ (vac.)	0.209	0.235	0.226	0.225	0.206	0.225	0.211	0.245
OH	3.433	3.555	3.526	3.510	3.608	3.547	3.492	3.473
F	0.567	0.444	0.474	0.490	0.392	0.453	0.508	0.527
species	F-elbaite	elbaite	elbaite	elbaite	elbaite	elbaite	F-elbaite	F-elbaite

Oxides	Lila-4-1	Lila-4-2	Lila-4-3	Lila-4-4	Lila-4-5	Lila-4-6	Lila-4-7	Lila-4-8
sample								
color	blue	blue	blue	blue	blue	blue	blue	blue
SiO ₂	37.28	37.34	37.34	37.41	37.21	37.33	37.43	37.32
TiO ₂	0.00	0.00	0.00	0.00	0.00	0.00	0.00	0.00
B ₂ O ₃ calc.	10.85	10.88	10.89	10.89	10.89	10.91	10.91	10.89
Al ₂ O ₃	38.75	39.00	38.89	38.80	39.11	38.89	38.95	38.77
Bi ₂ O ₃	0.00	0.00	0.03	0.00	0.02	0.00	0.00	0.06
V ₂ O ₃	0.00	0.00	0.00	0.00	0.00	0.07	0.00	0.00
FeO	3.27	3.63	3.70	3.67	3.60	3.85	3.81	3.61
MnO	1.19	1.09	1.06	1.14	1.06	1.11	1.10	1.09
MgO	0.00	0.00	0.00	0.01	0.00	0.00	0.00	0.00
CaO	0.35	0.30	0.31	0.32	0.31	0.33	0.32	0.29
CuO	0.00	0.00	0.00	0.00	0.00	0.00	0.00	0.00
PbO	0.00	0.00	0.00	0.01	0.00	0.00	0.00	0.00
ZnO	0.01	0.03	0.08	0.07	0.07	0.08	0.07	0.05
Li ₂ O calc.	1.73	1.65	1.69	1.68	1.67	1.67	1.67	1.74
Na ₂ O	2.38	2.25	2.42	2.38	2.36	2.44	2.33	2.62
K ₂ O	0.02	0.01	0.01	0.00	0.00	0.01	0.04	0.01
H ₂ O calc.	3.33	3.36	3.43	3.45	3.37	3.24	3.31	3.36
F	0.86	0.84	0.70	0.65	0.82	1.10	0.97	0.84
Sub-total	100.03	100.39	100.55	100.49	100.48	101.01	100.90	100.66
O=F	-0.36	-0.35	-0.29	-0.27	-0.34	-0.46	-0.41	-0.36
Total	99.67	100.03	100.25	100.22	100.13	100.55	100.49	100.30
Ions (apfu)								
T: Si	5.970	5.963	5.957	5.969	5.939	5.948	5.960	5.956
Al	0.030	0.037	0.043	0.031	0.061	0.052	0.040	0.044
B: B	3.000	3.000	3.000	3.000	3.000	3.000	3.000	3.000
Z: Al	6.000	6.000	6.000	6.000	6.000	6.000	6.000	6.000
Y: Al	1.283	1.301	1.268	1.265	1.296	1.250	1.270	1.246
Ti	0.000	0.000	0.000	0.000	0.000	0.000	0.000	0.000
Bi	0.000	0.000	0.001	0.000	0.001	0.000	0.000	0.003
V	0.000	0.000	0.000	0.000	0.000	0.009	0.000	0.000
Fe ²⁺	0.438	0.485	0.494	0.490	0.481	0.512	0.507	0.481
Mn ²⁺	0.162	0.147	0.144	0.155	0.143	0.149	0.149	0.147
Mg	0.000	0.000	0.000	0.002	0.000	0.000	0.000	0.000
Cu	0.000	0.000	0.000	0.000	0.000	0.000	0.000	0.000
Pb	0.000	0.000	0.000	0.001	0.000	0.000	0.000	0.000
Zn	0.001	0.004	0.009	0.009	0.008	0.009	0.008	0.006
Li	1.116	1.063	1.084	1.078	1.071	1.070	1.067	1.116
X: Ca	0.060	0.050	0.053	0.055	0.052	0.056	0.055	0.050
Na	0.740	0.698	0.750	0.735	0.731	0.752	0.719	0.811
K	0.003	0.001	0.002	0.001	0.001	0.001	0.009	0.002
□ (vac.)	0.197	0.251	0.195	0.209	0.216	0.190	0.217	0.137
OH	3.562	3.574	3.647	3.674	3.589	3.447	3.511	3.574
F	0.438	0.426	0.353	0.326	0.411	0.553	0.489	0.426
species	elbaite	elbaite	elbaite	elbaite	elbaite	F-elbaite	elbaite	elbaite

Oxides	Lila-5-1	Lila-5-2	Lila-5-3	Lila-5-4	Lila-5-5	Lila-5-6	Lila-5-7	Lila-5-8
sample								
color	blue	blue	blue	blue	blue	blue	blue	blue
SiO ₂	37.20	37.28	37.37	37.09	37.06	37.18	37.08	37.22
TiO ₂	0.00	0.00	0.01	0.00	0.00	0.00	0.00	0.00
B ₂ O ₃ calc.	10.88	10.88	10.89	10.85	10.81	10.83	10.81	10.82
Al ₂ O ₃	38.66	38.56	38.54	38.50	38.32	38.47	38.46	38.34
Bi ₂ O ₃	0.03	0.08	0.00	0.08	0.00	0.02	0.00	0.00
V ₂ O ₃	0.00	0.00	0.00	0.00	0.00	0.00	0.00	0.00
FeO	4.85	4.68	4.77	4.84	4.59	4.56	4.49	4.43
MnO	1.00	1.10	1.03	1.04	0.96	0.98	1.09	0.98
MgO	0.00	0.00	0.00	0.00	0.00	0.00	0.00	0.00
CaO	0.25	0.25	0.27	0.24	0.25	0.24	0.27	0.25
CuO	0.00	0.00	0.00	0.00	0.00	0.02	0.00	0.00
PbO	0.00	0.00	0.00	0.00	0.00	0.00	0.00	0.00
ZnO	0.06	0.12	0.09	0.09	0.13	0.12	0.17	0.14
Li ₂ O calc.	1.55	1.55	1.56	1.53	1.58	1.54	1.53	1.57
Na ₂ O	2.44	2.40	2.36	2.39	2.47	2.28	2.23	2.26
K ₂ O	0.01	0.00	0.00	0.01	0.01	0.00	0.01	0.03
H ₂ O calc.	3.30	3.30	3.27	3.32	3.30	3.39	3.33	3.42
F	0.97	0.97	1.03	0.88	0.90	0.74	0.86	0.65
Sub-total	101.19	101.16	101.17	100.85	100.40	100.35	100.31	100.11
O=F	-0.41	-0.41	-0.43	-0.37	-0.38	-0.31	-0.36	-0.27
Total	100.79	100.76	100.74	100.48	100.02	100.04	99.95	99.84
Ions (apfu)								
T: Si	5.940	5.954	5.964	5.942	5.956	5.966	5.958	5.979
Al	0.060	0.046	0.036	0.058	0.044	0.034	0.042	0.021
B: B	3.000	3.000	3.000	3.000	3.000	3.000	3.000	3.000
Z: Al	6.000	6.000	6.000	6.000	6.000	6.000	6.000	6.000
Y: Al	1.214	1.212	1.214	1.212	1.213	1.242	1.241	1.239
Ti	0.000	0.000	0.001	0.000	0.000	0.000	0.000	0.000
Bi	0.001	0.003	0.000	0.003	0.000	0.001	0.000	0.000
V	0.000	0.000	0.000	0.000	0.000	0.000	0.000	0.000
Fe ²⁺	0.648	0.625	0.636	0.649	0.617	0.612	0.604	0.595
Mn ²⁺	0.135	0.149	0.140	0.141	0.131	0.134	0.148	0.134
Mg	0.000	0.000	0.000	0.000	0.000	0.000	0.000	0.000
Cu	0.000	0.000	0.000	0.000	0.000	0.002	0.000	0.000
Pb	0.000	0.000	0.000	0.000	0.000	0.000	0.000	0.000
Zn	0.007	0.014	0.010	0.011	0.016	0.014	0.020	0.017
Li	0.995	0.996	0.999	0.984	1.023	0.997	0.987	1.016
X: Ca	0.042	0.043	0.046	0.042	0.042	0.041	0.047	0.044
Na	0.755	0.743	0.729	0.741	0.770	0.708	0.693	0.705
K	0.002	0.000	0.000	0.002	0.001	0.000	0.002	0.006
□ (vac.)	0.200	0.214	0.225	0.215	0.187	0.251	0.258	0.245
OH	3.512	3.512	3.481	3.552	3.541	3.624	3.564	3.669
F	0.488	0.488	0.519	0.448	0.459	0.376	0.436	0.331
species	elbaite	elbaite	F-elbaite	elbaite	elbaite	elbaite	elbaite	elbaite

Oxides	Lila-7-1	Lila-7-2	Lila-7-3	Lila-7-4	Lila-7-5	Lila-7-6	Lila-7-7	Lila-7-8
sample								
color	blue							
SiO ₂	37.10	37.24	37.09	37.01	37.17	37.15	37.03	37.03
TiO ₂	0.00	0.00	0.00	0.00	0.00	0.00	0.00	0.00
B ₂ O ₃ calc.	10.83	10.88	10.83	10.81	10.85	10.84	10.82	10.85
Al ₂ O ₃	38.32	38.37	38.41	38.31	38.34	38.41	38.40	38.49
Bi ₂ O ₃	0.00	0.01	0.00	0.10	0.01	0.00	0.00	0.00
V ₂ O ₃	0.00	0.00	0.00	0.00	0.01	0.05	0.00	0.00
FeO	5.05	5.35	4.82	5.29	5.05	4.80	4.88	4.93
MnO	1.52	1.41	1.36	1.35	1.41	1.37	1.38	1.51
MgO	0.00	0.00	0.00	0.00	0.00	0.00	0.00	0.00
CaO	0.20	0.18	0.16	0.13	0.19	0.18	0.18	0.20
CuO	0.00	0.00	0.00	0.00	0.00	0.00	0.00	0.00
PbO	0.00	0.00	0.00	0.00	0.00	0.00	0.00	0.00
ZnO	0.09	0.09	0.14	0.11	0.10	0.10	0.10	0.09
Li ₂ O calc.	1.41	1.41	1.46	1.36	1.44	1.46	1.43	1.43
Na ₂ O	2.23	2.30	2.32	2.13	2.27	2.27	2.22	2.32
K ₂ O	0.04	0.05	0.01	0.04	0.05	0.03	0.00	0.02
H ₂ O calc.	3.33	3.23	3.29	3.19	3.33	3.35	3.29	3.33
F	0.86	1.10	0.94	1.14	0.88	0.84	0.93	0.86
Sub-total	100.97	101.61	100.85	100.98	101.08	100.85	100.66	101.07
O=F	-0.36	-0.46	-0.40	-0.48	-0.37	-0.35	-0.39	-0.36
Total	100.61	101.15	100.45	100.50	100.72	100.50	100.27	100.70
Ions (apfu)								
T: Si	5.950	5.951	5.950	5.949	5.954	5.954	5.950	5.932
Al	0.050	0.049	0.050	0.051	0.046	0.046	0.050	0.068
B: B	3.000	3.000	3.000	3.000	3.000	3.000	3.000	3.000
Z: Al	6.000	6.000	6.000	6.000	6.000	6.000	6.000	6.000
Y: Al	1.195	1.176	1.211	1.208	1.193	1.210	1.221	1.200
Ti	0.000	0.000	0.000	0.000	0.000	0.000	0.000	0.000
Bi	0.000	0.000	0.000	0.004	0.000	0.000	0.000	0.000
V	0.000	0.000	0.000	0.000	0.001	0.006	0.000	0.000
Fe ²⁺	0.677	0.714	0.646	0.711	0.676	0.644	0.656	0.661
Mn ²⁺	0.206	0.191	0.185	0.184	0.191	0.186	0.188	0.205
Mg	0.000	0.000	0.000	0.000	0.000	0.000	0.000	0.000
Cu	0.000	0.000	0.000	0.000	0.000	0.000	0.000	0.000
Pb	0.000	0.000	0.000	0.000	0.000	0.000	0.000	0.000
Zn	0.010	0.011	0.017	0.013	0.012	0.012	0.011	0.010
Li	0.912	0.908	0.941	0.879	0.926	0.942	0.924	0.923
X: Ca	0.034	0.030	0.028	0.023	0.032	0.031	0.030	0.034
Na	0.693	0.713	0.722	0.665	0.706	0.704	0.692	0.719
K	0.008	0.010	0.003	0.009	0.010	0.006	0.001	0.004
□ (vac.)	0.266	0.248	0.247	0.304	0.252	0.259	0.276	0.242
OH	3.566	3.443	3.522	3.422	3.557	3.576	3.529	3.564
F	0.434	0.557	0.478	0.578	0.443	0.424	0.471	0.436
species	elbaite	F-elbaite	elbaite	F-elbaite	elbaite	elbaite	elbaite	elbaite

Oxides	Lila-8-1	Lila-8-2	Lila-8-4	Lila-8-5	Lila-8-6	Lila-8-7	Lila-8-8	Lila-9-1
sample								
color	blue							
SiO ₂	37.03	37.18	37.10	37.09	37.04	37.12	36.82	37.09
TiO ₂	0.00	0.00	0.00	0.00	0.00	0.00	0.00	0.00
B ₂ O ₃ calc.	10.76	10.75	10.74	10.78	10.75	10.78	10.77	10.82
Al ₂ O ₃	38.37	38.24	38.41	38.64	38.42	38.51	38.68	38.43
Bi ₂ O ₃	0.00	0.09	0.00	0.11	0.03	0.00	0.01	0.04
V ₂ O ₃	0.00	0.00	0.00	0.00	0.00	0.00	0.00	0.00
FeO	3.93	3.70	3.69	3.74	3.86	3.87	3.93	4.92
MnO	0.51	0.46	0.46	0.49	0.46	0.51	0.47	0.99
MgO	0.00	0.00	0.00	0.00	0.00	0.00	0.00	0.01
CaO	0.37	0.34	0.32	0.34	0.38	0.36	0.38	0.26
CuO	0.00	0.00	0.00	0.00	0.00	0.00	0.00	0.00
PbO	0.00	0.00	0.00	0.00	0.00	0.00	0.00	0.00
ZnO	0.04	0.05	0.05	0.07	0.06	0.05	0.05	0.05
Li ₂ O calc.	1.70	1.75	1.70	1.69	1.70	1.70	1.69	1.49
Na ₂ O	2.21	2.15	2.08	2.13	2.15	2.22	2.31	2.18
K ₂ O	0.04	0.01	0.00	0.02	0.01	0.01	0.01	0.02
H ₂ O calc.	3.36	3.36	3.30	3.31	3.18	3.23	3.16	3.32
F	0.73	0.72	0.86	0.87	1.12	1.04	1.17	0.88
Sub-total	99.05	98.81	98.71	99.26	99.15	99.38	99.44	100.49
O=F	-0.31	-0.30	-0.36	-0.37	-0.47	-0.44	-0.49	-0.37
Total	98.74	98.51	98.34	98.89	98.68	98.95	98.95	100.12
Ions (apfu)								
T: Si	5.984	6.013	6.004	5.980	5.987	5.983	5.943	5.958
Al	0.016	0.000	0.000	0.020	0.013	0.017	0.057	0.042
B: B	3.000	3.000	3.000	3.000	3.000	3.000	3.000	3.000
Z: Al	6.000	6.000	6.000	6.000	6.000	6.000	6.000	6.000
Y: Al	1.292	1.289	1.326	1.323	1.306	1.300	1.300	1.232
Ti	0.000	0.000	0.000	0.000	0.000	0.000	0.000	0.000
Bi	0.000	0.004	0.000	0.004	0.001	0.000	0.000	0.002
V	0.000	0.000	0.000	0.000	0.000	0.000	0.000	0.000
Fe ²⁺	0.531	0.500	0.499	0.504	0.521	0.521	0.531	0.661
Mn ²⁺	0.070	0.063	0.063	0.066	0.064	0.070	0.064	0.134
Mg	0.000	0.000	0.000	0.000	0.000	0.000	0.000	0.001
Cu	0.000	0.000	0.000	0.000	0.000	0.000	0.000	0.000
Pb	0.000	0.000	0.000	0.000	0.000	0.000	0.000	0.000
Zn	0.005	0.005	0.006	0.008	0.007	0.005	0.005	0.006
Li	1.102	1.139	1.105	1.094	1.102	1.103	1.099	0.963
X: Ca	0.063	0.060	0.055	0.058	0.065	0.062	0.065	0.045
Na	0.693	0.675	0.652	0.665	0.675	0.695	0.723	0.678
K	0.008	0.002	0.000	0.005	0.002	0.001	0.001	0.004
□ (vac.)	0.236	0.263	0.293	0.272	0.258	0.242	0.210	0.273
OH	3.625	3.630	3.558	3.555	3.427	3.471	3.405	3.552
F	0.375	0.370	0.442	0.446	0.573	0.529	0.595	0.448
species	elbaite	elbaite	elbaite	elbaite	F-elbaite	F-elbaite	F-elbaite	elbaite

Nigerian tourmaline plots

Fig. 10, X-site Ca-vacancy-Na plot: The end-member ternary plot of X-site occupancy for the Nigerian suite of stones shows that the three principal species examined have a broad diversity of colors. Pink, red and green specimens plot within the elbaite, liddicoatite and rossmanite fields. Elbaites can be greenish-yellow (sample “i”) and reddish-purple stone “k1” is a liddicoatite. Bluish-gray stones are liddicoatites, whereas those that are colorless to near colorless may be elbaite or liddicoatite. The blue stones are elbaite.

Fig. 11, Y-site Mn-Ti-Fe plot: The chromophoric ternary plot shows that colorless to near colorless, pink, red, bluish-gray and reddish-purple stones plot principally in the Mn-field whereas the green and blue tourmaline falls in the Fe-field. Ti-bearing samples are pink and red and do not plot in the Ti-field. Greenish-yellow stones plot only in the Mn-field. It is rare for tourmalines with greater Mn contents than Fe contents to plot in the Mn-field. Moreover, it is extremely rare for pink tourmalines to contain $\text{Fe} > \text{Mn}$ and plot in the Fe-field.

Fig. 12, Calculated Li vs. Fe plot: The calculated Li vs. Fe binary plot shows that the most Fe-rich, Li-poor tourmalines are blue and green elbaites. Fe and Li display an inverse relationship. As Fe decreases and Li increases, there is a gradual transition from greenish-yellow, red, red-purple, pink and colorless to near colorless liddicoatites, rossmanites and liddicoatites. The bluish-gray liddicoatites are slightly more Fe-rich than the pink and red elbaites, liddicoatites and rossmanites but less Fe-rich than the green elbaites, liddicoatites and rossmanites. Clustering is observed among the blue and green elbaites and liddicoatites and to a much lesser extent with the red elbaites.

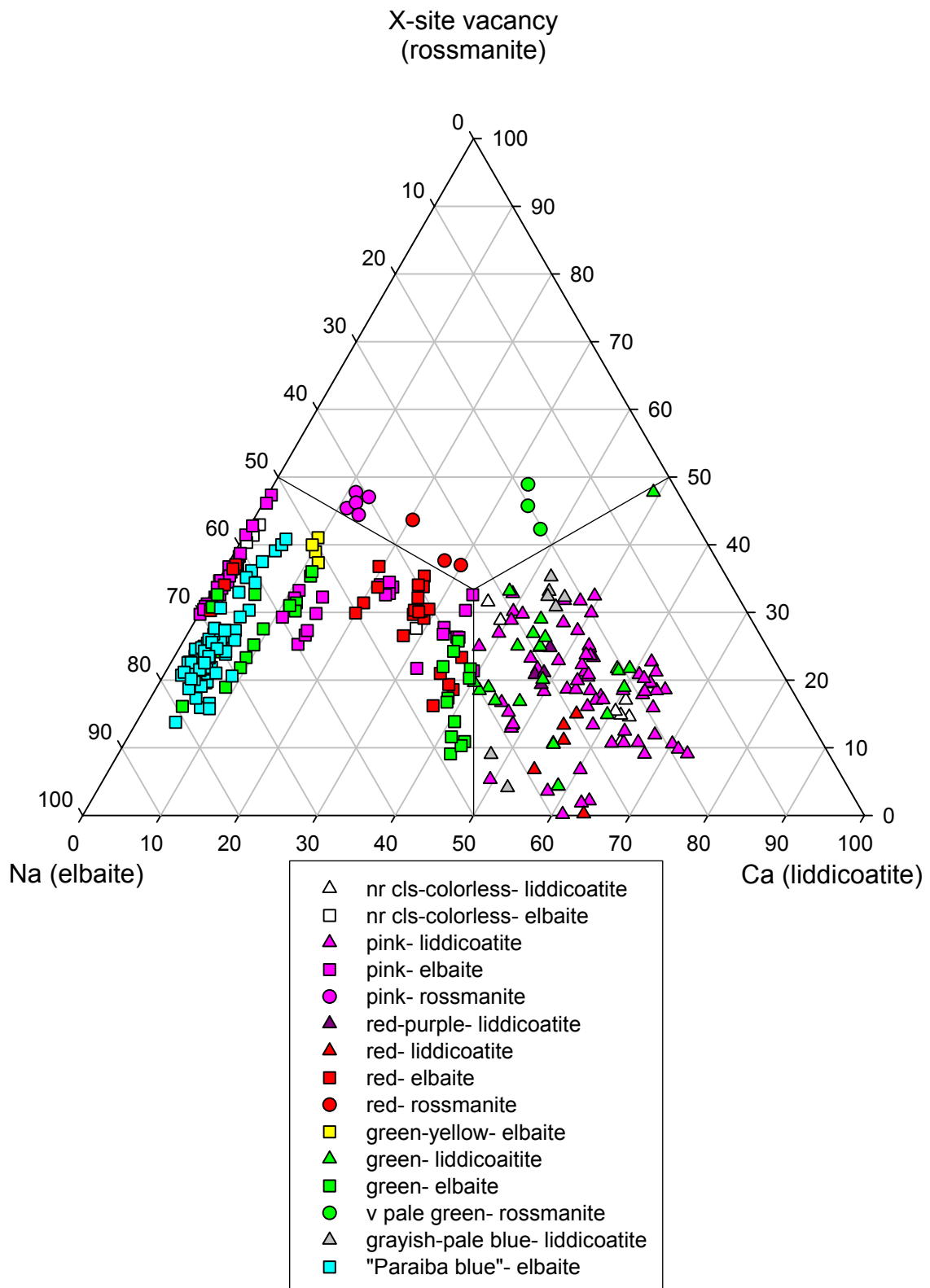


Fig. 10: Ca- X-site vacancy- Na ternary, Nigerian tourmaline.

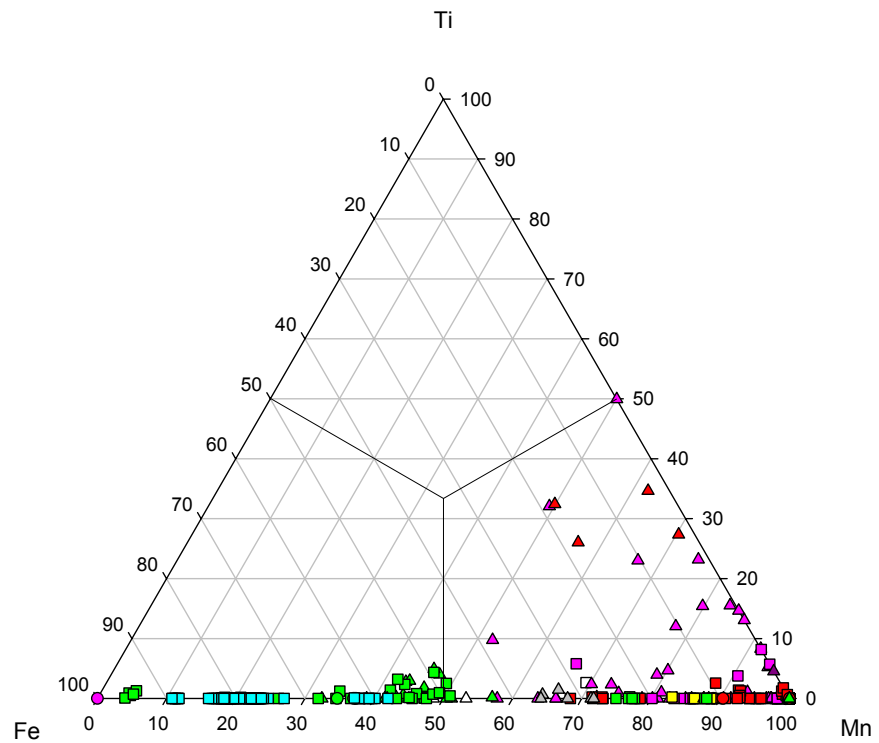


Fig. 11: Y-site Mn- Ti- Fe ternary, Nigerian tourmaline.

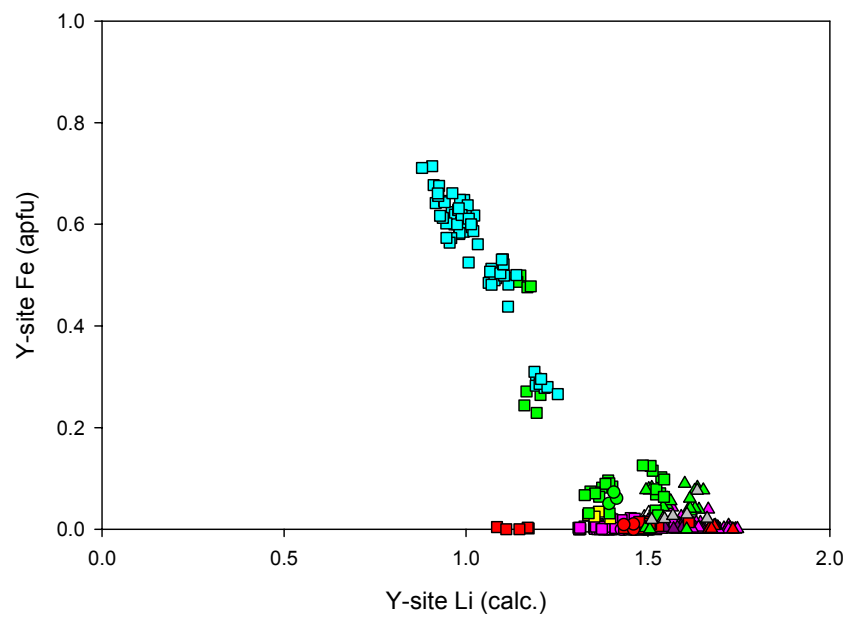


Fig. 12: Li vs. Fe binary, Nigerian tourmaline.

Fig. 13, Fe vs. Mn plot: The Fe vs. Mn binary diagram shows that the most Fe-dominant compositions are blue and green elbaites. The most Mn-rich sample is stone “e1”, a red liddicoatite. Stones may have a paucity of Fe and still be green. Generally, the pink, red, red-purple and colorless to near colorless stones are Fe-poor whereas the greenish-yellow elbaites and bluish-gray liddicoatites are more Fe-rich but generally contain less Fe than the green elbaites and liddicoatites. The green and blue elbaites contain as much Mn as red, reddish-purple, pink and colorless to near colorless elbaites. Pronounced clustering is observed with the blue and green elbaites.

Fig. 14, Calculated Li vs. Mn plot: The calculated Li vs. Mn covariation diagram shows that with the exception of red specimen “e1”, blue and green tourmalines from Nigeria contain equal quantities of Mn as do the colorless to near colorless pink, red and greenish-yellow gems but generally less Li. A weak and broad negative trend of increasing Li with decreasing Mn is observed. Accompanying this trend is the transition from elbaite to liddicoatite tourmaline. The 1.5 apfu Li line is the rather vague transition zone from elbaites to liddicoatites. The rossmanites cluster to the left of this line. Significant clustering occurs with the blue, green and red elbaites.

Fig. 15, Calculated Li vs. F plot: No decipherable trends are observed for this binary diagram. Two major groupings are observed among the entire population with blue elbaites being separated from the main grouping. Green stones “p1” and “f1” along with red stone “e1” are among these outliers. Generally, these stones contain less F than the remainder of the population. The liddicoatites have higher Li and F than the elbaites and rossmanites. Nearly half of the elbaites are fluor-elbaites with >50% F occupancy at the W-site.

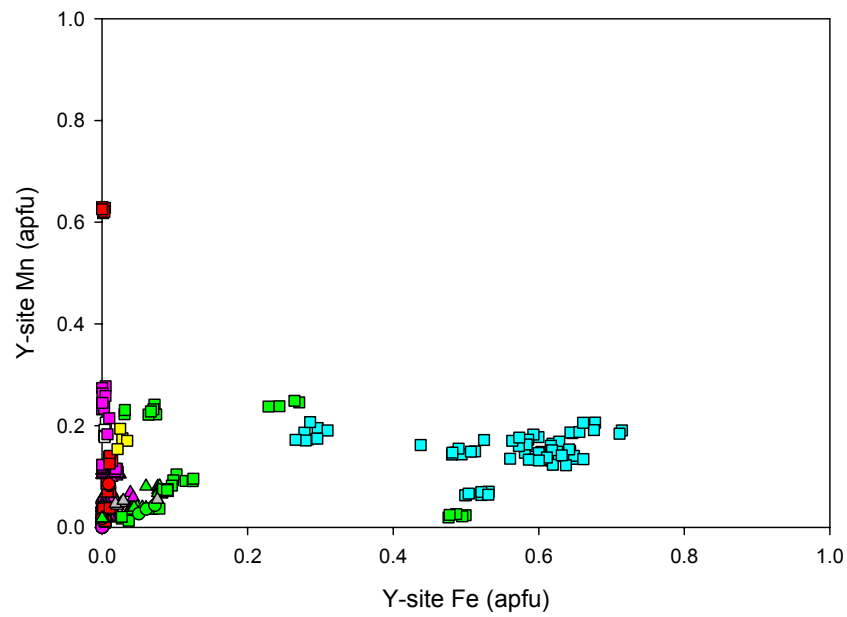


Fig. 13: Fe vs. Mn binary, Nigerian tourmaline.

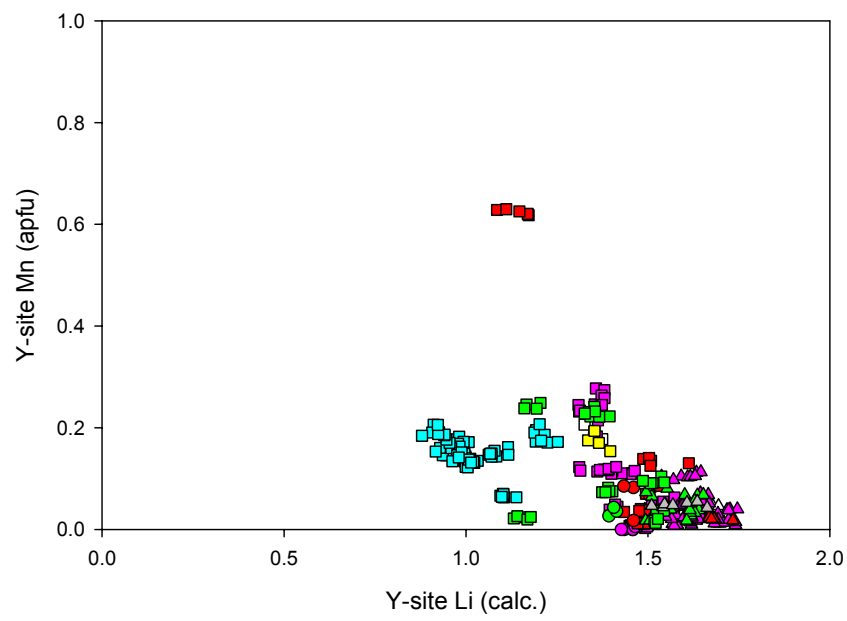


Fig. 14: Li (calc.) vs. Mn binary, Nigerian tourmaline.

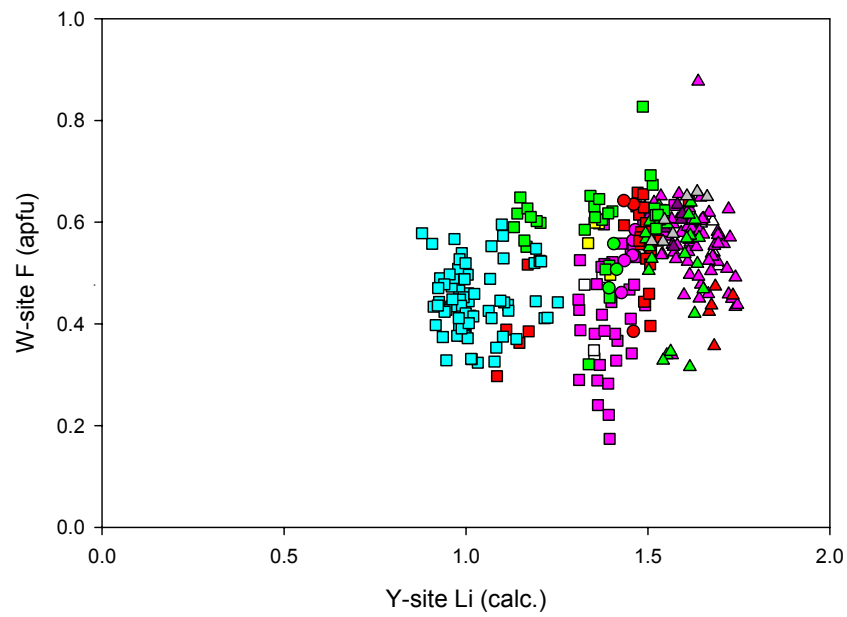


Fig. 15: Li (calc.) vs. F binary, Nigerian tourmaline.

Fig. 16, Calculated Li vs. Y-site Al plot: This diagram is rather complex. The blue elbaites along with the two green elbaites and one red elbaite follow a positive trend, displaying increasing Li with increasing Y-site Al. This is profoundly different from the rest of the colors and species from the Larson suite which exhibit a negative slope and exhibit decreasing Al with decreasing Li at the Y-site. The most Al-poor specimens include the blue elbaites and red stone “e1” as well as green and pink liddicoatites. The most Al-rich samples include the pink elbaites and rossmanites.

Fig. 17, Y-site Al vs. Fe plot: The general trend of this diagram shows that Fe and Al are inversely related. This is shown by a negatively sloping trend. The blue elbaites are the most Fe-rich and Al-poor samples, whereas the pink rossmanite contains the most Al and no Fe. Colorless to near colorless, pink, red, reddish-purple and colorless elbaites, liddicoatites and rossmanites are Fe-poor. A small number of green liddicoatites and elbaites exhibit this lack of Fe. Al varies widely among the green, greenish-yellow, orange, red, pink, bluish-gray and colorless elbaites, liddicoatites and rossmanites. However, the range of Al content is less extensive in the blue elbaites and some of the green elbaites (“p1” and “f1”). The blue and green elbaites exhibit a steep negative trend, whereas the other colors display a gentle negative trend. Clustering is again observed among the blue elbaites.

Fig. 18, Fe vs. Ti plot: The separation of colors with respect to Fe is significant. Generally the blue elbaites contain the most Fe, followed by the green elbaites and liddicoatites, bluish-gray liddicoatites and lastly the greenish-yellow elbaite. The colorless to near colorless, pink, red and reddish-purple samples have the least Fe. Slightly elevated Ti is observed in some areas of the green, red and pink samples.

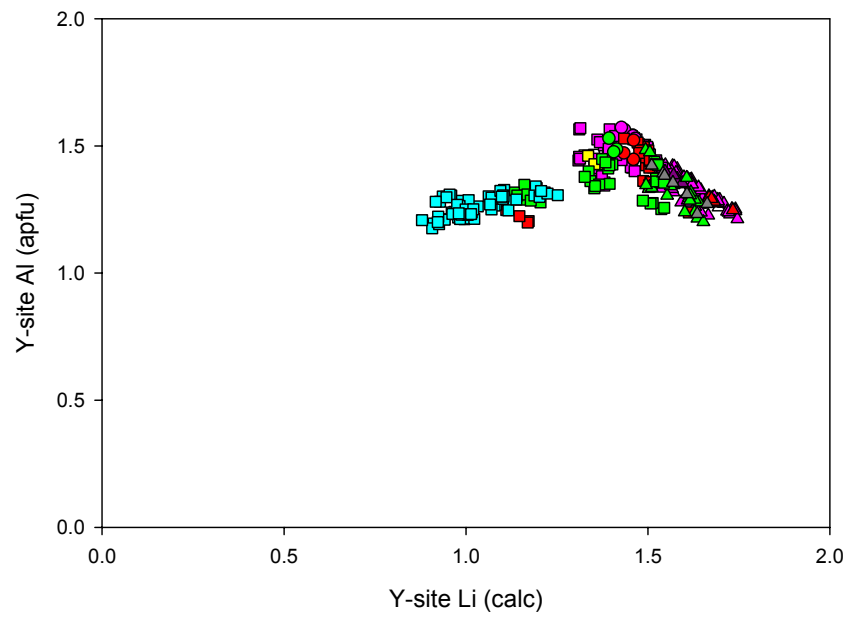


Fig. 16: Li (calc.) vs. Al binary, Nigerian tourmaline.

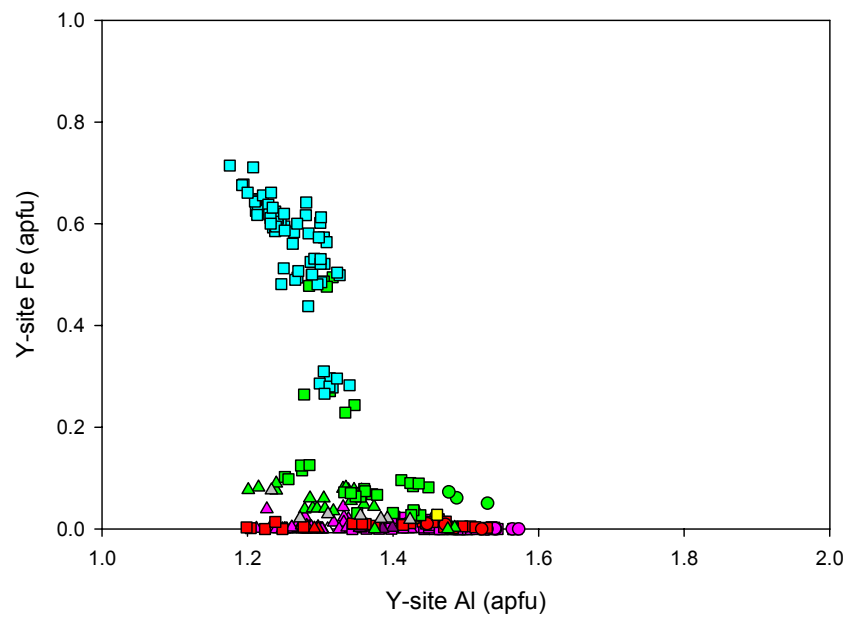


Fig. 17: Al vs. Fe binary, Nigerian tourmaline.

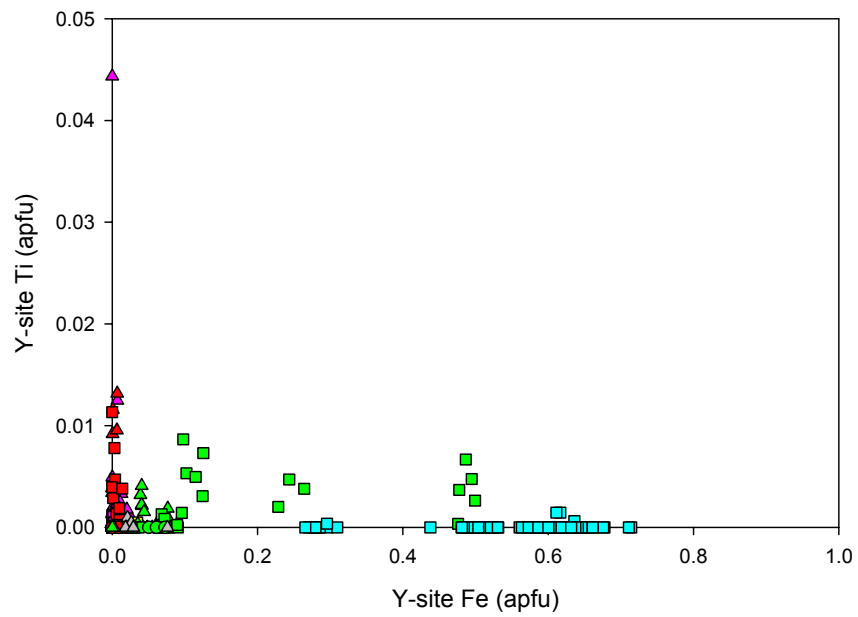


Fig. 18: Fe vs. Ti binary, Nigerian tourmaline.

Fig. 19, Mn vs. Ti plot: Separation of the Nigerian tourmalines by color is not distinct with respect to Mn vs. Ti concentration. Red elbaite sample “e1” has the highest Mn quantity with the other colors containing roughly the same amount of Mn. Larger relative amounts of Ti are observed among the red, green and pink stones.

Fig. 20, Na vs. F plot: As with the Li vs. F diagram, the Na vs. F plot has no distinct trends. The liddicoatites and rossmanites contain low Na and are separated at about 0.4 apfu Na from the elbaites which have high Na content. The elbaites, rossmanites and liddicoatites contain, on the average, equal quantities of F. The green elbaites are the most F-rich and contain 0.4 to 0.8 apfu Na.

Fig. 21, Na vs. Ti+Fe+Mn plot: The slope of this graph is positive and concave upward. The liddicoatites and rossmanites contain the least Ti+Fe+Mn (>0.2 apfu total for the green liddicoatites) and the elbaites contain the most with up to 0.9 apfu for the “Paraíba blue” stones. The red and pink elbaites may also contain high Na and low transition element contents. Color changes from pink/red to yellowish-green, green and blue accompany this trend.

Figs. 22 & 23, Mn vs. color intensity plots: The color intensity vs. average Mn per stone plot of the colorless, pink and red stones of the Nigerian suite does not show any distinct trends. The color intensity vs. the average Mn per color diagram has no distinct trends either. Both plots show that the colorless to near colorless, red and variously colored pink stones have approximately the same quantities of Mn.

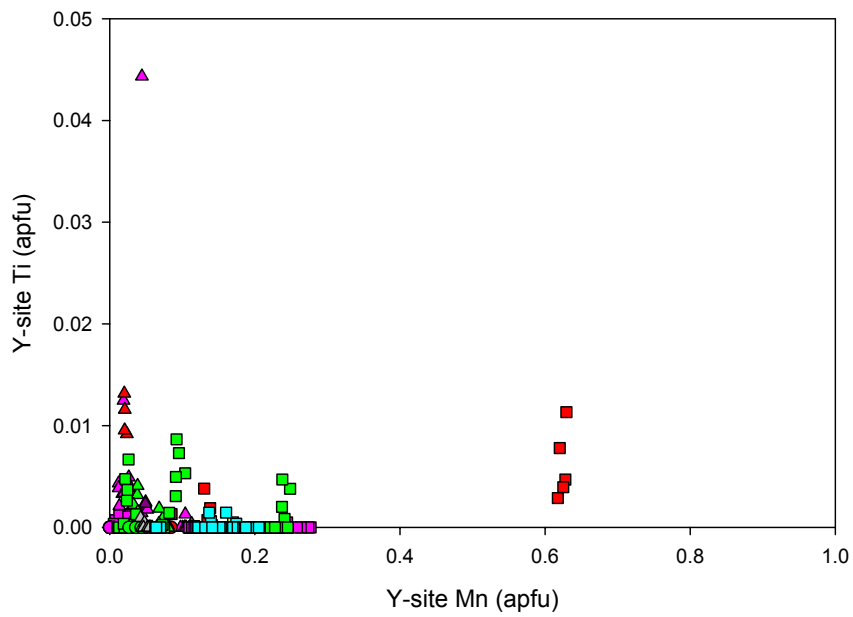


Fig. 19: Mn vs. Ti binary, Nigerian tourmaline.

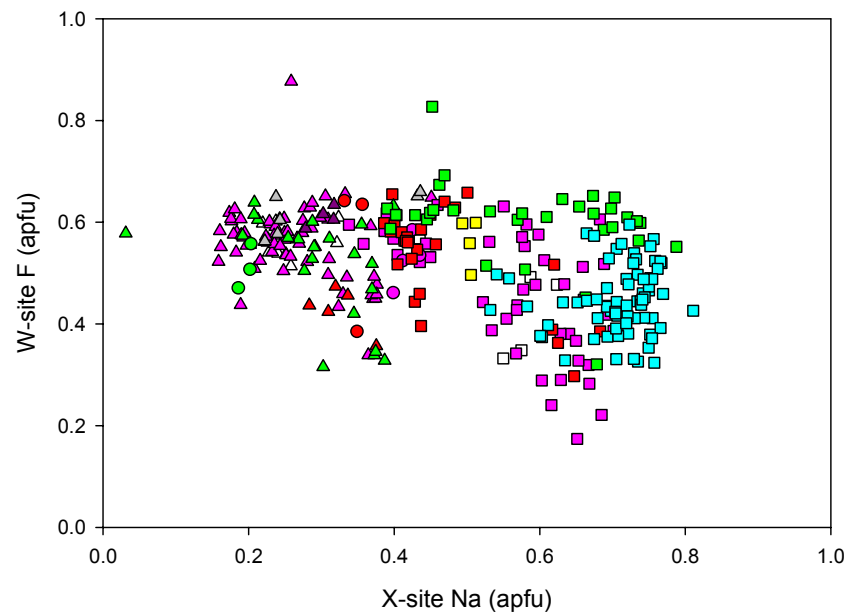


Fig. 20: Na vs. F binary, Nigerian tourmaline.

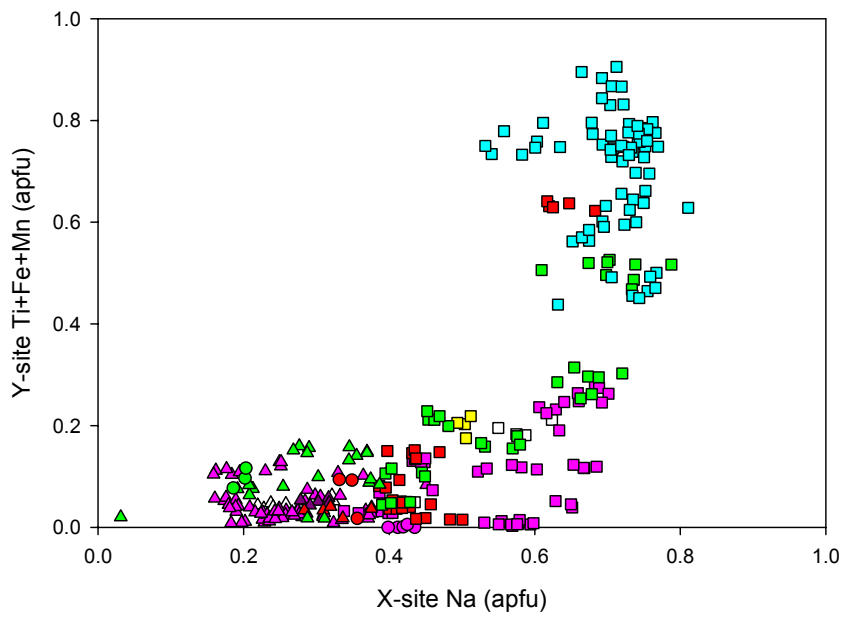


Fig. 21: Na vs. Ti+Fe+Mn binary, Nigerian tourmaline.

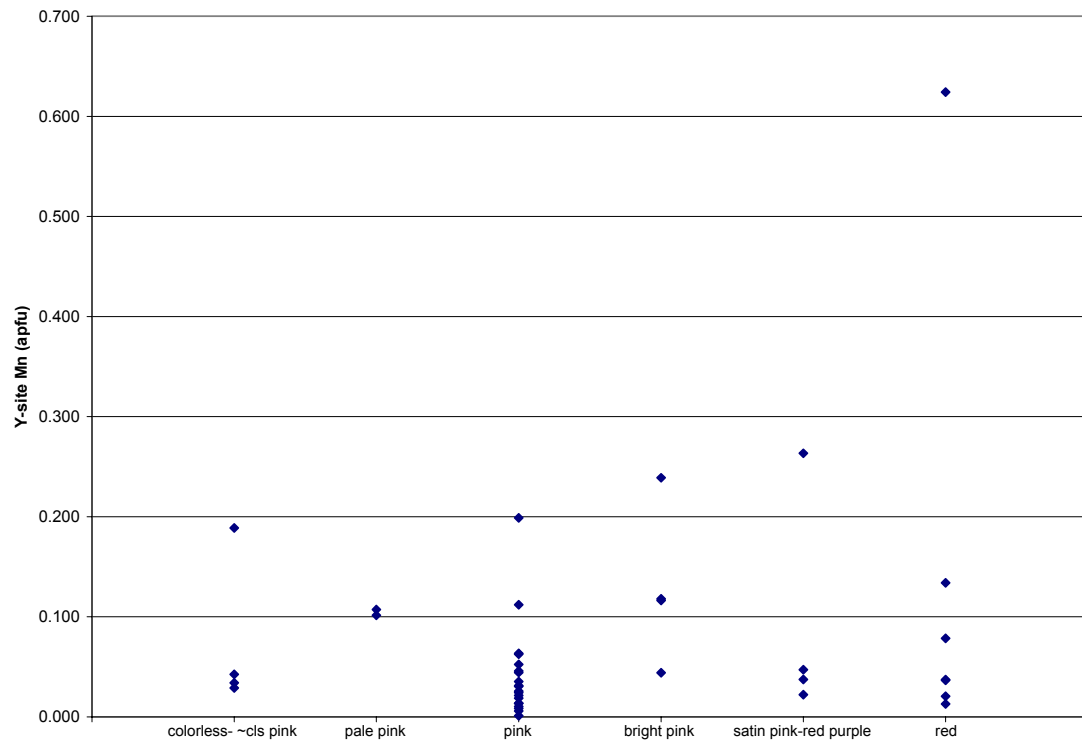


Fig. 22: Color intensity vs. Mn (avg. apfu per stone) binary, Nigerian tourmaline.

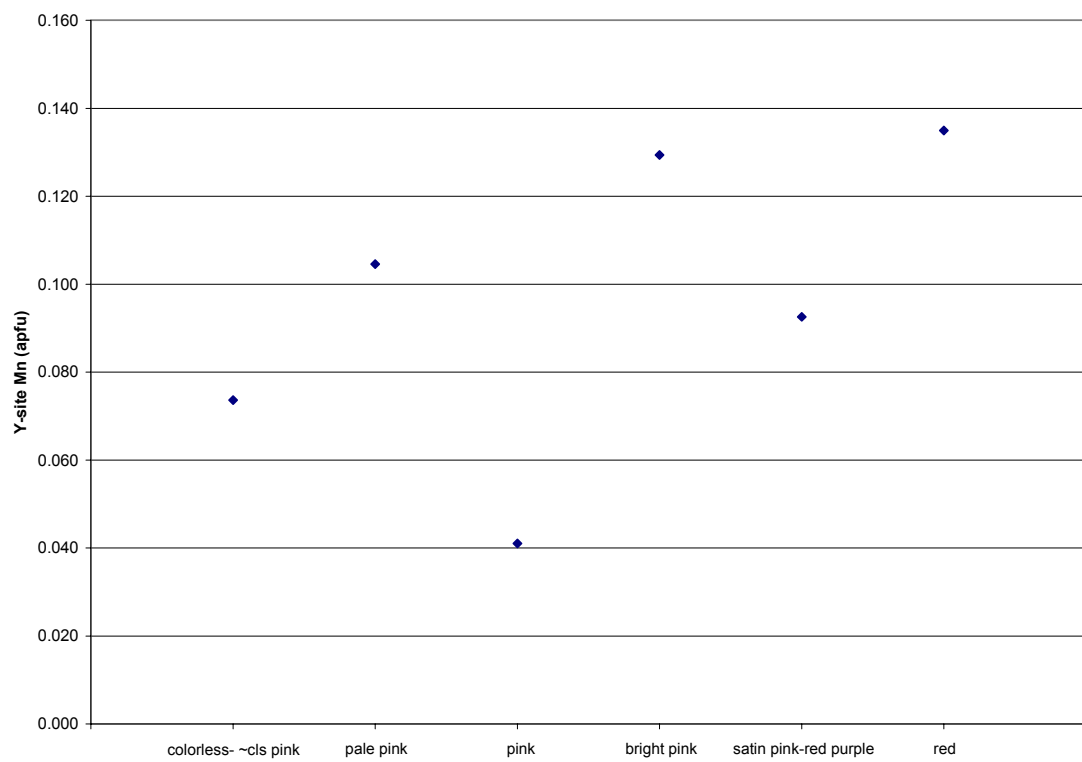


Fig. 23: Color intensity vs. Mn (avg. of avg. apfu per stone) binary, Nigerian tourmaline.

Namibian & Malian tourmaline slices & fragments

The tourmaline fragments and slices from various localities throughout Namibia and Gao, Mali are part of the liddicoatite-rossmanite-elbaite series, except for sample “3-10” which is a black schorl belonging to the schorl-elbaite series. Sample mounts of the Namibian tourmaline suite are shown in Figs. 24 and 25. Table 4 shows the microprobe analyses of the Namibian tourmaline suite. The Malian tourmaline analyses are given in Table 5. These specimens range in color from various shades of pink to red, green, blue and black. The pink, red (zones of slices), green and blue samples are all elbaites, save for spot 2 of sample 3-3 (this sample is composed of elbaite and rossmanite domains) which is a pink rossmanite. The green piece of rough from Gao, Mali is an elbaite.

The selected pieces of gem-quality rough from Namibia used for precision cell-edge refinements have a dimensions ranging from 15.814 to 15.859Å and c dimensions ranging from 7.095 to 7.116Å. The a dimension for the pink fragments ranges from 15.814 to 15.838Å and c ranges from 7.099Å to 7.116Å. The green rough has a ranging from 15.819 to 15.859Å and c ranging from 7.095 to 7.111Å. The blue rough has a dimensions ranging from 15.843 to 15.855Å and c ranging from 7.101 to 7.111Å. The black schorl fragment has a c dimension of 15.834Å and an a dimension of 7.112Å. The green fragment from Mali has an a dimension of 15.833Å and a c dimension of 7.095Å. Cell-edge data and analytical errors including data of a fragment from Mozambique is shown in Table 9 and the a vs. c cell-edge plot is shown in Fig. 78.



Fig. 24: Probe mount, Namibian and Malian tourmaline gem rough.

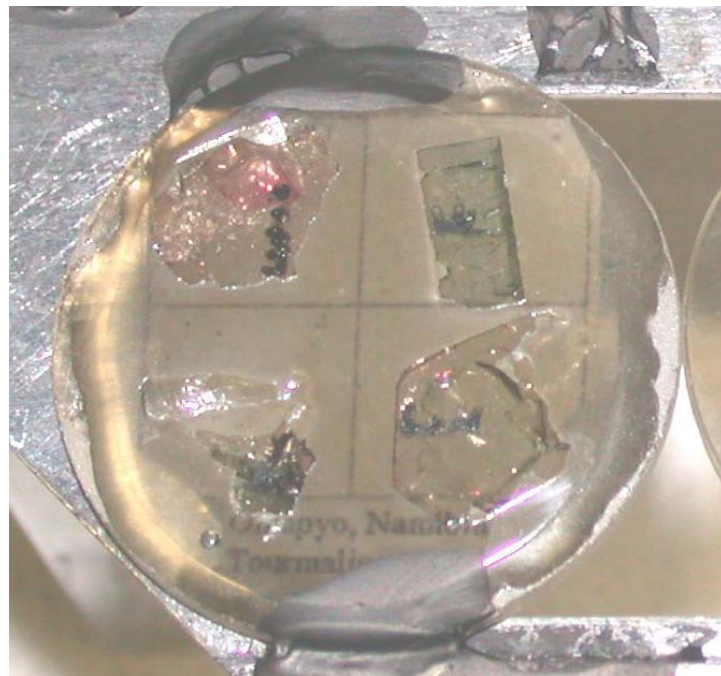


Fig. 25: Probe mount, Namibian tourmaline slices.

The T, B and Z-sites: SiO₂ quantities range from 35.88 to 38.68 wt. % and 5.863 to 6.195 apfu. Calculated B₂O₃ ranges from 10.16 to 11.22 wt. %. Al fills the Z-sites with 6.0 apfu and total Al varies from 31.367 to 42.761 wt. % with the schorl having the lowest Al and pink elbaites (rossmanite) containing the most.

Y-site Al: Al at the Y-site ranges from 0.282 to 1.713 apfu. Al contents at this site are highest for the elbaites and lowest for the schorl. Al varies from 1.528 to 1.713 apfu for the pink samples. The rossmanite spot has 1.704 apfu Al. Red elbaite zones contain between 1.619 to 1.673 apfu Al. The green samples have 1.173 to 1.654 apfu whereas the blue elbaite (sample “3-15”) contains significantly less Al (0.762 to 0.805 apfu). The schorl has a paucity of Al with 0.282 to 0.346 apfu in the Y-sites. The most Al-rich spot is sample 3-17, spot 2 with 1.707 apfu and the most Al-poor specimen is the schorl described above. The Malian green elbaite contains the lowest Y-site Al with 1.173 to 1.188 apfu.

Titanium: Ti contents are low for most of the samples varying from 0 to 0.31 wt. % TiO₂ and 0 to 0.008 apfu Ti. The red and blue samples have no detectable Ti. Among the pink samples, Ti is most prevalent in “3-11” with 0.01 to 0.04 wt. % and 0.001 to 0.005 apfu. The most Ti-rich green sample is spot 5 of sample “Nam-sl-a” with 0.10 wt. % and 0.012 apfu. Spots 2 to 3 and 6 to 7 of samples “Nam-sl-b” and “Nam-sl-c” also have substantial Ti contents. The schorl fragment is the most Ti enriched specimen among this suite with 0.26 to 0.31 wt. % and 0.033 to 0.040 apfu Ti. The elbaite from Mali contains no detectable Ti.

Bismuth: Bi in the blue elbaite and black schorl is not detectable but substantial Bi quantities are observed in the pink and green stones. Overall, Bi ranges from 0 to 0.21

wt % Bi_2O_3 and 0 to 0.008 apfu Bi. Bi attains quantities of up to 0.21 wt. % and 0.008 apfu among the pink tourmalines (sample 3-4, spot 1). Spot 2 of sample “Nam-sl-d” contains 0.11 wt. % and 0.004 apfu Bi. The most Bi-rich green fragment is sample “3-13” from Mali with 0.06 to 0.10 wt. % and 0.003 to 0.004 apfu Bi.

Vanadium: V is completely absent in this suite save for some traces in random samples. The Malian elbaite is V-free.

Iron: The Namibian tourmalines have a wide range of Fe content from 0 to 13.50 wt. % FeO and 0 to 1.919 apfu Fe. The most Fe-rich specimen is “3-10”, the schorl, with 12.52 to 13.50 wt. % and 1.791 to 1.919 apfu. Of the gem-quality tourmaline, blue elbaite sample “3-15” contains the most Fe with 5.90 to 6.02 wt. % and 0.809 to 0.823 apfu. Among the green specimens, Fe varies between 0.50 to 3.90 wt. % and 0.066 to 0.523 apfu. Fe quantities typically increase as the samples become darker. The most Fe-rich green sample is “3-14” with 3.85 to 3.90 wt. % and 0.515 to 0.523 apfu Fe whereas the least Fe-rich is slice “Nam-sl-a” with 0.50 to 2.53 wt. % and 0.066 to 0.334 apfu. Pink and red samples typically contain less Fe than the green and blue stones. Pink fragments may have 0 to 0.73 wt. % FeO and 0 to 0.096 apfu Fe whereas the red zones of the slices contain from 0.09 to 0.57 wt. % FeO and 0.012 to 0.074 apfu Fe. The most Fe-rich pink fragment is pale pink sample “3-18” with 0.62 to 0.73 wt. % and 0.081 to 0.096 apfu. The pink rossmanite spot has 0.14 wt. % and 0.019 apfu Fe. The Malian elbaite contains 3.22 to 3.33 wt. % and 0.436 to 0.451 apfu Fe, which is the most Fe-rich green stone.

Manganese: There is a wide range in Mn for the various colors of this suite. Mn ranges from 0 to 1.21 wt. % MnO and 0 to 0.161 apfu Mn. The highest Mn

concentrations are observed in the pink samples with sample “3-8” being the most Mn-rich (0.77 to 1.12 wt. % and 0.102 to 0.161 apfu). The pink rossmanite spot has 0.33 wt. % MnO and 0.042 apfu Mn. The red domains of the slices have substantially less Mn than the pink fragments with Mn ranging from 0.28 to 0.54 wt. % and 0.037 to 0.071 apfu. The green tourmalines may house nearly as much Mn as the pink stones with 0.14 to 1.13 wt. % and 0.019 to 0.151 apfu. Of these, the most Mn-rich specimens are the slices, particularly spot 5 of sample “Nam-sl-a” which contains 1.13 wt. % and 0.151 apfu Mn. The blue fragment shows a decrease in Mn with 0.44 to 0.51 wt % and 0.061 to 0.071 apfu whereas the schorl has 0.40 to 1.00 wt. % and 0.058 to 0.144 apfu. The Malian tourmaline has 0.14 to 0.27 wt. % and 0.019 to 0.037 apfu Mn.

Magnesium: There is no detectable Mg in the pink, red and blue fragments and slices. Otherwise Mg is sparse among the green zones of the slices and in the schorl. Green slice “Nam-sl-b” contains the most Mg of the set with 0.07 to 0.14 wt. % and 0.017 to 0.032 apfu. Mg in the schorl varies from 0.03 to 0.04 wt. % and 0.007 to 0.01 apfu. No Mg was detected in the green elbaite from Mali.

Calcium: Overall, Ca falls in the range of 0 to 0.63 wt. % CaO and 0 to 0.105 apfu Ca. The most Ca-rich samples are the pink elbaites, particularly sample “3-3” with 0.60 to 0.63 wt. % and 0.101 to 0.105 apfu. Spot 2 of this sample, the rossmanite, has 0.61 wt. % and 0.101 apfu Ca. The red portions of the slices contain 0.05 to 0.27 wt. % CaO and 0.009 to 0.044 apfu Ca. The green fragments and slices contain significant Ca in the range of 0.06 to 0.53 wt. % and 0.01 to 0.09 apfu. Slice “Nam-sl-b” has the most Ca (0.45 to 0.53 wt. % and 0.076 to 0.09 apfu) of the green elbaites. Ca is low in the blue

elbaite (0.03 to 0.05 wt. % and 0.006 to 0.009 apfu) and black schorl (0.02 to 0.02 wt. % and 0.004 apfu). The elbaite from Mali has 0.39 to 0.41 wt. % and 0.067 to 0.07 apfu Ca.

Calculated Lithium: Calculated Li quantities vary from 0.89 to 2.26 wt. % Li_2O and 0.611 to 1.414 apfu. In general, the pink elbaites have the highest Li concentrations, followed by the green, blue and red elbaites and lastly the black schorl. The range of Li contents for the pink samples is 1.92 to 2.26 wt. % and 1.214 to 1.414 apfu. The rossmanite spot has 1.97 wt. % Li_2O and 1.23 apfu Li. The most Li-dominant pink sample and most Li-rich of all the Namibian tourmalines is sample “3-1” with 2.11 to 2.26 wt. % and 1.32 to 1.414 apfu. The red zones have 1.98 to 2.04 wt. % and 1.239 to 1.276 apfu Li, a decrease from the pink stones. The green fragments and slices are second in Li abundance and contain 1.71 to 2.20 wt. % and 1.088 to 1.422 apfu. Of the green elbaites, sample “3-12” is the most Li-dominant with 1.96 to 2.20 wt. % and 1.248 to 1.422 apfu. The blue fragment has substantial calculated Li contents ranging from 1.99 to 2.05 wt. % and 1.31 to 1.345 apfu. The schorl contains a paucity of Li (0.90 to 1.11 wt. % and 0.611 to 0.764 apfu). The pale-green Malian elbaite is Li-rich with respect to the green samples with 2.02 to 2.10 wt. % and 1.314 to 1.366 apfu.

Sodium: Among the elbaites, Na varies from 1.48 to 2.69 wt. % Na_2O and 0.451 to 0.855 apfu Na. The pink elbaites have lower Na totals than the blue fragment and most of the green elbaites. The lowest Na totals are found in sample “3-3” (elbaite-rossmanite) with 1.46 to 1.88 wt. % and 0.441 to 0.564 apfu. The schorl contains 0.75 to 0.79 wt. % and 2.278 to 2.376 apfu Na. The Malian elbaite has 2.15 to 2.31 wt. % and 0.674 to 0.722 apfu Na.

Potassium: Quantities of K are very low in the Namibian and Malian samples. The overall range varies from 0.01 to 0.06 wt. % K₂O and 0.002 to 0.012 apfu K. This range applies to the pink gems as well. The highest K content for a pink elbaite is from 0.02 to 0.06 wt. % and 0.005 to 0.012 apfu. The rossmanite has low K with 0.03 wt. % and 0.005 apfu. In the red portions of the slices, K is low, ranging from 0.02 to 0.04 wt. % and 0.004 to 0.007 apfu. The green samples contain 0.01 to 0.05 wt. % and 0.002 to 0.01 apfu with sample “3-12”, the most K-dominant green elbaite, containing 0.03 to 0.05 wt. % and 0.006 to 0.01 apfu. Blue sample “3-15” contains 0.05 to 0.05 wt. % and 0.009 to 0.011 apfu K, whereas the schorl has 0.02 to 0.04 wt. % and 0.004 to 0.009 apfu respectively. The elbaite from Mali has 0.02 to 0.04 wt. % and 0.005 to 0.008 apfu K.

X-site totals: Occupancy at the alkali-site is generally high (especially in the pink specimens) with totals ranging from 0.441 to 0.855 apfu. The lowest X-site totals are found in sample “3-3” (with the rossmanite spot) with 0.441 to 0.71 apfu. The most occupied elbaite is blue sample “3-15” containing 0.78 to 0.86 apfu at the X-site. The schorl, sample “3-10” contains 0.752 to 0.768 apfu at the X-site. The elbaite from Mali has 0.674 to 0.722 apfu at the X-site.

Hydroxyl anion and calculated water: The wt. % of calculated H₂O varies from 3.01 to 3.45, whereas OH ranges from 3.311 to 3.67 apfu at the V and W-sites. The occurrence of hydroxyl-elbaites is rare in this suite. Sample “3-1” is a hydroxyl-elbaite with 3.524 to 3.57 apfu OH. The rossmanite spot of sample “3-3” contains 3.454 apfu OH and is a fluor-rossmanite. The schorl is OH deficient at the W-site with 3.436 apfu OH. The Malian elbaite has between 3.11 to 3.12 wt. % H₂O and 3.352 to 3.372 apfu OH at the X-site.

Fluorine: The F contents are widely variable between 0.67 to 1.38 wt. % F and 0.409 to 0.688 apfu F. Elbaites fall within this range and are primarily F-dominant at the W-site, thus they are fluor-elbaites. The rossmanite spot is fluor-rossmanite housing 1.11 wt. % and 0.546 apfu F. The schorl has 0.95 to 1.04 wt. % F and 0.514 to 0.564 apfu F, thus it is classified as a fluor-schorl. The Malian elbaite contains 1.23 to 1.27 wt. % F and 0.628 to 0.648 apfu at the W-site.

Table 4: Microprobe analyses, Namibian tourmaline.

Oxides	.3-1-1	.3-1-2	.3-1-3	.3-2-1	.3-2-2	.3-2-3	.3-3-1	.3-3-2
sample	.3-1-1	.3-1-2	.3-1-3	.3-2-1	.3-2-2	.3-2-3	.3-3-1	.3-3-2
color	pink	pink	pink	dkr pink	dkr pink	dkr pink	ple mk p	ple mk p
SiO ₂	37.87	38.68	38.34	37.73	38.02	37.83	38.01	37.82
TiO ₂	0.00	0.00	0.00	0.00	0.00	0.00	0.00	0.00
B ₂ O ₃ calc.	11.14	11.15	11.19	11.11	11.03	11.00	11.09	11.19
Al ₂ O ₃	42.15	41.22	42.01	42.00	40.87	40.92	41.68	42.76
Bi ₂ O ₃	0.05	0.01	0.02	0.00	0.00	0.00	0.00	0.11
V ₂ O ₃	0.00	0.00	0.00	0.00	0.00	0.00	0.00	0.00
FeO	0.01	0.02	0.01	0.01	0.00	0.00	0.14	0.14
MnO	0.00	0.11	0.28	0.33	0.97	0.89	0.33	0.33
MgO	0.00	0.00	0.00	0.00	0.00	0.00	0.00	0.00
CaO	0.26	0.27	0.27	0.32	0.33	0.31	0.60	0.61
Li ₂ O calc.	2.13	2.26	2.11	2.07	2.04	2.02	2.03	1.97
Na ₂ O	2.22	2.12	2.10	2.11	2.00	1.97	1.48	1.46
K ₂ O	0.03	0.04	0.03	0.01	0.02	0.02	0.04	0.03
H ₂ O calc.	3.37	3.41	3.42	3.35	3.28	3.30	3.26	3.33
F	0.99	0.93	0.93	1.02	1.11	1.05	1.20	1.11
Sub-total	100.22	100.22	100.71	100.05	99.66	99.30	99.86	100.86
O=F	-0.42	-0.39	-0.39	-0.43	-0.47	-0.44	-0.51	-0.47
Total	99.81	99.82	100.31	99.62	99.20	98.86	99.36	100.39
Ions (apfu)								
T: Si	5.909	6.026	5.953	5.905	5.990	5.977	5.959	5.875
Al	0.091	0.000	0.047	0.095	0.010	0.023	0.041	0.125
B: B	3.000	3.000	3.000	3.000	3.000	3.000	3.000	3.000
Z: Al	6.000	6.000	6.000	6.000	6.000	6.000	6.000	6.000
Y: Al	1.661	1.570	1.641	1.651	1.578	1.597	1.658	1.704
Ti	0.000	0.000	0.000	0.000	0.000	0.000	0.000	0.000
Bi	0.002	0.000	0.001	0.000	0.000	0.000	0.000	0.004
V	0.000	0.000	0.000	0.000	0.000	0.000	0.000	0.000
Fe ²⁺	0.001	0.002	0.001	0.001	0.000	0.000	0.018	0.019
Mn ²⁺	0.000	0.015	0.037	0.044	0.129	0.119	0.044	0.043
Mg	0.000	0.000	0.000	0.000	0.000	0.000	0.000	0.000
Li	1.335	1.414	1.320	1.305	1.292	1.285	1.280	1.230
X: Ca	0.043	0.045	0.045	0.054	0.055	0.052	0.101	0.101
Na	0.672	0.641	0.631	0.640	0.610	0.602	0.451	0.441
K	0.006	0.009	0.005	0.002	0.005	0.004	0.009	0.005
□ (vac.)	0.279	0.306	0.319	0.304	0.331	0.342	0.439	0.453
OH	3.511	3.539	3.541	3.495	3.447	3.478	3.405	3.454
F	0.489	0.460	0.459	0.505	0.553	0.522	0.595	0.546
species	elbaite	elbaite	elbaite	F-elbaite	F-elbaite	F-elbaite	F-elbaite	F-rossman

Oxides	.3-3-3	.3-4-1	.3-4-2	.3-4-3	.3-5-1	.3-5-2	.3-5-3	.3-6-1
sample	ple mk p	v pale p	v pale p	v pale p	tan pink	tan pink	tan pink	tan pink
SiO ₂	37.82	37.99	37.61	37.87	37.73	38.00	37.68	37.82
TiO ₂	0.00	0.00	0.00	0.00	0.02	0.01	0.00	0.00
B ₂ O ₃ calc.	11.21	11.10	10.96	11.02	10.98	11.02	10.99	11.00
Al ₂ O ₃	42.60	41.66	40.90	41.00	40.90	40.79	40.80	40.57
Bi ₂ O ₃	0.07	0.20	0.01	0.01	0.05	0.00	0.01	0.01
V ₂ O ₃	0.00	0.00	0.00	0.00	0.00	0.00	0.00	0.00
FeO	0.16	0.13	0.10	0.10	0.43	0.45	0.51	0.14
MnO	0.31	0.54	0.72	0.74	0.82	0.94	0.92	0.99
MgO	0.00	0.00	0.00	0.00	0.00	0.00	0.00	0.00
CaO	0.63	0.26	0.27	0.32	0.19	0.20	0.19	0.60
Li ₂ O calc.	2.07	2.02	2.01	2.03	1.93	1.95	1.96	2.08
Na ₂ O	1.88	1.95	2.00	1.95	1.90	1.96	2.16	1.99
K ₂ O	0.02	0.03	0.02	0.04	0.02	0.01	0.03	0.03
H ₂ O calc.	3.37	3.37	3.33	3.38	3.31	3.27	3.33	3.21
F	1.05	0.98	0.95	0.88	1.00	1.12	0.99	1.23
Sub-total	101.18	100.22	98.87	99.35	99.29	99.71	99.56	99.65
O=F	-0.44	-0.41	-0.40	-0.37	-0.42	-0.47	-0.41	-0.52
Total	100.74	99.81	98.47	98.98	98.86	99.24	99.14	99.13
Ions (apfu)								
T: Si	5.863	5.947	5.964	5.975	5.971	5.994	5.957	5.975
Al	0.137	0.053	0.036	0.025	0.029	0.006	0.043	0.025
B: B	3.000	3.000	3.000	3.000	3.000	3.000	3.000	3.000
Z: Al	6.000	6.000	6.000	6.000	6.000	6.000	6.000	6.000
Y: Al	1.646	1.632	1.608	1.599	1.600	1.575	1.560	1.528
Ti	0.000	0.000	0.000	0.000	0.002	0.001	0.000	0.000
Bi	0.003	0.008	0.000	0.000	0.002	0.000	0.000	0.000
V	0.000	0.000	0.000	0.000	0.000	0.000	0.000	0.000
Fe ²⁺	0.020	0.017	0.014	0.013	0.057	0.059	0.068	0.018
Mn ²⁺	0.041	0.071	0.097	0.099	0.110	0.125	0.124	0.132
Mg	0.000	0.000	0.000	0.000	0.000	0.000	0.000	0.000
Li	1.290	1.272	1.282	1.288	1.228	1.240	1.248	1.321
X: Ca	0.105	0.043	0.045	0.054	0.032	0.033	0.031	0.101
Na	0.564	0.592	0.613	0.596	0.583	0.599	0.661	0.610
K	0.004	0.007	0.005	0.008	0.003	0.002	0.006	0.005
□ (vac.)	0.326	0.358	0.337	0.341	0.382	0.366	0.301	0.284
OH	3.488	3.516	3.524	3.561	3.499	3.440	3.507	3.384
F	0.512	0.484	0.476	0.439	0.502	0.560	0.493	0.616
species	F-elbaite	elbaite	elbaite	elbaite	F-elbaite	F-elbaite	elbaite	F-elbaite

Oxides	.3-9-1	.3-9-2	.3-9-3	.3-10-1	.3-10-2	.3-10-3	.3-11-1	.3-11-2
sample	.3-9-1	.3-9-2	.3-9-3	.3-10-1	.3-10-2	.3-10-3	.3-11-1	.3-11-2
color	v pale p	v pale p	v pale p	black	black	black	pale pink	pale pink
SiO ₂	37.77	37.72	37.80	36.03	35.88	36.03	38.00	37.70
TiO ₂	0.00	0.00	0.00	0.26	0.26	0.31	0.01	0.04
B ₂ O ₃ calc.	11.03	11.05	11.06	10.23	10.16	10.20	11.05	11.00
Al ₂ O ₃	40.95	40.98	41.00	31.37	31.48	31.58	40.97	40.96
Bi ₂ O ₃	0.00	0.04	0.02	0.01	0.00	0.00	0.13	0.01
V ₂ O ₃	0.00	0.00	0.00	0.00	0.00	0.00	0.00	0.00
FeO	0.46	0.51	0.44	13.50	12.52	12.67	0.60	0.61
MnO	1.03	1.03	0.96	1.00	0.40	0.45	0.43	0.27
MgO	0.00	0.00	0.00	0.04	0.03	0.04	0.00	0.00
CaO	0.44	0.44	0.44	0.02	0.02	0.02	0.25	0.26
Li ₂ O calc.	1.98	1.99	2.02	0.89	1.11	1.08	2.03	2.04
Na ₂ O	1.96	2.07	2.11	2.29	2.38	2.28	2.09	2.12
K ₂ O	0.05	0.05	0.02	0.04	0.02	0.02	0.03	0.04
H ₂ O calc.	3.38	3.35	3.40	3.07	3.01	3.07	3.28	3.25
F	0.90	0.97	0.87	0.97	1.04	0.95	1.11	1.15
Sub-total	99.94	100.18	100.14	99.73	98.30	98.70	99.98	99.45
O=F	-0.38	-0.41	-0.36	-0.41	-0.44	-0.40	-0.47	-0.49
Total	99.56	99.78	99.78	99.32	97.86	98.30	99.51	98.96
Ions (apfu)								
T: Si	5.949	5.936	5.941	6.123	6.137	6.138	5.978	5.956
Al	0.051	0.064	0.059	0.000	0.000	0.000	0.022	0.044
B: B	3.000	3.000	3.000	3.000	3.000	3.000	3.000	3.000
Z: Al	6.000	6.000	6.000	6.000	6.000	6.000	6.000	6.000
Y: Al	1.550	1.534	1.537	0.282	0.346	0.341	1.573	1.583
Ti	0.000	0.000	0.000	0.034	0.033	0.040	0.001	0.005
Bi	0.000	0.002	0.001	0.000	0.000	0.000	0.005	0.000
V	0.000	0.000	0.000	0.000	0.000	0.000	0.000	0.000
Fe ²⁺	0.060	0.067	0.058	1.919	1.791	1.805	0.079	0.081
Mn ²⁺	0.137	0.137	0.127	0.144	0.058	0.065	0.057	0.037
Mg	0.000	0.000	0.000	0.010	0.007	0.009	0.000	0.000
Li	1.252	1.260	1.276	0.611	0.764	0.739	1.285	1.294
X: Ca	0.074	0.075	0.075	0.004	0.004	0.004	0.042	0.043
Na	0.597	0.631	0.643	0.753	0.788	0.752	0.637	0.649
K	0.009	0.009	0.004	0.009	0.005	0.004	0.007	0.008
□ (vac.)	0.319	0.286	0.278	0.233	0.203	0.240	0.314	0.300
OH	3.553	3.520	3.570	3.478	3.436	3.486	3.446	3.424
F	0.447	0.480	0.430	0.522	0.564	0.514	0.554	0.577
species	elbaite	elbaite	elbaite	F-schorl	F-schorl	F-schorl	F-elbaite	F-elbaite

Table 5: Microprobe analyses, Malian tourmaline.

Oxides			
sample	.3-13-1	.3-13-2	.3-13-3
color	pale g	pale g	pale g
SiO ₂	37.61	37.49	37.55
TiO ₂	0.00	0.00	0.00
B ₂ O ₃ calc.	10.73	10.74	10.76
Al ₂ O ₃	37.57	37.81	37.72
Bi ₂ O ₃	0.06	0.09	0.10
V ₂ O ₃	0.00	0.00	0.00
FeO	3.25	3.22	3.33
MnO	0.14	0.27	0.27
MgO	0.00	0.00	0.00
CaO	0.41	0.39	0.40
Li ₂ O calc.	2.10	2.02	2.04
Na ₂ O	2.15	2.21	2.31
K ₂ O	0.02	0.02	0.04
H ₂ O calc.	3.12	3.11	3.12
F	1.23	1.27	1.24
Sub-total	98.39	98.62	98.88
O=F	-0.52	-0.53	-0.52
Total	97.87	98.09	98.35
Ions (apfu)			
T: Si	6.092	6.066	6.067
Al	0.000	0.000	0.000
B: B	3.000	3.000	3.000
Z: Al	6.000	6.000	6.000
Y: Al	1.173	1.211	1.183
Ti	0.000	0.000	0.000
Bi	0.003	0.004	0.004
V	0.000	0.000	0.000
Fe ²⁺	0.440	0.436	0.451
Mn ²⁺	0.019	0.037	0.037
Mg	0.000	0.000	0.000
Li	1.366	1.314	1.325
X: Ca	0.071	0.067	0.070
Na	0.674	0.694	0.722
K	0.005	0.005	0.008
□ (vac.)	0.250	0.234	0.200
OH	3.372	3.352	3.366
F	0.628	0.648	0.634
species	F-elbaite	F-elbaite	F-elbaite

Namibian and Malian tourmaline plots

Fig. 26, X-site Ca-vacancy-Na plot: This diagram shows that the studied tourmalines are elbaites with one rossmanite analysis. The pink gems have the highest amounts of the liddicoatite and rossmanite components, whereas the blue stone is the most characteristically elbaitic. The green elbaites are generally intermediate with regard to quantities of liddicoatite and rossmanite incorporation.

Fig. 27, Mn-Ti-Fe plot: The tourmalines plot only along the Mn-Fe join. The green, blue and black samples fall into the Fe-field whereas the remaining pink and red stones plot in the Mn-field. There are several pink and red analyses which fall in the Fe-field.

Fig. 28, Calculated Li vs. Fe plot: The most Fe-rich, Li-poor sample is the black schorl, followed by the blue elbaite, the green elbaites and lastly the pink and red elbaites. The trend of this plot is negative and Li increases with decreasing Fe concomitant with the color changes above. The blue elbaite falls off the trend and clustering is observed among the green elbaites from Namibia and Mali.

Fig. 29, Fe vs. Mn plot: Each tourmaline color groups together forming trends with extremely steep, negative slopes. With increasing Fe content, the color changes from pink to red elbaites and rossmanites to green elbaites to blue elbaite and finally black schorl. The variously colored stones show no distinct separation with regard to Mn content. The green elbaites show pronounced clustering. The green Malian elbaite has low Mn quantities.

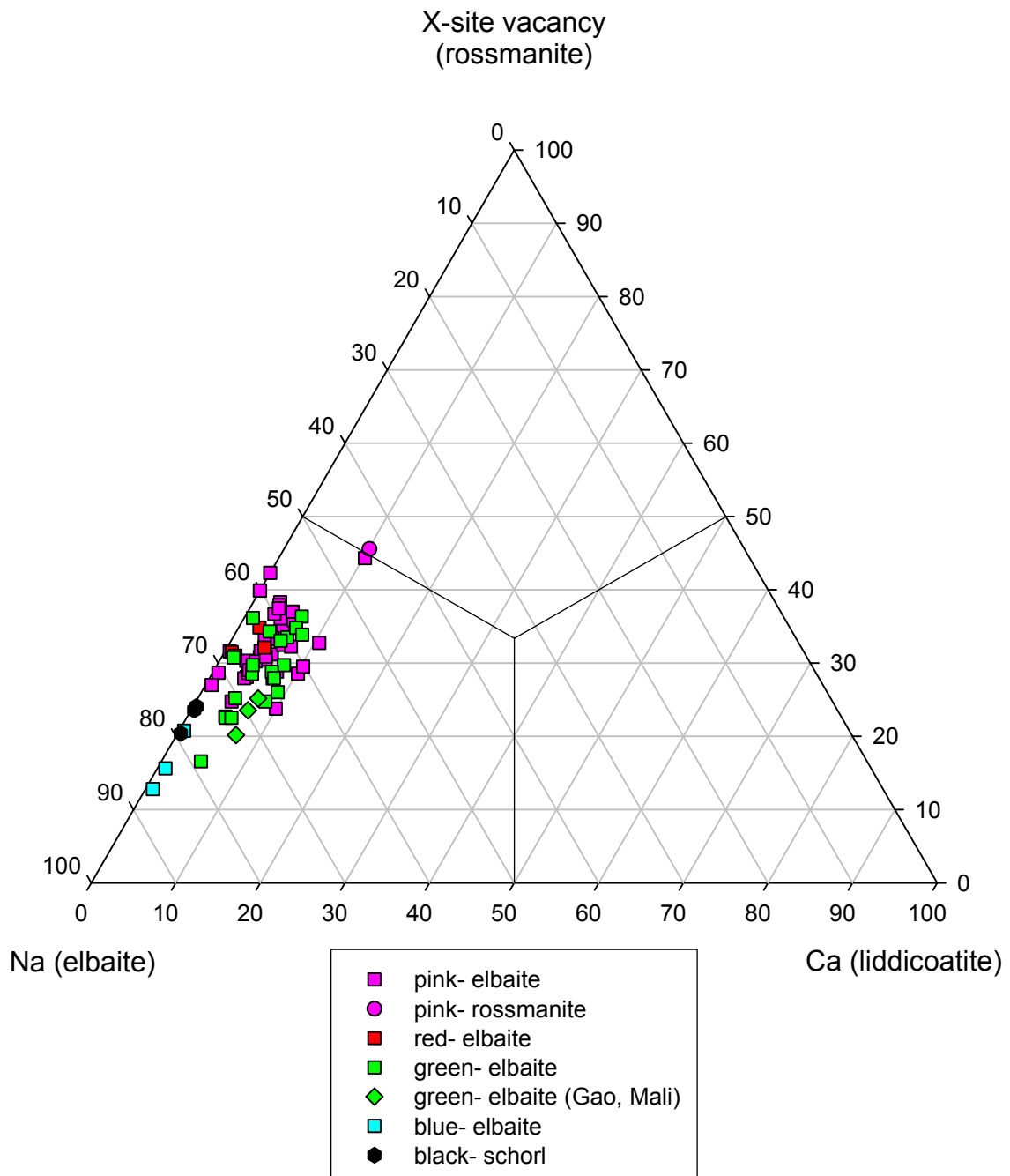


Fig. 26: Ca- X-site vacancy- Na ternary, Namibian and Malian tourmaline.

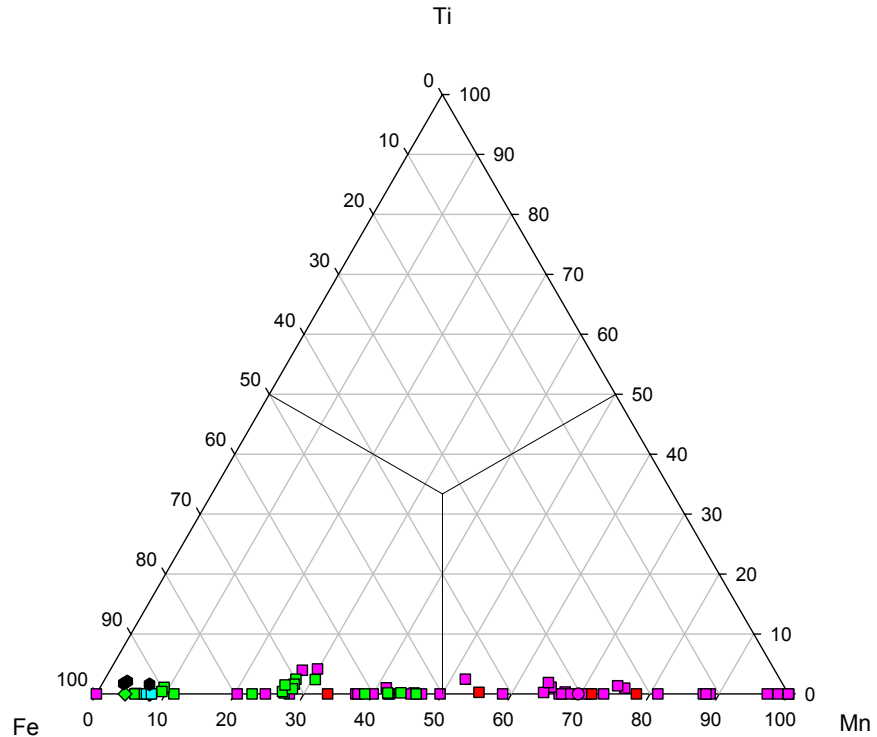


Fig. 27: Mn- Ti- Fe ternary, Namibian and Malian tourmaline.

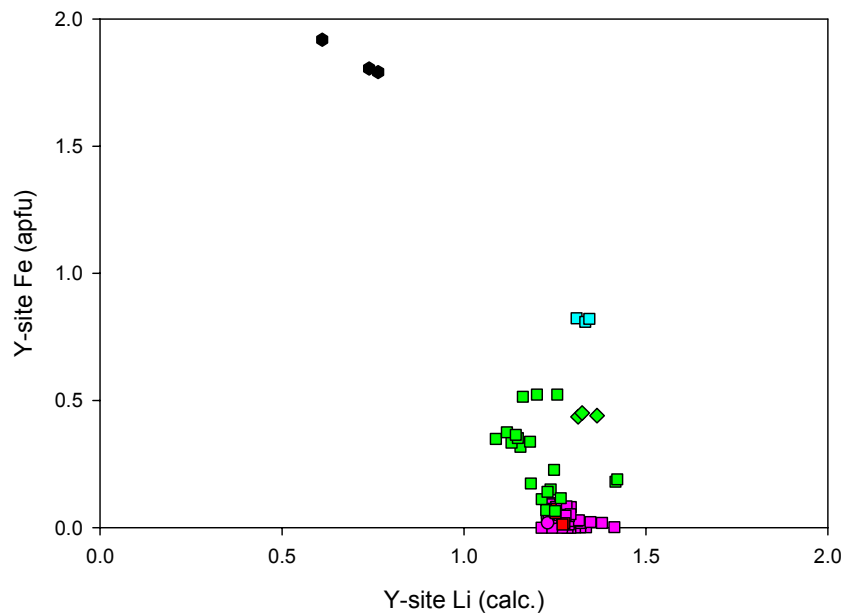


Fig. 28: Li (calc.) vs. Fe binary, Namibian and Malian tourmaline.

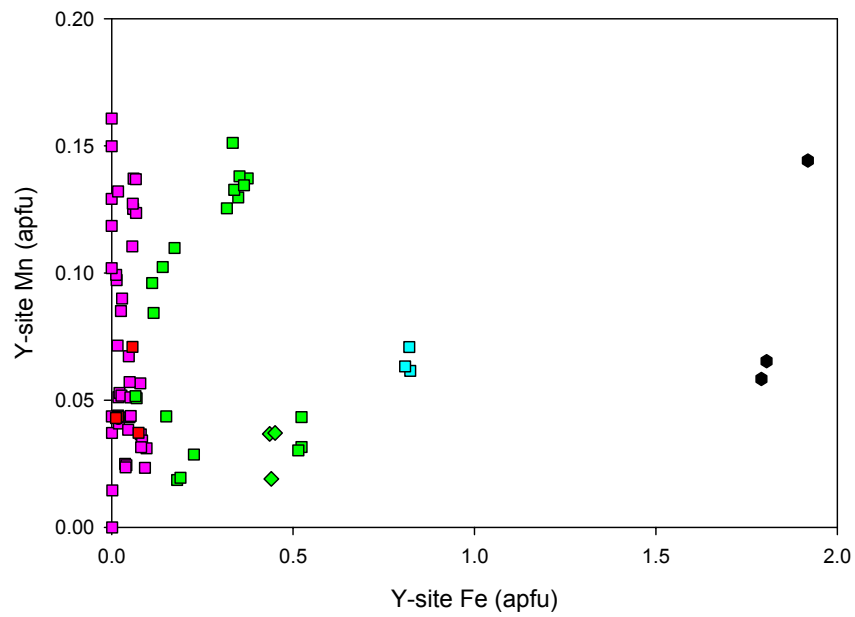


Fig. 29: Fe vs. Mn binary, Namibian and Malian tourmaline.

Fig. 30, Calculated Li vs. Mn plot: The slope of this graph is extremely negative. The schorl analyses plot far from the population of gem-quality material. Generally the colored stones have similar Mn quantities despite color. The sample from Mali has the lowest Mn content of the green elbaites.

Fig. 31, Calculated Li vs. F plot: This graph displays no definite trends or patterns. In general, the green and blue elbaites from Namibia and Mali contain the same quantities of F and Li as the pink and red elbaites and rossmanite spot. The schorl has approximately the same amount of F as the colored tourmalines but significantly less Li.

Fig. 32, Calculated Li vs. Y-site Al plot: As Li increases, Y-site Al increases forming a positive trend. The blue elbaite and green elbaite from Mali deviates from this trend. As Y-site Al increases, color changes from black (schorl) to blue, green, and finally various shades of red and pink. The rossmanite spot (sample 3-3, spot 2) is one of the most Al-rich specimens in the Namibian suite. Aside from the schorl (very low Al+Li), the colored tourmalines generally house the same calculated Li content.

Fig. 33, Y-site Al vs. Fe plot: A very distinct and tightly organized negative trend is displayed by this graph. As Al increases, Fe decreases at the Y-site. Accompanying this relationship are changes in color from black to blue, green and finally various hues of red and pink. The green elbaite from Mali contains the least Y-site Al of any green tourmaline analyzed in this suite.

Fig. 34, Fe vs. Ti plot: The only trend that these tourmaline samples display are the color changes described above as Y-site Fe quantities increase. The green elbaites

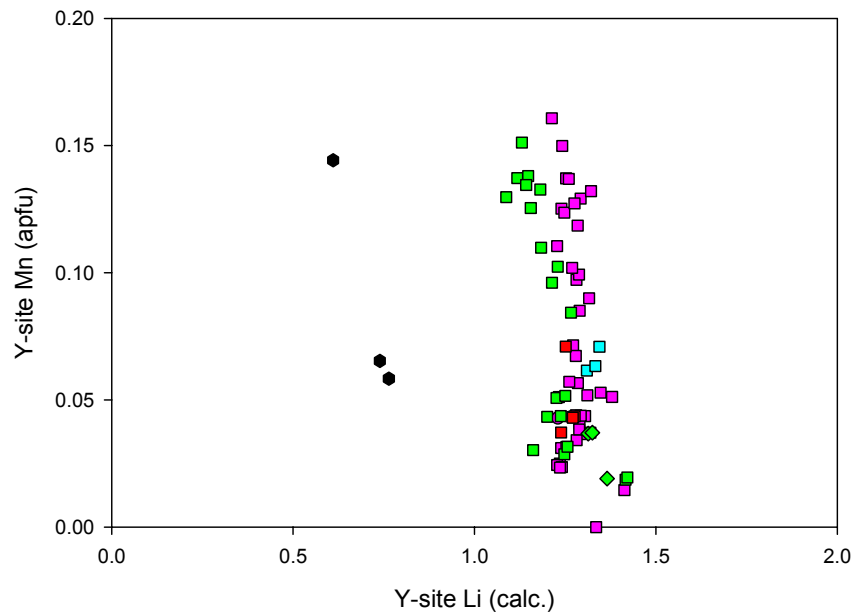


Fig. 30: Li (calc.) vs. Mn binary, Namibian and Malian tourmaline.

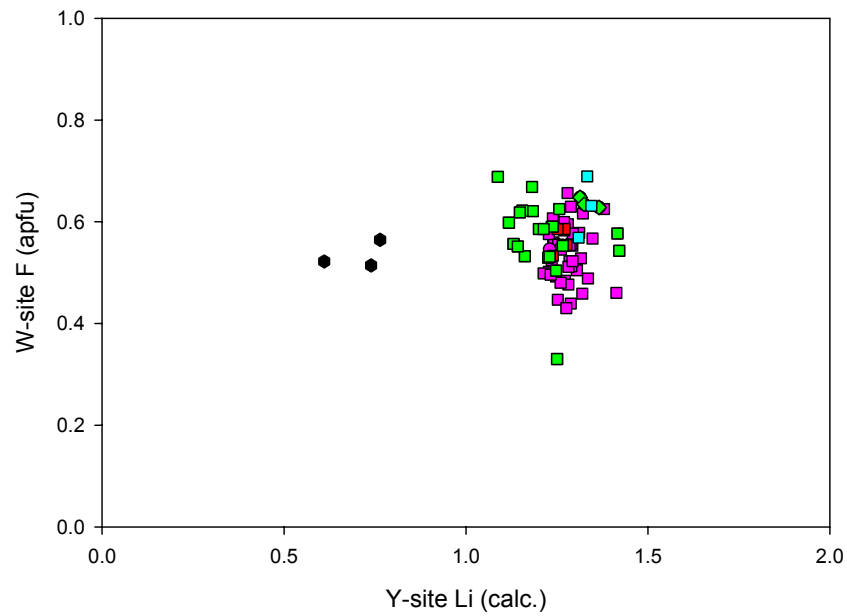


Fig. 31: Li (calc.) vs. W-site F binary, Namibian and Malian tourmaline.

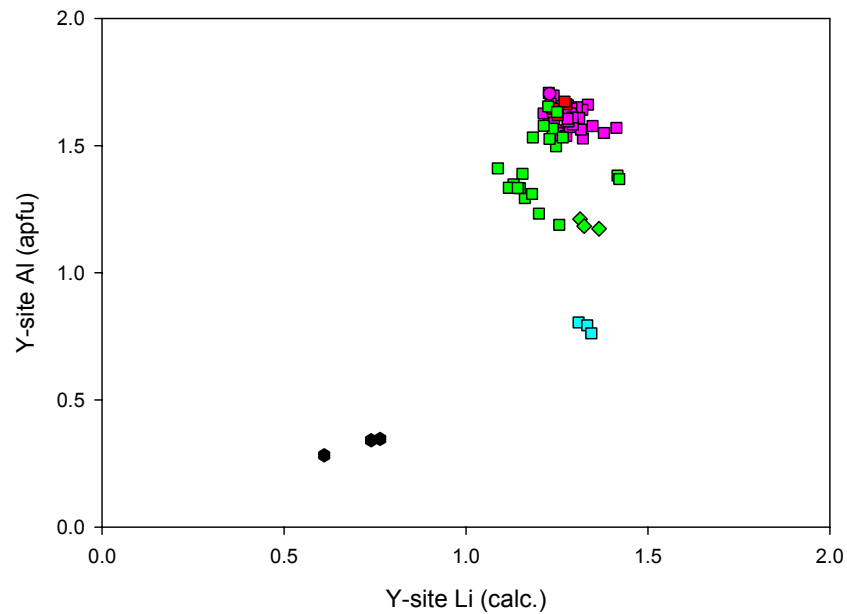


Fig. 32: Li (calc.) vs. Al binary, Namibian and Malian tourmaline.

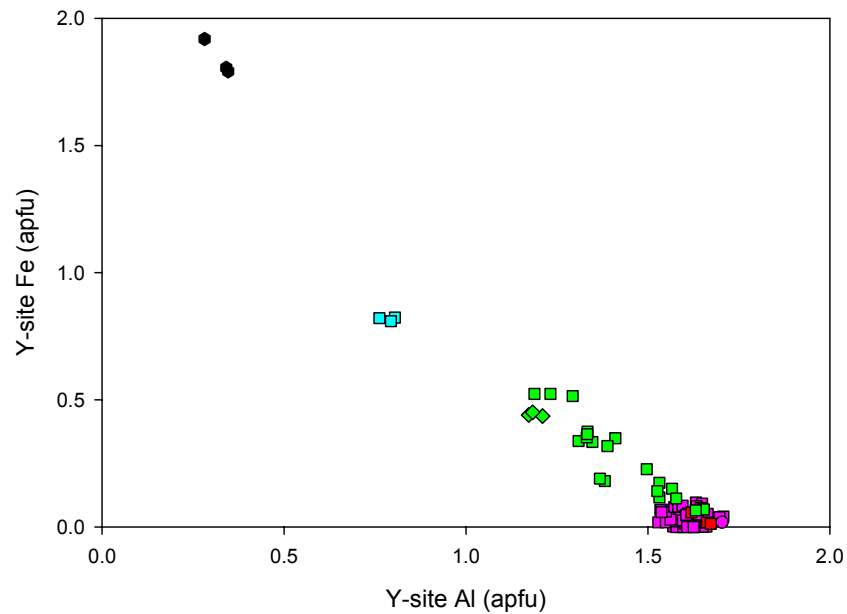


Fig. 33: Al vs. Fe binary, Namibian and Malian tourmaline.

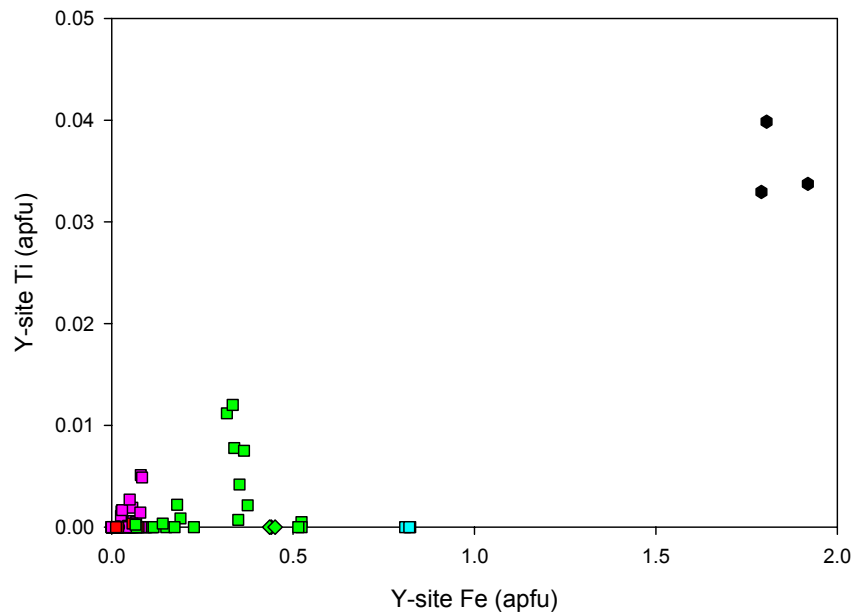


Fig. 34: Fe vs. Ti binary, Namibian and Malian tourmaline.

contain slightly more Ti than the other colored samples, whereas the elbaite from Mali contains no Ti. The schorl has up to 0.04 apfu and is considerably separated from the colored tourmaline data. However, when the schorls are included with the other samples, the graph shows a positive relationship.

Fig. 35, Mn vs. Ti plot: The colored tourmalines, especially the green and pink elbaites have approximately the same range of Mn quantities. A very slight Ti-enrichment is present in some green samples. Schorl covers the same Mn-range as do the colored tourmalines but has up to 0.04 apfu Ti, considerably more than the gem-quality material.

Fig. 36, Na vs. F plot: Samples cluster similarly to the Y-site Li vs. W-site F plot shown in Fig. 31. The pink rossmanite spot contains the least Na and the blue elbaite and black schorl contain the most. The green, blue and black stones contain slightly more F than the pink and red elbaites but generally, there is no separation between the variously colored stones with respect to F quantity.

Fig. 37, Na vs. Ti+Fe+Mn plot: This graph displays a positive, concave upward trend. Accompanying this trend are color changes from pink/red to green, blue and black. This chemistry changes from rossmanite to elbaite to schorl as total transition element contents increase.

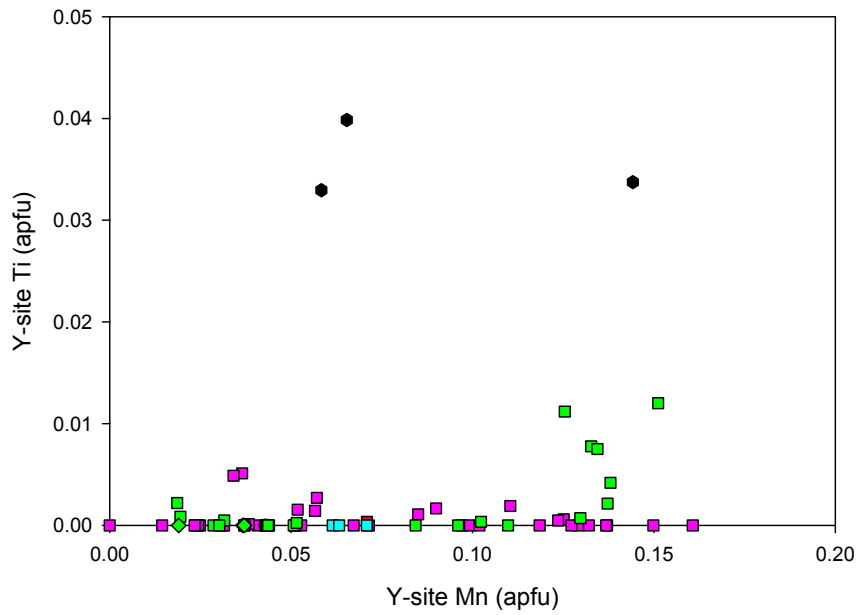


Fig. 35: Mn vs. Ti binary, Namibian and Malian tourmaline.

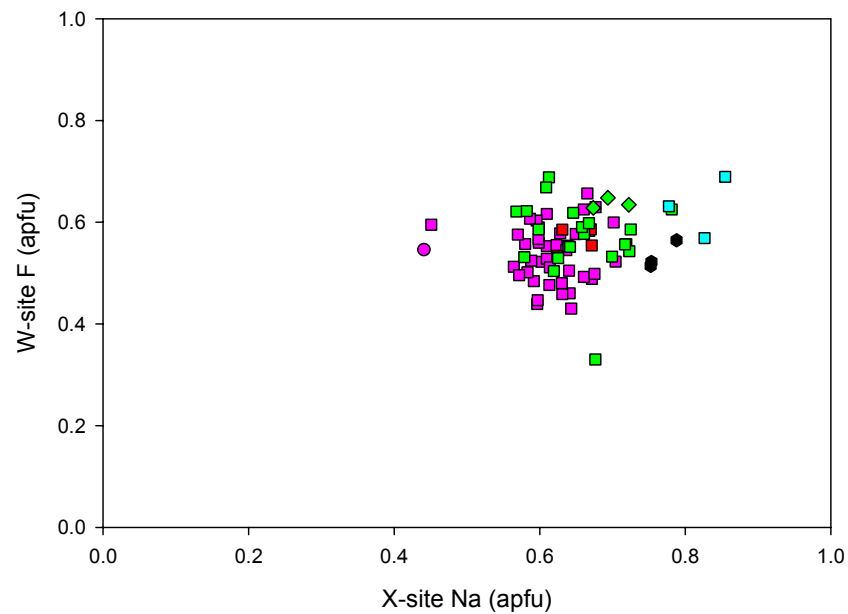


Fig. 36: Na vs. F binary, Namibian and Malian tourmaline.

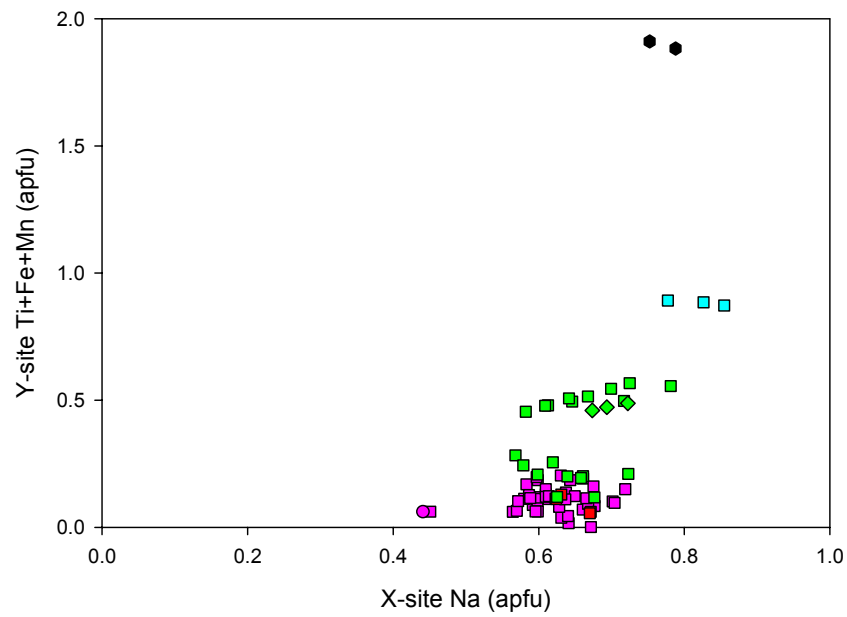


Fig. 37: Na vs. Ti+Fe+Mn binary, Namibian and Malian tourmaline.

Sanga Sanga, Tanzania tourmaline slices

The tourmaline slices and crystals from Sanga Sanga, Tanzania shown in Figs. 38 and 39 are comprised of liddicoatite, rossmanite (one analysis) and elbaite throughout the various chemical zones. Table 6 shows the microprobe data of these slices. From core to rim, slice "Sanga-w" is pink liddicoatite on the first four spots, then changes to pink rossmanite on the fifth spot and finally green liddicoatite on the last two spots. Slice "SS-wm" is liddicoatitic across the traverse but the color changes from pink to green on the final two spots. Sample "SS blue" is a blue elbaite slice. This sample suite is comprised of two watermelon tourmaline slices with pink cores and green rims and one slice which is blue throughout.



Fig. 38: Tanzanian "watermelon" tourmaline slices.



Fig. 39: "Watermelon" tourmaline crystals from Sanga Sanga, Tanzania.

The T, B and Z-sites: Si varies from 37.54 to 38.10 wt. % SiO_2 and 5.778 to 5.951 apfu Si. Calculated B is in the range of 10.97 to 11.34 wt. % B_2O_3 . The wt. % Al_2O_3 range is from 39.38 to 42.60. Liddicoatite zones contain the most total Al.

Ti, V and Mg: There is no detectable Ti, V or Mg in these slices.

Bismuth: Quantities of Bi are low in the slices with 0.01-0.12 wt. % and 0 to 0.005 apfu. Bi quantities are below detection limits in the blue slice and concentrations never rise above detection limits for the green zones. In “Sanga-w” Bi behaves somewhat irregularly with 0.005 apfu in the core, decreasing to 0.001 apfu in the rim. An increase of Bi is observed on intermediate spot 4 with 0.004 apfu Bi. The green portions of these slices have low, but significant Bi quantities.

Iron: Fe is most abundant in the blue elbaite slice and least abundant in the liddicoatite-rossmanite pink zones (spots 4-5) of sample “Sanga-w”. Overall Fe varies from 0 to 3.28 wt. % FeO and 0 to 0.431 apfu Fe. From core to rim, “Sanga-w” has decreasing Fe content from 0.014 to 0 apfu through the pink core and an increase to 0.012 apfu at the green rim with no Fe detected in the outermost spot. Slice “SS wm” has gradually increasing Fe in the pink core from 0 to 0.013 apfu, then increases from 0.188 to 0.204 apfu in the green rim. The blue elbaite has uniformly high Fe ranging from 0.399 to 0.431 apfu.

Manganese: The range of Mn contents is from 0.14 to 0.43 wt. % MnO and 0.018 to 0.055 apfu Mn. The pink core (spots 1-5) of “Sanga-w” contains 0.053 to 0.055 apfu Mn decreasing to 0.018 apfu. The green rim of this slice (spots 6-7) displays an increase in Mn with 0.018 to 0.035 apfu. From core to rim, the watermelon slice, “SS wm” has

uniform Mn quantities from 0.035 to 0.041 apfu with the most Mn in the pink core. The blue elbaite contains 0.03 to 0.036 apfu Mn.

Calcium: Ca varies from 1.23-3.33 wt. % CaO and 0.209-0.548 apfu Ca. Ca fluctuates erratically for “Sanga-w”. From core to rim, Ca varies erratically from 0.352 to 0.548 apfu for the pink core, then from 0.427 to 0.517 apfu at the green rim. Ca steadily decreases from 0.336 to 0.259 apfu at the pink core, then increases from 0.282 to 0.337 apfu in the green rim for sample “SS wm”. In the blue slice, Ca increases from 0.209 to 0.243 apfu, after which contents decrease to 0.232 apfu.

Calculated Lithium: Calculated Li is most abundant in the liddicoatite zones and lowest in the elbaite zones. Overall, calculated Li fluctuates from 1.97 to 2.46 wt. % and 1.257 to 1.526 apfu. In slice “Sanga-w”, Li contents vary widely with 1.444, 1.437, 1.487, 1.434 and 1.396 apfu for spots 1-5 respectively of the pink core. Li increases to 1.440 to 1.526 apfu for spots 6 to 7 respectively of the green rim of this slice. Li contents decrease in the pink core (spots 1-3) of “SS wm” with 1.471 to 1.421 apfu and contents continue to fall at the green rim (spots 4-5) with 1.396 to 1.382 apfu. Li stays relatively constant in slice “SS blue” with 1.257, 1.269 and 1.257 apfu for spots 2-4 respectively.

Sodium: Like Ca, Na shows pronounced fluctuations along core to rim traverses. Na ranges from 0.46-1.83 wt. % Na₂O and 0.136 to 0.548 apfu Na. Na content in sample “Sanga-w” is also highly variable from core to rim. Na increases from 0.459 to 0.548 apfu for spots 1-3 of the pink core of “SS wm” and decreases to 0.537 to 0.441 apfu in the green rim. In “SS blue”, Na falls from 0.569 to 0.546 apfu for spots 2-3 of the core respectively and rises to 0.574 apfu at spot 4 of the rim.

Potassium: Throughout the slices, K content remains very low but detectable. Quantities vary from 0.02 to 0.05 wt. % K₂O and 0.004 to 0.009 apfu K. K varies irregularly, without discernable patterns in the three slices.

X-site totals: The lowest X-site totals are found in the liddicoatite and rossmanite zones and the highest totals are in the elbaite zones. From core to rim of "Sanga-w", X-site totals are 0.736, 0.674, 0.688, 0.622 (rossmanite spot), 0.626 apfu for spots 1-5 of the pink core and 0.715 to 0.674 apfu for spots 6-7 of the green rim. Spots 1 to 3 of the pink core of "SS wm" contain 0.802, 0.824 and 0.811 apfu respectively, whereas the green rim has 0.824 to 0.787 apfu at the X-site for spots 4-5. Totals range from 0.785 to 0.811 apfu from core to rim for the blue slice.

Hydroxyl anion and calculated water: Samples "SS wm" and "Sanga-w" are OH-dominant members of their respective species (hydroxyl-liddicoatite, elbaite and rossmanite), whereas the blue elbaite is not OH-dominant. H₂O wt. % ranges from 3.21 to 3.63 whereas OH varies from 3.385 to 3.71 apfu.

Fluorine: The overall range of F for the three slices is 0.60 to 1.23 wt. % and 0.29 to 0.615 apfu. The F quantities of "Sanga-w", from core to rim are 0.363, 0.335, 0.290, 0.320, 0.376, 0.420 and 0.354 apfu for spots 1-7 respectively. Pink spots 1-3 of "SS wm" have decreasing F quantities of 0.459, 0.429 and 0.420 apfu respectively, whereas contents increase to 0.479 apfu on spot 4 and drop to 0.452 apfu on spot 5. F steadily increases from 0.568 to 0.615 apfu from core to rim of slice "SS blue".

Table 6: Microprobe analyses, Tanzanian tourmaline.

Oxides	Sanga-w1	Sanga-w2	Sanga-w3	Sanga-w4	Sanga-w5	Sanga-w6	Sanga-w7	SS wm-1
sample color	salmon p	salmon p	v pale p	bright p	bright p	pale g	pale g col	pink
SiO ₂	37.89	37.77	37.69	37.54	37.72	37.58	37.66	38.10
TiO ₂	0.00	0.00	0.00	0.00	0.00	0.00	0.00	0.00
B ₂ O ₃ calc.	11.25	11.30	11.33	11.24	11.24	11.24	11.23	11.32
Al ₂ O ₃	41.92	42.42	42.60	42.42	42.53	41.96	42.12	42.23
Bi ₂ O ₃	0.12	0.07	0.03	0.09	0.03	0.04	0.04	0.01
V ₂ O ₃	0.00	0.00	0.00	0.00	0.00	0.00	0.00	0.00
FeO	0.11	0.09	0.01	0.00	0.00	0.00	0.10	0.01
MnO	0.40	0.43	0.27	0.21	0.14	0.14	0.27	0.31
MgO	0.00	0.00	0.00	0.00	0.00	0.00	0.00	0.00
CaO	2.22	2.81	3.33	2.84	2.12	3.30	2.58	2.04
Li ₂ O calc.	2.33	2.32	2.41	2.31	2.24	2.45	2.31	2.38
Na ₂ O	1.21	0.69	0.46	0.49	0.90	0.55	0.81	1.54
K ₂ O	0.03	0.03	0.03	0.02	0.03	0.03	0.02	0.03
H ₂ O calc.	3.53	3.57	3.63	3.57	3.51	3.47	3.53	3.46
F	0.74	0.69	0.60	0.65	0.77	0.86	0.72	0.95
Sub-total	101.75	102.18	102.39	101.37	101.23	101.62	101.37	102.40
O=F	-0.31	-0.29	-0.25	-0.28	-0.32	-0.36	-0.30	-0.40
Total	101.44	101.89	102.13	101.10	100.91	101.26	101.07	102.00
Ions (apfu)								
T: Si	5.853	5.806	5.778	5.804	5.833	5.810	5.828	5.848
Al	0.147	0.194	0.222	0.196	0.167	0.190	0.172	0.152
B: B	3.000	3.000	3.000	3.000	3.000	3.000	3.000	3.000
Z: Al	6.000	6.000	6.000	6.000	6.000	6.000	6.000	6.000
Y: Al	1.484	1.493	1.474	1.535	1.585	1.454	1.511	1.486
Ti	0.000	0.000	0.000	0.000	0.000	0.000	0.000	0.000
Bi	0.005	0.003	0.001	0.004	0.001	0.002	0.001	0.000
V	0.000	0.000	0.000	0.000	0.000	0.000	0.000	0.000
Fe ²⁺	0.014	0.011	0.002	0.000	0.000	0.000	0.012	0.002
Mn ²⁺	0.053	0.055	0.035	0.028	0.018	0.018	0.035	0.041
Mg	0.000	0.000	0.000	0.000	0.000	0.000	0.000	0.000
Li	1.444	1.437	1.487	1.434	1.396	1.526	1.440	1.471
X: Ca	0.368	0.462	0.548	0.471	0.352	0.547	0.427	0.336
Na	0.363	0.206	0.136	0.148	0.268	0.163	0.242	0.459
K	0.005	0.006	0.005	0.004	0.006	0.005	0.004	0.007
□ (vac.)	0.264	0.326	0.312	0.378	0.374	0.285	0.326	0.198
OH	3.637	3.665	3.710	3.680	3.624	3.580	3.646	3.541
F	0.363	0.335	0.290	0.320	0.376	0.420	0.354	0.459
species	OH-liddi	OH-liddi	OH-liddi	OH-liddi	rossman	OH-liddi	OH-liddi	elbaite

Oxides	sample	SS wm-2	SS wm-3	SS wm-4	SS wm-5	SS blue-2	SS blue-3	SS blue-4
color		pink	pink	green	green	blue	blue	blue
SiO ₂		37.97	37.84	37.72	37.56	37.54	37.61	37.71
TiO ₂		0.00	0.00	0.00	0.00	0.00	0.00	0.00
B ₂ O ₃ calc.		11.33	11.28	11.08	11.09	10.96	10.99	11.05
Al ₂ O ₃		42.41	42.32	40.32	40.51	39.41	39.38	39.62
Bi ₂ O ₃		0.03	0.03	0.03	0.03	0.01	0.01	0.01
V ₂ O ₃		0.00	0.00	0.00	0.00	0.00	0.00	0.00
FeO		0.03	0.10	1.43	1.55	3.01	3.11	3.28
MnO		0.33	0.34	0.32	0.32	0.23	0.27	0.23
MgO		0.00	0.00	0.00	0.00	0.00	0.00	0.00
CaO		1.97	1.57	1.68	2.01	1.23	1.43	1.38
Li ₂ O calc.		2.37	2.29	2.21	2.19	1.97	2.00	1.99
Na ₂ O		1.66	1.83	1.77	1.45	1.85	1.78	1.88
K ₂ O		0.04	0.03	0.03	0.05	0.03	0.04	0.03
H ₂ O calc.		3.49	3.48	3.36	3.39	3.25	3.21	3.26
F		0.89	0.86	0.97	0.91	1.13	1.23	1.17
Sub-total		102.50	101.97	100.91	101.06	100.63	101.06	101.59
O=F		-0.37	-0.36	-0.41	-0.38	-0.48	-0.52	-0.49
Total		102.13	101.61	100.50	100.67	100.16	100.55	101.10
Ions (apfu)								
T: Si		5.824	5.832	5.917	5.887	5.951	5.946	5.934
Al		0.176	0.168	0.083	0.113	0.049	0.054	0.066
B: B		3.000	3.000	3.000	3.000	3.000	3.000	3.000
Z: Al		6.000	6.000	6.000	6.000	6.000	6.000	6.000
Y: Al		1.491	1.520	1.372	1.371	1.313	1.283	1.281
Ti		0.000	0.000	0.000	0.000	0.000	0.000	0.000
Bi		0.001	0.001	0.001	0.001	0.000	0.001	0.000
V		0.000	0.000	0.000	0.000	0.000	0.000	0.000
Fe ²⁺		0.004	0.013	0.188	0.204	0.399	0.411	0.431
Mn ²⁺		0.043	0.045	0.042	0.042	0.030	0.036	0.030
Mg		0.000	0.000	0.000	0.000	0.000	0.000	0.000
Li		1.461	1.421	1.396	1.382	1.257	1.269	1.257
X: Ca		0.323	0.259	0.282	0.337	0.209	0.243	0.232
Na		0.492	0.548	0.537	0.441	0.569	0.546	0.574
K		0.008	0.005	0.005	0.009	0.007	0.008	0.005
□ (vac.)		0.176	0.189	0.176	0.213	0.215	0.203	0.189
OH		3.571	3.580	3.521	3.548	3.432	3.385	3.417
F		0.429	0.420	0.479	0.452	0.568	0.615	0.583
species		elbaite	elbaite	elbaite	elbaite	F-elbaite	F-elbaite	F-elbaite

Sanga Sanga, Tanzania tourmaline plots

Fig. 40, X-site Ca-vacancy-Na plot: Slices “SS blue” and “SS wm” are elbaites and “Sanga-w” contains both liddicoatite and rossmanite zones with substantial amounts of the elbaite molecule based on the X-site occupancy ternary. Elbaite zones may be blue, green or pink and blue analyses are elbaites only. The liddicoatites are pink and green whereas the rossmanite spot is pink. The pink liddicoatite zones have the highest relative quantities of the rossmanite molecule.

Fig. 41, Mn-Ti-Fe plot: The blue and green elbaite analyses plot in the Fe-field and the pink liddicoatite, elbaite and rossmanite spots fall in the Mn-dominant field. Green liddicoatite analyses plot in the Mn-field.

Fig. 42, Calculated Li vs. Fe plot: This plot shows a steeply negative trend with increasing Li as Fe quantities decrease. The variously colored zones are separated and change color from blue to green to pink accompanying this chemical trend. The very light green to nearly colorless liddicoatite zones plot with the pink liddicoatite, elbaite and rossmanite data.

Fig. 43, Fe vs. Mn plot: The pink, green and blue zones have the same range of Mn contents. Pink to green to blue color changes take place as Fe increases. The colored chemical zones cluster together. The pink zones have the most diverse Mn contents. The very light green liddicoatite zones plot among the pink elbaite zones.

Fig. 44, Calculated Li vs. Mn plot: This graph shows no trend. Considerable overlap of Mn content occurs with all three colors. The pink portions have the widest range of Mn content and the most Mn overall.

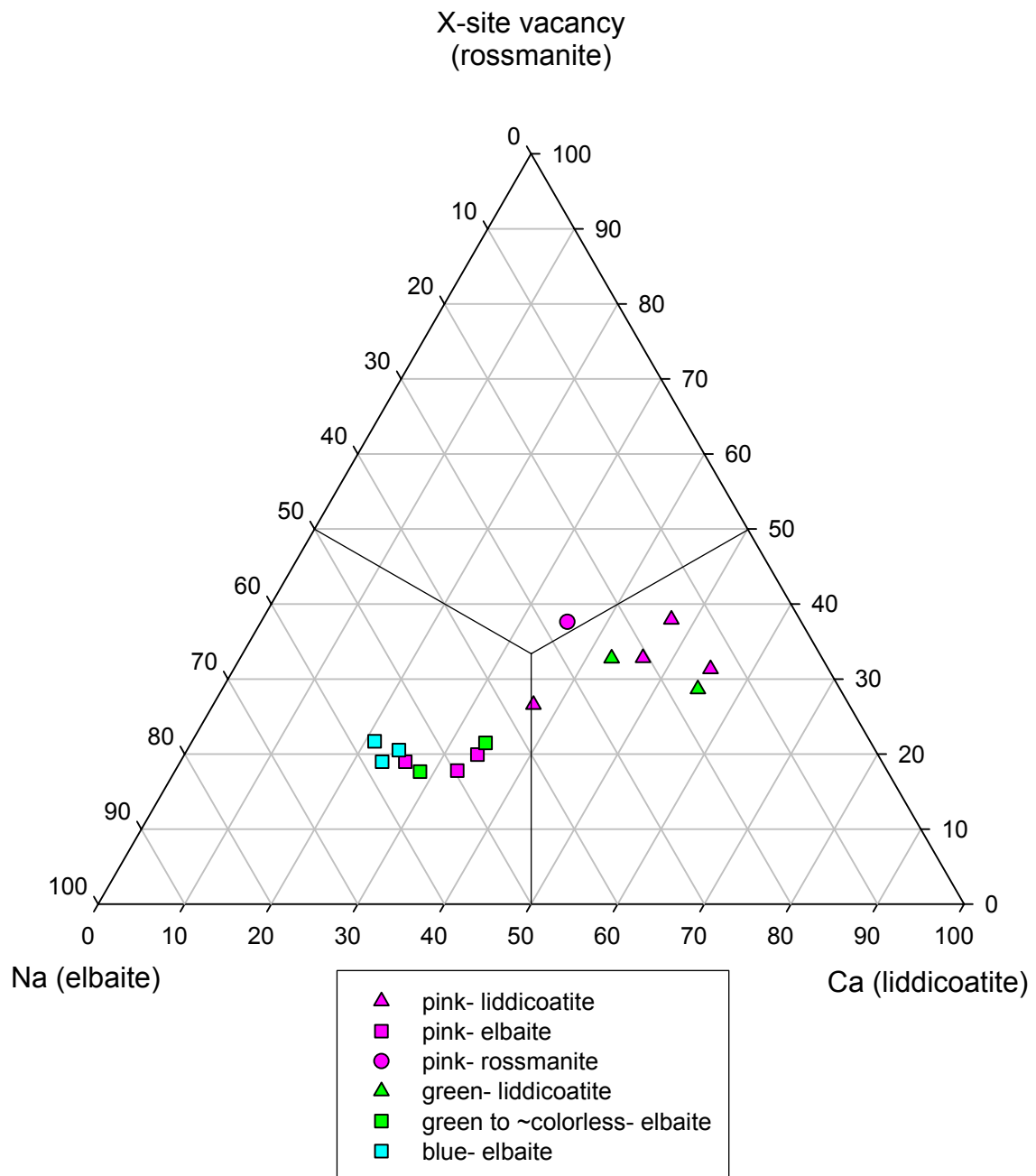


Fig. 40: Ca- X-site vacancy- Na ternary, Tanzanian tourmaline.

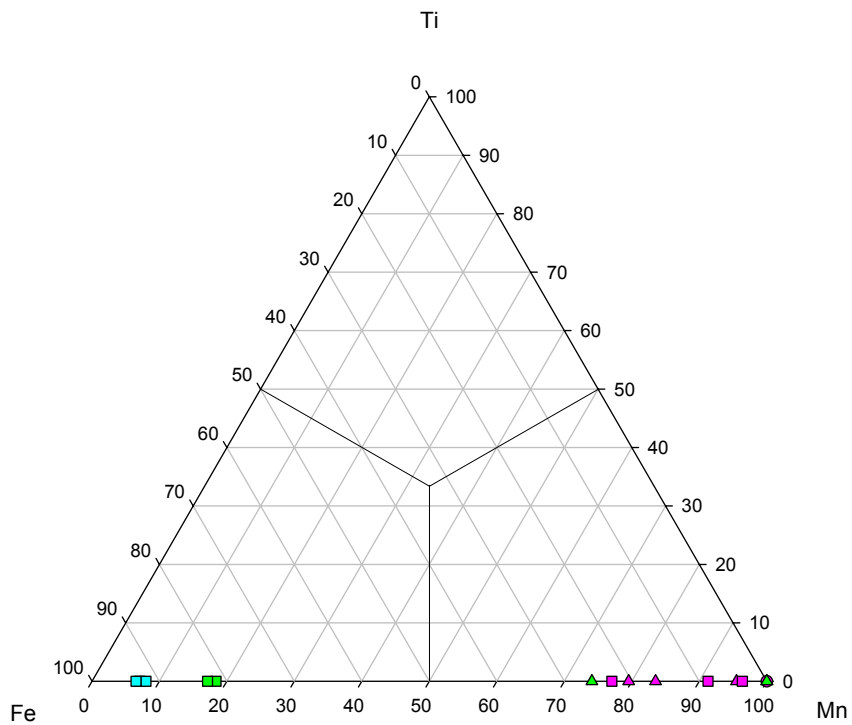


Fig. 41: Mn- Ti- Fe ternary, Tanzanian tourmaline.

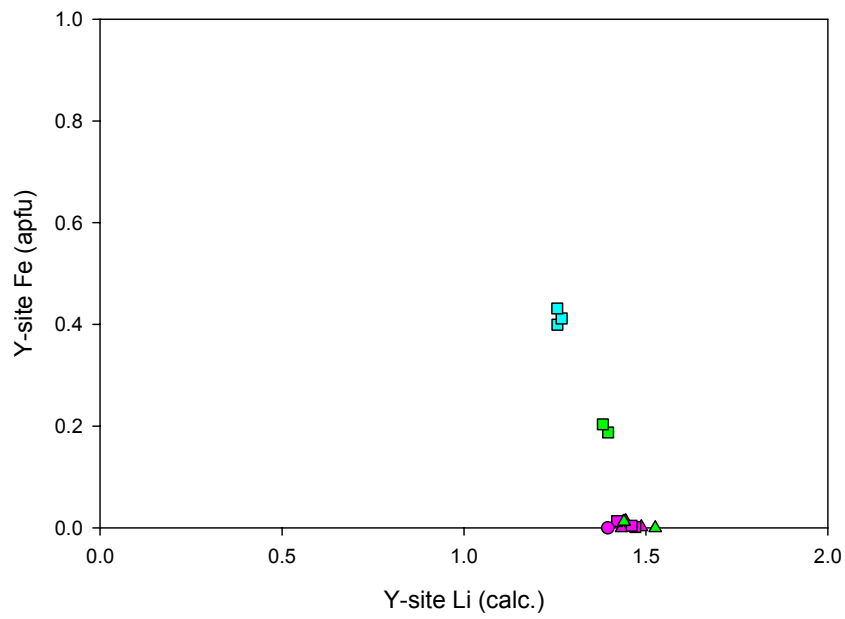


Fig. 42: Li (calc.) vs. Fe binary, Tanzanian tourmaline.

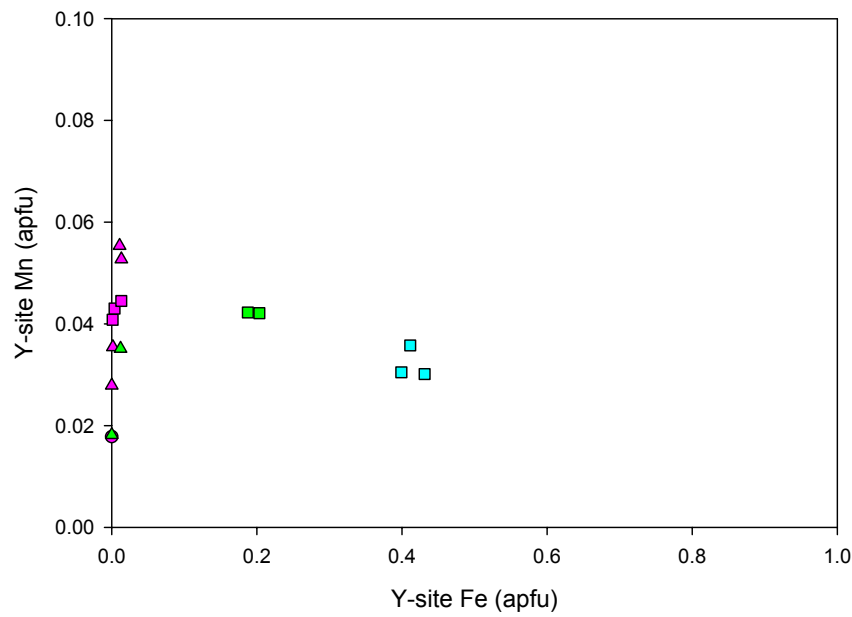


Fig. 43: Fe vs. Mn binary, Tanzanian tourmaline.

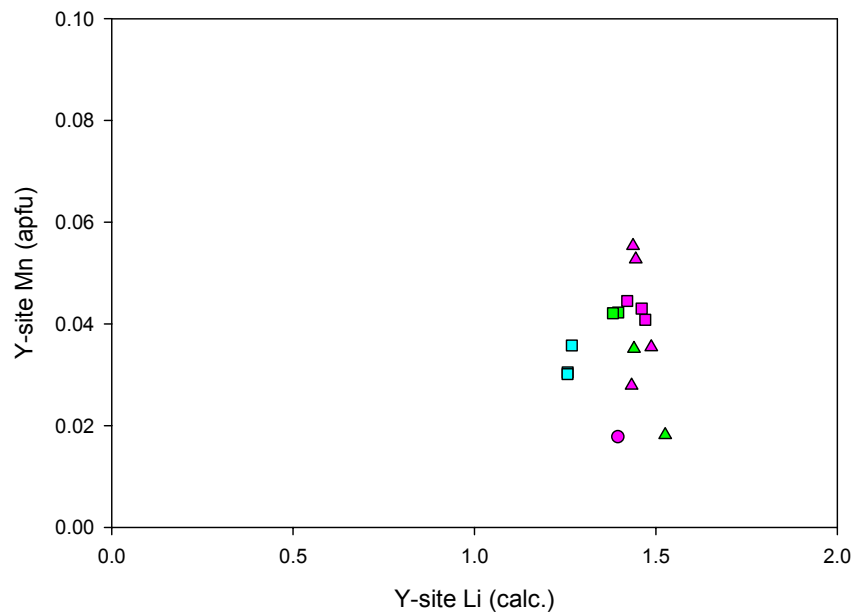


Fig. 44: Li (calc.) vs. Mn binary, Tanzanian tourmaline.

Fig. 45, Calculated Li vs. F plot: With increasing Li, F decreases. A somewhat noticeable separation of the data with regard to color is observed and corresponds to the above trend. The light green liddicoatite zones plot with the pink elbaite, liddicoatite and rossmanite zones. The blue elbaite slice is the most F-rich of the Tanzanian tourmaline.

Fig. 46, Calculated Li vs. Y-site Al plot: As Li contents rise, a simultaneous increase of Y-site Al content takes place forming a positive relationship as the colors change from blue to green to pink. The blue elbaites have the lowest Li+Al quantities and the pink/light green liddicoatites and rossmanite have the most.

Fig. 47, Y-site Al vs. Fe plot: A negative correlation between Al and Fe is observed. As Y-site Al increases, Fe decreases as the colors change from blue to green to pink. The blue elbaite has the lowest Y-site Al and the highest Fe. Conversely, the pink rossmanite spot contains the least Fe and most Al.

Fig. 48, Fe vs. Ti plot: There are no trends expressed by this graph and there is no Ti in the samples. Blue samples contain the most Fe whereas pink samples contain the least Fe. The green rims of slices “SS wm” and “Sanga w” contain intermediate Fe content.

Fig. 49, Mn vs. Ti plot: Analyses cling to the x-axis and there is no Ti. The blue elbaite generally has the least Mn and the pink liddicoatite analyses have the most. Considerable overlap of color irrespective of Mn content is observed.

Fig. 50, Na vs. F plot: The tourmaline slices from Sanga Sanga, Tanzania display a weakly positive correlation of Na increasing with increasing F. The slope of the graph is nearly zero. The blue slice contains the most Na and F and deviates from the main

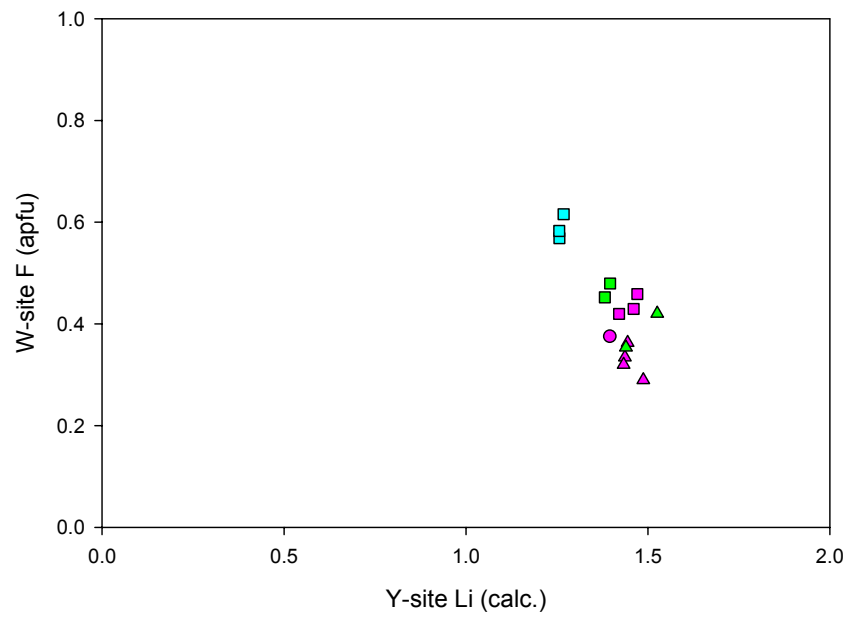


Fig. 45: Li (calc.) vs. F binary, Tanzanian tourmaline.

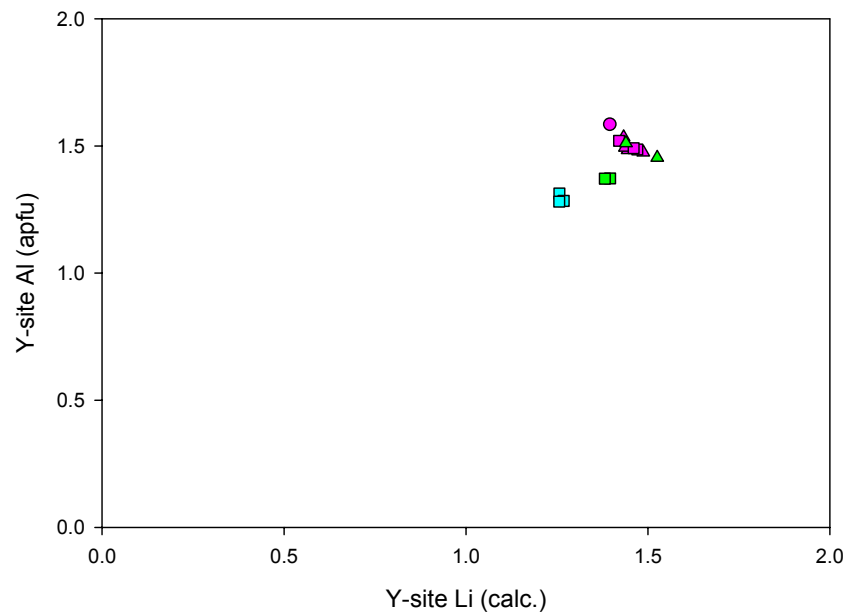


Fig. 46: Li (calc.) vs. Al binary, Tanzanian tourmaline.

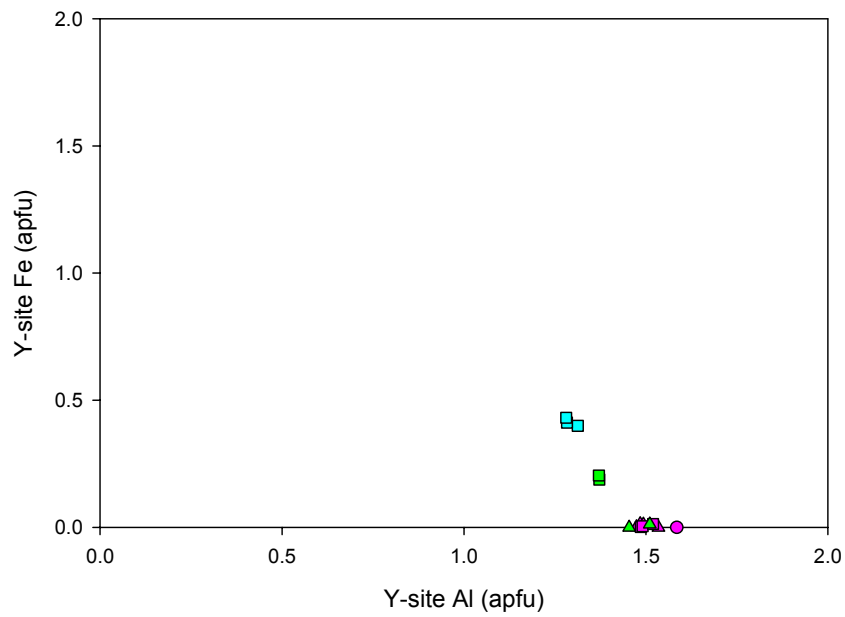


Fig. 47: Al vs. Fe binary, Tanzanian tourmaline.

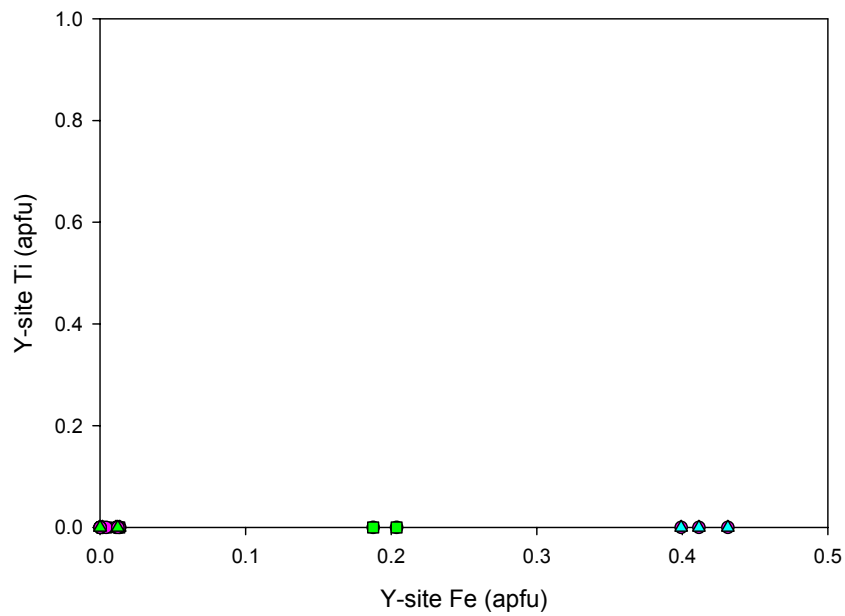


Fig. 48: Fe vs. Ti binary, Tanzanian tourmaline.

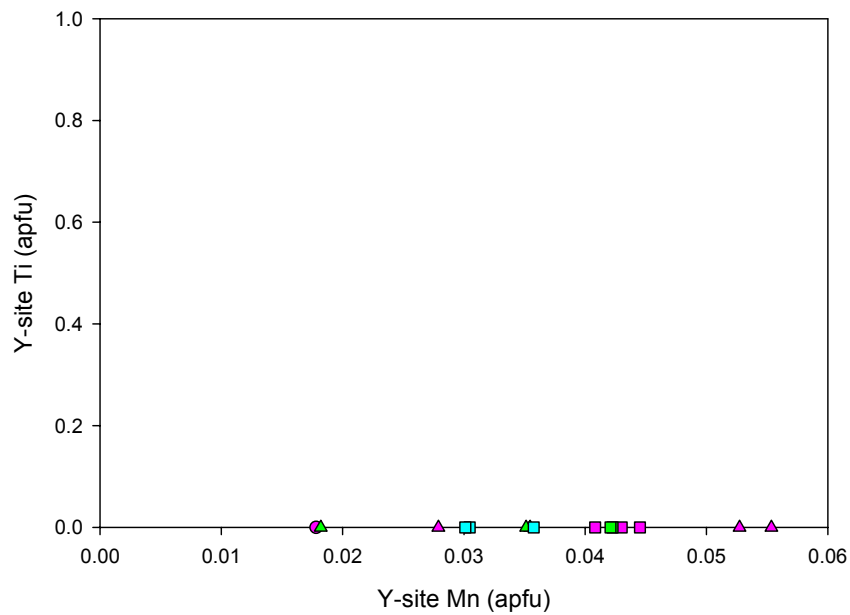


Fig. 49: Mn vs. Ti binary, Tanzanian tourmaline.

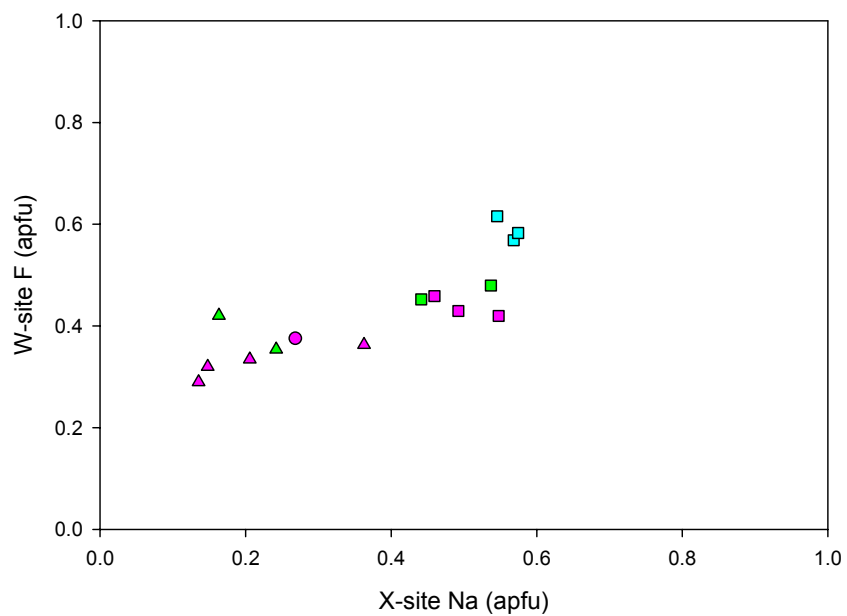


Fig. 50: Na vs. F binary, Tanzanian tourmaline.

trend. Generally the liddicoatite and rossmanite portions have lower Na and F quantities than do the elbaitic zones.

Fig. 51, Na vs. Ti+Fe+Mn plot: A positive, concave upward trend is observed as Na contents increase with increasing chromophoric transition element quantities. As with the Nigerian stones, elbaitic samples may contain high Na contents and low quantities of transition elements. The colors change from pink to green to blue as the mineralogy changes from liddicoatite to rossmanite to elbaite with the above trend.

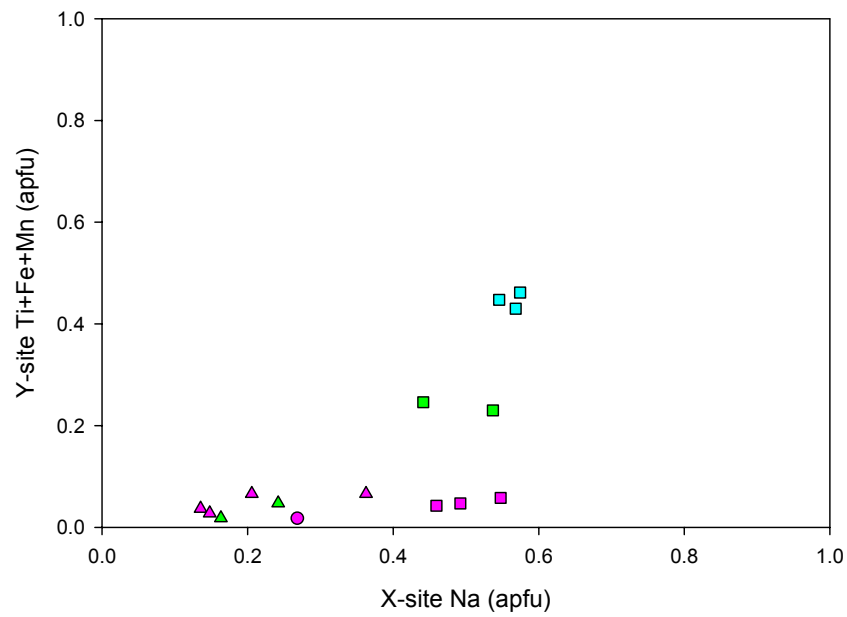


Fig. 51: Na vs. Ti+Fe+Mn binary, Tanzanian tourmaline.

Democratic Republic of Congo tourmaline slices

The tourmaline slices from the Democratic Republic of Congo shown in Fig. 52 are elbaites. Microprobe data of these slices is shown in Table 7. These slices contain pink, green, yellowish-brown, brown and dark-brown zones. Generally, the pink zones of "Congo I" are the most liddicoatitic and rossmanitic in character and the brownish zones contain the greatest proportions of the elbaite molecule.



Fig. 52: Congolese tourmaline slices.

The T, B and Z-sites: The range of Si content is between 36.97 to 37.44 wt. % SiO_2 and 5.923 to 6.114 apfu Si. Calculated B_2O_3 wt. % varies from 10.51 to 10.93. Total Al quantities are between 33.51 to 39.81 wt. % Al_2O_3 . Total Al is highest for the pink elbaite zones of sample “Congo l” and lowest for the dark-brown core of “Congo i”.

Y-site Al: This has a very broad range from 0.535-1.411 apfu Al. The pink zones of sample Congo “l” contain the most Y-site Al with 1.271 to 1.411 apfu. In the yellow-brown zones of “Congo k” and “Congo i”, Al is between 0.812 to 1.162 apfu. The green rim of sample “Congo l” contains 1.211 apfu Al. Lastly, the brown to dark-brown elbaite zones of “Congo k” and “Congo i” generally contain a paucity of Y-site Al with 0.535 to 0.948 apfu.

Titanium: Ti is very prevalent in these samples and attains quantities as high as the Nigerian and Namibian tourmalines. Overall, Ti ranges between 0 to 0.37 wt. % TiO_2 and 0 to 0.044 apfu Ti. The pink zones of “Congo l” have up to 0.05 wt. % and 0.006 apfu Ti and there is a spike of Ti up to 0.24 wt. % and 0.029 apfu in the green rim. Ti is initially high in the brown core of “Congo k” and progressively decreases from 0.032 to 0.021 apfu from the brown core to the yellow-brown rim. In slice “Congo i”, Ti quantities are 0.037 (dark-brown core), 0.044 and 0.043 apfu from core to rim with an increase in the yellowish-brown intermediate zone.

Bismuth and Vanadium: These two elements were not detected in the Congolese slices.

Iron: The variation of Fe ranges from 0.12 to 5.05 wt. % FeO and 0.016 to 0.699 apfu Fe. From core to rim, Fe has quantities of 0.208, 0.233, 0.239 (murky-pink), 0.082, 0.090, 0.086 (pink) and 0.127 apfu (green rim) for spots 1-7 of “Congo l” respectively.

From the brown core to the yellowish-brown rim of “Congo k”, there is 0.018, 0.086, 0.055 and 0.127 apfu Fe for spots 2, 5, 6 and 7 respectively. The dark-brown core of “Congo i” contains 0.699 apfu Fe and this decreases to 0.023 to 0.016 apfu in the yellow-brown rim.

Manganese: Mn is highly variable for the three slices with 1.01 to 7.11 wt. % MnO and 0.137 to 0.98 apfu overall. Mn is lowest throughout the “Congo l” traverse with 0.219, 0.219, 0.217, 0.225, 0.235, 0.216 apfu for spots 1-6 pink core and 0.137 apfu at the green rim. The dark-brown core of sample “i” has 0.824 apfu Mn whereas Mn increases to 0.98 apfu then drops to 0.96 apfu at the yellowish-brown rim. The brown core of slice “Congo k” initially has between 0.907 to 0.867 apfu Mn and these contents decrease to 0.687 to 0.594 apfu in the yellow-brown rim.

Magnesium: There is a preponderance of Mg in these slices with contents ranging from 0 to 0.46 wt. % and 0 to 0.11 apfu. On spots 1-7 of “Congo l” (core-rim), Mg fluctuates from 0.046 to 0.042, 0.048, 0.018, 0.038, 0.039 and jumps to 0.11 apfu in the green rim. No Mg was detected in slice “Congo k”. Mg steadily decreases from 0.069 apfu in the dark-brown core of “i” to 0.006 to 0.005 apfu in the yellow-brown rim.

Calcium: Ca quantities are very low for these samples. Concentrations range from 0.03 to 0.80 wt. % CaO and 0.005 to 0.137 apfu Ca. For sample “Congo l”, from core to rim, Ca ranges from 0.137 to 0.107, 0.102, 0.133, 0.104, 0.118 apfu for the pink core, then drops to 0.045 apfu in the green rim. Ca behavior is erratic in “Congo k” with 0.097, 0.048 (brown core), 0.086 and 0.071 apfu (yellow-brown rim). Ca is initially low with 0.005 apfu in the dark-brown core of “Congo i”, rising to 0.09 to 0.074 apfu at the rim.

Calculated Lithium: Li is rather low for these slices compared to others in the study. The range of Li is from 1.25 to 1.91 wt. % Li₂O and 0.831 to 1.263 apfu. In the pink core of “l”, Li rises from 1.179 to 1.263 apfu over spots 1-4, then steadily decreases from 1.241 to 1.093 apfu over the final three spots. Li in “Congo k” is initially at 1.198 apfu (spot 2), drops to 1.072 to 1.074 apfu over spots 5 to 6 of the brown core to yellow-brown rim and rises to 1.105 apfu at the final spot of the yellow-brown rim. At the dark-brown rim at “sample i”, Li is initially low with 0.831 apfu at the dark-brown core but increases to 1.129 apfu through the yellow-brown rim.

Sodium: There is significant Na fluctuation in all three slices. Its composition varies from 1.94 to 2.50 wt. % and 0.606 to 0.81 apfu overall. The pink core of “Congo l” contains from 0.606 to 0.76 apfu Na, whereas quantities increase to 0.774 apfu at the green rim. Na decreases then increases in sample “k”, fluctuating from 0.761 to 0.732 at the brown core and from 0.645 to 0.710 apfu at the yellow-brown rim. The Na content of sample “i” rises then falls with 0.745, 0.810 and 0.757 apfu for spots 2, 4 and 5 respectively.

Potassium: K is extremely low in the slices. It is barely detected in the yellow-brown rim of “k” at spots 6 to 7 with 0.002 to 0.004 apfu K and the brown core, spot 5 of sample “k” with 0.002 apfu K. The dark-brown core of “Congo i” has 0.003 apfu K. There was no K detected in “Congo l”.

X-site totals: Occupancy at the X-site remains high throughout with 0.724 to 0.9 apfu overall. X-site totals are 0.761, 0.755, 0.862 0.794, 0.769, 0.724 and 0.819 apfu for spots 1-7 respectively of pink-green sample “Congo l”. X-site totals in “Congo k” decrease from 0.858 to 0.733 over spots 2, 5 and 6 and increase to 0.785 apfu at spot 7.

Totals in sample “Congo i” rise then fall with 0.753, 0.900 and 0.831 over spots 2, 4 and 5 respectively.

Hydroxyl anion and calculated water: The wt. % of H₂O varies from 3.16 to 3.27 and OH quantities range from 3.389 to 3.558 apfu at the W-site. “Congo l” is OH subordinate in all seven spots. “Congo k” is OH-dominant save for brown core spot 2. “Congo i” is OH-dominant at all spots except for spot 4 on the yellow-brown rim.

Fluorine: F varies from 0.87 to 1.21 wt. % and 0.442 to 0.611 apfu. Slice “Congo l” is fluor-elbaitic throughout containing from 0.528 to 0.611 apfu F from core to rim. F quantities decrease from core to rim with 0.516 (fluor-elbaite), 0.499, 0.442 and 0.442 apfu for spots 2, 5, 6 and 7 of “Congo k”. From core to rim of sample “i”, F varies from 0.464 to 0.537 over fluor-elbaitic spots 2 and 4 and 0.490 apfu at spot 5.

Table 7: Microprobe analyses, Congolese tourmaline.

Oxides	Congo k2	Congo k5	Congo k6	Congo k7	Congo I1	Congo I2	Congo I3	Congo I4
sample color	brown	brown	yel-brown	yel-brown	murky pi	murky pi	murky pi	pink
SiO ₂	37.36	37.11	37.32	37.32	37.33	37.44	37.37	37.12
TiO ₂	0.27	0.20	0.18	0.18	0.00	0.00	0.02	0.00
B ₂ O ₃ calc.	10.67	10.64	10.79	10.79	10.93	10.86	10.90	10.89
Al ₂ O ₃	35.60	36.10	37.72	37.61	39.52	38.86	38.92	39.81
Cr ₂ O ₃	0.08	0.01	0.01	0.07	0.07	0.04	0.11	0.02
Bi ₂ O ₃	0.00	0.01	0.02	0.00	0.01	0.00	0.00	0.00
V ₂ O ₃	0.00	0.00	0.00	0.00	0.00	0.00	0.00	0.00
FeO	0.13	0.63	0.41	0.94	1.56	1.66	1.79	0.62
MnO	6.58	6.27	5.03	4.35	1.63	1.61	1.60	1.66
MgO	0.01	0.01	0.00	0.00	0.19	0.18	0.20	0.08
CaO	0.56	0.27	0.50	0.41	0.80	0.62	0.60	0.78
Li ₂ O calc.	1.83	1.63	1.66	1.71	1.84	1.84	1.89	1.97
Na ₂ O	2.41	2.31	2.07	2.27	2.03	2.09	2.46	2.14
K ₂ O	0.00	0.01	0.01	0.02	0.00	0.00	0.00	0.00
H ₂ O calc.	3.21	3.21	3.31	3.31	3.27	3.22	3.24	3.18
F	1.00	0.97	0.87	0.88	1.07	1.11	1.11	1.21
Sub-total	99.69	99.38	99.88	99.85	100.25	99.54	100.20	99.48
O=F	-0.42	-0.41	-0.37	-0.37	-0.45	-0.47	-0.47	-0.51
Total	99.27	98.97	99.52	99.48	99.80	99.07	99.73	98.97
Ions (apfu)								
T: Si	6.084	6.061	6.012	6.014	5.934	5.994	5.957	5.923
Al	0.000	0.000	0.000	0.000	0.066	0.006	0.043	0.077
B: B	3.000	3.000	3.000	3.000	3.000	3.000	3.000	3.000
Z: Al	6.000	6.000	6.000	6.000	6.000	6.000	6.000	6.000
Y: Al	0.833	0.948	1.162	1.143	1.339	1.324	1.271	1.409
Ti	0.032	0.024	0.021	0.021	0.000	0.000	0.002	0.000
Cr	0.010	0.001	0.001	0.008	0.009	0.005	0.014	0.003
Bi	0.000	0.001	0.001	0.000	0.000	0.000	0.000	0.000
V	0.000	0.000	0.000	0.000	0.000	0.000	0.000	0.000
Fe ²⁺	0.018	0.086	0.055	0.127	0.208	0.223	0.239	0.082
Mn ²⁺	0.907	0.867	0.687	0.594	0.219	0.219	0.216	0.225
Mg	0.001	0.001	0.000	0.000	0.046	0.042	0.048	0.018
Li	1.198	1.072	1.074	1.105	1.179	1.187	1.209	1.263
X: Ca	0.097	0.048	0.086	0.071	0.137	0.107	0.102	0.133
Na	0.761	0.732	0.645	0.710	0.624	0.648	0.760	0.660
K	0.000	0.002	0.002	0.004	0.000	0.000	0.000	0.000
□ (vac.)	0.142	0.218	0.267	0.215	0.239	0.245	0.138	0.206
OH	3.484	3.501	3.558	3.553	3.464	3.436	3.442	3.389
F	0.516	0.499	0.442	0.447	0.536	0.564	0.558	0.611
species	F-elbaite	elbaite	elbaite	elbaite	F-elbaite	F-elbaite	F-elbaite	F-elbaite

Oxides						
sample	Congo I5	Congo I6	Congo I7	Congo i2	Congo i4	Congo i5
color	pink	pink	green	dk br ~blk	yel brown	yel brown
SiO ₂	37.17	37.07	37.22	36.96	37.21	37.24
TiO ₂	0.05	0.02	0.24	0.30	0.36	0.35
B ₂ O ₃ calc.	10.83	10.79	10.86	10.51	10.68	10.73
Al ₂ O ₃	39.27	39.22	38.47	33.51	35.50	36.29
Cr ₂ O ₃	0.01	0.07	0.03	0.03	0.05	0.03
Bi ₂ O ₃	0.00	0.01	0.00	0.01	0.00	0.00
V ₂ O ₃	0.00	0.00	0.00	0.01	0.00	0.00
FeO	0.67	0.64	3.10	5.05	0.17	0.12
MnO	1.73	1.59	1.01	5.88	7.11	7.00
MgO	0.16	0.16	0.46	0.28	0.02	0.02
CaO	0.60	0.68	0.26	0.03	0.52	0.42
Li ₂ O calc.	1.92	1.91	1.70	1.25	1.72	1.61
Na ₂ O	2.14	1.94	2.50	2.32	2.57	2.41
K ₂ O	0.00	0.00	0.00	0.02	0.00	0.00
H ₂ O calc.	3.19	3.16	3.25	3.20	3.19	3.25
F	1.16	1.20	1.04	0.89	1.04	0.96
Sub-total	98.88	98.46	100.16	100.23	100.14	100.44
O=F	-0.49	-0.51	-0.44	-0.37	-0.44	-0.40
Total	98.40	97.96	99.72	99.86	99.70	100.03
Ions (apfu)						
T: Si	5.964	5.968	5.956	6.114	6.058	6.031
Al	0.036	0.032	0.044	0.000	0.000	0.000
B: B	3.000	3.000	3.000	3.000	3.000	3.000
Z: Al	6.000	6.000	6.000	6.000	6.000	6.000
Y: Al	1.390	1.411	1.211	0.535	0.812	0.926
Ti	0.006	0.002	0.029	0.037	0.044	0.043
Cr	0.002	0.009	0.004	0.003	0.007	0.004
Bi	0.000	0.000	0.000	0.000	0.000	0.000
V	0.000	0.000	0.000	0.002	0.000	0.000
Fe ²⁺	0.090	0.086	0.415	0.699	0.023	0.016
Mn ²⁺	0.235	0.217	0.137	0.824	0.980	0.960
Mg	0.038	0.039	0.110	0.069	0.006	0.005
Li	1.241	1.235	1.093	0.831	1.129	1.046
X: Ca	0.104	0.118	0.045	0.005	0.090	0.074
Na	0.666	0.606	0.774	0.745	0.810	0.757
K	0.000	0.000	0.000	0.003	0.000	0.000
□ (vac.)	0.231	0.276	0.181	0.247	0.100	0.169
OH	3.414	3.389	3.472	3.536	3.463	3.510
F	0.586	0.611	0.528	0.464	0.537	0.490
species	F-elbaite	F-elbaite	F-elbaite	elbaite	F-elbaite	elbaite

Congolese tourmaline plots

Fig. 53, X-site Ca-vacancy-Na plot: The three slices from Congo cluster together in the elbaite field. There is a grouping of the pink zones of “Congo l” plotting towards the rossmanite field. The green zone of this sample along with the brown, dark-brown and yellow-brown zones of “k” and “l” plot more towards the elbaite end-member.

Fig. 54, Mn-Ti-Fe plot: The colored zones of slices “Congo l”, “Congo k” and “Congo i” plot along the Fe-Mn join. The pink, brown, dark-brown and yellow-brown zones fall in the Mn-dominant field except for two pink spots which plot near the 50-50 line but within the Fe-dominant field. The green zone of sample “l” falls squarely in the Fe-field.

Fig. 55, Calculated Li vs. Fe plot: The dark-brown, green and pink zones of “Congo i and l” form a negative trend with increasing Li and decreasing Fe. The murky pink zone of “Congo l” has more Fe than the pink zone of this sample. Deviating from this trend are the yellow-brown and brown zones of “Congo k” and “Congo i” which contain the least Fe and have less Li than the pink zones of “Congo l”.

Fig. 56, Fe vs. Mn plot: As Fe increases, the colors change from yellow-brown, brown, pink, murky pink, green and finally to dark-brown. As Mn increases, colors change from pink, yellow-brown, brown and lastly yellow-brown. The brown and yellow-brown zones contain the highest Mn.

Fig. 57, Calculated Li vs. Mn plot: Li content stays relatively constant with increasing Mn content as colors change. Increasing Mn correlates to color changes from green to pink to colors with brown overtones in the various zones of slices “Congo

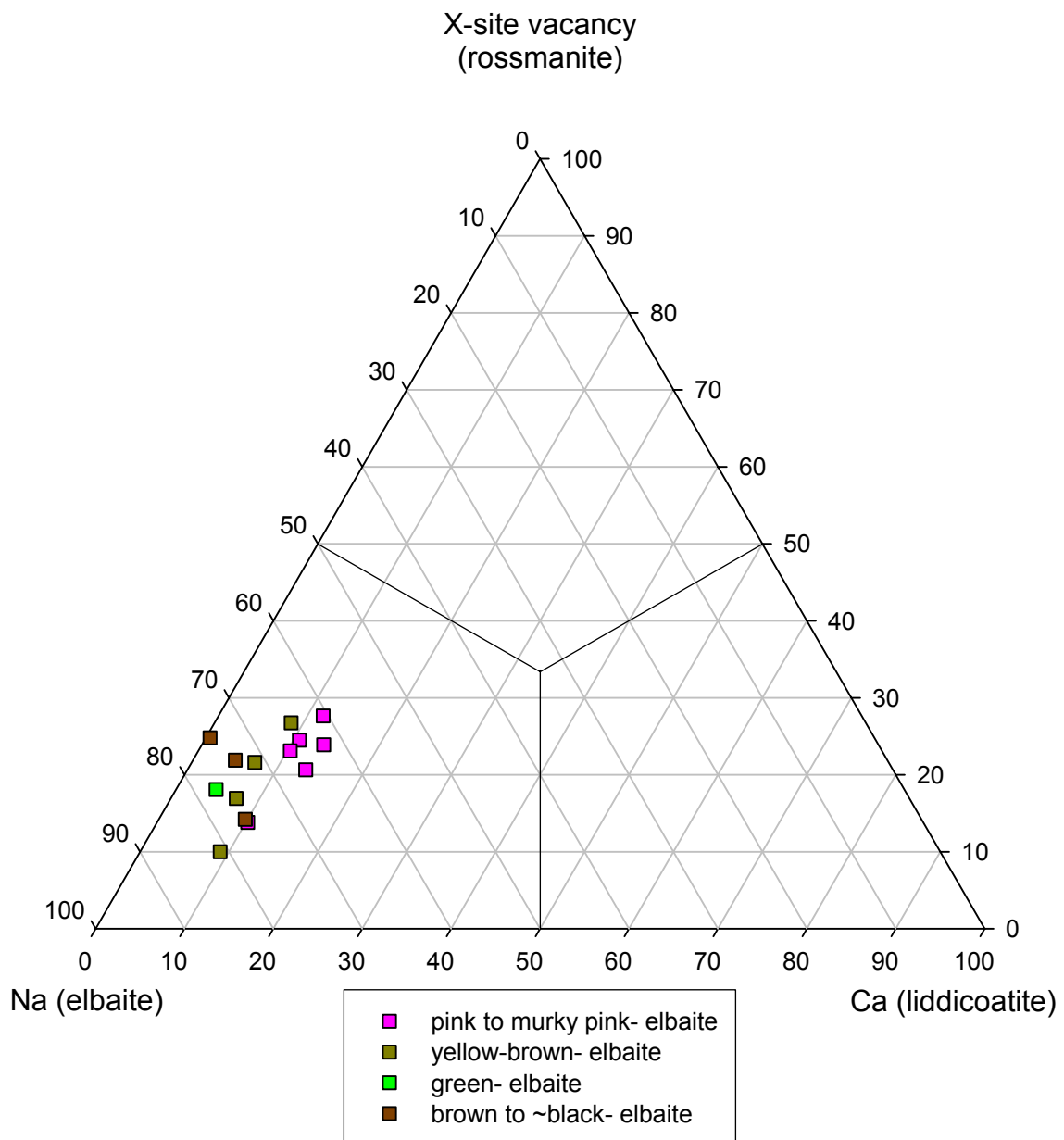


Fig. 53: Ca- X-site vacancy- Na ternary, Congolese (D.R.C.) tourmaline.
(D.R.C. = Democratic Republic of Congo, formerly Zaire)

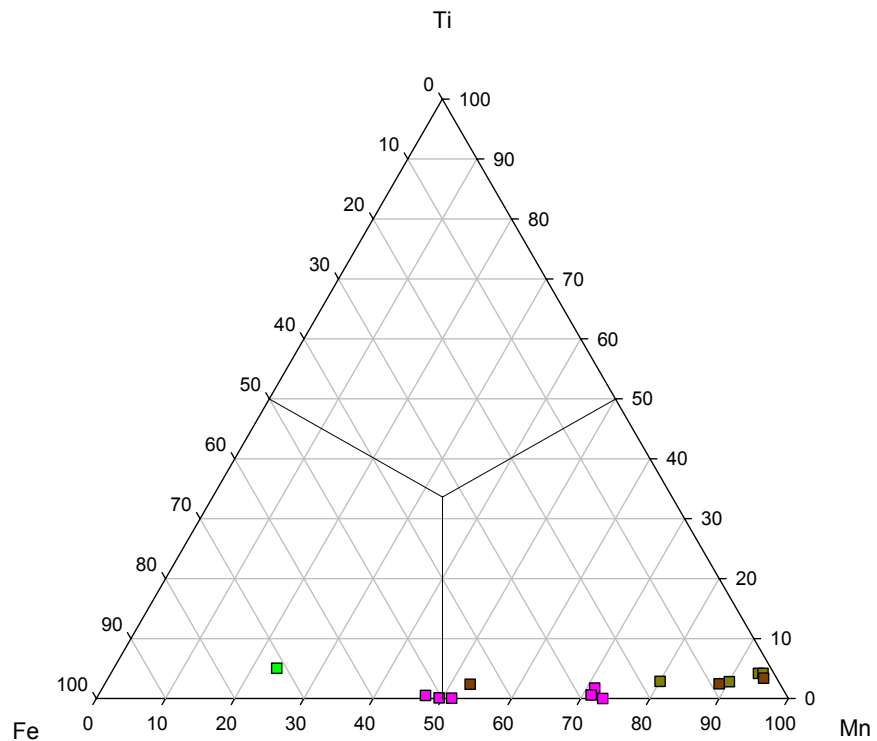


Fig. 54: Mn- Ti- Fe ternary, Congolese tourmaline.

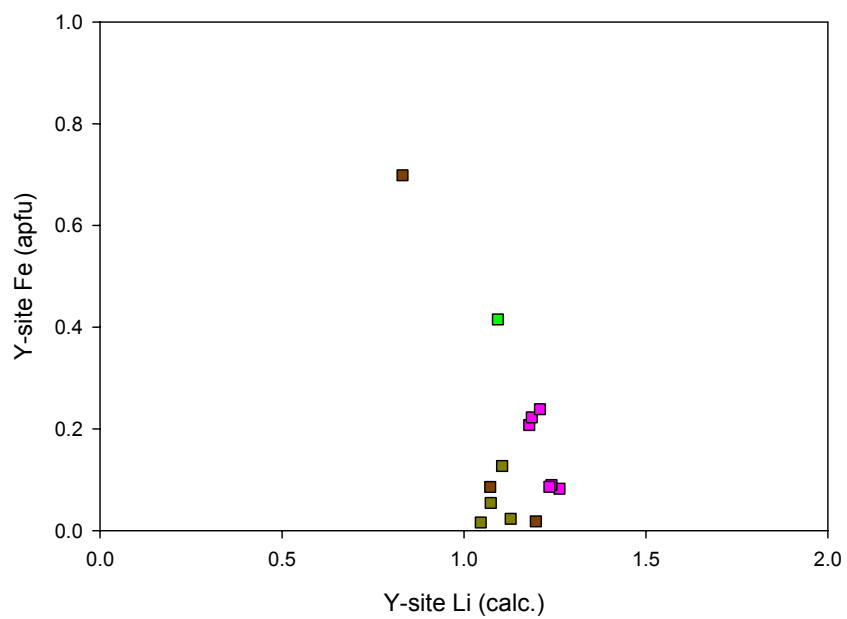


Fig. 55: Li (calc.) vs. Fe binary, Congolese tourmaline.

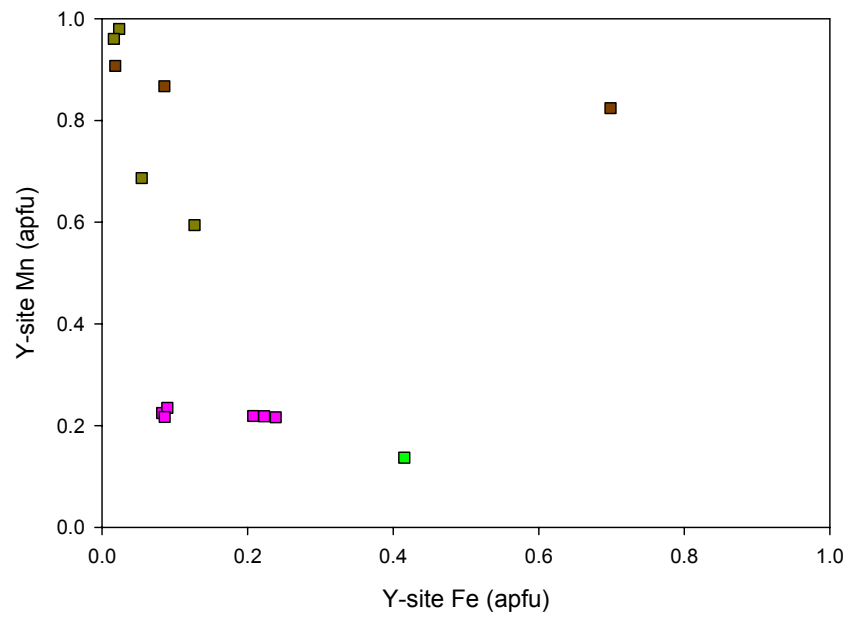


Fig. 56: Fe vs. Mn binary, Congolese tourmaline.

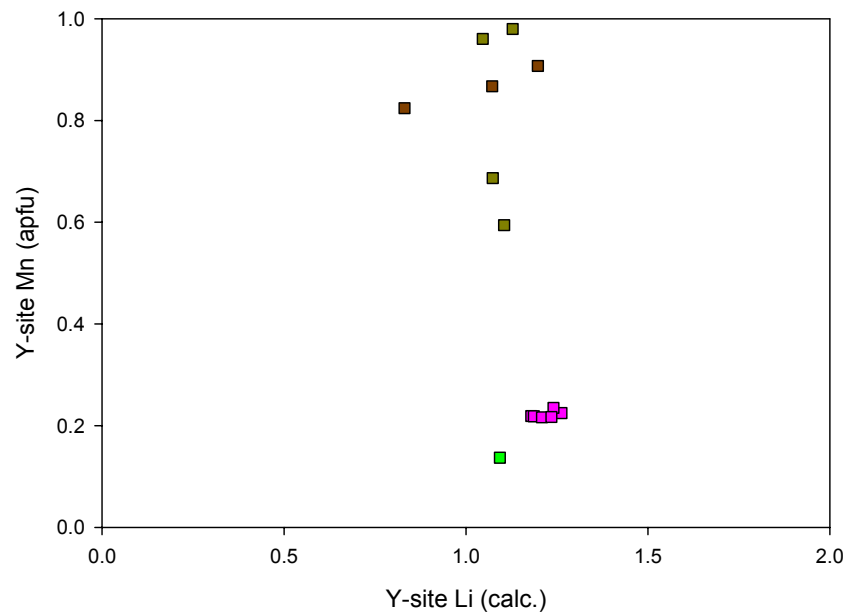


Fig. 57: Li (calc.) vs. Mn binary, Congolese tourmaline.

k" and "Congo i". This graph displays the best tourmaline color separation of the various Li vs. Mn plots for all the countries examined.

Fig. 58, Calculated Li vs. F plot: Contrary to the other Li vs. F plots from other countries, Congolese tourmalines clearly show a trend of increasing Li with increasing F. The brownish zones of "Congo k and I" cluster together along with the green rim analysis of "Congo l" and contains the least Li+F quantities, whereas the pink to murky-pink zone of "Congo l" has the most F. The dark-brown core of "i" contains a paucity of Li and deviates from the main trend.

Fig. 59, Calculated Li vs. Y-site Al plot: As Li increases, Al increases at the Y-site forming a positive relationship. The colors change from dark-brown, brown, yellow-brown, green, murky-pink to pink with the above trend.

Fig. 60, Y-site Al vs. Fe plot: Fe and Al constitute a negative trend with sample "Congo l" which has increasing Al and decreasing Fe as colors change from green to murky pink to pink. The brownish zones fall far off this trend and contain substantially less Al and Fe save the dark-brown spot which contains the most Fe and the least Al.

Fig. 61, Fe vs. Ti plot: Correlations are really not observed on this graph, rather the colors are separated with increasing Fe content. As Fe increases, colors change from pink, murky-pink, green to dark-brown. Yellowish-brown, brown and green zones contain greater than 0.02 apfu Ti with the yellowish-brown zones containing low Fe.

Fig. 62, Mn vs. Ti plot: As Mn quantities rise, so does Ti forming a directly proportional relationship. The colors change from pink to brownish shades as Mn and Ti increase. The green zone of "Congo l" deviates from the main trend and contains less Mn and considerably more Ti than the pink zones.

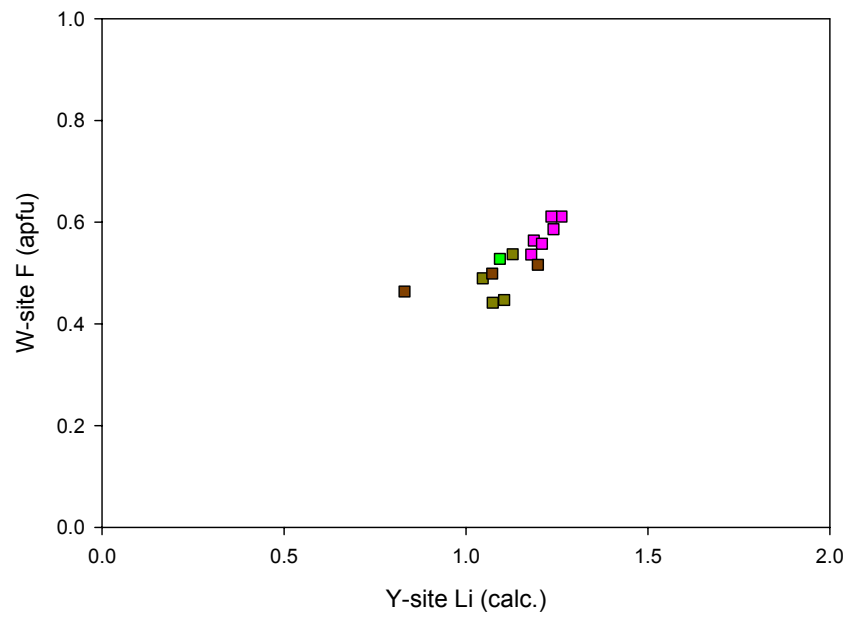


Fig. 58: Li (calc.) vs. F binary, Congolese tourmaline.

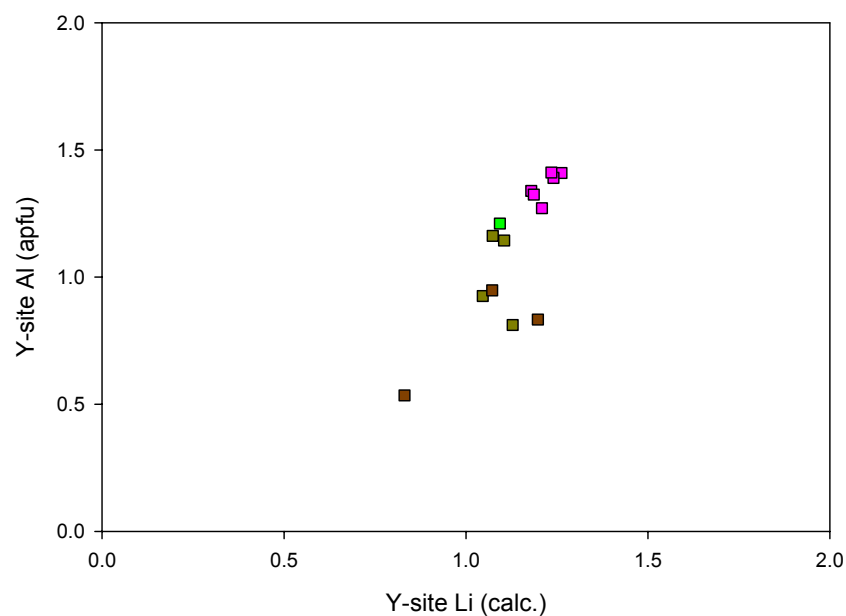


Fig. 59: Li (calc.) vs. Al binary, Congolese tourmaline.

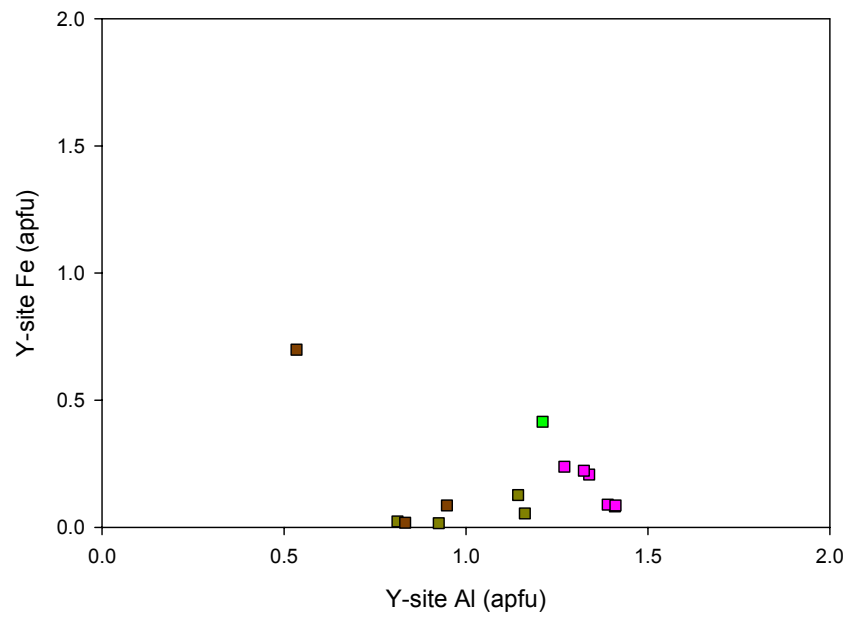


Fig. 60: Al vs. Fe binary, Congolese tourmaline.

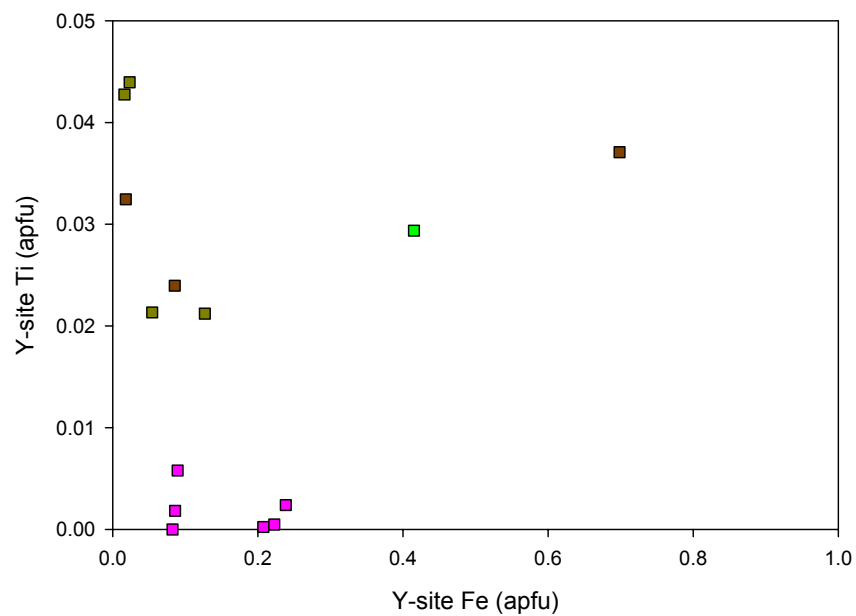


Fig. 61: Fe vs. Ti binary, Congolese tourmaline.

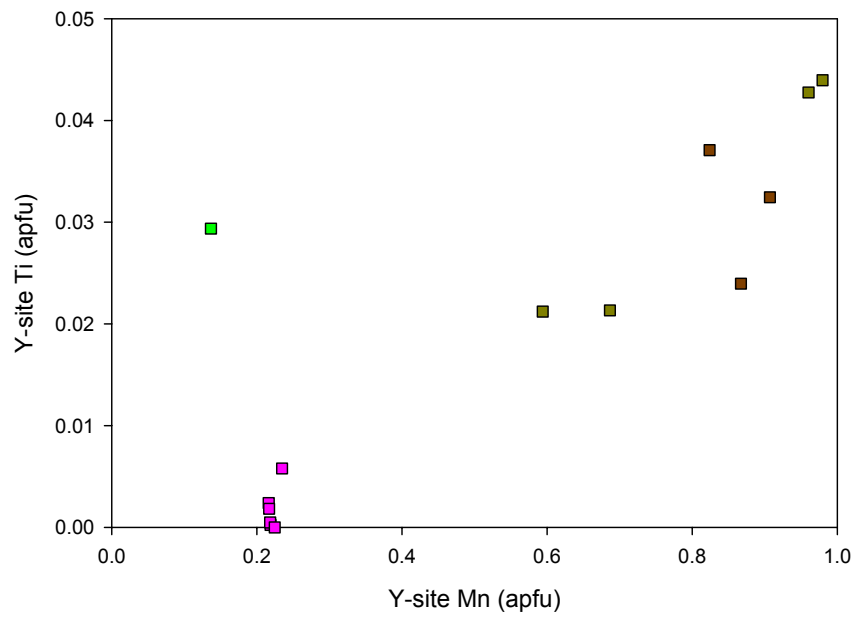


Fig. 62: Mn vs. Ti binary, Congolese tourmaline.

Fig. 63, Na vs. F plot: This graph displays the same clustering trend as do the Namibian and Nigerian Na vs. F diagrams. There are discernable trends among the variously colored zones. Analyses of the pink domains group together.

Fig. 64, Na vs. Ti+Fe+Mn plot: There is a broad, slightly positive trend displayed by this covariation diagram. Accompanying this trend, the colors change from pink to green, yellowish-brown, brown and dark-brown. As Na increases, transition metal content increases.

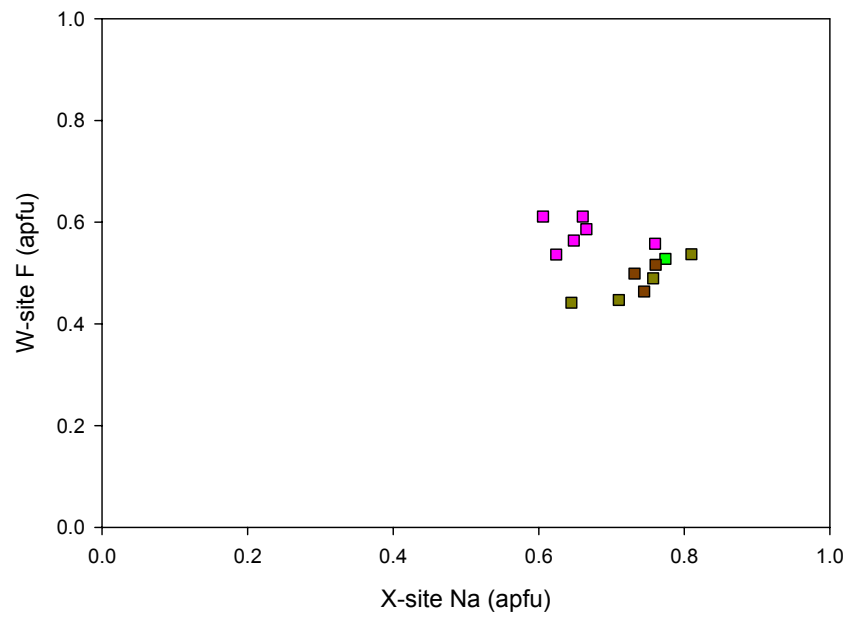


Fig. 63: Na vs. F binary, Congolese tourmaline.

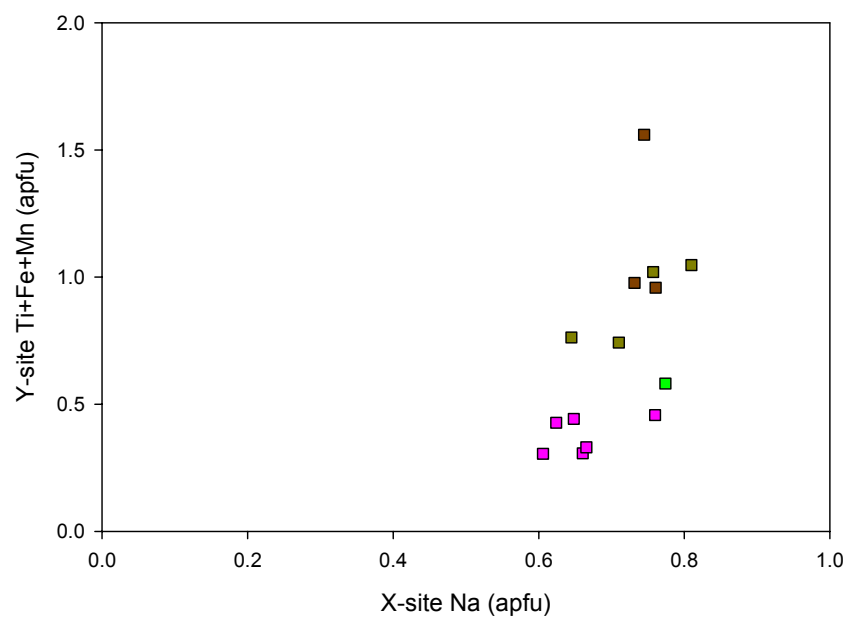


Fig. 64: Na vs. Ti+Fe+Mn binary, Congolese tourmaline.

Mozambique Tourmaline

The tourmaline from Mozambique consists only of elbaite. Fig. 65 shows a photograph of a green tourmaline crystal from Mozambique analyzed for this project. Table 8 shows microprobe analyses of the two fragments analyzed. The specimens contain low quantities of the liddicoatite and rossmanite components when plotted on the X-site end-member ternary diagram. The selected piece of pink rough used for cell-edge analysis has an a dimension of 15.838Å and a c dimension of 7.100Å.



Fig. 65: Green tourmaline crystal from Mozambique.

The T, B and Z-sites: Si varies from 37.05 to 37.84 wt. % and 5.824 to 5.979 apfu Si. The green fragment has elevated Si quantities compared to the pink sample. Calculated B_2O_3 ranges from 10.79 to 11.28 wt. %. Al totals fall between 37.36 to 43.00 wt. %. Al quantities are higher for the pink sample.

Y-site Al: The range of Al at the Y-site is from 1.044 to 1.662 apfu. This is highest for the pink specimen and lowest for the green fragment. Spots 1 to 5 of the green fragment contain 1.049, 1.044, 1.053, 1.059, and 1.067 apfu Al respectively. These quantities are 1.649, 1.657, 1.636, 1.662 and 1.641 apfu in for spots 6 to 10 respectively of the pink specimen.

Titanium: Ti was not detected in the green fragment. The pink specimen has from 0 to 0.04 wt. % TiO_2 and 0 to 0.004 apfu Ti. Spots 7, 9 and 10 of this sample contain 0.004, 0.002 and 0.004 apfu Ti respectively.

Bismuth: Bi attains very low quantities at or near detection limits in these samples. Bi varies from 0.01 to 0.02 wt. % Bi_2O_3 and up to 0.001 apfu. Spots 6 through 8 and 10 of the pink fragment have 0.001 apfu Bi whereas spots 1 and 4 of the green sample also contain 0.001 apfu Bi.

Vanadium: This element was not detected in the Mozambique tourmalines.

Iron: Overall, Fe contents range from 0.07 to 5.34 wt. % FeO and 0.008 to 0.718 apfu. Fe quantities are high in the green specimen and range from 0.718 to 0.687, 0.671, 0.676 and 0.670 on spots 1 to 5 respectively. A significant drop in Fe quantity occurs in the pink specimen with contents of 0.013, 0.016, 0.018, 0.021 and 0.008 apfu over spots 6-10 respectively.

Manganese: The general range of Mn is from 0.18 to 3.04 wt. % MnO and 0.023 to 0.414 apfu Mn. The green sample possesses the most Mn with 0.393, 0.401, 0.381, 0.400 and 0.414 apfu over spots 1 to 5 respectively. Mn dramatically decreases in the pink sample from 0.042 to 0.033, 0.041, 0.026 and 0.023 apfu on the final five spots.

Magnesium: Mg was not detected in these specimens.

Calcium: Ca contents are low throughout but fluctuate erratically for both specimens. Overall the range is between 0.32 to 0.71 wt. % CaO and 0.055 to 0.118 apfu Ca. The green fragment has 0.055, 0.072, 0.095, 0.071 and 0.095 apfu Ca at spots 1 to 5 respectively. Spots 6 to 10 of the pink sample contain higher amounts of Ca with 0.108, 0.099, 0.118, 0.101 and 0.093 apfu respectively.

Calculated Lithium: The green sample contains substantially less Li than the pink. Quantities vary from 1.30 to 2.11 wt. % Li₂O and 0.837 to 1.322 apfu. Analyses 1 to 5 of the green specimen contain 0.837, 0.867, 0.893, 0.863 and 0.848 apfu Li. The pink fragment contains 1.294, 1.288, 1.301, 1.288 and 1.322 apfu Li respectively.

Sodium: Na contents range from 1.95 to 2.31 wt. % Na₂O and 0.582 to 0.719 apfu Na. The green sample is slightly more Na-rich than the pink. In the green specimen, Na behaves erratically with 0.692, 0.719, 0.690, 0.964 and 0.639 over spots 1 to 5. Quantities of Na for spots 6-10 of the pink sample are 0.603, 0.591, 0.596, 0.582 and 0.606 respectively.

Potassium: Quantities of K are very low throughout both the pink and green pieces but are above detection limits. The overall range of K is between 0 and 0.02 wt. % K₂O and 0.001 to 0.004 apfu. These values are applicable to both samples from Mozambique.

X-site totals: Occupancy at the X-site of the green specimen is higher than in the pink fragment with 0.752, 0.795, 0.787, 0.766 and 0.737 apfu respectively for spots 1 to 5. The pink specimen contains 0.713, 0.693, 0.717, 0.684 and 0.703 apfu at the X-site for spots 6 to 10 respectively.

OH anion and calculated water: The wt. % of H₂O varies from 3.21 to 3.34. The green sample is mostly OH-dominant with 3.445 to 3.545 apfu OH. The pink fragment has a paucity of OH at the W-site with 3.413 to 3.446 apfu over spots 6 to 10 respectively.

Fluorine: F predominates at the W-site for 7 out of the 10 analyses of these specimens. The general range of F content is from 0.87 to 1.20 wt. % and 0.455 to 0.587 apfu F. The green sample is relatively F-depleted and has large F fluctuations from 0.510 to 0.485, 0.455, 0.555 and 0.457 apfu for spots 1 to 5. The pink fragment is fluor-elbaite and contains 0.587 to 0.554 apfu F at spots 6 through 10.

Table 8: Microprobe analyses, Mozambique tourmaline.

Oxides	Moz-1	Moz-2	Moz-3	Moz-4	Moz-5	Moz-6	Moz-7	Moz-8
Sample color	green	green	green	green	green	pink	or-pink	or-pink
SiO ₂	37.23	37.12	37.13	37.05	37.09	37.66	37.60	37.84
TiO ₂	0.00	0.00	0.00	0.00	0.00	0.00	0.04	0.00
B ₂ O ₃ calc.	10.82	10.83	10.83	10.79	10.83	11.24	11.21	11.28
Al ₂ O ₃	37.36	37.47	37.52	37.37	37.63	42.93	42.84	43.00
Bi ₂ O ₃	0.02	0.01	0.01	0.02	0.01	0.02	0.03	0.03
V ₂ O ₃	0.00	0.00	0.01	0.00	0.00	0.00	0.01	0.01
FeO	5.34	5.12	5.00	5.02	5.00	0.10	0.12	0.14
MnO	2.89	2.95	2.80	2.93	3.04	0.32	0.26	0.32
MgO	0.00	0.00	0.00	0.00	0.00	0.00	0.00	0.00
CaO	0.32	0.42	0.55	0.41	0.55	0.65	0.60	0.71
Li ₂ O calc.	1.30	1.34	1.38	1.33	1.31	2.08	2.07	2.10
Na ₂ O	2.22	2.31	2.22	2.22	2.06	2.01	1.97	2.00
K ₂ O	0.02	0.02	0.01	0.01	0.01	0.01	0.01	0.02
H ₂ O calc.	3.26	3.28	3.31	3.21	3.31	3.31	3.31	3.34
F	1.00	0.96	0.90	1.09	0.90	1.20	1.18	1.16
Sub-total	101.81	101.83	101.68	101.46	101.75	101.53	101.23	101.94
O=F	-0.42	-0.40	-0.38	-0.46	-0.38	-0.51	-0.50	-0.49
Total	101.38	101.43	101.31	101.00	101.37	101.03	100.73	101.46
Ions (apfu)								
T: Si	5.979	5.957	5.958	5.967	5.951	5.824	5.829	5.829
Al	0.021	0.043	0.042	0.033	0.049	0.176	0.171	0.171
B: B	3.000	3.000	3.000	3.000	3.000	3.000	3.000	3.000
Z: Al	6.000	6.000	6.000	6.000	6.000	6.000	6.000	6.000
Y: Al	1.049	1.044	1.053	1.059	1.067	1.649	1.657	1.636
Ti	0.000	0.000	0.000	0.000	0.000	0.000	0.004	0.000
Bi	0.001	0.000	0.000	0.001	0.000	0.001	0.001	0.001
V	0.000	0.000	0.001	0.000	0.000	0.000	0.001	0.002
Fe ²⁺	0.718	0.687	0.671	0.676	0.670	0.013	0.016	0.018
Mn ²⁺	0.393	0.401	0.381	0.400	0.414	0.042	0.033	0.041
Mg	0.000	0.000	0.000	0.000	0.000	0.000	0.000	0.000
Li	0.837	0.867	0.893	0.863	0.848	1.294	1.288	1.301
X: Ca	0.055	0.072	0.095	0.071	0.095	0.108	0.099	0.118
Na	0.692	0.719	0.690	0.694	0.639	0.603	0.591	0.596
K	0.004	0.003	0.002	0.001	0.002	0.002	0.002	0.004
□ (vac.)	0.248	0.205	0.213	0.234	0.263	0.287	0.307	0.283
OH	3.490	3.515	3.545	3.445	3.543	3.413	3.422	3.435
F	0.510	0.485	0.455	0.555	0.457	0.587	0.578	0.565
species	F-elbaite	elbaite	elbaite	F-elbaite	elbaite	F-elbaite	F-elbaite	F-elbaite

Oxides		
Sample	Moz-9	Moz-10
color	or-pink	or-pink
SiO ₂	37.80	37.70
TiO ₂	0.02	0.03
B ₂ O ₃ calc.	11.25	11.15
Al ₂ O ₃	42.98	42.27
Bi ₂ O ₃	0.01	0.02
V ₂ O ₃	0.00	0.00
FeO	0.17	0.07
MnO	0.20	0.18
MgO	0.00	0.00
CaO	0.61	0.56
Li ₂ O calc.	2.07	2.11
Na ₂ O	1.95	2.00
K ₂ O	0.00	0.02
H ₂ O calc.	3.34	3.31
F	1.14	1.12
Sub-total	101.53	100.55
O=F	-0.48	-0.47
Total	101.06	100.08

Ions (apfu)		
T: Si	5.838	5.876
Al	0.162	0.124
B: B	3.000	3.000
Z: Al	6.000	6.000
Y: Al	1.662	1.641
Ti	0.002	0.004
Bi	0.000	0.001
V	0.000	0.000
Fe ²⁺	0.021	0.008
Mn ²⁺	0.026	0.023
Mg	0.000	0.000
Li	1.288	1.322
X: Ca	0.101	0.093
Na	0.582	0.606
K	0.001	0.004
□ (vac.)	0.316	0.297
OH	3.446	3.446
F	0.554	0.554
species	F-elbaite	F-elbaite

Mozambique Tourmaline Plots

Fig. 66, X-site Ca-vacancy-Na: This figure shows that the Mozambique samples are elbaite. The green and pink fragments contain approximately the same quantity of the liddicoatite component, however the green specimen is more elbaitic whereas the pink sample contains a higher proportion of the rossmanite molecule. Each of the following plots display a tight clustering of data points with respect to color.

Fig. 67, Mn-Ti-Fe plot: This ternary displays a distinct separation of the green and pink specimens. The green fragment plots in the Fe-field whereas the pink sample falls in the Mn-field. There are no spots which plot in the Ti-field but three analyses of the pink fragment contain small amounts of Ti.

Fig. 68, Calculated Li vs. Fe plot: This binary graph shows that as Li increase, Fe decreases forming a negative trend. The green fragment is Fe-rich and Li-poor relative to the pink sample.

Fig. 69, Fe vs. Mn plot: As with tourmaline from other countries, there is pronounced separation of pink and green analyses as Fe increases. This graph shows that Fe has a positive relationship with Mn. The green sample is rich in Fe and Mn relative to the pink fragment.

Fig. 70, Calculated Li vs. Mn plot: This plot shows that as Li increases, Mn quantities decrease constituting a negative trend. The color changes from green to pink corresponding to the above trend.

Fig. 71, Calculated Li vs. F plot: This binary graph exhibits a slightly positive trend. Li increases as the W-site becomes increasingly occupied by F accompanied by a

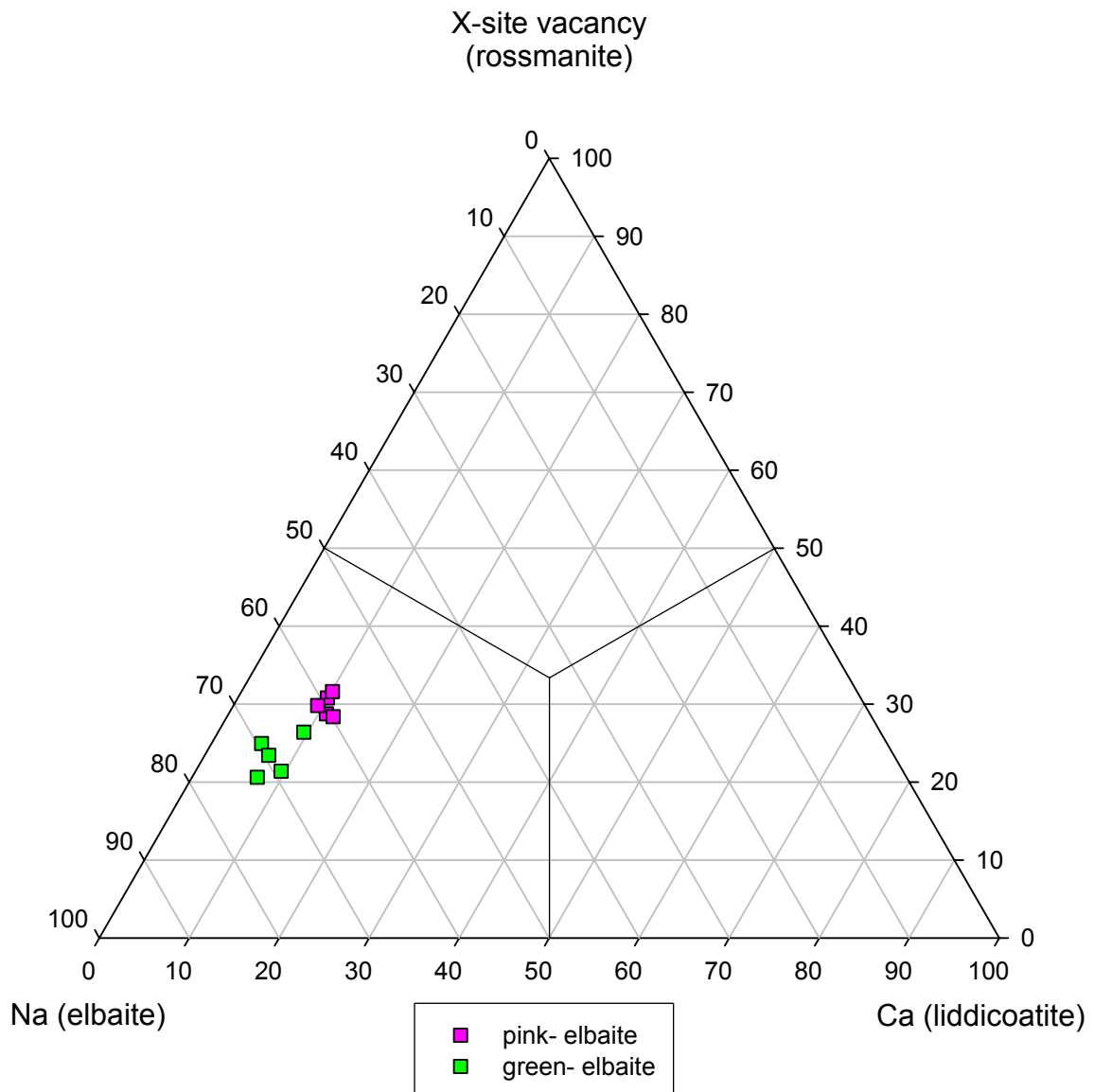


Fig. 66: Ca- X-site vacancy- Na ternary, Mozambique tourmaline.

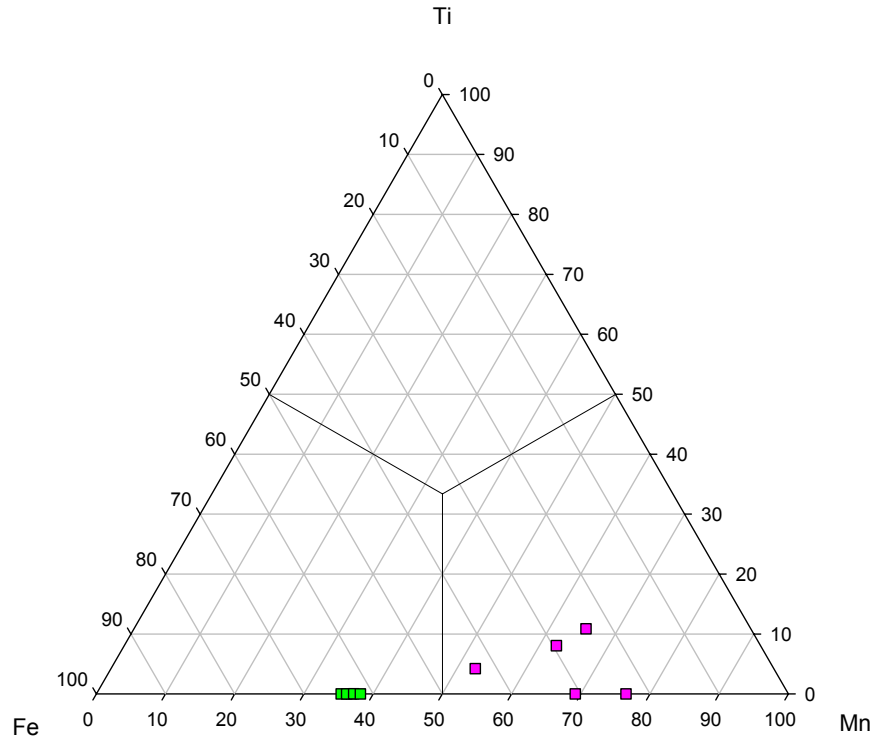


Fig. 67: Mn- Ti- Fe ternary, Mozambique tourmaline.

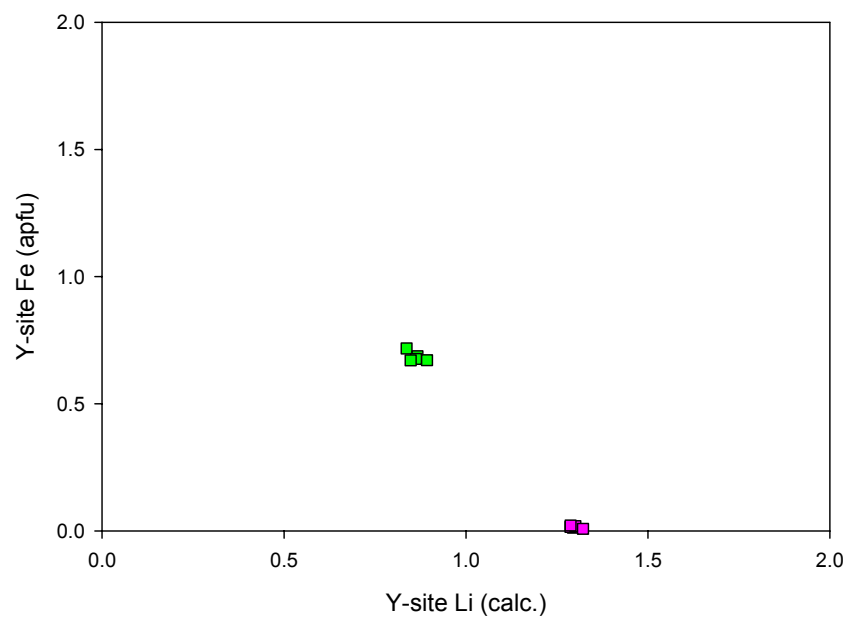


Fig. 68: Li (calc.) vs. Fe binary, Mozambique tourmaline.

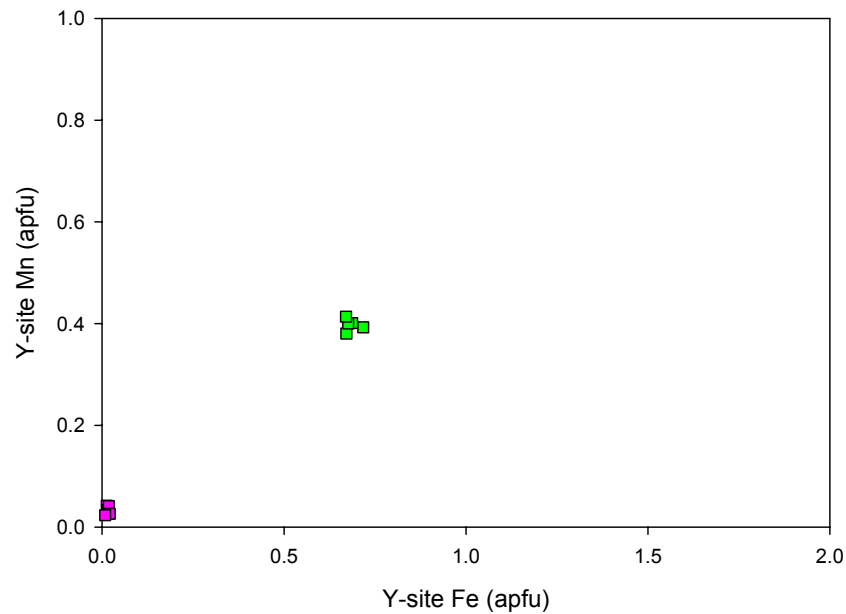


Fig. 69: Fe vs. Mn binary, Mozambique tourmaline.

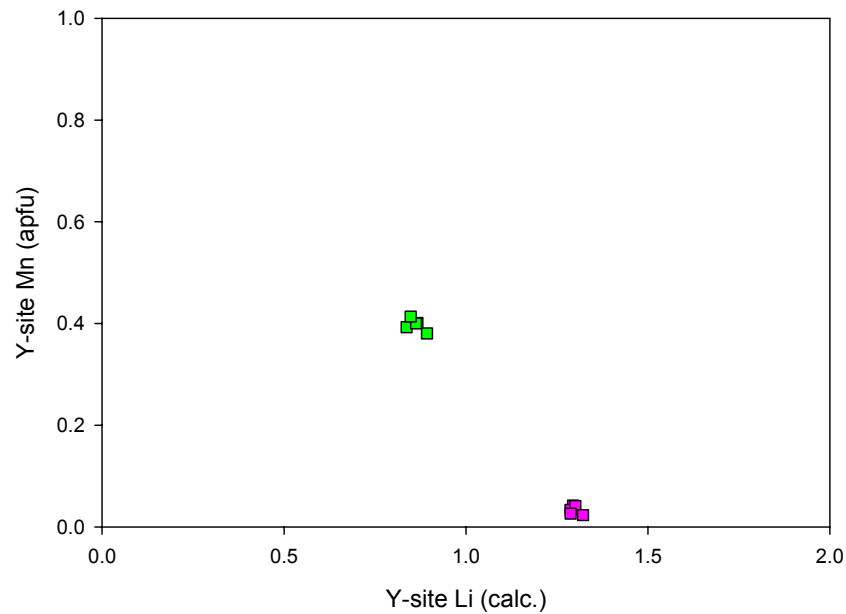


Fig. 70: Li (calc.) vs. Mn binary, Mozambique tourmaline.

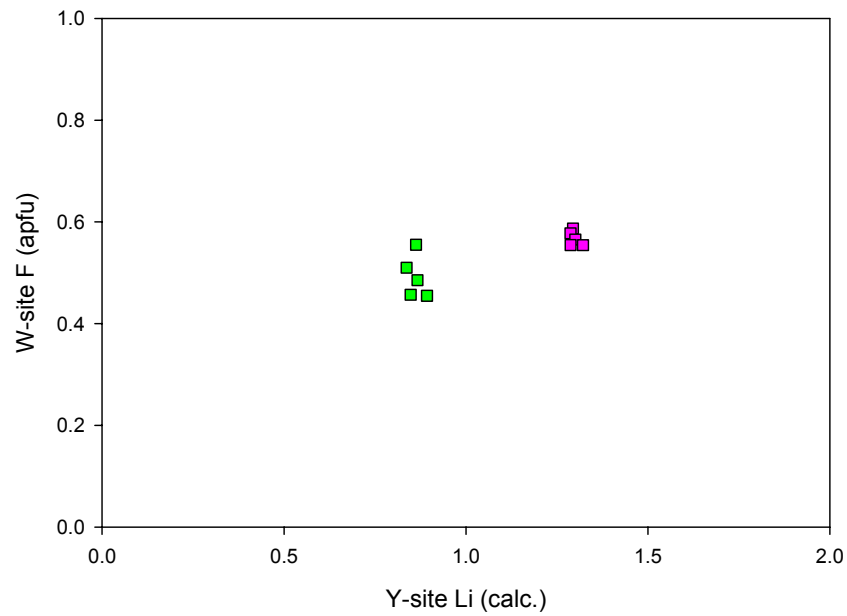


Fig. 71: Li (calc.) vs. F binary, Mozambique tourmaline.

green to pink color change. The pink specimen is completely fluor-elbaite and two of the five green sample spots are fluor-elbaite.

Fig. 72, Calculated Li vs. Y-site Al plot: A positive trend is displayed by this plot. At the Y-site, Li increases, Y-site calculated Li increases. This corresponds to a pink to green color change.

Fig. 73, Y-site Al vs. Fe plot: This plot exhibits a negative trend. Fe decreases as Al increases. Accompanying this trend is a color change from green to pink.

Fig. 74, Fe vs. Ti plot: The green and pink specimens both contain low quantities of Ti overall but the pink fragment contains significantly more Ti than the green sample. Elevated Fe is present in the green sample whereas the pink fragment has only trace Fe.

Fig. 75, Mn vs. Ti plot: This graph shows that Ti is more prevalent in the pink sample as opposed to the green sample. Mn quantities remain constant for both fragments with the green sample containing greater Mn contents than the pink specimen.

Fig. 76, Na vs. F plot: No trends are displayed by this covariation diagram. The data clusters in the same manner as the Na vs. F graphs for the Nigerian and Namibian stones. The pink and green fragments are separated with the pink specimen containing more F and less Na than the green sample which has less F and more Na.

Fig. 77, Na vs. Ti+Fe+Mn plot: The trend of this plot is steeply positive. The pink sample contains very low transition element quantities whereas the green fragment has much higher transition element contents.

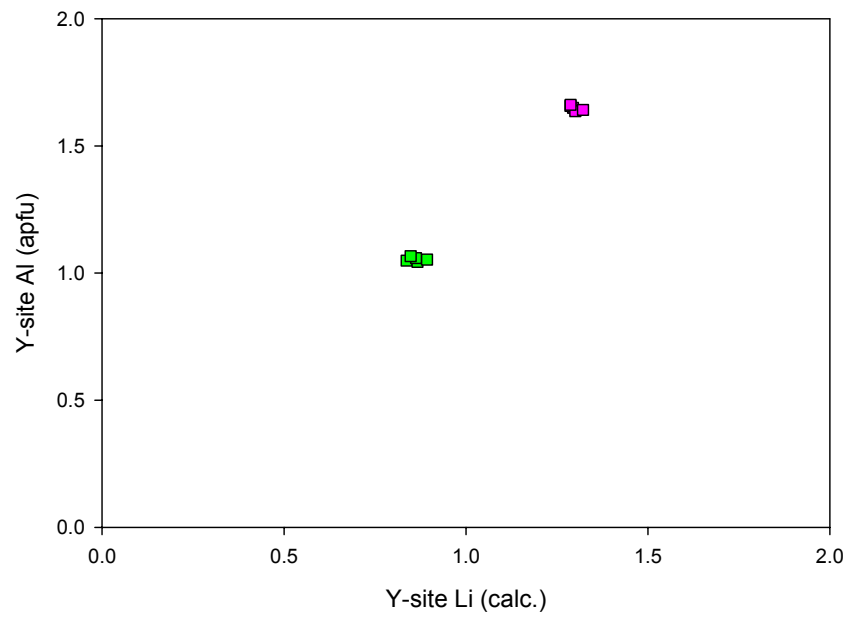


Fig. 72: Li (calc.) vs. Al binary, Mozambique tourmaline.

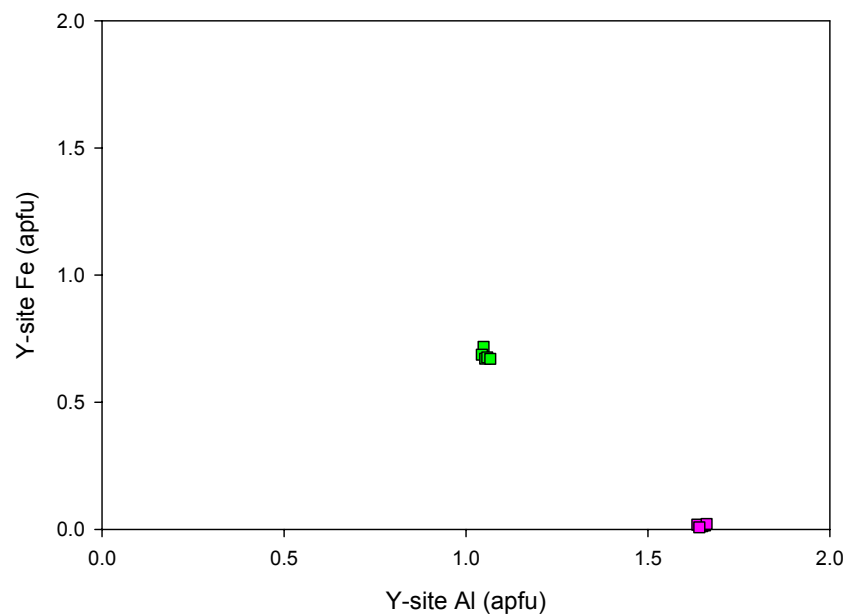


Fig. 73: Al vs. Fe binary, Mozambique tourmaline.

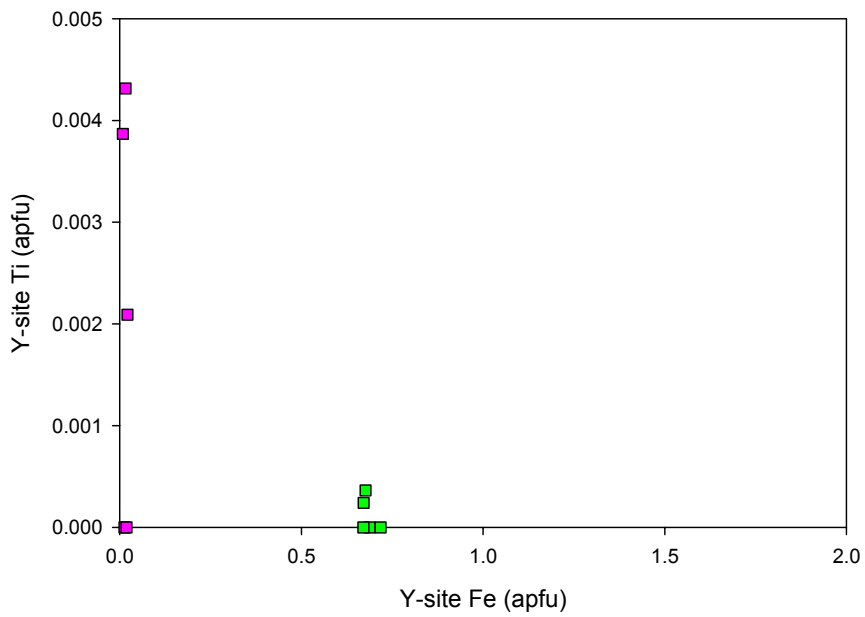


Fig. 74: Fe vs. Ti binary, Mozambique tourmaline.

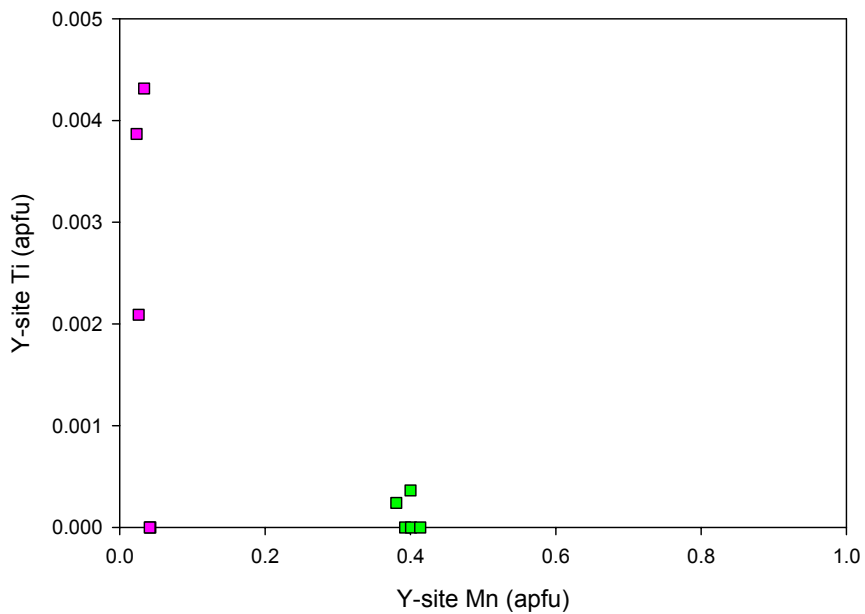


Fig. 75: Mn vs. Ti binary, Mozambique tourmaline.

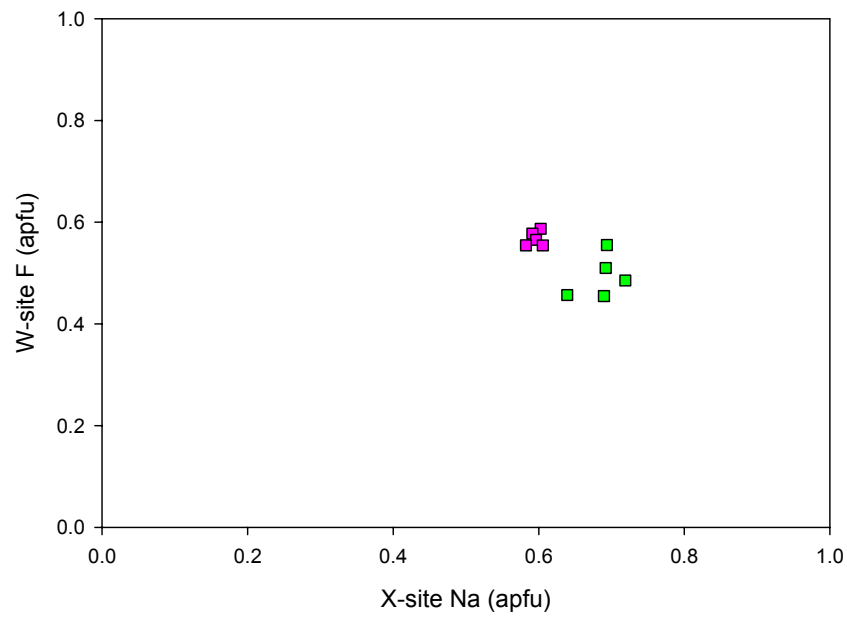


Fig. 76: Na vs. F binary, Mozambique tourmaline.

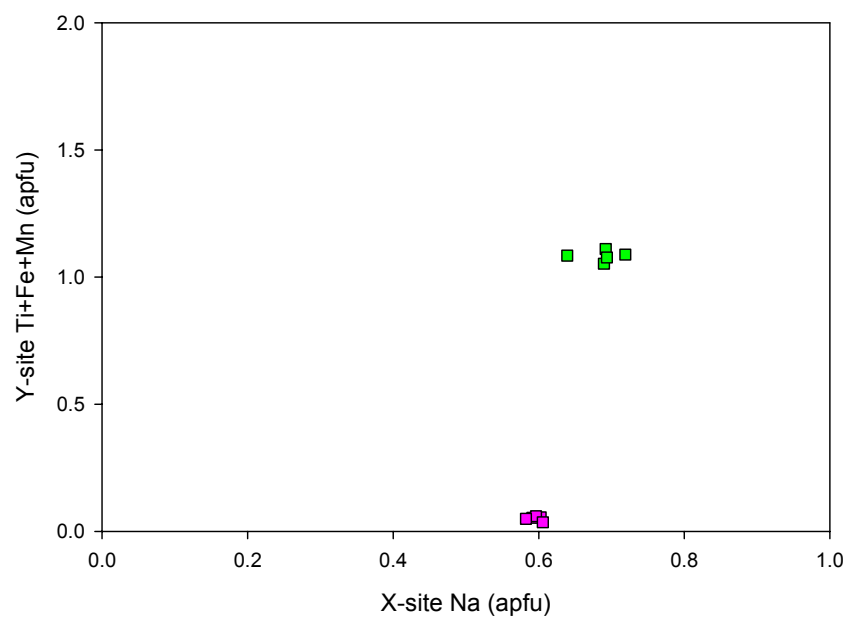


Fig. 77: Na vs. Ti+Fe+Mn binary, Mozambique tourmaline.

Namibian, Malian and Mozambique cell-edge refinements

The a vs. c unit cell plot in Fig. 78 shows that the variously colored gem rough from Namibia, Mali and Mozambique generally falls along the olenite-elbaite and elbaite- liddicoatite joins. The samples cluster around the elbaite reference point. The pink fragments which range in color from pink to dark pink, orange-pink and greenish-pink tend to have shorter a cell dimensions and the most variable c dimensions of the studied samples. The green samples ranging in color from light green to yellowish-green and green have the widest range of a cell dimensions and relatively variable c dimensions. The blue stones generally contain the most expanded a dimensions of the population. Lastly, the black schorl-elbaite has intermediate a and c dimensions with respect to the other colors and plots very close to the elbaite reference point.

Table 9: Cell-edge data of selected Namibian, Malian and Mozambique tourmaline.

sample	color	species	location	a (Å)	c (Å)
pNe19437	pink	elbaite	Namibia	15.821 (5)	7.103 (4)
pinkON	pink	elbaite	Namibia	15.814 (4)	7.116 (4)
pON2	pink	elbaite	Namibia	15.820 (4)	7.111 (5)
dpONBL4	dark pink	elbaite	Namibia	15.820 (4)	7.106 (4)
dpONBL6	dark pink	elbaite	Namibia	15.821 (3)	7.100 (3)
oON	orange-pink	elbaite	Namibia	15.831 (1)	7.102 (1)
oON2	orange-pink	elbaite	Namibia	15.824 (2)	7.104 (2)
pg170721	greenish-pi	elbaite	Namibia	15.823 (2)	7.099 (2)
pM178180	pink	elbaite	Mozambique	15.838 (1)	7.100 (1)
gNeR3937	green	elbaite	Namibia	15.859 (3)	7.103 (2)
lgONBL5	light green	elbaite	Namibia	15.829 (2)	7.101 (2)
gCorON10	green	elbaite	Namibia	15.823 (4)	7.108 (4)
gONeBL3	green	elbaite	Namibia	15.825 (2)	7.100 (2)
yONBL2	yel-green	elbaite	Namibia	15.819 (4)	7.111 (5)
yON124155	yel-green	elbaite	Namibia	15.838 (1)	7.102 (1)
gMali	green	elbaite	Mali	15.833 (3)	7.095 (3)
bN149508	blue	elbaite	Namibia	15.843 (2)	7.101 (2)
bON2	blue	elbaite	Namibia	15.845 (1)	7.102 (1)
bONjp	blue	elbaite	Namibia	15.855 (5)	7.111 (2)
bpON	blue	elbaite	Namibia	15.848 (3)	7.110 (2)
bkONcore	black	schorl	Namibia	15.834 (5)	7.112 (4)

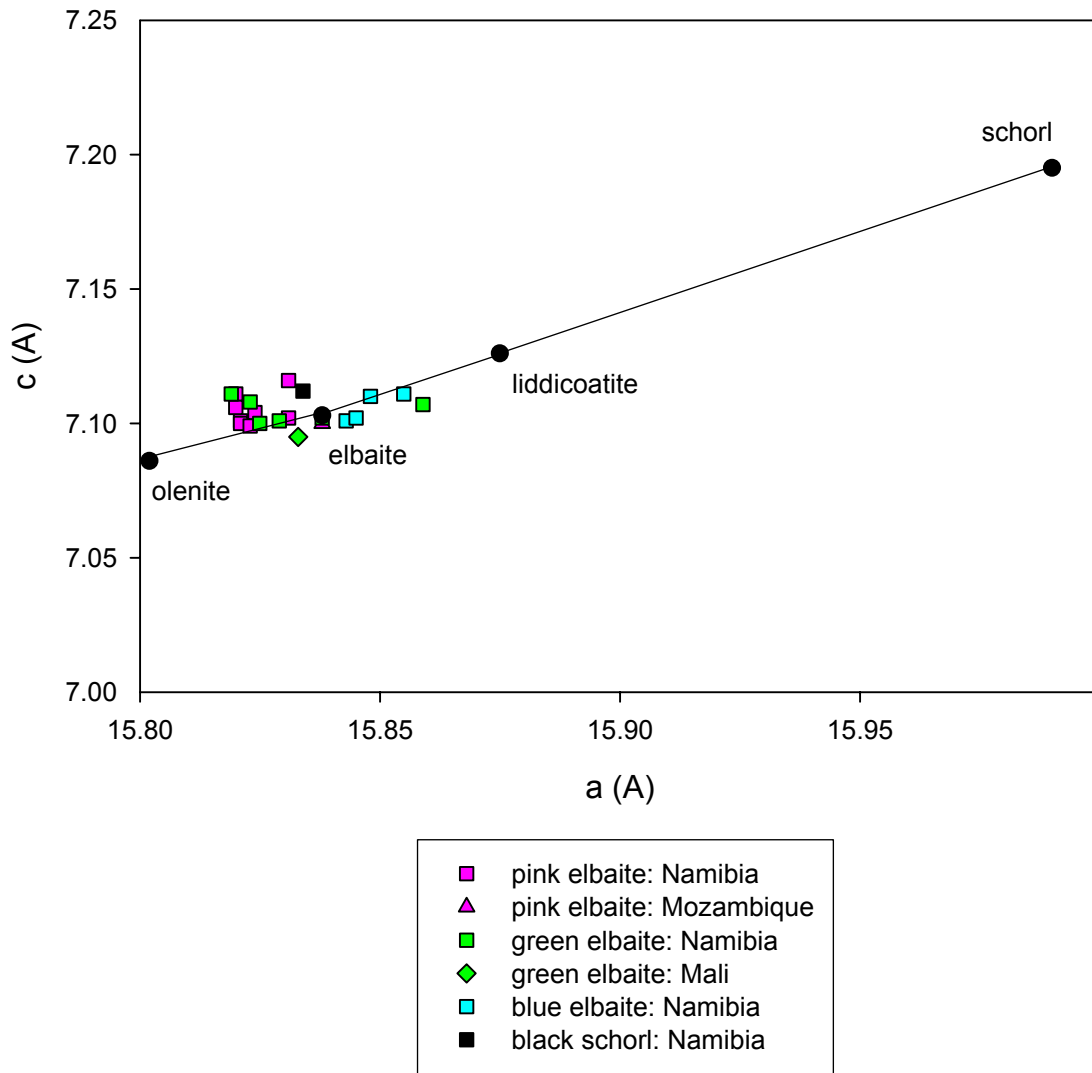


Fig. 78: a vs. c diagram, Namibian, Malian and Mozambique tourmaline rough.
(reference points from Deer *et al.*, (1962) & Anthony *et al.*, (1995))

DISCUSSION

The general chemistry shown by the Mg- Y-site Al- Fe and Ca-Y-site- Na ternaries of Figs. 5 and 6 is typical of gem-quality tourmaline from LCT-family pegmatites. The Mg enrichment of the Congolese samples is peculiar and is probably the result of magma contamination or original magma chemistry. Only the three Namibian analyses that plot closest to the Fe and Na end-members of these two plots are schorl. The remaining specimens examined are Al [Li] tourmalines.

The principal substitution responsible for the chemistry of the studied tourmaline is the elbaite-liddicoatite ${}^X\text{Na}^+ + {}^Y(\text{Al}^{3+})_{0.5} \rightarrow {}^X\text{Ca}^{2+} + ({}^Y\text{Li}^+)_{0.5}$ coupled substitution vector. The ${}^X\text{Ca}^{2+} + {}^Y\text{Li}^+ \rightarrow {}^X\text{□} + {}^Y\text{Al}^{3+}$ (liddicoatite-rossmanite) and ${}^X\text{□} + ({}^Y\text{Al}^{3+})_{0.5} \rightarrow {}^X\text{Na}^+ + ({}^Y\text{Li}^+)_{0.5}$ (rossmanite-elbaite) substitutions are operating but are less significant. The Namibian schorl fragment is part of the elbaite-schorl series which is facilitated by the $({}^Y\text{Li}^+)_{1.5} + ({}^Y\text{Al}^{3+})_{1.5} \rightarrow ({}^Y\text{Fe}^{2+})_{3.0}$.

The presence of rossmanite in this study is very significant because this mineral has never been previously described as a cut stone and has yet to be reported from Nigeria, Namibia or Tanzania. The broad range of colors among the faceted Nigerian liddicoatites and rossmanites is particularly interesting with colors ranging from near-colorless to colorless, pink, pink-red, red, yellowish-green, light green and bluish-gray.

Specimens with low Si contents (i.e. 5.83 apfu) contain high Al totals because small quantities of Al may substitute for Si at the T-sites. There are a few samples in this

study that were calculated to contain >6.000 apfu of Si and this is likely the result of analytical error.

Ti does not play a role in coloring the faceted tourmalines from Africa save for the tourmaline from Democratic Republic of Congo. There is detectable Ti in the pink and red liddicoatites and elbaites of the Nigerian suite but these quantities are not significant and do not result in any noticeable color changes. For the Congolese slices, elevated Mn plus Ti facilitates the $Mn^{2+} \leftrightarrow Ti^{4+}$ I.C.V.T which causes the yellowish-brown to brown colors.

The Congolese slices exhibit relatively constant or decreasing Ti quantities from core to rim. The overall low Ti content of these samples may be related to low initial Ti parent pegmatitic magma or the incorporation of this element into earlier phases. The cause of the Ti enrichment in the rim of “Congo I” is uncertain but it is postulated that a complexing agent, possibly F was present in the melt/fluid that was able to sequester Ti until the final stages of crystallization. Fe may also be conserved in the melt through a similar complexing process and Ca may also be conserved by some as yet unexplained mechanism.

The elevated Bi concentrations of certain samples in the Nigerian, Namibian and Tanzanian suites may have profound implications for the chemistry and paragenesis of these host pegmatites. Bi generally increases with progressive magmatic evolution in LCT-family pegmatites. Thus, the tourmaline samples with Bi in this study may provide evidence that the host melts that produced these tourmaline crystals may have contained substantial Bi late in the consolidation history of these pegmatites. Moreover, tourmaline

crystals with high Bi quantities could potentially serve as a prospecting tool for very rare and highly sought after Bi minerals.

The rare V occurrences in the blue Nigerian elbaites may stem from the contamination of the host melts via external sources. V is normally a constituent of minerals associated with mafic to ultramafic rocks, marine sedimentary rocks and resulting metamorphic rocks and is not typically observed in granitic pegmatites of the LCT affiliation, unless the pegmatitic melt has become contaminated with these sources.

Of the three chromophoric transition metal cations responsible for coloring the studied samples (Fe, Mn and Ti), Fe is the most dominant. As Y-site Fe contents increase, hues become darker and colors change from yellowish-green to green, blue-gray, blue and black. It takes very little Fe (~0.003 apfu) to cause a slight change in color. The bi-colored stones of the Nigerian suite range in color from pink to green and vice versa as quantities of Fe change. Fe is considerably higher in the green portions and Mn contents remain relatively constant in these samples. The blue stones which are rich in Fe and low in Ti are proof that high Fe content alone can cause blue hues instead of the $\text{Fe}^{2+} \leftrightarrow \text{Ti}^{4+}$ I.V.C.T. suggested by Rossman (1997).

Mn is an important coloring agent for the studied tourmalines. However, it is a much less dominant chromophore than is Fe as Mn is a weaker absorber of visible photons (Rossman, 1997). Only when Fe quantities are low (<0.04 apfu) do the chromophoric effects of Y-site Mn become apparent. In general, colors change to yellow-brown and brown with increasing Mn. Some pink Namibian elbaite fragments contain greater quantities of Fe than Mn but retain a pink hue. This phenomenon will be discussed later.

The quantities of Mn have no relationship to the Fe content of the samples of this study because the green, blue and black samples contain approximately the same range of Mn contents as the colorless, pink and red samples. Thus, the use of Mn alone is not the most useful indicator of fractionation. However, the observed decreases in Mn from core to rim of the Congolese and Tanzanian slices are probably the result of these residual melts becoming depleted in Mn.

The Mn content versus pink color intensity plots given in Figs. 22 and 23 show that there is no correlation between the Mn content and the degree of coloration of colorless, pink and red stones. This phenomenon has not been fully discussed in previous literature. A plausible explanation is natural γ -radiation from K, U and Th-bearing phases within proximity of low Fe, Mn-bearing tourmaline. This radiation is energetic enough to strip a valence electron from the Mn^{2+} cation, oxidizing it to Mn^{3+} (Reinitz & Rossman, 1988). This may cause tourmaline to change from colorless to brilliant pink hues. Tourmaline may contain up to 3.0 wt. % MnO and remain colorless (Rossman, 1997). Thus the intensity of the color of these stones may be related to the flux of γ -radiation that these low Fe specimens have been exposed to and not the Mn-content.

Evolved LCT-family pegmatitic melts do not have appreciable Mg, unless this element is introduced via contamination from more mafic country rocks or other Mg-bearing rocks (Selway *et al.*, 2000a; Tindle *et al.*, 2002). The abundance of Mg in the Nigerian, Namibian and Congolese stones (green rims) violates the classical fractionation trends of LCT pegmatites of Mg decreasing with progressive evolution (Jolliff *et al.*, 1986) and leaves open the possibility that Mg, like Fe and Ca may be conserved until the

final stages of consolidation. The Namibian schorl fragment with high Mg likely crystallized earlier when Mg was more prevalent in the melt.

The Ca activity of the melt as well as the presence of competing Ca-bearing phases determines whether elbaite or liddicoatite will crystallize (Teertstra *et al.*, 1999). The Nigerian liddicoatites of this study may have crystallized from melts contaminated with Ca-rich rocks, particularly dolomite or calcite marbles.

The broad variation of Li content of these samples is a direct function of the species of tourmaline examined (i.e. liddicoatite, rossmanite or elbaite). Under ideal circumstances, uncontaminated B-rich, LCT-family melts should have considerable quantities of Na, allowing elbaite to precipitate. Magmas contaminated with Ca preferentially crystallize liddicoatite. Thus, the parental melt must be enriched in Ca, as well as Al, B and Li for liddicoatite to form. Rossmanite and Na-poor elbaite crystallize in only the last stages of pegmatitic consolidation when Na-poor, Li-rich conditions have been attained in the micro-environments that these crystals nucleate in (Simmons, 2003; Brown & Wise, 2001; Selway *et al.*, 1999 and Selway *et al.*, 1998a).

There is a paucity of K throughout the various suites of tourmaline as the structure does not easily accommodate this element. This is due to the large ionic radius of K, which limits its substitutions for smaller cations at the X-site.

The occupancy of the X-site of tourmalines from this study results from the relative activities of Ca, Na and K late in the history of the host pegmatite. Each of the samples examined has some quantity of X-site vacancies and this site is never completely filled.

W-site occupancy is a function of the abundance of F and OH anions in the melt. The Nigerian and Tanzanian hydroxyl-liddicoatite occurrences are significant as they are the first examples of these species from these countries and represent the first report of this mineral on the gem market. The same applies to the fluor-elbaites, fluor-rossmanites and fluor-schorls from the six localities. These findings prove that F-activity may be low and still result in the formation of liddicoatite in pegmatites. The amount of F present in the tourmaline crystals examined is a function of the original amount of F in the melt and the presence of phases that could compete with tourmaline for F.

The Mn-Ti-Fe ternary diagrams (Figs. 11, 27, 41, 54 and 67) for the six countries are similar. These plots show that stones which are near colorless to colorless, pink, red, reddish-purple, yellow-brown and brown contain Mn with very low Fe at the Y-sites, whereas the yellowish green, green, blue and black stones have more Fe. Rare overlap of green specimens into the Mn-dominant field occurs because Fe is such a powerful absorber of visible photons (Mattson & Rossman, 1987). Pink stones which have more Fe than Mn contain very low quantities of both elements.

The Fe vs. Mn plots given in Figs. 13, 29, 43, 56 and 69 show a distinct separation of the various colors present as well as the species. These graphs show that the colorless, pink, red, reddish-purple, yellow-brown and brown samples of this study contain low concentrations of Fe. As Fe quantities increase, colors abruptly change to shades of green, blue, dark-brown and black. Small quantities of Fe cause the Nigerian liddicoatites and rossmanites to be light-green. Fe-rich green, blue, dark-brown and black specimens usually contain as much Mn as the near colorless, pink, red, yellow-brown and brown samples. In these stones color is controlled by Fe and not by Mn.

The Li vs. Mn graphs given in Figs. 14, 30, 44, 57 and 70 show that no distinction can be made regarding the colors of these populations based on Mn alone. Mn for Li substitution throughout these populations is minimal except in tourmaline from Nigeria and the Congo where there are significant quantities of Mn present in these samples. The negative trends of the Nigerian (Fig. 14) and Congolese Li vs. Mn (Fig. 57) plots stems from the fact that Li replaces Mn at the Y-sites. As Mn contents increase there is a concomitant increase in X-site Na quantities as the chemistry trends toward the hypothetical “tsilaisite” end-member.

Contrary to findings from previous studies, the Nigerian, Namibian and Malian populations have no correlations between Li vs. F (Figs. 15 and 31) and Na vs. F (Figs. 20 and 36). Other workers have reported that Li and F and Na and F share intimate crystal chemical relationships (Tindle *et al.*, 2002; Selway *et al.*, 2000b; Hawthorne & Henry, 1999; Robert *et al.*, 1997; Hawthorne, 1996).

The Li vs. Al covariation diagrams are given in Figs. 16, 32, 46, 59 and 72. The black and blue elbaite samples form a positive trend as Li and Al quantities increase. As compositions trend from elbaite to rossmanite, Al increases and Li essentially remains constant. As the samples become more liddicoatitic, Li increases and Al decreases as Li replaces Al in the structure. The trends of these plots are due to the relative quantities of Li and Al in elbaite, rossmanite and liddicoatite.

The negative trends of the Al vs. Fe diagrams shown in Figs. 17, 33, 47, 60 and 73 are the result of Al↔Fe substitution and possibly fractionation. The Mn-rich samples of the Nigerian and Congolese suites deviate from the main trend because Mn substitutes for Al. The relative Fe contents cause the observed color changes.

The Fe vs. Ti (Figs. 13, 34, 48, 61 and 74) and Mn vs. Ti plots (Figs. 19, 35, 49, 62 and 75) show that Ti affects colors only among the slices from the Congo. The effect of Ti plus high Mn quantities promotes the $Mn^{2+} \leftrightarrow Ti^{4+}$ I.C.V.T. which causes the yellow-brown to brown color zones of these slices (Rossman, 1997). The dark brown core of “Congo i” is the result of high Fe and the $Mn^{2+} \leftrightarrow Ti^{4+}$ I.C.V.T. The schorl from Namibia contains >0.03 apfu Ti but any contributing chromophoric effects of the Ti are muted by extremely high Fe contents.

The patterns exhibited by the Na vs. Ti+Fe+Mn plots shown in Figs. 21, 37, 51, 64 and 77 of the studied tourmaline crystals are the result of the geochemistry of the late-stage parental pegmatitic magmas from which they crystallized in. The liddicoatites of Anjanabonoina, Madagascar display a paucity of transition element content (Dirlam *et al.*, 2002) and this finding is consistent with the results of this study. Increasing quantities of transition elements correlate with tourmaline becoming more elbaitic and eventually schorlitic (Fe) or “tsilaisitic” (Mn). It is very probable that the low transition element content of the liddicoatites and rossmanites of this study is due to the low content of these elements in the late-stage magma from which these minerals crystallized.

Cell-edge analysis of multi-colored gem tourmaline rough from Namibia, Mali and Mozambique shows limited correlations between color, chemistry and cell-edge lengths. As colors change from pink to green to blue and as Y-site Fe increases, the a cell dimension expands. Accompanying this trend, there is a small increase in the c cell dimension. The wide range of lengths of the a dimensions of the green crystals may be related to the broad range of color and hence Fe content of these samples. The variability of lengths of the c dimensions of the pink crystals is likely a function Mn content since

these samples all have low Fe. The black schorl fragment (sample .3-10-1, Table 4) is anomalous because it plots in the middle of the elbaite population. This fragment does not have a large a dimension that would be expected from such an Fe-rich tourmaline. This sample does contain considerable Li and Al quantities as well as high Ti and this could be the reason that it plots with the elbaites.

CONCLUSIONS

1. The Mg- Y-site Al- Fe ternary shown in Fig. 5 indicates that the tourmaline from Nigeria, Namibia, Mali, Tanzania, Congo and Mozambique are predominantly Li-Al-rich with five Namibian analyses and one Congolese analysis that plot towards the schorl end-member. The Congolese samples have a Mg signature which indicates that the host melt contained Mg or was contaminated by Mg-rich rocks. The Ca- Y-site Al-Na ternary given in Fig. 6 more specifically shows that the tourmaline from these six countries is of the liddicoatite-rossmanite-elbaite solid solution series with several analyses of the Namibian, Congolese and Mozambique suites belonging to the elbaite-schorl solid solution series.

2. The Nigerian faceted stones belong to the liddicoatite-rossmanite-elbaite solid solution series. There is an approximately equal proportion of liddicoatite and elbaite stones in this suite and four stones that are at least in part rossmanite. The Nigerian samples are the most chemically diverse population of samples of any African locality sampled. The slices from Sanga Sanga, Tanzania are also part of this series with one zone of one slice being rossmanite. The Namibian rough samples and slices are dominantly elbaite and trend toward the rossmanite field with one stone that is part rossmanite. There is a schorl fragment within this set, which represents the Fe-rich core of one of the samples. Tourmaline from the Democratic Republic of Congo, Mozambique and Mali are elbaite with small quantities of the liddicoatite and rossmanite molecules.

3. The color of gem-quality tourmaline is largely controlled by the Y-site Fe content. Fe is the most dominant chromophore in tourmaline and causes light greenish-yellow to light yellowish-green, light-green, green, dark-green, bluish-green, blue and black colors as Fe-content increases. The chromophoric effects of Mn are only apparent when Fe quantities are very low. Ti does not influence colors in the tourmalines from any of the suites except for the yellow-brown to brown zones of the Congolese slices. The $Mn^{2+} \leftrightarrow Ti^{2+}$ I.V.C.T combined with very low Fe contents are the cause of these hues. The color of the dark-brown core of "Congo i" is the result of very high Fe content and the $Mn^{2+} \leftrightarrow Ti^{2+}$ I.V.C.T. The causes of the unusual grayish-blue colors of Nigerian samples "c" and "s1" do not appear to correlate with transition element content. They appear to be the result of interactions of color from bi-colored samples with tables cut parallel to color zones.

4. The color zoning observed in the Namibian, Tanzanian and Congolese tourmaline slices of this study provides a record of what cations were present in the micro-environments of the parental pegmatitic magmas where these crystals were nucleating. These sharply defined heterogeneities may be the result of fluctuating chemical conditions or possibly boundary layer effects in a rapidly crystallizing system.

5. Patterns linking the chemistry of the tourmaline suites to their provenance are weak. Of the countries examined, rossmanite was found only in Nigeria, Namibia and Tanzania and liddicoatite was found only in Nigeria and Tanzania. Considering the relative rarity of these two minerals, there is a good chance that faceted African stones which are compositionally liddicoatite or rossmanite could be from one of these countries. The bottom-line is that locality information is not discernable on the basis of

minor element chemistry unlike the Mn-rich liddicoatites from Tsilaisina, Madagascar (Dirlam *et al.*, 2002) or the cuprian elbaites from Paraíba, Brazil (Rossman *et al.*, 1991).

6. Only a weak relationship between color, chemistry and the lengths of the *a* and *c* unit cell dimensions is observed. Generally the *a* and *c* dimensions increase as Fe contents increase and colors change from pink to green to blue. The likely reason that the schorl fragment does not plot more toward the schorl reference point in Fig. 78 is because of this samples high Li, Al and Ti contents. X-ray diffraction does not appear to be a viable method for studying gem tourmaline.

7. The rossmanite occurrences of Nigeria, Namibia and Tanzania are significant and represent the first reported occurrence of this species on the gem market and the first reports of this mineral from these countries. Additionally, the W-site occupancy of tourmaline from the six countries is F and OH-dominant in about equal proportions and represents the first report of fluor-elbaite, fluor-rossmanite and hydroxyl-liddicoatite (Hawthorne & Henry, 1999) from these respective localities and the first report of these species on the gem market. This is evidence that tourmaline from Africa as well as other world-wide localities can no longer simply be labeled as “elbaite”.

8. There is no correlation between the degree of color for colorless, near-colorless, pink or red samples from the Nigerian suite, and the Mn-content of these stones. Gem-quality tourmaline can contain up to 3.0 wt. % MnO and still be colorless (Rossman, 1997). The lack of a relationship of color with Mn quantity is likely the result of natural γ -radiation from K, U or Th-bearing phases capable of oxidizing $Mn^{2+} \rightarrow Mn^{3+}$, intensifying pink and red hues. Structural defects could also be a cause of this discrepancy. It is also possible that some of these stones have been exposed to synthetic

radiation to enhance their color to more desirable intensities and increase their value.

Further work needs to be completed to determine the exact nature of this phenomenon.

REFERENCES

- ANTHONY, J.W., BIDEAUX, R.A., BLADH, K.W. & NICHOLS, M.C. (1995): *Handbook of Mineralogy: Silica, Silicates-Part 1*. Mineral Data Publishing. Tucson, Arizona. **1**.
- _____, _____, _____, _____ (1995): *Handbook of Mineralogy: Silica, Silicates-Part 2*. Mineral Data Publishing. Tucson, Arizona. **2**.
- APPLEMAN, D.E. & EVANS, H.T., JR. (1973): Job 9214: indexing and least squares refinement of powder diffraction data. *U.S. Geol. Surv. Comput. Contrib.* **20** (*NTIS Doc. PB2-16188*).
- AURISICCHIO, C. & PEZZOTTA, F. (1997): Tourmaline group minerals of the LCT-miarolitic pegmatites of the Elba Island, (Italy): chemical composition and genetic and paragenetic inferences. *Tourmaline 1997., Int. Symp. on Tourmaline (Nové Město na Moravě), Abstr. Vol.*, 1-2.
- AYUSO, R.A. & BROWN, C.E. (1984): Manganese-rich red tourmaline from Fowler, New York. *Can. Mineral.* **32**, 327-331.
- BILAL, E., CÉSAR-MENDES, J. & CORREA-NEVES, J.M. (1997): Chemistry of tourmalines in some granitic pegmatites of São José da Safira, Minas Gerais, Brazil. *Tourmaline 1997., Int. Symp. on Tourmaline (Nové Město na Moravě), Abstr. Vol.*, 7-9.
- BROWN, C.D. & WISE, M.A. (2001): Internal zonation and chemical evolution of the Black Mountain granitic pegmatite, Maine. *Can. Mineral.* **39**, 45-55.
- ČERNÝ, P. (2000): Constitution, petrology, affiliations and categories of miarolitic pegmatites. *Memorie della Società Italiana di Scienze Naturali e del Civico di Storia Naturale di Milano.* **30**, 5-12.
- DEER, W.A., HOWIE, R.A. & ZUSSMAN, J. (1962): *Rock Forming Minerals-Ortho and Ring Silicates*. Lougmans, Green and Co. Ltd. **1**.
- _____, _____, _____ (1986): *Rock Forming Minerals-Disilicates and Ring Silicates* (2nd edition). Lougmans, Green and Co. Ltd. **1B**, 559-602.
- DIETRICH, R.V. (1985): *The Tourmaline Group*. Von Nostrand Reinhold, New York, N.Y.

- DIRLAM, D.L., LAURS, B.M., PEZZOTTA, F. & SIMMONS, W.B. (2002): Liddicoatite tourmaline from Anjanabonoina, Madagascar. *Gems and Gemology*. **38**, 28-35.
- DUTROW, B.L. & HENRY, D.J. (2000): Complexly zoned fibrous tourmaline, Cruziero Mine, Minas Gerais, Brazil: A record of evolving magmatic and hydrothermal fluids. *Can. Mineral.* **38**, 131-143.
- FALSTER, A.U., SIMMONS, W.B. and WEBBER, K.L. (1997): Unusual chemistry of tourmaline in the Animikie Red Ace pegmatite in Florence County, Wisconsin, U.S.A. *Tourmaline 1997., Int. Symp. on Tourmaline (Nové Město na Moravě), Abstr. Vol.*
- FOORD, E.E. (1976): *Mineralogy and petrogenesis of layered pegmatite-aplite dikes in the Mesa Grande district, San Diego County, California*. PhD. thesis, Stanford University. 326p.
- FRONDEL, C., BIEDL, A. & ITO, J. (1966): A new type of ferric iron tourmaline. *Am. Mineral.* **51**, 1501-1505.
- FOIT, F.F. & ROSENBERG, P.E. (1975): Aluminobuergerite, $\text{Na}_{1-x}\text{Al}_3\text{Al}_6\text{B}_3\text{Si}_6\text{O}_{27}\text{O}_{3-x}(\text{OH})_{1+x}$, a new end-member of the tourmaline group. *Am. Geophys. Union, Trans. (Eos)* **56**, 461.
- _____ & _____ (1979): The structure of vanadium-bearing tourmaline and its implications regarding tourmaline solid solutions. *Am. Mineral.* **64**, 788-798.
- GORDIENKO, V.V., CHARIKOV, A.V., KARETKOVA, N.N. & VASILJEVA, M.V. (1997): Zn in tourmaline-schorls as an indicator of evolution in pegmatite process. *Tourmaline 1997., Int. Symp. on Tourmaline (Nové Město na Moravě), Abstr. Vol.*, 27-28.
- GRICE, J.D., ERCIT, T.S. & HAWTHORNE, F.C. (1993): Povondraite, a redefinition of the tourmaline ferridravite. *Am. Mineral.* **78**, 433-436.
- _____ & ROBINSON, G.W. (1989): Feruvite, a new member of the tourmaline group, and its crystal structure. *Am. Mineral.* **75**, 706-707. Abstr.
- HAWTHORNE, F.C. (1996): Structural mechanisms for light element variations in tourmaline. *Can. Mineral.* **34**, 123-132.
- HAWTHORNE, F.C. (1997): The crystal chemistry of tourmaline: current status. *Tourmaline 1997., Int. Symp. on Tourmaline (Nové Město na Moravě), Abstr. Vol.*
- _____ & HENRY, D.J. (1999): Classification of the minerals of the tourmaline group. *Eur. J. Mineral.* **11**, 201-215.

- _____, SELWAY, J.B., KATO, A., MATSUBARA, S., SHIMIZU, M., GRICE, J.D. & VAJDAK, J. (1999): Magnesiofoitite, $\square(\text{Mg}_2\text{Al})\text{Al}_6\text{Si}_6\text{O}_{18}(\text{BO}_3)_3(\text{OH})_4$, a new alkali deficient tourmaline. *Can. Mineral.* **37**, 1439-1443.
- HENRY, D.J. & DUTROW, B.L. (2001): Compositional zoning and element partitioning in nickeloan tourmaline from a metamorphosed karstbauxite from Samos, Greece. *Am. Mineral.* **86**, 1130-1142.
- _____, & _____ (2000): Fibrous tourmaline as a recorder of evolving magmatic and hydrothermal fluids. *Can. Mineral.* **38**, 131-143.
- _____, & _____ (1996): Metamorphic tourmaline and its petrologic implications. In Boron mineralogy, petrology and geochemistry. (E.S. Grew & L.M. Anovitz, eds.). *Rev. Mineral.* **33**, 503-557.
- _____, & GUIDOTTI, C.V. (1985): Tourmaline as a petrogenetic indicator mineral: an example from the staurolite-grade metapelites of NW Maine. *Am. Mineral.* **70**, 1-15.
- HUGHES, J.M., ERTL, A., DYAR, M.D., GREW, E.S., SHEARER, C.K., YATES, M.G. & GUIDOTTI, C.V. (2000): Tetrahedrally coordinated boron in a tourmaline: Boron-rich olenite from Stoffhütte, Koralpe, Austria. *Can. Mineral.* **38**, 861-868.
- HUGHES, K.A., HUGHES, J.M. & DYAR, M.D. (2001): Chemical and structural evidence for $^{[4]}\text{B} \leftrightarrow ^{[4]}\text{Si}$ substitution in natural tourmalines. *Eur. J. Mineral.* **13**, 743-747.
- JIANG, S.Y., PALMER, M.R., McDONALD, A.M., SLACK, J.F. & LEITCH, C.H.B. (1996): Feruvite from the Sullivan Pb-Zn-Au deposit, British Columbia. *Can. Mineral.* **34**, 733-740.
- JOLLIFF, B.L., PAPIKE, J.J. & SHEARER, C.K. (1986): Tourmaline as a recorder of pegmatite evolution: Bob Ingersoll pegmatite, Black Hills, South Dakota. *Am. Mineral.* **71**, 472-500.
- KASSOLI-FOURNARAKI, A. & MICHAELIDIS, K. (1994): Chemical composition of tourmaline in quartz veins from Nea Roda and Thasos Areas in Macedonia, northern Greece. *Can. Mineral.* **32**, 607-615.
- KELLER, P., ROBLES, E.R., PERÉZ, A.P. & FONTAN, F. (1999): Chemistry, petrogenesis and significance of tourmaline in pegmatites of the southern tin belt, central Namibia. *Chem. Geol.* **158**, 203-225.
- KOIVULA, J.I. (1982): Tourmaline as an inclusion in Zambian emeralds. *Gems and Gemology*. **18**, 225-227.
- _____, & FRYER, C.W. (1985): Interesting red tourmaline from Zambia. *Gems and Gemology*. **21**, 40-42.

- LOWENSTEIN, W. (1956): Boron in tetrahedra of borates and borosilicates. *Am. Mineral.* **41**, 349-351.
- LYNCH, G. & ORTEGA, J. Hydrothermal alteration and tourmaline/albite equilibria at the Coxheath Porphyry Cu-Mo-Au deposit, Nova Scotia, Canada. *Can. Mineral.* **35**, 79-94.
- MACDONALD, D.J., HAWTHORNE, F.C. & GRICE, J.D. (1993): Foitite, a new alkali deficient tourmaline: description and crystal structure. *Am. Mineral.* **78**, 1299-1303.
- MANDARINO, J.A. (1999): *Fleisher's Glossary of Mineral Species*. The Mineralogical Record Inc., Tuscon, Arizona.
- MATTSON, S.M. & ROSSMAN, G.R. (1987): Fe²⁺-Fe³⁺ interactions in tourmaline. *Phys. Chem. Minerals.* **14**, 163-171.
- NOVÁK, M. & SELWAY, J.B. (1997): Tourmaline composition as a recorder of crystallization in open and closed systems in the elbaite sub-type pegmatite from Bližná. *Tourmaline 1997., Int. Symp. on Tourmaline (Nové Město na Moravě), Abstr.*
- _____ & TAYLOR, M.C. (2000): Foitite: Formation during late stages of evolution of complex granitic pegmatites at Dobrá Voda, Czech Republic, and Pala, California, U.S.A. *Can. Mineral.* **38**, 1399-1408.
- NUBER, B. & SCHMETZER, K. (1981): Strukturverfeinerung von liddicoatite. *Neues Jahrb. Mineral. Monatsh.*, 215-219. (in German)
- PEZZOTTA, F, HAWTHORNE, F.C., COOPER, M.A. & TEERTSTRA, D.K. (1996): Fibrous foitite from San Piero in Campo, Elba, Italy. *Can. Mineral.* **34**, 741-744.
- POVONDRA, P. & NOVÁK, M. (1986): Tourmaline in metamorphosed carbonate rocks from western Moravia, Czechoslovakia. *Neues Jahrb. Mineral. Monatsh.*, 273-282.
- REINITZ, I.M. & ROSSMAN, G.R. (1988): Role of natural radiation in tourmaline coloration. *Am. Mineral.* **73**, 822-825.
- REZNITSKY, E.Z., SKLYAROV, E.V., USHCHAPOVSKAYA, Z.F., NARTOVA, N.V., KASHAEV, A.A., KARMANOV, N.S., KANAKIN, S.V., SMOLIN, A.S. & NEKRASOVA, E.A. (2001): Vanadiumdravite, NaMg₃V₆(BO₃)₃Si₆O₁₈(OH)₃(OH), a new mineral of the tourmaline group. *Zap. Vses. Mineral. Obshchest.* **130**, 59-72. (in Russian)
- ROBERT, J.L., GOURDANT, J.P., LINNEN, R.L., PIOVER, O & BENOIST, P. (1997): Crystal chemical relationships between OH, F and Na in tourmaline. *Tourmaline 1997., Int. Symp. on Tourmaline (Nové Město na Moravě), Abstr. Vol.*, 84-85.

- ROSSMAN, G.R. (1997): Color in tourmaline. *Tourmaline 1997., Int. Symp. on Tourmaline (Nové Město na Moravě), Abstr. Vol.*
- ____ & MATTSON, S.M. (1986): Yellow, Mn-rich elbaite with Mn-Ti intervalence charge transfer. *Am. Mineral.* **71**, 599-602.
- _____, FRITSCH, E. & SHIGLEY, J.E. (1991): Origin of color in cuprian elbaite from São Jose da Batalha, Paraíba, Brazil. *Am. Mineral.* **76**, 1479-1484.
- RUMYANTSEVA, E.V. (1983): Chromdravite, a new mineral from Karelia. *Zap. Vses. Mineral. Obshchest.* **112**, 222-226.
- _____(1985): Some minerals of the chromium-vanadium glimmerites of Karelia. *Zap. Vses. Mineral. Obshchest.* **114**, 55-62. (in Russian)
- SCHMETZER, K. & BANK, H. (1984a): Intensive yellow tsilaisite (manganese tourmaline) of gem quality from Zambia. *The Journal of Gemology and Proceedings of the Gemological Assoc. of Great Britain.* **19**, 218-223.
- ____ & _____ (1984b): Crystal chemistry of tsilaisite (manganese tourmaline) from Zambia. *Neues Jahrb. Mineral. Monatsh.*, 61-69.
- SELWAY, J.B. (1999): *Compositional evolution of tourmaline in granitic pegmatites.* Ph.D. thesis, Univ. Manitoba, Winnipeg, Manitoba.
- _____, ČERNÝ, P. & HAWTHORNE, F.C. (1998b): Feruvite from lepidolite pegmatites at Red Cross Lake, Manitoba. *Can. Mineral.* **36**, 433-439.
- _____, _____, _____ & NOVÁK, M. (2000b): The Tanco pegmatite of Bernic Lake, Manitoba. XIV. Internal tourmaline. *Can. Mineral.* **38**, 877-891.
- _____, NOVÁK, M., ČERNÝ, P. & HAWTHORNE, F.C. (1999): Compositional evolution of tourmaline in lepidolite-subtype pegmatites. *Eur. J. Mineral.* **11**, 569-584.
- _____, _____, _____ & _____ (2000a): The Tanco pegmatite at Bernic Lake, Manitoba. XIII. Exocontact tourmaline. *Can. Mineral.* **38**, 869-876.
- _____, _____, HAWTHORNE, F.C., ČERNÝ, P., OTTOLINI, L. & KYSER, T.K. (1998a): Rossmanite, $\square(\text{Li},\text{Al}_2)\text{Al}_6\text{Si}_6\text{O}_{18}(\text{BO}_3)_3(\text{OH})_3(\text{OH})$, a new alkali deficient tourmaline; description and crystal structure. *Am. Mineral.* **83**, 896-900.
- SIMMONS, W.B. (2003): *Mineralogy of the tourmaline group.* In Tourmaline, extraLapis English no. 3: A gemstone spectrum. (A.U. Falster, M.D. Jarnot, G.A. Neumeier, W.B. Simmons & G.A. Staebler, eds.). 10-23.

- _____. (2003): *Pegmatites-An Overview*. In Tourmaline, extraLapis English no. 3: A gemstone spectrum. (A.U. Falster, M.D. Jarnot, G.A. Neumeier, W.B. Simmons & G.A. Staebler, eds.). 70-72.
- _____, FALSTER, A.U., WEBBER, K.L., & LYCKBERG, P. (1997): Elbaite from pegmatites of the Malkhanski pegmatite district, Transbaikalia, Siberia, Russia. *Tourmaline 1997., Int. Symp. on Tourmaline (Nové Město na Moravě), Abstr. Vol.*, 93-94.
- _____, WEBBER, K.L., FALSTER, A.U. & NIZAMOFF, J.W. (2001): Gem tourmaline chemistry and paragenesis. *Australian Gemmologist*. **21**, 24-29.
- SINKANKAS, J. (1981): *Emerald and other beryls*. Chilton Book Co., Radnor, PA.
- SHIGLEY, J.E., KANE, R.E. & MANSON, D.V. (1986): A notable Mn-rich gem elbaite and its relationship to tsilaisite. *Am. Mineral.* **71**, 1214-1216.
- SLIVKO, M.M. (1959): Manganese tourmalines. *Mineral. Sborn. Lvov*. **13**, 139-148. (in Russian)
- SOKOLOV, P.B., GORSKAYA, M.G., GORDIENKO, V.V. PETROVA, M.G., KRETZER & FRANK-KAMENETSKII, V.A. (1986): Olenite $\text{Na}_{1-x}\text{Al}_3\text{B}_3\text{Si}_6\text{O}_{27}(\text{O},\text{OH})_4$ -A new high alumina mineral of the tourmaline group. *Zap. Vses. Mineral. Obshchest.* **115**, 119-123. (in Russian)
- TAGG, S.L., CHO, H., DYAR, M.D. & GREW, E.S. (1999): Tetrahedral boron in naturally occurring tourmaline. *Am. Mineral.* **84**, 1451-1455.
- TAYLOR, M.C., SELWAY, J.B. & NOVÁK, M. (1997): Tourmaline as a recorder of pegmatite evolution: Belo Horizonte no. 1 pegmatite, Peninsular Ranges batholith, Southern California. *Tourmaline 1997., Int. Symp. on Tourmaline (Nové Město na Moravě), Abstr. Vol.*, 121.
- TEERTSTRA, D.K., ČERNÝ, P. & OTTOLINI, L. (1999): Stranger in paradise: liddicoatite from the High Grade Dike pegmatite, southeastern Manitoba, Canada. *Eur. J. Mineral.* **11**, 227-235.
- TINDLE, A.G., BREAKS, F.W. & SELWAY, J.B. (2002): Tourmaline in petalite-subtype pegmatites: Evidence for fractionation and contamination from the Pakeagama Lake and Separation Lake areas of northwestern Ontario, Canada. *Can. Mineral.* **40**, 753-788.
- TIPPE, A. & HAMILTON, W.C. (1971): A neutron diffraction study of the ferric tourmaline, buergerite. *Am. Mineral.* **56**, 101-113.

- TOMISAKA, T. (1968): Syntheses of some end-members of the tourmaline group. *Mineral J.* **5**, 355-364.
- WALLENTA, K. & DUNN, P.J. (1979): Ferridravite, a new mineral of the tourmaline group from Bolivia. *Am. Mineral.* **64**, 945-948.
- ZANG, J., FALSTER, A.U. & SIMMONS, W.B. (2003): *News about the star. In Tourmaline, extraLapis English no. 3: A gemstone spectrum.* (A.U. Falster, M.D. Jarnot, G.A. Neumeier, W.B. Simmons & G.A. Staebler, eds.). 39-41.
- ZOLOTAREV, A.A. (1997): Crystal chemistry of tourmaline from pegmatites of the East-Pamirs, Tajikistan. *Tourmaline 1997., Int. Symp. on Tourmaline (Nové Město na Moravě), Abstr. Vol.*, 115.

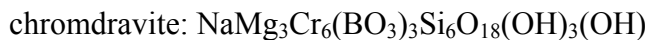
APPENDIX 1

The Tourmaline Group

The 14 species of the tourmaline group can be divided into sub-groups based on X-site chemistry. This classification yields the alkali, calcic and X-site vacant sub-groups. Schorl, dravite, elbaite, olenite, buergerite, chromdravite, povondraite and vanadiumdravite belong to the alkali sub-group. Liddicoatite, uvite and feruvite comprise the calcic sub-group and rossmanite, foitite and magnesiofoitite compose the X-site vacant sub-group. The tourmaline group can be further broken down on the basis of W-site anionic occupancies yielding the hydroxyl, fluor, and oxy sub-groups and end-members (Hawthorne & Henry, 1999). This new classification system has not yet been approved by the I.M.A.



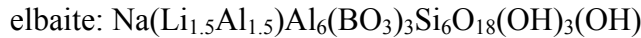
Buergerite is the Na-Fe³⁺-Al-dominant end-member of the tourmaline group. Na, Fe³⁺ and Al are housed by the X-site, Y-sites and Z-sites respectively (Foit & Rosenberg, 1979; Tippe & Hamilton, 1971; Frondel *et al.*, 1966).



Chromdravite is the Na-Mg-Cr-dominant species of the tourmaline group. Na, Mg and Cr are housed by the X-site, Y-sites and Z-sites respectively (Anthony *et al.*, 1995; Rumyantseva, 1985; Rumyantseva, 1983).



Dravite is the Na-Mg-Al-rich species of the tourmaline group. Na, Mg and Al are held by the X-site, Y-sites and Z-sites respectively (Novák & Selway, 1997; Dietrich, 1985; Koivula & Fryer, 1985; Koivula, 1982; Sinkankas, 1981; Slivko, 1959).



Elbaite is the Na-Li-Al-rich end-member of the tourmaline group. Na is housed in the X-site. Li and Al are equally distributed among the three Y-sites of the ideal elbaite molecule. The Z-site is fully occupied by Al. OH anions are held by the V and W-sites. Elbaite is one of the most variably colored species of tourmaline. This is a result of its diverse incorporation of chromophoric transition elements, intervalence charge transfers and color changes due to irradiation. The unit cell parameters of elbaite vary as a result of solid solution with a and c dimensions ranging from 15.80-15.93 Å and 7.09-7.13 Å respectively (Anthony *et al.*, 1995).

Elbaite forms solid solution series with schorl, rossmanite, liddicoatite, dravite, olenite, “tsilaisite”, and possibly feruvite. The elbaite-schorl series is based on Y-site substitutions of $(^Y\text{Li}^+)^{1.5} + (^Y\text{Al}^{3+})^{1.5} \rightarrow (^Y\text{Fe}^{2+})_3$ (Dietrich, 1985). There is a small immiscibility gap in this series. The elbaite-rossmanite series is facilitated by ${}^X\text{Na}^+ + {}^Y\text{Li}_{0.5}^+ \rightarrow {}^X\text{□} + {}^Y\text{Al}_{0.5}^{3+}$ coupled exchange vector. The elbaite-liddicoatite series operates via the substitution vector ${}^X\text{Na}^+ + {}^Y(\text{Al}^{3+})_{0.5} \rightarrow {}^X\text{Ca}^{2+} + (^Y\text{Li}^+)_{0.5}$. Because of crystal chemical constraints, elbaite has a greater Li:Al ratio than liddicoatite. A small immiscibility gap exists in this series (Henry & Dutrow, 1996). Elbaite and dravite comprise a partial series with a large immiscibility gap separating the two end-members

(Dietrich, 1985). According to Novák & Selway (1997) elbaite and dravite may form a nearly complete series based on tourmaline compositions from the pegmatite near Bližná, Czech Republic. Elbaite and olenite belong to a series based on $(^Y\text{Li}^+)_{1.5} \rightarrow (^Y\text{Al}^{3+})_{1.5}$ substitution vector. Elbaite and “tsilaisite” form a complete hypothetical series based on the $(^Y\text{Li}^+)_{1.5} + (^Y\text{Al}^{3+})_{1.5} \rightarrow (^Y\text{Mn}^{2+})_3$ substitution vector (Schmetzer & Bank, 1984b). Elbaite and feruvite may form a partial series based on the ${}^X\text{Na}^+ \rightarrow {}^X\text{Ca}^{2+}$, $(^Y\text{Li}^+)_{1.5} + (^Y\text{Al}^{3+})_{1.5} \rightarrow (^Y\text{Fe}^{2+})_3$ and ${}^Z\text{Al}^{3+} \rightarrow {}^Z\text{Mg}^{2+}$ substitution vectors. Evidence for this is that the feruvite from the Red Cross Lake pegmatite field, Manitoba which is Li-bearing (Selway *et al.*, 1998b).

Elbaite crystallizes most commonly in rare-element and miarolitic class, LCT family pegmatites. Compositions of elbaite generally become more enriched in Li from the exocontact to the core zones within these pegmatites.

Tourmaline from the Animikie Red Ace pegmatite in Wisconsin is part of the elbaite-olenite series (Falster *et al.*, 1997). At this locality, tourmaline is commonly found in the wall and middle intermediate zones with the mineral rarely occurring in the other pegmatite zones. Microprobe analyses show that MnO quantities of tourmaline in the wall and border zones range from near detection limits to greater than 5.0 wt. %. From the middle intermediate zone to the wall zone, FeO fluctuates between near detection limits to 1.5 wt. % in the green rims of the crystals. The dark blue tourmaline contains greater than 3.0 wt. % FeO and between 0.X to 1.0 wt. % of MnO. Cu has been detected in the “roots” of tourmaline crystals occurring in the wall zone. The authors state that this is due to contamination from the surrounding country rocks (Falster *et al.*, 1997).

Brown & Wise (2001) performed a mineralogical survey of the Black Mountain granitic pegmatite, Maine, U.S.A. to decipher its internal zonation and chemical evolution. The general tourmaline crystallization sequence from the exocontact to the core is schorl-dravite to elbaite-rossmanite. Mg and Fe decrease whereas Al, Mn and Li increase from the exocontact to the third intermediate zone with increasing fractionation. Tourmaline colors vary from black to green, pink and lastly colorless with the chemical trends described above (Brown & Wise, 2001).

The authors have found relationships between the color, chemistry and the zonal positions of the tourmaline crystals in the pegmatite. The most evolved crystals of pink to colorless elbaite-rossmanite in the third intermediate zone are nearly devoid of Fe, Mg, Ca and K. These crystals contain minor Mn and Zn quantities (≈ 1.0 wt. % MnO and ZnO), whereas the schorl crystals from the wall zone contain up to 13.0 wt. % FeO (Brown & Wise, 2001). Fe and Mn are the principal factors controlling the color of Li-Al tourmaline at this locality as well as countless other localities worldwide.



Feruvite is the Ca-Fe²⁺-Mg-Al-rich member of the tourmaline group (Selway *et al.*, 1998b; Jiang *et al.*, 1996; Henry & Dutrow, 1996; Grice & Robinson, 1990).



Foitite is the \square -Fe²⁺-Fe³⁺-Al-dominant tourmaline group species (Novák & Taylor, 2000; Selway *et al.*, 1998b; Pezzotta *et al.*, 1996; MacDonald *et al.*, 1993).



Liddicoatite is the Ca-Li-Al dominant tourmaline group end-member. Ca is housed in the X-site. Li and Al occupy the Y-sites in a 2:1 ratio in the ideal liddicoatite molecule. Al completely fills the Z-sites. The V-sites contain OH anions and F is held by the W-site. The F content of liddicoatite is a reflection of the volatile-rich conditions of the LCT family pegmatite melts that it crystallizes from. The unit cell parameters of liddicoatite are $a=15.875$ (Deer *et al.*, 1986) and $c=7.126$ (Nuber & Schmetzer, 1981). These dimensions vary with changing chemistry.

It is widely agreed upon that liddicoatite and elbaite comprise a complete solid solution series with a small immiscibility gap (Nuber & Schmetzer, 1981; Henry & Dutrow, 1996). This series is based on the ${}^X\text{Ca}^{2+} + {}^Y\text{Li}^+ \rightarrow {}^X\text{Na}^+ + {}^Y\text{Al}^{3+}$ coupled substitution vector (Dietrich, 1985). Liddicoatite and rossmanite constitute a series operating by the coupled substitution vector, ${}^X\text{Ca}^{2+} + {}^Y\text{Li}^+ \rightarrow {}^X\text{□} + {}^Y\text{Al}^{3+}$ (Teertstra *et al.*, 1999). The Al:Li ratio of liddicoatite is 1:2 as opposed to the approximately 1:1 ratio to that of elbaite.

Liddicoatite is found in the LCT family High Grade Dike pegmatite, southeastern Manitoba, Canada. The cores of tourmaline crystals found here are corroded and replaced by albite, quartz, white mica and cookeite after elbaite, followed by a rim of liddicoatite containing substantial elbaite and rossmanite components. In these zoned crystals, there is a relationship of Na and Ca with Na being higher in the altered cores corresponding to elbaite and Ca being more abundant in the late stage liddicoatite rims. The most Ca-rich liddicoatite has 0.498 apfu in the X-site with minor Y-site Mn (0.414 apfu) and Fe (0.065 apfu).

The general crystallization sequence of tourmaline in this pegmatite is from schorl-dravite (exocontact) to elbaite var. verdellite (intermediate zones) to liddicoatite in the last stages of pegmatite crystallization (Teertstra *et al.*, 1999). The authors attribute the formation of liddicoatite to be primary and the result of a microlite and apatite deficient pegmatite. This allowed for the partitioning of Ca into the liddicoatite structure instead of these competing phases.

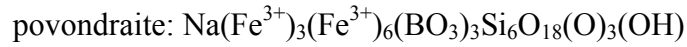
Perhaps the world's premier locality for liddicoatite is the Anjanabonoina pegmatite, central Madagascar. Liddicoatite from this locality exhibits exotic triangular zoning in the cores, concentric zoning of the rims and the so called "Mercedes Benz" three pointed stars (Zang *et al.*, 2003). The 191 analyses performed by Dirlam *et al.*, (2002) plot in both the liddicoatite and elbaite compositional fields. The authors found that the chromophoric transition elements Fe, Mn and Ti of the studied samples was generally low with the gray (2.66 wt. % FeO), green and blue zones containing much more Fe than the colorless and pink zones. The highest Mn contents (3.22 wt. % MnO) were found in purplish-red samples. A yellow zone contained the highest Ti (0.82 wt. % TiO₂) quantity (Dirlam *et al.*, 2002).



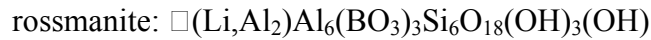
Magnesiofoitite is the \square -Mg-Al dominant end-member of the tourmaline group (Hawthorne *et al.*, 1999).



Olenite is the Na-Al dominant tourmaline group species (Falster *et al.*, 1997; Sokolov *et al.*, 1987; Sokolov *et al.*, 1986).



Povondraite is the Na-Fe³⁺-rich tourmaline species (Lynch, 1997; Grice *et al.*, 1993; Wallenta & Dunn, 1979).



Rossmannite is the □-Li-Al dominant tourmaline species. The X-site is vacant. The Y-sites are occupied by one Li⁺ and two Al³⁺ cations in the ideal formula. Al is held at the Z-sites. The V and W-sites are filled by OH anions. Rossmannite was first classified by Selway *et al.*, (1998a).

The chemistry of rossmannite is very similar to elbaite. It is because of this similarity that rossmannite forms a solid solution series with elbaite. This series is based on the substitution vector ${}^X\Box + {}^Y\text{Al}^{3+})_{0.5} \rightarrow {}^X\text{Na}^+ + {}^Y\text{Li}^+_{0.5}$ (Selway *et al.*, 1999). Rossmannite forms a series with liddicoatite based on the ${}^X\Box + {}^Y\text{Al}^{3+} \rightarrow {}^X\text{Ca}^{2+} + {}^Y\text{Li}^+$ substitution vector (Teertstra *et al.*, 1999). Rossmannite may form a series with alkali deficient species foitite or magnesiofoitite.

Selway *et al.*, (1999) studied the compositional evolution of tourmaline in lepidolite-subtype, LCT family pegmatites and found that rossmannite plays a small role in the consolidation of these pegmatites. The rossmannite-elbaite series mid-point is defined by the X-site Na/(Na+□) ratio equaling 0.5. When Na/(Na+□) ratios are greater than 0.5,

they are considered elbaite by the authors (Selway *et al.*, 1999). Rossmanite was first described from a rare-element pegmatite in the Hradisko quarry, near Rožná, western Moravia, Czech Republic (Selway *et al.*, 1998a).



Schorl is the Na-Fe²⁺-Al-rich species of the tourmaline group. Ideally, Na, Fe²⁺ and Al are housed by the X-site, Y-sites and Z-sites respectively. OH anions completely occupy the V and W-sites. The chemistry of schorl can vary widely with the incorporation of other tourmaline formula units via partial or complete isomorphous solid solution series with other end-members. The unit cell dimensions of schorl are variable with *a* and *c* ranging between 15.93-16.03 Å and 7.12-7.19 Å respectively (Anthony *et al.*, 1995). These values vary with changes in chemistry.

Schorl constitutes isomorphous solid solution series with five other tourmaline group species. This includes but is not limited to elbaite, dravite, feruvite, foitite and uvite. Schorl could conceivably form solid solution series with buergerite and the hypothetical species, “tsilaisite”.

The schorl-elbaite series is based on Y-site substitution vector $(^Y\text{Fe}^{2+})_3 \rightarrow (^Y\text{Al}^{3+})_{1.5} + (^Y\text{Li}^+)_{1.5}$ (Dietrich, 1985). The schorl-dravite series is facilitated by substitution vector $^Y\text{Fe}^{2+} \rightarrow ^Y\text{Mg}^{2+}$ (Dietrich, 1985). The schorl-feruvite series involves the coupled substitution of $^X\text{Ca}^{2+} \rightarrow ^X\text{Na}^+$ in the X-site which is charge balanced by the substitution vector $^Z\text{Al}^{3+} \rightarrow ^Z\text{Mg}^{2+}$ (Henry & Dutrow, 1996). MacDonald *et al.*, (1993) proposed the existence of a schorl-foitite series where foitite is derived from schorl by the coupled substitution $^X\text{Na}^+ \rightarrow ^X\text{□}$ and $^Y\text{Fe}^{2+} \rightarrow ^Y\text{Al}^{3+} + ^Y\text{Fe}^{3+}$ (MacDonald *et al.*, 1993). The

schorl-uvite series is based on ${}^X\text{Ca}^{2+} \rightarrow {}^X\text{Na}^+$, ${}^Y\text{Mg}^{2+} \rightarrow {}^Y\text{Fe}^{2+}$ and ${}^Z\text{Mg}^{2+} \rightarrow {}^Z\text{Al}^{3+}$ substitutions. If a schorl-buergerite series exists, it would involve the substitution vector, ${}^Y\text{Fe}^{2+} \rightarrow {}^Y\text{Fe}^{3+}$ with full O²⁻ occupancy at the V-sites and F at the W-site (Dietrich, 1985). The schorl-“tsilaisite” series would be based on ${}^Y\text{Fe}^{2+} \rightarrow {}^Y\text{Mn}^{2+}$ substitutions. Given the structural and chemical complexity of the tourmaline group, many other isomorphous solid solution series with schorl are possible.

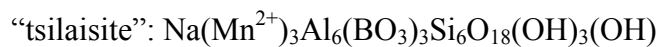
Schorl is the most common species of tourmaline and is found as an accessory mineral in many igneous environments (granitoid plutons and associated pegmatites, aplites and hydrothermal deposits) and pelitic metamorphic regimes (low to high grade barrovian, skarns) containing sufficient B (Henry & Guidotti, 1985). Schorl also occurs as authigenic overgrowths in sedimentary rocks.

Henry & Dutrow (2001) have described a schorl with very unusual chemistry from a micaceous marble in Samos, Greece. This tourmaline is zoned and ranges in chemistry from schorl-dravite-foitite. The first zone is enriched in Mg, Ti and F with depleted Al, Fe and X-site vacancies. The second zone is composed of a nickeloan dravite enriched in Mg, Co, Ca and F and depleted in Fe, Zn, Cr and V. The chemistry of the overgrowths varies extensively between the (c^+) and (c^-) poles. These specimens contain up to 3.5 wt. % NiO (0.5 apfu), 1.3 wt. % CoO and 0.8 wt. % ZnO (Henry & Dutrow, 2001).

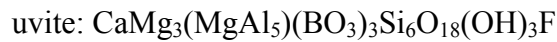
Kassoli-Fournaraki & Michailidis (1994) studied schorl from the Nea Roda and Thasos areas, Macedonia, Greece. The schorl in Nea Roda has two distinct chemical zones and crystallized in quartz veins crosscutting migmatitic gneisses. On Thasos Island, the bi-zoned schorl formed in quartz veins intruding sericite-chlorite schists. The

examined tourmalines belong to the schorl-dravite series. The tourmaline from Thasos is dravitic whereas the Nea Roda samples are schorlitic.

These schorl-dravites have an unusually high Ga content which the authors attribute as a sedimentary origin of the host rocks where Ga can be present in the clay minerals comprising the shales. Tourmalines from Nea Roda and Thasos contain 1.03 and 1.33 wt. % Ga_2O_3 respectively. Other minor elements (in apfu) detected were Mn (0-0.016), Ti (0.012-0.133), Ni (0-0.03), Cr (0-0.015), V (0-0.3), Zn (0-0.034) and Cu (0-0.033) (Kassoli-Fournaraki & Michailidis, 1994).



“Tsilaisite” is a hypothetical tourmaline group end-member. Its molecule has been identified in other species of tourmaline and therefore, true “tsilaisite” might exist. Na, Mn^{2+} and Al are housed by the X-site, Y-sites and Z-sites respectively (Simmons, 2003; Dirlam *et al.*, 2002; Shigley *et al.*, 1986; Schmetzer & Bank, 1984a; Schmetzer & Bank, 1984b; Tomisaka, 1968; Slivko, 1959).



Uvite is the Ca-Mg-Al-rich species of tourmaline (Povondra & Novák, 1986; Ayuso, 1984).



Vanadiumdravite is the newest tourmaline group species. It is the Na-Mg-V-rich tourmaline group end-member. Na, Mg and V are housed by the X, Y-sites and Z-sites respectively (Reznitsky *et al.*, 2001).

APPENDIX 2

sample	country	dist./peg.	sample	country	dist./peg.
a	Nigeria	Ibadan	t1	Nigeria	Ibadan
b	Nigeria	Ibadan	u1	Nigeria	Ibadan
c	Nigeria	Ibadan	v1	Nigeria	Ibadan
d	Nigeria	Ibadan	w1	Nigeria	Ibadan
e	Nigeria	Ibadan	x1	Nigeria	Ibadan
f	Nigeria	Ibadan			
g	Nigeria	Ibadan	Lila-1	Nigeria	Ibadan
h	Nigeria	Ibadan	Lila-2	Nigeria	Ibadan
i	Nigeria	Ibadan	Lila-3	Nigeria	Ibadan
j	Nigeria	Ibadan	Lila-4	Nigeria	Ibadan
k	Nigeria	Ibadan	Lila-5	Nigeria	Ibadan
l	Nigeria	Ibadan	Lila-6	Nigeria	Ibadan
m	Nigeria	Ibadan	Lila-7	Nigeria	Ibadan
n	Nigeria	Ibadan	Lila-8	Nigeria	Ibadan
o	Nigeria	Ibadan	Lila-9	Nigeria	Ibadan
p	Nigeria	Ibadan			
q	Nigeria	Ibadan	.3-1	Namibia	Omapyo
r	Nigeria	Ibadan	.3-2	Namibia	Omapyo
s	Nigeria	Ibadan	.3-3	Namibia	Omapyo
t	Nigeria	Ibadan	.3-4	Namibia	Omapyo
u	Nigeria	Ibadan	.3-5	Namibia	Omapyo
v	Nigeria	Ibadan	.3-6	Namibia	Omapyo
w	Nigeria	Ibadan	.3-7	Namibia	Omapyo
x	Nigeria	Ibadan	.3-8	Namibia	Omapyo
y	Nigeria	Ibadan	.3-9	Namibia	Omapyo
z	Nigeria	Ibadan	.3-10	Namibia	Omapyo
a1	Nigeria	Ibadan	.3-11	Namibia	Omapyo
b1	Nigeria	Ibadan	.3-12	Namibia	Omapyo
c1	Nigeria	Ibadan	.3-14	Namibia	Omapyo
d1	Nigeria	Ibadan	.3-15	Namibia	Brusius
e1	Nigeria	Ibadan	.3-17	Namibia	Omapyo
f1	Nigeria	Ibadan	.3-18	Namibia	Omapyo
g1	Nigeria	Ibadan	.3-19	Namibia	Omapyo
h1	Nigeria	Ibadan	.3-20	Namibia	Omapyo
i1	Nigeria	Ibadan	Nam-sl-d	Namibia	Swakopwund
j1	Nigeria	Ibadan	Nam-sl-c	Namibia	Omapyo
k1	Nigeria	Ibadan	Nam-sl-a	Namibia	Omapyo
l1	Nigeria	Ibadan	Nam-sl-b	Namibia	Omapyo

sample	country	dist./peg.	sample	country	dist./peg.
m1	Nigeria	Ibadan			
n1	Nigeria	Ibadan	.3-13	Mali	Gao
o1	Nigeria	Ibadan			
p1	Nigeria	Ibadan	Sanga-w	Tanzania	Sanga
q1	Nigeria	Ibadan	SS wm	Tanzania	Sanga
r1	Nigeria	Ibadan	SS blue	Tanzania	Sanga
s1	Nigeria	Ibadan			
Congo k	D.R. of C.	unknown			
Congo l	D.R. of C.	unknown			
Congo i	D.R. of C.	unknown			
Moz (grn)	Mozamb.	unknown			
Moz (pink)	Mozamb.	Morrua			

VITA

Brian Seth Giller was born on April 26, 1977 to parents Martin and Susan Giller in Fairfax County, Virginia. He studied under Dr. Lance E. Kearns and received his B.S. in geology from James Madison University, Harrisonburg, Virginia on May 6, 2000. From September, 2000 until April, 2001, Brian interned with pegmatite mineralogist, Dr. Michael A. Wise at the Smithsonian Institution, Washington, D.C. He received his M.S. in geology at the University of New Orleans on May 16, 2003 under the tutelage of Dr. William B. "Skip" Simmons Jr., Alexander U. Falster, Dr. Karen L. Webber and Dr. Michael A. Wise.

EXAMINATION AND THESIS REPORT

Candidate: Brian Seth Giller

Major Field: Geology

Title of Thesis: An Overview of Tourmaline Mineralogy from Gem Tourmaline Producing Pegmatite Districts in Africa

Approved:

Approved:
W.B. Murray
Major Professor & Chair

Robert C. Casler
Dean of the Graduate School

EXAMINING COMMITTEE:

John S. W.

Karen Luehken

Per oddz

Date of Examination: March 25, 2003